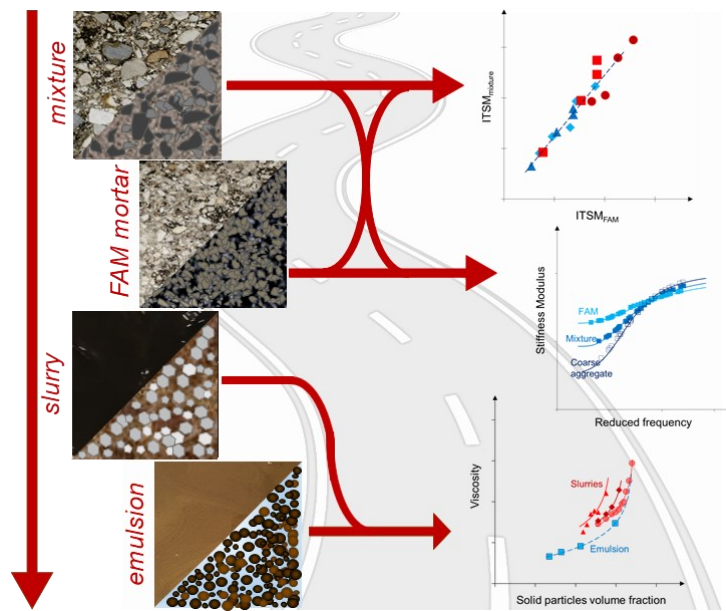




Università Politecnica delle Marche
Scuola di Dottorato di Ricerca in Scienze dell'Ingegneria
Curriculum in Ingegneria Civile, Ambientale, Edile e Architettura
XIX edition - new series

Multiscale Approach for Characterising the Behaviour of Cold Bitumen Emulsion Materials

Ph.D Dissertation of:
Chiara Mignini



Advisor:

Prof. Ph.D. Andrea Graziani

Co-Advisor:

Prof. Ph.D. Fabrizio Cardone

Curriculum Supervisor:

Prof. Ph.D. Francesco Fatone



Università Politecnica delle Marche
Scuola di Dottorato di Ricerca in Scienze dell'Ingegneria
Curriculum in Ingegneria Civile, Ambientale, Edile e Architettura
XIX edition - new series

Multiscale Approach for Characterising the Behaviour of Cold Bitumen Emulsion Materials

Ph.D. Dissertation of:

Mignini Chiara

Advisor:

Prof. Ph.D. Andrea Graziani

Co Advisor:

Prof. Ph.D. Fabrizio Cardone

Curriculum Supervisor:

Prof. Ph.D. Francesco Fatone

XIX edition - new series

Università Politecnica delle Marche
Dipartimento di Ingegneria Civile, Edile e Architettura
Via Brezze Bianche — 60131 - Ancona, Italy

Acknowledgements

The research work discussed in this thesis would never have been possible without the inestimable help given to me by some fundamental people who supported me for the PhD study duration.

First and foremost, I am extremely grateful to my advisor Prof. Andrea Graziani for the continuous support, for all of the opportunities I was given to further my research, for his patience, motivation, and immense knowledge. He convincingly guided me in all the time of research and writing of this thesis. I could never have to ask having a better advisor and mentor for my PhD study. I would also like to thank my co-advisor, Prof. Fabrizio Cardone, for his contribution and valuable advice for my research work.

I want to express my sincere gratitude to Prof. Davide Lo Presti and Prof. Gordon Airey for giving me the valuable opportunity to work at the Nottingham Transportation Engineering Centre (NTEC). It was extraordinary cooperation and an unrepeatable occasion to meet new motivating people, which I thank for their support and friendship.

I would like to extend my sincere thanks to Prof. Maurizio Bocci, Prof. Francesco Canestrari, Prof. Gilda Ferrotti and Prof. Amedeo Virgili for their valuable guidance throughout my studies. You provided me with the tools I needed to follow the right direction and successfully complete research work.

Thanks to the technical staff of the department ICEA (infrastructure area) and all my former and actual colleagues. A special mention to Davide Ragni, Arianna Stimilli, Elena Gaudenzi and Giorgia Mazzoni for the continuous encouragement, and first of all, their true friendship. Thank you to my “Canadian” colleague and friend Simone Raschia, with whom I shared the research topic and who has always offered me his support.

My endless gratitude is for my friends Martina, Francesca, Katia, Alessandra and Giuseppe. Without their tremendous understanding and encouragement in the past few years, it would be impossible to complete my study.

Thank you to my flatmates Andrea and Giulia for their inestimable support. Thank you also to my “SIIV” friends, especially Antonio and Federica, who provided stimulating discussions as well as happy amusement to rest my mind outside of my research.

The deepest gratitude ever is for my mom Clara and my dad Giuseppe for their continuous love and for always helping me to pursue my dreams.

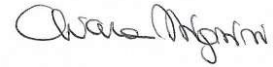
I am deeply grateful to Italcementi – HeidelbergCement Group and the CRABforOERE-*Cold Recycled Asphalt Bases for Optimised Energy & Resource Efficient*

Acknowledgements

Multiscale Approach for Characterising the Behaviour of Cold Bitumen Emulsion Materials

Pavements project (funded by Conference of European Directors of Roads) for partially supporting my fellowships during the 3 years PhD study.

Ancona, 15th April 2021



Abstract

Cold bitumen emulsion (CBE) materials are sustainable pavement construction and rehabilitation technologies. They are obtained using bitumen emulsion as the main binder. Cement or other types of mineral additions can be employed as co-binders or secondary stabilising agents. Frequently, CBE materials are produced using high amounts of reclaimed asphalt aggregate, maximising their sustainable benefits. However, CBE materials can lead to real economic advantages only if their performance is comparable to traditional hot mix asphalt. The achievement of CBE materials with satisfactory performances is strongly linked to a superior design of their composition and to a deep awareness about the mechanisms influencing their mechanical behaviour. Hence, type and dosages of the constituents, and their interaction, are key features to be investigated and optimised. Within this framework, this thesis aims to provide the scientific community with a multiscale approach for the fundamental characterisation of CBE materials. The multiscale approach here presented considers CBE materials as multiphase composites and investigates four scales of engineering interest: mixtures, fine aggregate matrix (FAM) mortars, fresh mastics (i.e. slurries) and bitumen emulsions. Specifically, the experimental investigation first attempted to define the FAM mortar concept. The evolutive behaviours of mixtures and FAM mortars were evaluated, as well as their linear viscoelastic (LVE) response. Then, a procedure for testing the viscosity of CBE slurries was investigated. In parallel, the adoption of innovative constituents for enhancing the CBE materials performances was assessed as well. Results showed that the developed multiscale approach is an effective tool for characterising CBE materials. FAM mortars showed a satisfactory predicting ability of CBE mixtures evolutive behaviour indeed. Besides, mortars and mixtures exhibited a similar sensitivity in terms of LVE response. A reliable novel methodology for characterising the rheological behaviour of CBE slurries was proposed. Finally, the use of innovative materials was found beneficial for enhancing the mechanical properties of CBE materials.

Sommario

I materiali a freddo prodotti con emulsione bituminosa rappresentano tecnologie sostenibili nel campo della costruzione e riabilitazione delle pavimentazioni. Si ottengono utilizzando l'emulsione bituminosa come legante principale. Come co-leganti o agenti stabilizzanti secondari possono essere impiegati cemento o altri tipi di aggiunte. Spesso, i materiali a freddo con emulsione vengono prodotti utilizzando quantità elevate di conglomerato bituminoso di recupero, massimizzando i loro benefici in termini di sostenibilità. Tuttavia, i materiali a freddo possono apportare reali vantaggi economici solo se le loro prestazioni sono paragonabili a quelle del tradizionale conglomerato bituminoso. L'ottenimento di materiali a freddo con emulsione bituminosa aventi prestazioni soddisfacenti è fortemente legato ad una progettazione avanzata della loro composizione e ad una profonda consapevolezza dei meccanismi che influenzano il loro comportamento meccanico. Di conseguenza, il tipo e i dosaggi dei componenti, ma anche la loro interazione, sono caratteristiche chiave da studiare e ottimizzare. In quest'ottica, la presente tesi mira a fornire alla comunità scientifica un approccio multiscala per la caratterizzazione fondamentale dei materiali a freddo prodotti con emulsione bituminosa. L'approccio multiscala qui presentato considera i materiali a freddo con emulsione bituminosa come compositi multifase e indaga quattro scale di interesse ingegneristico: le miscele, le malte, i mastici allo stato fresco e l'emulsione bituminosa. Nello specifico, l'indagine sperimentale ha tentato di definire il concetto di malta. È stato poi valutato il comportamento evolutivo di miscele e malte, nonché le loro proprietà viscoelastiche lineari (LVE). Quindi, è stata studiata una procedura per misurare la viscosità dei mastici allo stato fresco. Parallelamente, è stata valutata anche l'adozione di componenti innovative per migliorare le prestazioni dei materiali a freddo. I risultati hanno mostrato che l'approccio multiscala sviluppato è uno strumento efficace per caratterizzare i materiali a freddo con emulsione bituminosa. Le malte hanno evidenziato una soddisfacente capacità predittiva del comportamento evolutivo delle miscele. Inoltre, malte e miscele hanno mostrato una sensibilità simile in termini di risposta LVE. È stata proposta una nuova metodologia affidabile per caratterizzare il comportamento reologico dei mastici freschi. Infine, l'uso di materiali innovativi si è dimostrato utile per migliorare le proprietà meccaniche dei materiali CBE.

Table of Contents

Acknowledgements	i
Abstract.....	iii
Sommario	iv
Table of Contents	v
List of Figures.....	xi
List of Tables	xv
List of Standard Specifications	xvii
List of Abbreviations	xix
Chapter 1. Introduction.....	1
Chapter 2. Literature Review	3
2.1. Cold bitumen emulsion materials	3
2.1.1. Cold paving materials	3
2.1.1.1. Cold recycling technologies.....	4
2.1.1.2. Classification of cold mixtures.....	5
2.1.2. Constituents of CBE materials	8
2.1.2.1. Bitumen emulsion.....	8
2.1.2.2. Cementitious binder	17
2.1.2.3. Aggregate.....	18
2.1.2.4. Water.....	21
2.1.2.5. Bitumen emulsion-aggregate interaction.....	21
2.1.2.6. Bitumen emulsion-cementitious binders interaction.....	22
2.1.3. The evolutive behaviour of CBE materials.....	22

Table of Contents

Multiscale Approach for Characterising the Behaviour of Cold Bitumen Emulsion Materials

2.1.3.1. <i>Modelling curing behaviour of cold mixtures</i>	23
2.1.4. Viscoelastic properties of CBE materials	25
2.1.4.1. <i>Measuring the complex modulus of cold mixtures</i>	28
2.1.4.2. <i>Modelling the viscoelastic behaviour of cold mixtures</i>	29
2.2. The multiscale approach	37
2.2.1. Study of FAM mortars	38
2.2.2. Viscosity of fresh mastics: CBE slurries.....	41
Chapter 3. Research Description and Objectives	46
3.1. Introduction	46
3.2. Objective Statement	47
3.3. Methodology: the multiscale approach	47
3.4. Outline of the dissertation	49
Chapter 4. Materials and Methods	51
4.1. Materials	51
4.2. Sample preparation	53
4.2.1. Mixing.....	53
4.2.1.1. <i>Mixtures and FAM mortars</i>	53
4.2.1.2. <i>Slurries</i>	53
4.2.2. Compaction	53
4.2.3. Curing	54
4.3. Volumetric analysis	54
4.3.1. Fresh state CBE mixtures and mortars.....	55
4.4. CBE materials composition	57
4.4.1. Mixtures	57
4.4.2. FAM mortars.....	60
4.4.3. Slurries	62
4.5. Test methods	65

Table of Contents

Multiscale Approach for Characterising the Behaviour of Cold Bitumen Emulsion Materials

4.5.1. Water loss by evaporation.....	65
4.5.2. Indirect Tensile Stiffness Modulus	65
4.5.3. Indirect Tensile Strength.....	65
4.5.4. Complex modulus	66
4.5.4.1. <i>Data analysis: construction of the master curves and rheological modelling</i>	67
4.5.5. Viscosity	69
Chapter 5. Mixture to FAM Mortar Downscaling.....	71
5.1. Introduction	71
5.2. Objectives	71
5.3. Methodology	71
5.4. Analysis of the Results	74
5.5. Summary	77
Chapter 6. Curing Behaviour of CBE Materials	78
6.1. Introduction	78
6.2. Objectives	78
6.3. Methodology	78
6.4. Analysis of the Results	80
6.4.1. Water loss by evaporation.....	80
6.4.2. Stiffness and strength.....	82
6.4.3. Effect of sealed curing conditions.....	85
6.4.4. Relationship between CBE mixtures and mortars properties.....	87
6.5. Validation of the FAM mortar concept	90
6.5.1.1. <i>Relationship between CBE mixtures and FAM mortars</i>	91
6.6. Summary	95
Chapter 7. Linear Viscoelastic Study of CBE Materials.....	97
7.1. Introduction	97

Table of Contents

Multiscale Approach for Characterising the Behaviour of Cold Bitumen Emulsion Materials

7.2. Objectives.....	97
7.3. Methodology	97
7.4. Analysis of the Results	99
7.4.1. Complex modulus results.....	99
7.4.2. Thermo-rheological modelling.....	102
7.4.3. Relationship between CBE mixtures and FAM mortars	110
7.4.3.1. CBE composites modelling: influence of the coarse aggregate	115
7.5. Summary	120
Chapter 8. Rheological Characterisation of CBE Slurries.....	121
8.1. Introduction	121
8.2. Objectives.....	121
8.3. Methodology	121
8.4. Analysis of the Results	124
8.4.1. Part 1: Definition of the testing procedure.....	124
8.4.2. Part 2: Viscosity of CBE slurries	127
8.5. Summary	134
Chapter 9. Conclusions	135
9.1. Concluding Remarks.....	135
9.1.1. Multiscale approach	135
9.1.2. Impact of CBE materials constituents and compositions.....	136
9.1.3. Testing methods and models for CBE materials	137
9.2. Recommendations	137
References.....	139
Appendix A Properties of Materials Employed	154
A.1. Aggregates.....	154
A.2. Bitumen emulsions	157
A.3. Cementitious binders	159

Table of Contents

Multiscale Approach for Characterising the Behaviour of Cold Bitumen Emulsion Materials

Appendix B	Mixing procedures for CBE Mixtures and FAM Mortars	160
B.1.	Mixtures	160
B.2.	FAM mortars	163
Appendix C	Study of the Composition of CBE Mixtures with Different Cements for Base Courses	167
C.1.	Introduction	167
C.2.	Methodology	167
C.3.	Analysis of the Results	168
C.4.	Summary	171
Appendix D	Effect of Curing on the Indirect Tensile Failure Energy of CBE Mixtures	172
D.1.	Introduction	172
D.2.	Methodology	172
D.3.	Analysis of the Results	173
D.4.	Summary	176
Appendix E	Effect of Grading Distribution on the Volumetric Properties of CBE Mixtures for Binder Courses	177
E.1.	Introduction	177
E.2.	Methodology	177
E.3.	Analysis of the Results	179
E.4.	Summary	181
Appendix F	Study of the Composition of CBE Mixtures with High Strength Cements for Binder Courses	182
F.1.	Introduction	182
Appendix G	Fatigue Behaviour of CBE Mixtures for Binder Courses Produced with High Strength Cements	189
G.1.	Introduction	189
G.2.	Methodology	190

Table of Contents

Multiscale Approach for Characterising the Behaviour of Cold Bitumen Emulsion Materials

G.3. Analysis of the Results	191
G.4. Summary	196
Appendix H Cracking Resistance of CBE FAM mortars	197
H.1. Introduction	197
H.2. Methodology	197
H.3. Analysis of the Results	199
H.4. Summary	203
Appendix I Graphic Representation of the Results For Complex Modulus Test	204
Lists of 3-years PhD Publications	207
Lists of 3-years PhD Awards	209

List of Figures

Figure 2.1. Classification by temperature and fuel usage of road paving techniques (Del Carmen Rubio <i>et al.</i> 2013)	4
Figure 2.2. Sustainability benefits of cold technologies over traditional HMA (Xiao <i>et al.</i> 2018).....	4
Figure 2.3. Conceptual composition of cold mixtures adapted from Grilli <i>et al.</i> 2012.....	7
Figure 2.4. Bitumen emulsion a) types: O/W, W/O, and multiple W/O/W (from top to bottom), b) typical particle size distribution of the bituminous droplets (AkzoNobel Surface Chemistry 2017).....	9
Figure 2.5. Types of emulsion charges: a) anionic emulsion , b) cationic emulsion (adapted from AkzoNobel Surface Chemistry, 2017).....	11
Figure 2.6. Bitumen emulsion breaking stages (adapted from James, 2006).....	12
Figure 2.7. Potential emulsion breaking scenarios: a) film forming, b) gel contraction (adapted from Lesueur and Potti 2004).....	13
Figure 2.8. a) RA stockpiled in a production plant, b) RA aggregate.....	19
Figure 2.9. CBE material volume change during curing	23
Figure 2.10. Modified Michaelis Menten model representation (Equation 2.2).....	24
Figure 2.11. Domains of behaviour for bituminous mixtures, (strain amplitude as a function of the number of cycles) (Olard <i>et al.</i> 2005)	26
Figure 2.12. Complex modulus test: a) stress and strain trends, b) complex plan representation	26
Figure 2.13. Construction of the stiffness modulus master curve: a) horizontal shifting ($T_{ref} = 25\text{ }^{\circ}\text{C}$), b) CFS algorithm application.....	28
Figure 2.14. Analogical LVE models: a) Kelvin-Voigt, b) generalised Kelvin-Voigt	30
Figure 2.15. Analogical LVE models: a) Maxwell, b) generalised Maxwell	30
Figure 2.16. Analogical LVE model: a) Huet-Sayegh (HS), b) 2S2P1D.....	31
Figure 2.17. Comparison between the Huet–Sayegh (HS) and HS-HY models.....	33
Figure 2.18. Analogical DBN model.....	33
Figure 2.19. Scales involved in the multiscale investigation of bituminous mixtures (Underwood 2015).....	38
Figure 3.1. Schematic diagram showing the general definition of the various scale of observation of CBE materials.....	48
Figure 3.2. Scheme of the dissertation.....	50
Figure 4.1. Aggregates grading distributions.....	52

List of Figures

Figure 4.2. CBE mixtures and mortars composition at the fresh state (by mass and by volume).....	56
Figure 4.3. Volumetric analysis of fresh CBE materials: a) volumetric properties progress during compaction (Equations (4.1) and (4.2)), b) specimen aspect right after compaction with $VFL > 90\%$, c) specimen aspect right after compaction with $VFL < 90\%$	57
Figure 4.4. Mixtures grading distributions	59
Figure 4.5. FAM mortars grading distributions	61
Figure 4.6. CBE mixtures and mortars mechanical testing: a) <i>ITSM</i> test, b) <i>ITS</i> test.....	66
Figure 4.7. Complex modulus testing: a) mixtures specimens, b) FAM mortar specimen coring, c) AMPT PRO device, d) testing configuration detail	68
Figure 4.8. CBE slurries viscosity testing equipment a) Brookfield viscometers employed in the experimental study: LV model (on the left) and HA model (on the right) b) impellers used within the experimental study.....	70
Figure 5.1. CBE mixture and FAM mortar volumetric composition model (fresh state) ...	72
Figure 5.2. Mixture to FAM mortar downscaling: experimental programme organisation	73
Figure 5.3. FAM mortar-to-mixture <i>ITS</i> ratio as a function of FAM mortar-to-mixture air voids content ratio obtained with $vW, FAM / vW, mixture = 1.00$	76
Figure 5.4. FAM mortar-to-mixture <i>ITS</i> ratio as a function of FAM mortar-to-mixture air voids content ratio obtained for CBE produced with cement C2 and C3, B/C=1.3	76
Figure 6.1. Study of CBE materials curing behaviour: experimental programme organisation	79
Figure 6.2. Evolution of <i>DW</i> for mixtures and FAM mortars produced with binders C1 and C4. Experimental data and modified MM model (Equation (2.2)).....	81
Figure 6.3. Comparison of <i>DW</i> of mixtures and FAM mortars (from 1 day to 28 days) ...	81
Figure 6.4. Evolution of <i>ITSM</i> for mixtures and FAM mortars produced with cementitious binders C1 and C3. Experimental data and modified MM model (Equation (2.2))	83
Figure 6.5. Regression parameters of the curing model (Equation (2.2)) for the <i>ITSM</i> of mixtures a) <i>ITSM1</i> , b) <i>ITSMa</i>	83
Figure 6.6. Evolution of <i>ITS</i> for mixtures and FAM mortars produced with cementitious binders C1 and C3. Experimental data and modified MM model (Equation (2.2))	84
Figure 6.7. Regression parameters of the curing model (Equation (2.2)) for the <i>ITS</i> of mixtures a) <i>ITS1</i> , b) <i>ITSa</i>	84
Figure 6.8. Evolution of <i>ITSM</i> as a function of curing time of CBE mixtures and FAM mortars produced with cement C2 (unsealed and sealed “S” curing conditions) ..	86
Figure 6.9. Evolution of <i>ITS</i> as a function of curing time of CBE mixtures and FAM mortars produced with cement C2 (unsealed and sealed “S” curing conditions)	86
Figure 6.10. Correlation between <i>ITSM</i> and <i>ITS</i> in unsealed and sealed (“S”) curing conditions	87

List of Figures

Figure 6.11. Mechanical properties of CBE mixtures as a function of mechanical properties of FAM mortars: a) <i>ITSM</i> , b) <i>ITS</i>	88
Figure 6.12. Schematic 1D representation of modulus composite models: a) original Hirsch model b) modified Hirsch model.....	88
Figure 6.13. FAM mortars composition in terms of volume of water and air respect of the total mixture volume.....	91
Figure 6.14. Comparison of <i>DW</i> of mixtures (MIX3 and MIX 4) and FAM mortars (FAM3 and FAM4) from 6 hours to 90 days	93
Figure 6.15. Mechanical properties of MIX3 (CC) and MIX4 (GG) as a function of mechanical properties of FAM3 and FAM4: a) <i>ITSM</i> , b) <i>ITS</i>	94
Figure 7.1. Study of CBE materials LVE behaviour: experimental programme organisation	98
Figure 7.2. Isothermal curves: a) <i>E0</i> of MIX3-C3_R1, b) φ of MIX3-C3_R1, c) <i>E0</i> of FAM3-C3_R1 and d) φ of FAM3-C3_R1	100
Figure 7.3. Stiffness modulus and phase angle data, plotted in the Black diagram, a) mixtures with cement C2, b) mixtures with cement C3, c) FAM mortars with cement C2 and d) FAM mortars with cement C3.....	101
Figure 7.4. Loss modulus and storage modulus data plotted in the Cole-Cole diagram, a) mixtures with cement C2, b) mixtures with cement C3, c) FAM mortars with cement C2 and d) FAM mortars with cement C3.....	102
Figure 7.5. Shift factors and WLF models ($T_{ref} = 25\text{ }^{\circ}\text{C}$): a) CBE mixtures b) FAM mortars	105
Figure 7.6. CBE mixtures experimental data and 2S2P1D-HY model a) Black diagram, b) Cole-Cole plan, c) stiffness modulus master curves ($T_{ref} = 25\text{ }^{\circ}\text{C}$) and d) phase angle master curves ($T_{ref} = 25\text{ }^{\circ}\text{C}$).....	107
Figure 7.7. Accuracy of 2S2P1D-HY model prediction (Equations (7.2 and (7.3) for CBE mixtures: a) stiffness modulus, b) phase angle.....	108
Figure 7.8. FAM mortars experimental data and 2S2P1D-HY model a) Black diagram, b) Cole-Cole plan, c) stiffness modulus master curves ($T_{ref} = 25\text{ }^{\circ}\text{C}$) d) phase angle master curves ($T_{ref} = 25\text{ }^{\circ}\text{C}$)	109
Figure 7.9. Accuracy of 2S2P1D-HY model prediction (Equations (7.2 and (7.3) for FAM mortars: a) stiffness modulus, b) phase angle.....	110
Figure 7.10. Comparison of CBE mixtures and FAM mortars 2S2P1D-HY model parameters a) <i>Ee</i> , b) <i>Eg</i> . Error bars represent the variability of the parameters.....	111
Figure 7.11. Comparison of MIX3 and FAM3 a) normalised Black diagram b) normalised Cole–Cole plan.....	111
Figure 7.12. Comparison of MIX4 and FAM4 a) normalised Black diagram b) normalised Cole–Cole plan.....	112
Figure 7.13. Comparison of MIX5 and FAM5 a) normalised Black diagram b) normalised Cole–Cole plan.....	112

List of Figures

Figure 7.14. Comparison of CBE mixtures and FAM mortars 2S2P1D-HY model parameters a) k , b) h , c) δ , d) $\text{Log } \tau$, e) β and f) φ_0 . Error bars represent the variability of the parameters	114
Figure 7.15. FAM3-C3 to MIX3-C3 master curves upscaling a) stiffness modulus, b) phase angle	115
Figure 7.16. 1D schematic representation of CBE mixture in parallel arrangement	115
Figure 7.17. Average complex modulus results and fitted 2S2P1D-HY obtained for CBE materials with grading CC and cement C3 a) Black diagram, b) Cole-Cole plan, c) stiffness modulus master curves ($T_{ref} = 25\text{ }^\circ\text{C}$) and d) phase angle master curves ($T_{ref} = 25\text{ }^\circ\text{C}$)	118
Figure 7.18. Average complex modulus results and fitted 2S2P1D-HY obtained for CBE materials with grading GG and cement C2 a) Black diagram, b) Cole-Cole plan, c) stiffness modulus master curves ($T_{ref} = 25\text{ }^\circ\text{C}$) and d) phase angle master curves ($T_{ref} = 25\text{ }^\circ\text{C}$)	119
Figure 8.1. Viscosity of CBE slurries: experimental programme organisation	123
Figure 8.2. Test procedure followed during the experimental study a) Part1A, b) Part 1B, c) Part 2 - LV model viscometer, d) Part 2 - HA model viscometer.....	123
Figure 8.3. Viscosity changes over time of bitumen emulsion and CBE slurries measured using a) S27, b) DHR. Error bars represent the standard deviation of the experimental data	124
Figure 8.4. . CBE slurries appearance: a) BWC_580 immediately after the hand-stirring (emulsion breaking), b) BPWF_680 right after the lowering of the impeller.....	125
Figure 8.5. Viscosity measured during Phase 1B a) B_596 (emulsion), b) BWF_511, c) BWC_437, d) BWFC_511. Error bars represent the standard deviation of the experimental data	126
Figure 8.6. Viscosity as a function of shear rate measured during the rising phase of speed (up) and decreasing phase of speed (down) for a) B_596 and BWC_437, b) BWF_511 and BWFC_511, c) BP_596 and BPWC_437, d) BPWF_511 and BPWFC_511. Error bars represent the standard deviation of the experimental data.	128
Figure 8.7. Viscosity versus shear rate for a) BPW, b) BPWF, c) BPWC, d) BPWFC. Error bars represent the standard deviation of the experimental data	129
Figure 8.8. Effect of bitumen emulsion type on the viscosity of bitumen emulsion dispersions and CBE slurries.....	130
Figure 8.9. Viscosity versus solid particles volume fraction a) B, b) BP ($\gamma = 34\text{ s}^{-1}$)	131
Figure 8.10. Relative viscosity as a function of the ratio between solid particles volume fraction and maximum packing volume fraction.....	133

List of Tables

Table 2.1. Comparison of advantages and disadvantages of bituminous and cementitious stabilising agents (Xiao <i>et al.</i> 2018)	8
Table 2.2. Bitumen emulsions classification according to EN 13808, ASTM-D977 ASTM and D2397/D2397M	15
Table 2.3. Typical emulsion pH and emulsifiers types and levels (AkzoNobel Surface Chemistry 2017)	15
Table 2.4. Applications of bitumen emulsions (adapted from AkzoNobel Surface Chemistry, 2017).....	16
Table 2.5. Summary of CRM properties and thermo-rheological characterization approaches based on cyclic axial tests on cylindrical specimens	35
Table 2.6. Summary of the approaches proposed for defining HMA FAM composition ...	40
Table 2.7. Summary of the procedures proposed for mixing and viscosity testing of CBE slurries	44
Table 4.1. Gravimetric composition of the aggregate blends of the mixtures.....	59
Table 4.2. Composition of mixtures investigated within the thesis	60
Table 4.3. Gravimetric composition of the aggregate blends of FAM mortars.....	61
Table 4.4. Composition of FAM mortars investigated within the thesis.....	62
Table 4.5. Typical compositions of CBE mixtures derived from scientific literature.....	63
Table 4.6. Composition by mass and volumetric fractions of the CBE dispersions (bitumen emulsions and slurries).....	64
Table 5.1. Water and air voids fractions adopted for the trial FAM mortar compositions .	74
Table 6.1. Regression parameters of the curing model for MIX3 and MIX4	92
Table 6.2. Regression parameters of the curing model for FAM3 and FAM4.....	93
Table 6.3. Model parameters (Equations (6.1 and (6.2) and regression parameters for relating <i>ITSM</i> and <i>ITS</i> of FAM3 and FAM 4 with MIX3 and MIX4 (CC and GG, respectively)	95
Table 7.1. CBE mixtures parameters of the 2S2P1D-HY model (Equation (7.1)) and WLF model (Equation (4.6)), $T_{ref} = 25\text{ }^{\circ}\text{C}$	103
Table 7.2. FAM mortars parameters of the 2S2P1D-HY model (Equation (7.1)) and WLF model (Equation (4.6)), $T_{ref} = 25\text{ }^{\circ}\text{C}$	104
Table 7.3. CBE materials compositions in terms of binders	104
Table 7.4. Parallel arrangement and 2S2P1D-HY model average parameters ($T_{ref} = 25\text{ }^{\circ}\text{C}$) obtained in the study of the influence of coarse aggregate	117

List of Tables

Multiscale Approach for Characterising the Behaviour of Cold Bitumen Emulsion Materials

Table 8.1. Krieger-Dougherty model parameters (Equation (8.1)) obtained for all the tested dispersions.....	133
--	-----

List of Standard Specifications

- AASHTO T 316: Standard Method of Test for Viscosity Determination of Asphalt Binder Using Rotational Viscometer, 2019.
- AASHTO T 342: Standard Method of Test for Determining Dynamic Modulus of Hot Mix Asphalt (HMA), 2011.
- AASHTO TP 62: Standard Method of Test for Determining Dynamic Modulus of Hot Mix Asphalt (HMA), 2007.
- AASHTO TP 79: Standard Method of Test for Determining the Dynamic Modulus and Flow Number for Asphalt Mixtures Using the Asphalt Mixture Performance Tester (AMPT), 2015.
- ASTM C109/C109M: Standard Test Method for Compressive Strength of Hydraulic Cement Mortars (Using 2-in. or [50 mm] Cube Specimens), 2020.
- ASTM D2397/D2397M: Standard Specification for Cationic Emulsified Asphalt. 2020.
- ASTM-D977: Standard Specification for Emulsified Asphalt, 2020.
- EN 12697-23: Bituminous mixtures - Test methods - Part 23: Determination of the indirect tensile strength of bituminous specimens, 2017-
- EN 12697-24: Bituminous mixtures - Test methods - Part 24: Resistance to fatigue, 2018.
- EN 12697-26: Bituminous mixtures - Test methods - Part 26: Stiffness, 2016.
- EN 12697-44: Bituminous mixtures - Test methods - Part 44: Crack propagation by semi-circular bending test, 2019.
- EN 12697-8: Bituminous mixtures - Test methods - Part 8: Determination of void characteristics of bituminous specimens, 2018.
- EN 13043: Aggregates for bituminous mixtures and surface treatments for roads, airfields and other trafficked areas, 2002
- EN 13108-1: Bituminous mixtures - Material specifications - Part 1: Asphalt Concrete, 2016.

List of Standard Specifications

Multiscale Approach for Characterising the Behaviour of Cold Bitumen Emulsion Materials

- EN 13108-2: Bituminous mixtures - Material specifications - Part 2: Asphalt Concrete for Very Thin Layers (BBTM) , 2016.
- EN 13108-3: Bituminous mixtures - Material specifications - Part 3: Soft Asphalt , 2016.
- EN 13108-4: Bituminous mixtures - Material specifications - Part 4: Hot Rolled Asphalt, 2016.
- EN 13108-5: Bituminous mixtures - Material specifications - Part 5: Stone Mastic Asphalt, 2016.
- EN 13108-6: Bituminous mixtures - Material specifications - Part 6: Mastic Asphalt, 2016.
- EN 13108-7: Bituminous mixtures - Material specifications - Part 7: Porous Asphalt, 2016.
- EN 13108-8: Bituminous mixtures - Material specifications - Part 8: Reclaimed Asphalt, 2016.
- EN 13108-9: Bituminous mixtures - Material specifications - Part 9: Asphalt for Ultra-Thin Layer (AUTL) , 2016.
- EN 13242: Aggregates for unbound and hydraulically bound materials for use in civil engineering work and road construction, 2002+A1:2007.
- EN 13302: Bitumen and bituminous binders - Determination of dynamic viscosity of bituminous binder using a rotating spindle apparatus. 2018.
- EN 13808: Bitumen and bituminous binders - Framework for specifying cationic bituminous emulsions, 2013.
- EN 15368: Hydraulic binder for non-structural applications - Definition, specifications and conformity criteria, 2008 + A1 2010.
- EN 196-1: Methods of testing cement - Part 1: Determination of strength, 2016.
- EN 197-1: Cement Part 1: Composition, specifications and conformity criteria for common cements, 2011.
- prEN 13108-31: Bituminous mixtures - Material specifications - Part 31: Asphalt Concrete with Bituminous Emulsion, *draft*.

List of Abbreviations

2S2P1D	2 springs, 2 parabolic elements, 1 dashpot
2S2P1D-HY	2 springs, 2 parabolic elements, 1 dashpot – hysteretic
ARRA	Asphalt Recycling and Reclaiming Association
B/C	Bitumen to cement
B/F	Residual bitumen to filler
BSM	Bitumen-Stabilised Materials
C/F	Cement to filler
CAC	Calcium aluminate cement
CAM	Christensen-Anderson-Marasteanu
CBE	Cement-Bitumen Emulsion
CBTM	Cement-Bitumen Treated Materials
CCPR	Cold Central Plant Recycling
CFS	Closed-Form Shifting
CIR	Cold In-Place Recycling
CM	Cold Mixtures
CMA	Cold Mix Asphalt
CR	Cold Recycling
CRABforOERE	Cold Recycled Asphalt Bases for Optimised Energy & Resource Efficient Pavements
CRM	Cold Recycled Mixtures
CSA	Calcium sulfoaluminate cement
CTM	Cement-Treated Materials
DBN	Di Benedetto-Neifar
DBNPDS	Di Benedetto-Neifar Plastic Dissipation for Small Cycles
DHR	Dual Helical Ribbon

List of Abbreviations

Multiscale Approach for Characterising the Behaviour of Cold Bitumen Emulsion Materials

DW	Water loss by evaporation
EB	Emulsion bitumen
EP	Elasto-plastic
FAM	Fine Aggregate Matrix
FDE	Fractional Derivative Elements
FDR	Full Depth Reclamation
GE	Grave Emulsion
HA	High Torque
HMA	Hot Mix Asphalt
HS	Huet-Sayegh
HS-HY	Huet-Sayegh-Hysteretic
ITS	Indirect Tensile Strength
ITSM	Indirect Tensile Stiffness Modulus
ITSR	Indirect Tensile Fatigue test
ITSR	Indirect Tensile Strength ratio
LV	Low torque
LVDT	Linear Variable Differential Transducers
MM	Michaelis-Menten
MS	Medium-setting emulsions
NMAS	Nominal Maximum Aggregate Size
O/W	Oil-in-water
OPC	Ordinary Portland cement
RA	Reclaimed Asphalt
RB	Recycled binder
RBR	Recycled binder ratio
RH	Relative Humidity
RILEM	Réunion Internationale des Laboratoires et Experts des Matériaux, systèmes de construction et ouvrages
RS	Rapid-setting emulsions
SCB	Semi-circular bending
SGC	Superpave Gyratory Compactor

List of Abbreviations

Multiscale Approach for Characterising the Behaviour of Cold Bitumen Emulsion Materials

SMC	Spindle Multiplier Constant
SRC	Shear Rate Constant
SS	Slow-setting emulsions
SSD	Saturated Surface Dry
TK	Torque Constant
TTSP	Time-Temperature Superposition Principle
VFL	Voids filled with liquids
V _m	Voids in the mixture
W/B	Water to residual bitumen
W/C	Water to cement
W/F	Water to filler
W/O	Water-in-oil
W/O/W	Water-in-oil-in-water

Chapter 1.

Introduction

The pursuit of sustainability is one of the primary issues of contemporary society and affects all sectors, including the construction sector. 35% of the European Union total waste comes from construction sector. Compared to the total national greenhouse gas emissions, it is estimated that 5-12% comes from material extraction, manufacturing of construction products, construction and renovation of buildings. Then, reducing waste and greenhouse emissions is among the priorities of the European Green Deal (European Commission 2020). The transport infrastructure engineering sector is obviously part of these challenges, as it is constantly increasing due to the growing demand and the need for a well-connected transport network. The current practices about road materials application are moving on to claim sustainable solutions, supported by research progress in the last decades. Thinking about sustainability, the first thought generally regards the reduction of the environmental impact. A sustainable paving material should reduce pollutants emissions, save non-renewable resources and energy, and increase the re-use of waste materials. Nevertheless, so that a material can actually be considered sustainable, it should engender economic benefits, such as costs reductions and economic growth. Social sustainability must be accomplished, as well. It can be obtained, for example, guaranteeing the health of the workers and the conservation of the resources. In this framework, cold bitumen emulsion (CBE) materials are an effective road paving solution. They are indeed increasingly gaining attention as part of a progressive transition to a sustainable economic system.

However, all the peculiarities that make them sustainable, including the potential use of an important amount of reclaimed asphalt (RA) or the presence, instead of bitumen, of bitumen emulsion, cementitious co-binders and water, makes them extremely complex materials. The present thesis deals with the interaction of the different constituent materials and their impact on the CBE materials response. In particular, the experimental investigation aimed at developing and applying a multiscale approach for characterising the behaviour of CBE materials analysed as multi-phase composites.

Specifically, Chapter 2 provides a review of the scientific literature about CBE materials, the object of the thesis. The application of the multiscale approach in traditional bituminous mixtures, and its application for investigating cold materials are also discussed. This leads to the research description and objectives reported in Chapter 3. Chapter 4 gives

Chapter 1

Introduction

Multiscale Approach for Characterising the Behaviour of Cold Bitumen Emulsion Materials

an overview of the materials adopted within the investigation and, the adopted procedures for preparing and testing the CBE materials. The results discussion is presented in four chapters, each one focusing on a specific aspect of the multiscale approach. Chapter 5, Chapter 6 and Chapter 7 focus on mixtures and fine aggregate matrix (FAM) mortars, and their relationship. Chapter 8 investigates the rheological properties of CBE slurries. Finally, Chapter 9 reports the main findings of this thesis and some recommendations for future researches.

Chapter 2. Literature Review

2.1. Cold bitumen emulsion materials

2.1.1. Cold paving materials

Cold paving technologies represent an effective answer to sustainability needs. While traditional hot mix asphalt (HMA) mixtures are manufactured at 150-180 °C, cold paving technologies are manufactured at temperatures lower than 60 °C, allowing a reduction up to 50% of the fuel consumption needed for the heating (D'Angelo *et al.* 2008, Del Carmen Rubio *et al.* 2013) (**Figure 2.1**). The lack of heating leads to the abatement of energy consumption and greenhouse, sulphur dioxide and nitric oxide/nitrogen dioxide pollutant emissions (Thenoux *et al.* 2007, Cross *et al.* 2011, Giani *et al.* 2015, Xiao *et al.* 2018).

All these benefits are maximised in the case of cold recycling technologies, which allows the recycling of reclaimed asphalt (RA) aggregate coming from the milling of end of life pavement structures (Xiao *et al.* 2018) (**Figure 2.2**). Indeed, in striving to preserve natural resources, cold recycling is one of the most effective paving technologies since it allows using a high amount of RA, generally between 50% and 100% of the total aggregate blend. The large usage of RA also permits the reduction of costs for the disposal of waste materials.

Chapter 2
Literature Review

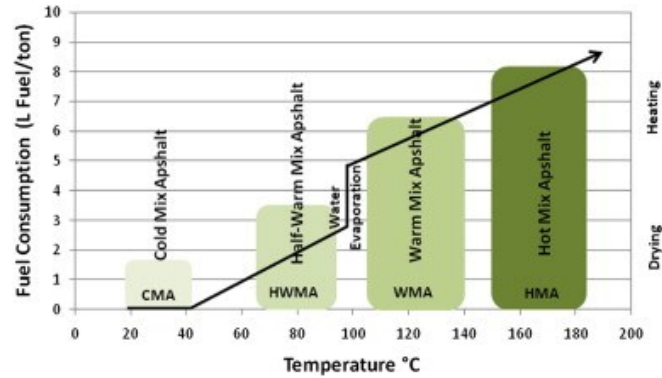


Figure 2.1. Classification by temperature and fuel usage of road paving techniques (Del Carmen Rubio *et al.* 2013)

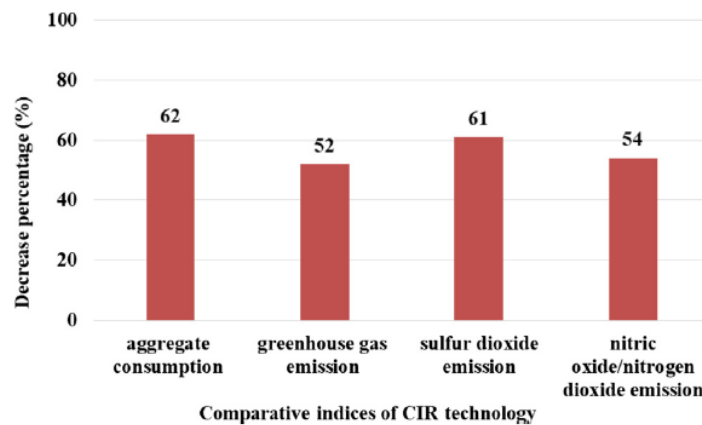


Figure 2.2. Sustainability benefits of cold technologies over traditional HMA (Xiao *et al.* 2018)

2.1.1.1. Cold recycling technologies

Cold recycling technologies can be distinguished into two main categories (ARRA 2001):

- Full-depth reclamation (FDR), which includes several sub-categories:
 - o pulverisation;
 - o mechanical stabilisation;
 - o bituminous stabilisation;
 - o chemical stabilisation.
- Cold recycling (CR), which includes two sub-categories:

Chapter 2

Literature Review

- Cold In-Place Recycling (CIR);
- Cold Central Plant Recycling (CCPR).

FDR interests the full thickness of the bound pavement and a certain amount of the underlying unbound layers, which are milled and blended to obtain a homogenous material. The milled materials can be stabilised using a binding agent, e.g. hydraulic binders, bitumen emulsion or foamed bitumen. The treatment thickness generally ranges between 100 and 300 mm, and the final material is suitable for base and subbase layers (Fedrigo *et al.* 2020).

Generally, CR allows obtaining a better quality material compared to FDR. It interests the reclaiming of the bituminous pavement layers only. The treatment thickness can range between 50 and 100 mm when only a bituminous binder is employed, i.e. bitumen emulsion or foamed bitumen. It can reach 150 mm if a co-binder is added, e.g. Portland cement, lime, fly ash. CIR takes place directly on site using the so-called “recycling train”. The technique allows recycling 100% RA, although natural aggregate is sometimes added to adjust the grading distribution (Mollenhauer and Simnofske 2015, Lin *et al.* 2017, Sangiorgi *et al.* 2017, Bocci *et al.* 2020). CIR allows cost savings between 41% and 47% compared to traditional HMA mill and overlays (Offenbacher *et al.* 2021). The CCPR process is carried out in a fixed or mobile cold mix plant: here, the employed RA aggregate may be subjected to further crushing and sieving operations. Also in this case, natural aggregate is introduced to adjust the grading distribution. The final recipe also undergoes better control (Diefenderfer *et al.* 2016, Gu *et al.* 2019). In this context, the final material has superior properties and reliability than those obtained with CIR, making it suitable for being used in high-traffic roads as base and binder courses (Timm *et al.* 2018, Ferrotti, Grilli, *et al.* 2020).

2.1.1.2. Classification of cold mixtures

Cold mixtures (CM) and cold recycled mixtures (CRM) are produced with aggregate (natural and RA), and one or more binding/stabilising agents, i.e. bituminous and cementitious binders. The mixing takes place at ambient temperature. Then, bitumen as it is, cannot be used as a binder and it is replaced with bitumen emulsion or foamed bitumen. Bitumen emulsion (BE) is a dispersion of bitumen droplets in water characterised by a much lower viscosity than bitumen, which makes it suitable for being used at low temperatures (James 2006). In foamed bitumen, a temporary viscosity reduction is obtained by mixing cold water with hot bitumen to create a foam of air bubbles coated with the binder. To compensate for the lack of heating, water is frequently added to improve the diffusion of the binder and promote the mixing and compaction operations (Grilli *et al.* 2012, Kuna *et al.* 2017). Based on the type and dosage of the binding agents, cold materials can be classified in many categories (**Figure 2.3**) that give practical information about their mechanical behaviour, failure mode and thus, influence the design criteria (Grilli *et al.* 2012):

Chapter 2

Literature Review

- Cement-treated materials (CTM). A cementitious binder binds the aggregate blend in a dosage ranging between 1 and 6%. These materials are generally characterised by high stiffness and proneness to cracking.
- Bitumen-stabilised materials (BSM). The binding agent is bitumen in the form of emulsion or foam, in a dosage ranging between 1 and 3%. BSM are characterised by good flexibility. A small cement quantity, acting as “*active filler*”, can be added to increase the strength. However, the residual bitumen to cement ratio (B/C) must be greater than one to not compromise the material flexibility. The particle coating is poor and interests mostly the finest aggregate. Thus BSM show a stress-dependent mechanical behaviour similar to those of granular materials. The failure generally occurs by permanent deformation or shear stress.
- Cement-bitumen treated materials (CBTM). Both the bituminous and cementitious binders contribute to the aggregate binding and mechanical properties. The composition of CBTM mixtures can be extremely variable (Bocci *et al.* 2011, Fang, Garcia-Hernandez, Winnefeld, *et al.* 2016, Dolzycki *et al.* 2017). The residual bitumen dosage ranges between 1.5% and 3%, whereas the cement dosage goes from 1% to 4%. These materials can be considered enhanced CTM because the presence of the bitumen reduces the stiffness and confers more flexibility. On the other side, CBTM are much stiffer and cohesive concerning BSM thanks to the cementitious binder. The value of B/C is commonly around 1. CBTM have properties that are halfway between those of asphalt concrete mixtures and CTM. The bitumen confers them their typical frequency- and temperature-dependent behaviour and fatigue susceptibility (Fu and Harvey 2007, Kavussi and Modarres 2010, Bocci *et al.* 2011, Cardone *et al.* 2015, Dolzycki *et al.* 2020, Graziani, Mignini, *et al.* 2020). The cementitious binder enhances strength, stiffness and permanent deformation resistance. It may cause a prone-cracking behaviour, though (Oruc *et al.* 2007, Niazi and Jalili 2009, García *et al.* 2013, Al-Hdabi *et al.* 2014a, Graziani *et al.* 2016, Valentin *et al.* 2016).
- Cold mix asphalt (CMA). The main binding agent is bitumen, in a dosage generally ranging between 2.5% and 6%. A small quantity of cement can be added as active filler. The B/C is generally higher than 1.5. CMA has high flexibility, and its mechanical behaviour is comparable to asphalt concrete. One of the most well-known CMA is the *grave emulsion* (GE) used, especially in France in base courses or for reprofiling and overlaying old pavements. It is also used in the construction or rehabilitation of lightly trafficked roads. GE is produced with only natural aggregate, using a dense-graded distribution, high sand content, and no cement.

CTM and BSM are mostly used in subbase and base layers. CBTM and CMA can be employed for base and binder courses. **Table 2.1** compares the main advantages and disadvantages resulting from using the different stabilising agents, i.e. bituminous and

Chapter 2
Literature Review

cementitious (Xiao *et al.* 2018). Cold materials can be produced using only natural aggregate, although high amounts of RA are added with sustainable purposes in the majority of cases.

The present thesis focuses on cold materials in which the bituminous binder is the bitumen emulsion: cold bitumen emulsion (CBE) materials. Specifically, CBTM with bitumen emulsion are mainly investigated. Part of the study, focusing on slurries, examines BSM, CBTM and CMA produced with bitumen emulsion.

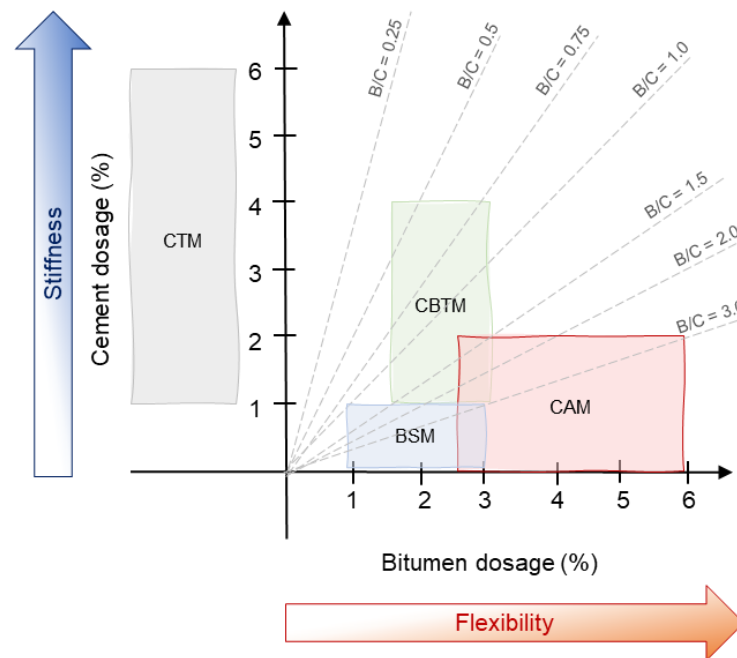


Figure 2.3. Conceptual composition of cold mixtures adapted from Grilli *et al.* 2012

Chapter 2
Literature Review

Multiscale Approach for Characterising the Behaviour of Cold Bitumen Emulsion Materials

Table 2.1. Comparison of advantages and disadvantages of bituminous and cementitious stabilising agents (Xiao *et al.* 2018)

Stabilising agent	Advantages	Disadvantages
Bituminous	1. Flexibility. It can create a viscoelastic type of material with improved shear property. 2. Ease of application and acceptance. 3. Quick strength development. Traffic can be opened soon after compaction, especially stabilized with BSM-foam.	1. Relatively empirical. 2. Rutting and instability distresses.
Cementitious	1. Availability, cost saving and ease of application. 2. Acceptance. Standard test methods and specifications are usually available. 3. Significant improvement of compressive strength and durability properties of most material.	1. Shrinkage cracking distress. 2. Requires proper curing and protection from early trafficking, particularly heavy slow-moving vehicles.

2.1.2. Constituents of CBE materials

As already mentioned, CBE materials are obtained by mixing:

- Bitumen emulsion;
- Cementitious binder, acting as co-binder (CBTM) or active filler (BSM and CAM) if needed;
- Aggregate, only natural (in the case of CM) or also RA (in the case of CRM);
- Water.

This section reports the main features of the constituents of CBE materials.

2.1.2.1. Bitumen emulsion

An emulsion is a dispersion of liquid droplets in a continuous liquid medium (Willenbacher and Georgieva 2013). Most of the time, one of the two liquids is water. Emulsions can be distinguished in (Tadros 2013) (**Figure 2.4a**):

- Oil-in-water (O/W) emulsions when water is the continuous medium, and the dispersed droplets are an “oily” liquid;
- Water-in-oil (W/O) emulsions when water droplets are dispersed in a continuous oil phase;

Chapter 2

Literature Review

- Multiple water-in-oil-in-water (W/O/W) emulsions if oil droplets contain smaller water droplets within them.

The use of bitumen emulsion started in the early 20th century. Bitumen emulsions are typical O/W or W/O/W emulsions: bitumen droplets, with a dimension between 1 and 20 μm diameter, are dispersed in water.

Bitumen emulsions are obtained by mixing hot bitumen (at 110 – 160 °C) with water containing emulsifying agents (at 30 - 70 °C) and applying mechanical energy sufficient to break up the bitumen into droplets. The production takes place in colloid mills, at about 100 – 120 °C and high-speed rotation, about 1000-6000 revolutions/min (AkzoNobel Surface Chemistry 2017).

The particle size and particle size distribution (**Figure 2.4b**) strongly affect the physical properties of the emulsions, e.g. viscosity and storage stability. In particular, larger particle size and a broad distribution cause a lower viscosity. The bitumen emulsion viscosity ranges between 0.05 and 1 Pa·s at 60 °C whereas the bitumen viscosity ranges between 10 - 400 Pa·s. Thus, the reduced viscosity makes emulsion suitable for being used at ambient temperature, as happens in cold mixing (James 2006).

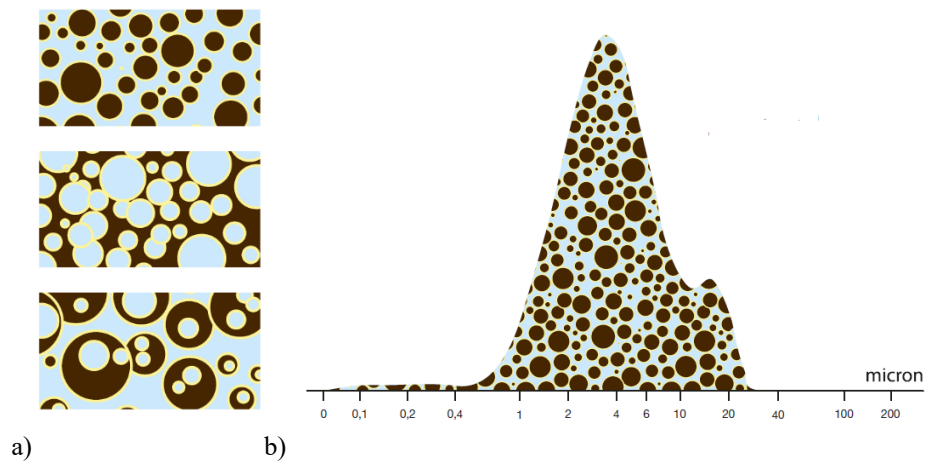


Figure 2.4. Bitumen emulsion a) types: O/W, W/O, and multiple W/O/W (from top to bottom), b) typical particle size distribution of the bituminous droplets (AkzoNobel Surface Chemistry 2017)

Bitumen emulsions generally include from 40% to 75% residual bitumen, 25% to 60% water, 0.1% to 2.5% emulsifier, plus some minor components. They appear as brownish, milky-creamy liquids (James 2006, AkzoNobel Surface Chemistry 2017).

Chapter 2

Literature Review

Emulsifiers are surface-active agents, also called surfactants. They help the emulsification process by reducing the interfacial tension between bitumen and water and prevent coalescence of the droplets once formed. The energy of water molecules at the interface between water and oil is, indeed, higher than those in the water. Therefore, it tends to reduce the interfacial area. Emulsifiers act on the charge of bitumen droplets and water causing their repulsion. A common emulsifier has a hydrophilic “*head*” group and lipophilic “*tail*”: the latter orientates in the oily bituminous phase, whereas the hydrophilic portion orientates in the water phase. Emulsifiers can be classified into anionic, cationic, ampholytic and non-ionic types based on the charge adopted in water by the head group, albeit this charge may depend on pH. Anionic emulsifiers usually have oxygen atoms in the head group and ionise in water, creating negatively charged ions, whereas cationic emulsifiers, with nitrogen atoms in the head, creating positively charged ions (**Figure 2.5**). Ampholytic emulsifiers ionize in the function of the pH of the water, having more than one functional group. Nonionic emulsifiers do not create ions in water. The first two classes are the most used till now.

Bitumen droplets have surface-active species, which can also concentrate on the interface as well. The size and sign of the charge are measured and expressed as the zeta potential of the droplet. Zeta potential depends on pH. This is because the pH depends on the charge on the emulsifier, but it is also due to the polar components of the bitumen itself. Rising the pH, the bitumen droplets charge tends to become more negative (James 2006).

Part of the emulsifiers is concentrated at the interface between water and bitumen droplets. Another part is unbound, dispersed in the water phase, and is crucial to maintaining the emulsion stable, preventing the coalescence during storage and transport.

The dosage of emulsifier, especially in unbound form, is strictly connected to the emulsion breaking speed. Indeed, emulsifier molecules are partially hydrophobic, so they are most likely to exist as colloids. When an emulsion and aggregates come into contact, charged sites will attract the unbound emulsifier. Consequently, if the emulsifier uses these sites, the emulsion will not break as quickly. On the opposite, the high content of unbound emulsifier could have a negative effect on the adhesion of bitumen with aggregate. If the emulsifier occupies the aggregate surface, the bitumen droplets coalescence will take place far from the aggregate surface indeed.

Chapter 2
Literature Review

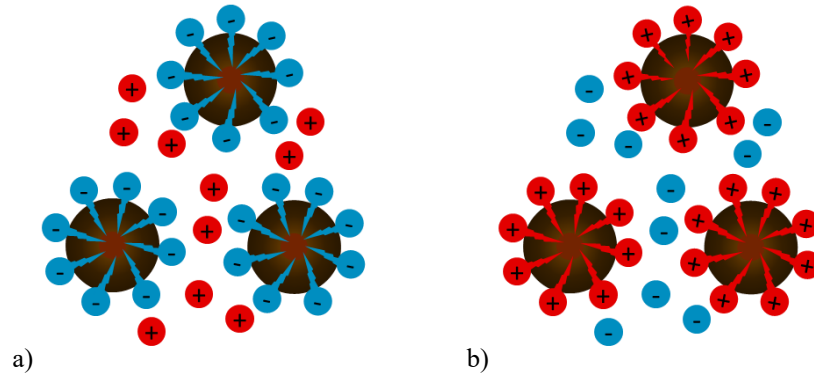


Figure 2.5. Types of emulsion charges: a) anionic emulsion , b) cationic emulsion (adapted from AkzoNobel Surface Chemistry, 2017)

Other minor components of bitumen emulsions are calcium and sodium chlorides, promoters of the adhesion, solvents and latex. Calcium chloride or sodium chloride are included in the emulsion at a small concentration, from 0.1 to 0.2 %, to reduce osmosis phenomena and minimise the viscosity changes. This is needed because bitumen contains a small amount of salt. The latter can lead to osmotic swelling of the droplets in the emulsion as water is drawn into the droplet, resulting in the viscosity of emulsion increase, often followed by a decrease due to the salt slowly escaping. Adhesion promoters (generally surface active amine compounds) can be added because anionic emulsions, and sometimes also cationic ones, may not have sufficient adhesion to aggregate, resulting in poor water resistance of the final mixture. Solvents can improve emulsification, reduce settlement, improve curing rate at low temperatures, or provide the right binder viscosity after curing. If the emulsion is used for cold recycling, solvent and flux can rejuvenate the aged RA aggregate. Their content can be up to 15% to provide the right workability characteristics and stockpile life to asphalt mixtures. Finally, polymer modification can be added to the emulsion for improving the bitumen characteristics in terms of cohesion, resistance to cracking at low temperatures, and resistance to flow at high temperatures. In this context, the emulsion modification can be made using latex, a water-based dispersion of polymer. Latex can be anionic, non-ionic or cationic, and must be compatible with the emulsion. Among the most commonly used latexes for emulsions for road paving applications there are styrene-butadiene rubber, polychloroprene, and natural rubber (James 2006).

Emulsions are not stable; water and bitumen droplets tend to separate in a process called breaking, which can take a variable period of time, from hours to years. Emulsion breaking happens in the form of coalescence, consisting of the thinning and disruption of the liquid film between the bitumen droplets and resulting in the fusion of two or more droplets into larger ones (Tadros 2013). Bitumen droplets in the emulsion are actually separate from

the other thanks to an electrostatic barrier created by small charges present on them, provided by the emulsifier and the ionisable components in the bitumen itself. When the droplets attain enough energy to overcome the barrier and approach closely, they flocculate, adhering to each other. The flocculation is not irreversible: the droplets can be returned to their original separated state by agitation, dilution, or addition of more emulsifier. With time, the water layer between the droplets gets thinner, and coalescence occurs. Coalescence is not reversible anymore (**Figure 2.6**). Many factors can accelerate the flocculation and coalescence: settlement under gravity, evaporation of the water, shear or freezing. Also, the pH value of the aqueous medium plays a key role (James 2006).

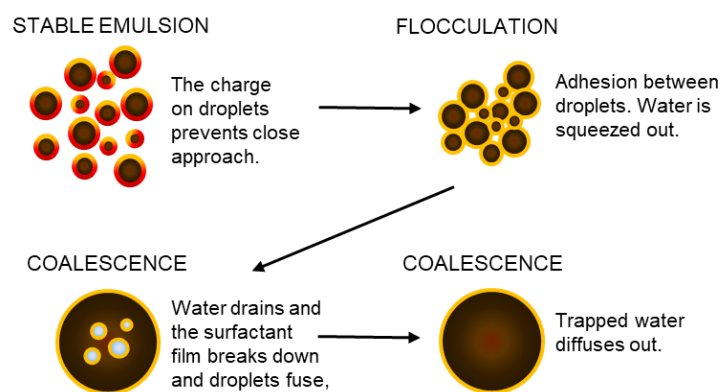


Figure 2.6. Bitumen emulsion breaking stages (adapted from James, 2006)

Analysing the emulsion stability phenomenon from a physicochemical perspective, it can be stated that it is mainly due to repulsive electrostatic forces between the bitumen droplets. These forces can be described through the Derjaguin-Landau-Verwey-Overbeek (DLVO) theory (Israelachvili 2011). The interactions between droplets are due to the sum of the electrostatic repulsion and the Van der Waals attraction. Thus, when the repulsion forces are higher than the attraction forces, the emulsion is stable, and coalescence does not occur. On the contrary, when the attraction forces prevail, droplets tend to contact, and coalescence occurs. Hence, according to Lesueur and Potti (2004), the breaking is a consequence of the concentration of bitumen droplets, i.e. film-forming and the disappearance of the electrostatic repulsion forces, i.e. gel contraction. The first one is a result of water evaporation. The resulting increase in the bitumen droplets concentration induces a growing pressure that overcomes the repulsive forces leading to the coalescence. The higher is the water evaporation rate, the faster is the film-forming process. The gel contraction happens when emulsion and other reactive species, e.g. aggregate, cementitious binders or other mineral additions, are brought into contact. In this case, changing the charges within the emulsion system occurs, which inducing the coalescence (**Figure 2.7**).

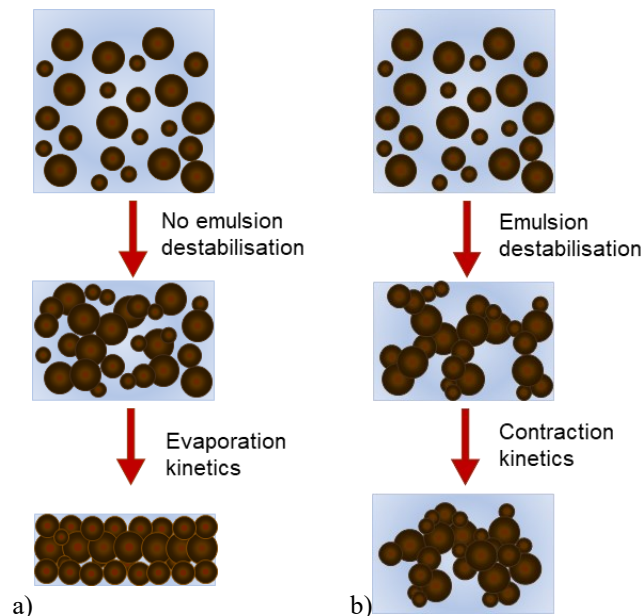


Figure 2.7. Potential emulsion breaking scenarios: a) film forming, b) gel contraction (adapted from Lesueur and Potti 2004)

Further details about emulsion interaction with the other CBE materials constituent and its effects on the emulsion breaking kinetic will be discussed later.

The time needed for flocculation (setting) and coalescence (curing) occurring is linked to the emulsion individual system. However, it can be stated that, in general, flocculation, during which some water is squeezed from the system and some cohesive strength develops, is quicker. The formation of a continuous bitumen phase throughout the coalescence takes longer. Indeed, during coalescence, an inversion process happens, converting O/W into W/O emulsion, which then slowly loses its internal water phase. When the bitumen to water ratio is higher, the inversion is favoured (James 2006).

Bitumen emulsions are distinguished based on the charge of the bitumen droplets:

- Cationic emulsions droplets have a positive charge;
- Anionic emulsions droplets are negatively charged;

and emulsion reactivity, i.e. breaking speed:

- Rapid-setting (RS) emulsions set quickly in contact with clean aggregates of low-surface area, such as the chippings used in chip seals (surface dressings). Because of their high reactivity. RS emulsions should be used with unreactive aggregates;

Chapter 2

Literature Review

- Medium-setting (MS) emulsions set sufficiently less quickly, and they can be mixed with aggregates of low surface area, such as those used in open-graded mixes;
- Slow-setting (SS) emulsions can be mixed with reactive aggregates of high surface area. Being unreactive, SS emulsion can be mixed with reactive aggregates. Some national standards identify an additional category within SS, called over-stabilised or super-stable, whose setting is prolonged.

Bitumen emulsion characteristics come from the different aspects of the emulsion formulation: emulsifier type and concentration, choice and concentration of acids or bases used to adjust pH, and the grade and source of the bitumen used (AkzoNobel Surface Chemistry 2017). Besides, the real setting and curing time in the field will be connected to the techniques applied, the materials adopted, and environmental conditions (James 2006).

Within the European standards framework for specifications, only cationic bitumen emulsions are considered and hence, are most commonly used in paving applications. The European Standard EN 13808 specifies the requirements in terms of performance characteristics of cationic bitumen emulsions. According to EN 13808, emulsions are classified using an alphanumeric code:

- Bitumen charge, cationic (character “C”);
- Residual bitumen content (two-digit numbers);
- Type of binder (characters “B” or “BP” for plain or polymers modified bitumen);
- Possible addition of flux (if > 3% of the emulsion, indicated by the character “F”);
- Class of breaking or setting rate (number from “2” to “12”, from RS to over-stabilised emulsions).

For example, C60BP10 is used for a cationic emulsion, with 60% residual polymer modified bitumen with slow setting breaking behaviour. **Table 2.2** summarises the bitumen emulsion classification according to EN13808 and ASTM-D977 or D2397/D2397M. **Table 2.3** and **Table 2.4** report the typical emulsifiers (types and levels) and the typical bitumen emulsion applications for paving (AkzoNobel Surface Chemistry 2017).

Chapter 2
Literature Review

Multiscale Approach for Characterising the Behaviour of Cold Bitumen Emulsion Materials

Table 2.2. Bitumen emulsions classification according to EN 13808, ASTM-D977 ASTM and D2397/D2397M

Droplets charge	Breaking characteristics	Reference standard	
		EN 13808 ^a	ASTM-D977 & ASTM D2397/D2397M
Cationic	Rapid setting	C##XY1	CRS
		C##XY2	
		C##XY3	
	Medium setting	C##XY4	CMS
		C##XY5	
		C##XY6	
	Slow setting	C##XY7	CSS
		C##XY8	
		C##XY9	
	Very slow setting	C##XY10	
		C##XY11	
		C##XY12	
Anionic	Rapid setting		ARS
	Medium setting	n.a.	AMS
	Slow setting		ASS

a) ## = numbers, from 35 to 72, XY = bitumen type, n.a. = not available

Table 2.3. Typical emulsion pH and emulsifiers types and levels (AkzoNobel Surface Chemistry 2017)

Emulsion type	Emulsion pH	Typical emulsifier	Emulsifier level (%)
CRS	2 - 3	tallow diamine	0.15 - 0.25
CMS	2 - 3	tallow diamine	0.3 - 0.6
CSS	2 - 5	quaternary amine	0.8 - 2.0
ARS	10.5 - 12	tall acid	0.2 - 0.4
AMS	10.5 - 12	tall acid	0.4 - 0.8
ASS	7.5 - 12	nonionic + lignosulphonate	1.2 - 2.5

Chapter 2
Literature Review

Multiscale Approach for Characterising the Behaviour of Cold Bitumen Emulsion Materials

Table 2.4. Applications of bitumen emulsions (adapted from AkzoNobel Surface Chemistry, 2017)

	Anionic			Cationic			
	RS	MS	SS	RS	MS	SS	Super stable
Spray Applications							
Surface Dressing (Chip Seals)	x			x			
Fog Seal		x	x		x	x	x
Tack Coat		x ^a	x	x	x ^a	x	
Prime Coat			x	x		x	x
Penetration Macadam				x			
Slurry Surfacing							
Slurry Seal			x			x ^b	x
Cape Seal			x			x ^b	x
Microsurfacing						x ^b	
Plant Mixes							
Open graded/Semi Dense		x ^a			x		
Dense Graded			x			x	x
RAP		x				x	x
Stockpile mix		x ^a			x ^a		x
Pre-coated chips					x	x	
Mix Paving							
Open Graded					x ^a		
In place Mixes							
RAP		x ^a			x ^a	x	x
Soil Stabilization			x				x
Dense Graded			x			x	x

a) may content solvent, b) need to pass cement test

Chapter 2

Literature Review

2.1.2.2. Cementitious binder

In CM and CRM, not only the bituminous binders can be employed. Often, supplementary cementitious binders, such as cement, can be employed as stabilising agents. Also, cementitious binders are generally used to accelerate the emulsion breaking (Wang *et al.* 2013) and achieve suitable structural and durability properties of the mixtures (Schwartz *et al.* 2017).

Cement is a hydraulic binder widely used in the construction of concrete buildings and infrastructures. Thanks to the contact with water, cement changes its properties during setting and hardening processes and finally adheres to other materials forming a binding matrix.

The most common cementitious binder type adopted in cold mixing is Ordinary Portland cement (OPC). OPC is composed of at least two-thirds by mass of calcium silicates (C_3S and C_2S). The remaining part consists of aluminium and iron, containing clinker phases and other compounds. According to the European Standard EN 197-1, which defines the composition, specifications and conformity criteria for common cements, five types of Portland cements exist (from type I to type V). They differ by the production process, particularly in terms of the percentage of clinker and other constituents (i.e. blast-furnace slag, silica fume, pozzolana, fly ash, burnt shale, limestone). The most widely used cement in Italy is Portland limestone cement type II/A-LL, strength class 32.5R or 42.5R.

When OPC reacts with water, the calcium silicates, C_3S and C_2S , hydrate to form new solid materials, the calcium hydroxide and calcium-silicate hydrate (C-S-H) gel. Hydrated OPC contains between 15 and 20% of calcium hydroxide and about 50% of C-S-H by mass. The strength of the paste made of cement and water is mainly conferred by the latter. The pH of the pore solution is high, ranging from 12.6 to 14 (Alonso *et al.* 2010).

Powers' theory can be used for describing the OPC hardening process (Powers 1958). According to Powers' theory, the hardened OPC paste consists of cement gel, capillary pores and unreacted cement. The cement gel, basically constituting the cement hydration products, consists of solid hydrated cement and water-filled gel pores, i.e. absorbed water, bound with cement. Whereas the capillary water is "*gravimetric water*". The total porosity comprises both capillary pores and gel pores. Differences in capillary porosity can lead to structural differences among pastes. On the other hand, the different OPC chemical compositions can influence the physical characteristics of hardened cement gel in some small way (Lura *et al.* 2017). The hydrated cement consists of reacted cement and the non-evaporable water, sometimes called "*chemically combined water*". The non-evaporable water is the water that is bound chemically with the cement. Also, the physically bound water is adsorbed at the surfaces of gel particles and occupies the gel pores. Free unbound water occupies the larger capillary pores. Both physically bound water and free water constitute the evaporable water (Brouwers 2004, Lura *et al.* 2017). Nonevaporable water can be driven off only at temperatures higher than 105 °C. According to Powers' measurement, chemically

Chapter 2

Literature Review

bound water is about 0.23 g per gram of cement reacted during hydration, whereas the physically bound water is about 0.19 g per gram of cement reacted. The volume of the reaction products developed during the hydration is lower than the volume of cement and water reacted. This volume reduction, called chemical shrinkage, is about 6.4 ml/100 g cement reacted (Jensen and Hansen 2001). The volumetric composition of the cement paste depends on the degree of the hydration reaction α . Its value ranges from 0 for the unhydrated cement, to 1 if the cement is fully hydrated. As only the capillary water is freely accessible for cement hydration, the complete cement hydration is possible only if the water to cement (W/C) ratio is above 0.42 ($= 0.23 + 0.19$). If the W/C ratio is lower, part of the cement will not hydrate ($\alpha < 1$). On the contrary, if $W/C > 0.42$, cement fully hydrates ($\alpha = 1$) and some capillary water will still be available (Powers 1958, Jensen and Hansen 2001).

Not only OPC is used for producing CM and CRM. For example, non-Portland cementitious binders, like calcium aluminate (CAC) and calcium sulfoaluminate (CSA) binders, can be used. They are characterised by rapid setting and hardening processes and therefore allow to accelerate the strength development, improving the mechanical properties of cold mixtures in the early stage of curing (Thanaya *et al.* 2009, Fang, Garcia, *et al.* 2016, Saadon *et al.* 2018). Fang, Garcia, *et al.* (2016) observed that CAC and CSA confer to mixtures mechanical properties after one day comparable to those reached after about one week when OPC is used. The use of other supplementary blended cementitious fillers results in the increased early strength due to an enhanced hydration reaction. Moreover, these kinds of filler can improve cold mixtures mechanical response and water sensitivity (Al-Hdabi *et al.* 2014b, Nassar *et al.* 2016, Dulaimi *et al.* 2017).

Within the present investigation, along with OPC binders, CSA is employed. In CSA, the main phase of the clinker is yeelimite ($C_4A_3\bar{S}$). When CSA cement hydrates, ettringite ($C_6A_3\bar{S}_3H_{32}$) is formed. The resulting pore solution pH values are highly variable but generally lower than those of ordinary OPC, ranging from 8.5 to 13 (Alonso *et al.* 2010). CSA production requires less energy and reduces CO₂ emissions (Phair 2006, Juenger *et al.* 2011, Habert 2013), leading to sustainability benefits compared to OPC. Moreover, it binds a higher amount of water than ordinary Portland-based cement: 1 g of CSA binds approximately 0.75 g of water (Lura *et al.* 2017).

Other cementitious stabilising agents commonly used in cold mixing are fly ash, ground blast furnace slag and other such pozzolanic materials, and other types of blends obtained mixing them.

2.1.2.3. Aggregate

In general, no specific requirements are provided about aggregate for cold materials production. Usually, each aggregate suitable for HMA is considered appropriate for cold materials (Fang, Garcia-Hernandez, and Lura 2016). However, the aggregate must be

Chapter 2

Literature Review

compatible with the type of emulsion adopted. For example, limestone aggregates are widely used for cold recycling applications in Europe because of their good affinity with cationic emulsions, which are the most common emulsion for paving applications (Section 2.1.2.1).

Even though there are some cold materials applications in which only natural aggregate is used (Needham 1996, Khalid and Monney 2009, Serfass *et al.* 2012, Al-Hdabi *et al.* 2014b, Fang, Garcia, *et al.* 2016, Saadoon *et al.* 2018), most of the time the primary aggregate is RA, in the perspective of applying CR techniques to maximise environmental benefits. The amount of RA available for being re-used or, in the alternative, to be disposed of is constantly increasing. Indeed, the construction of new infrastructures is becoming rare. At the same time, the major part of the existing roads is produced with asphalt layers. The road network constantly needs maintenance and update operations, often consisting of removing the damaged pavement layers and paving new ones. RA obtained from the milling of old pavement layers is usually stockpiled in production plants waiting to be re-used to produce hot, warm or cold recycled mixtures (**Figure 2.8**). In these conditions, the aggregate is completely exposed to environmental factors, e.g. air, solar radiation etc., that can modify its characteristics, such as ageing or oxidation. Also, the material is greatly heterogeneous because of the wide variety of sources. As a consequence, characterising RA is an important step for producing quality bituminous mixtures.

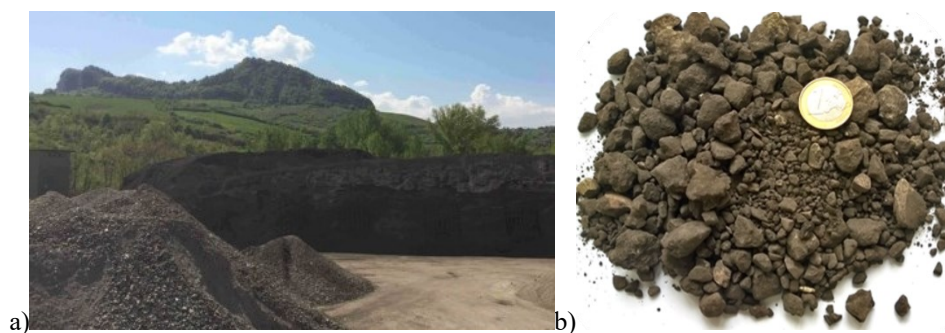


Figure 2.8. a) RA stockpiled in a production plant, b) RA aggregate

The European Standard EN 13043 indicates the requirements for aggregate and filler obtained by processing natural, manufactured or recycled materials, and mixtures of these aggregates, to adopt them in bituminous mixtures and surface treatments for roads, airfields and other trafficked areas. However, EN 13043 does not cover the use of reclaimed bituminous mixtures despite the increasing spreading of recycling techniques, which demands the identification of RA as a valuable construction material. The European Standard EN 13242 considers the use of RA as aggregate for unbound and hydraulically bound layers (road embankment, subgrade and foundation). European Standards from EN 13108-1 to EN 13108-7 and EN13808-9 allow the addition of RA in asphalt products (asphalt concrete,

Chapter 2

Literature Review

asphalt concrete for very thin layers, soft asphalt, hot rolled asphalt, stone mastic asphalt, mastic asphalt, porous asphalt, ultra-thin layers) with requirements related to the percentage addition. The qualification of RA aggregate is currently carried out according to EN 13108-8, which focuses on the reuse of RA in HMA.

It must be pointed out that, during hot and warm recycling, the aged bitumen contained in the RA aggregates is re-heated and made “*active*” again, often using specific additive (Stimilli *et al.* 2015, Lo Presti *et al.* 2020). A new binder, consisting of the re-activated aged bitumen and added bitumen, coats the aggregates, gives cohesion to the mixture and affects its mechanical properties. The role that RA aggregate plays on CRM is more questionable due to a lack of knowledge. This inadequate knowledge is also present in the European Standard for Asphalt Concrete with Bituminous Emulsion currently under development (prEN 13108-31). The Standard states, indeed, that the “binder in the reclaimed asphalt can be considered as active, partially active or inactive in the contribution to the properties of the mixture”. In CR, RA aggregate can be assumed to act as a “*black rock*”. Indeed, the ambient production temperature does not allow the aged binder reactivation during mixing and compaction. Consequently, the aged bitumen does not blend with the fresh bitumen and does not contribute to the lubrication of the solids. It is worth noting that the black rock concept is valid only from the physical point of view: the aged bitumen is still present in the material. Hence, it may contribute to the mechanical response of CRM because of its temperature dependency, even if it is not blended with the new binder. Besides, the aged binder in RA surely affects particles dimension, shape, resistance to fragmentation, water absorption and many other physical, mechanical and chemical properties. More importantly, aged binder affects the surface charge of the particles and, thus, the compatibility with the emulsion.

To facilitate the use of the RA, it would be beneficial, therefore, to measure and declare its properties using the same approach currently adopted for natural or other recycled aggregates, formally considering RA as black rock. In this context, the European research project CRABforOERE (Cold Recycled Asphalt Bases for Optimised Energy & Resource Efficient Pavements) funded by the Conference of European Directors of Roads, has, among its objectives, the definition of a simple and practical testing protocol to assess the effect of the RA aggregate on CR materials properties (CRABforOERE 2018). Also, within RILEM (International Union of Laboratories and Experts in Construction Materials, Systems and Structures) technical committee 237-SIB (about testing and characterisation of sustainable innovative bituminous materials and systems) a procedure for characterising the fragmentation resistance and for classifying RA throughout a cohesion test was proposed (Perraton *et al.* 2016, Preti *et al.* 2019).

As regards the aggregate blend grading distribution, continuously dense-graded curves are adopted generally adopted in CM and CRM production (Bocci *et al.* 2011, García *et al.* 2013, Graziani *et al.* 2016, Valentin *et al.* 2016, Dolzycki *et al.* 2017, Nassar *et al.* 2018, Raschia *et al.* 2020). Nevertheless, recent studies attempted to evaluate the effect the

Chapter 2

Literature Review

effect of different grading curves on the mechanical properties of cold mixtures (Xu *et al.* 2017, Raschia, Mignini, *et al.* 2019). An open gradation has been used in porous asphalt production (Al-Hdabi *et al.* 2014a).

2.1.2.4. Water

The total water content of CBE materials includes emulsion water and additional water. The latter is frequently added to compensate for the lack of heating, improve the diffusion of the binder, and promote the mixing and laying operations (Graziani *et al.* 2016, Grilli *et al.* 2016). The water plays a lubricant role in coating the aggregates and compaction (Fang, Garcia-Hernandez, and Lura 2016, Kuchiishi *et al.* 2019). A fraction of the additional water is absorbed by the aggregate, whereas the remaining fraction, along with the emulsion water, is intergranular, free water.

2.1.2.5. Bitumen emulsion-aggregate interaction

As mentioned in Section 2.1.2.1, bitumen emulsion stability can be affected by the others CBE materials constituents, such as aggregate and co-binders.

The reactivity of the aggregate influences emulsion breaking. The rise in pH test was introduced for measuring the chemical reactivity of aggregates in bitumen emulsion (Ziyani *et al.* 2014). However, it was found that the emulsion breaking is not only linked to the rise in pH but also the particles surface area: the higher is the surface area, the easier the breaking. Also, aggregate mineralogy should be considered. Aggregate is characterised by a surface charge that can interact with the emulsion ones. For example, carbonates and fillers, including cement which is highly basic, may neutralise the acid in cationic emulsions, leading to an increase in pH, which causes emulsion destabilisation. Anionic emulsions may be destabilised by soluble multivalent ions instead (James 2006). The cationic emulsion has a better adsorbing ability on the mineral aggregate surface than anionic asphalt emulsion because most aggregates are characterised by a negative surface charge (Ouyang, Li, *et al.* 2017).

The selection of the emulsion type to employ should take into account the emulsion/aggregate interaction. Thus, rapid setting emulsions can be used with low reactive aggregate, i.e. with low surface area. In contrast, SS emulsions should be adopted in the presence of reactive aggregate, having a high surface area.

Evaluating the interaction with emulsion is more complex when stockpiled RA is used since its undefined nature. However, the mechanical properties of CBE mixtures can significantly be affected by the aggregate-emulsion combinations and should be considered in the mixing design phase.

Chapter 2

Literature Review

2.1.2.6. Bitumen emulsion-cementitious binders interaction

Cementitious binders were initially added to cold materials for favouring the emulsion breaking. Indeed, cement hydration greatly affects the stability of the bitumen emulsion (García *et al.* 2013, Tan *et al.* 2014, Ouyang *et al.* 2016). Firstly, cement binds to water for its hydration, reducing the water content and favouring the water forming (Needham 2000, Montepara and Giuliani 2001, Wang *et al.* 2013). Also, the addition of cement, which is characterised by alkaline pH, increases the pH of cationic emulsion, promoting its setting (Wang *et al.* 2013, Ouyang, Li, *et al.* 2017). On the other side, during cement hydration, a number of counter ions, including Ca^{2+} , influence the electric charge layer of anionic emulsions (Wang *et al.* 2013). Rapid-hardening cementitious binders, such as the CSA cement, can accelerate the emulsion setting, reducing the working time of cold materials (Wang *et al.* 2008).

Likewise, the emulsion affects the hydration process of cementitious binders, generally delaying its rate and the formation of well-structured cementitious bonds (Du 2014, Saadon *et al.* 2018). This effect depends on many factors, including the cement concentration, types of emulsion and emulsifiers and W/C ratio (Pouliot *et al.* 2003, Zhang *et al.* 2012, Tan *et al.* 2013, 2014). The cement hydration could be prematurely arrested if the emulsifier dosage is too low and the water evaporation too fast, with a consequent reduction of W/C ratio below the value needed for the full hydration (see Section 2.1.2.2) (Miljković *et al.* 2017). Fang, Garcia, *et al.* (2016) observed that the rate of hydration of the cement is initially accelerated or retarded also in function of cement type and dosage. In contrast, no significant effects were observed on the later hydration development.

2.1.3. The evolutive behaviour of CBE materials

CBE materials show an evolutive behaviour: with time, bitumen emulsion breaks, cement hydrates, and water evaporates. The set of these processes, known as curing, can take months or years before being totally completed (Du 2018, Godenzoni *et al.* 2018). During curing, the physical structure of CBE materials changes (**Figure 2.9**): cement increases its volume, as the hydration products occupy a greater volume than the unhydrated cement (Section 2.1.2.2). Water mostly evaporates and, as a consequence, the volume of the air voids increases. Some negligible amount of water can be remain trapped in not interconnected voids, though. In parallel, the material mechanical properties improve (Pouliot *et al.* 2003, Miljković and Radenberg 2014, Graziani *et al.* 2018). Therefore, the performance of CBE materials must be evaluated, taking into account their curing behaviour (Kim *et al.* 2011, Doyle *et al.* 2013, Cardone *et al.* 2015, Graziani *et al.* 2016).

The aggregate blend nature influences curing (Ziyani *et al.* 2014), as well as the dosage of binders and their interaction. Cement hydration affects the pH and reduces water content, promoting emulsion setting (García *et al.* 2013, Wang *et al.* 2013). Likewise, emulsion affects the hydration rate and the formation of well-structured cementitious bonds

Chapter 2

Literature Review

(Pouliot *et al.* 2003, Du 2014, Saadoon *et al.* 2018). Environmental conditions affect the curing process. High temperature and low relative humidity (RH) promote water evaporation and increase the curing rate (Lura *et al.* 2001, Du 2018). High temperatures also increase cement hydration rate but may hinder the long-term strength of the cementitious matrix. Besides, a moist environment (García *et al.* 2013) enhances cement hydration and hinders emulsion breaking. Controlling the curing rate of CBE materials during time is crucial. Indeed, during pavement construction activities, the proper evaluation of the curing level is needed because it governs the timing for laying upper layers and opening the road to the traffic. Also, the right evaluation of the material long-term properties is required to properly design the pavement structure and predict its performance properly.

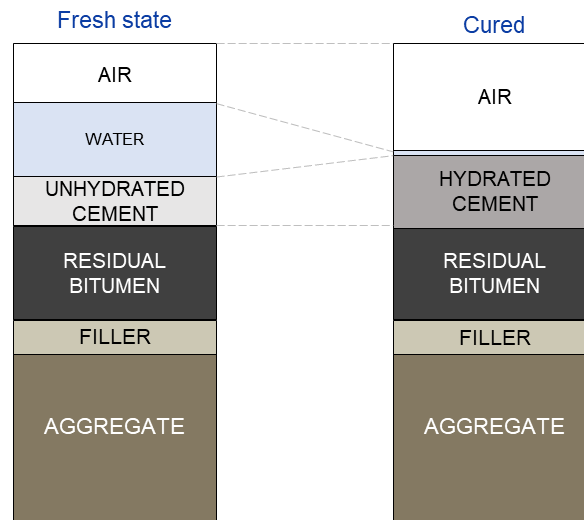


Figure 2.9. CBE material volume change during curing

2.1.3.1. Modelling curing behaviour of cold mixtures

Modelling the curing of CBE materials can be useful for predicting the evolution of their physical and mechanical properties. At first, the use of the non-linear asymptotic Michaelis-Menten model was proposed (Michaelis *et al.* 1913, Graziani *et al.* 2016, 2017). The model was originally developed in biochemistry and biology to describe the velocity of formation of a product in a chemical reaction as a function of the substrate concentration. The MM model was adapted for characterising the evolutive behaviour of CBE materials using the equation:

Chapter 2
Literature Review

$$y(t) = \frac{y_a \cdot t}{h_y + t} \quad (2.1)$$

where $y(t)$ is the property under investigation, y_a is the asymptotic value (long-term property). The parameter h_y represents the time needed to reach the value $(y_a - y_i)/2$ by $y(t)$.

However, some issue was observed about the predicting ability of the model due to the time interval in which it is applied. In particular, because the first measurement of the material properties comes after a certain period of time (hours or days), the model showed some inaccuracy in predicting the early curing. For this reason, a modified version of the MM model was proposed (Mignini *et al.* 2018, 2019, Raschia, Graziani, *et al.* 2019, Ferrotti, Grilli, *et al.* 2020) :

$$y(t) = y_i + (y_a - y_i) \frac{t - t_i}{(h_y - t_i) + (t - t_i)} \quad (2.2)$$

where y_i is its value at the time t_i . The time t_i represents the early-stage of curing (first measurement time) (**Figure 2.10**).

Other models are proposed in the literature, for example, the maturity method. It considers the temperature history of the material during curing for estimating the hydration degree, which is connected to the strength development (Galobardes *et al.* 2015).

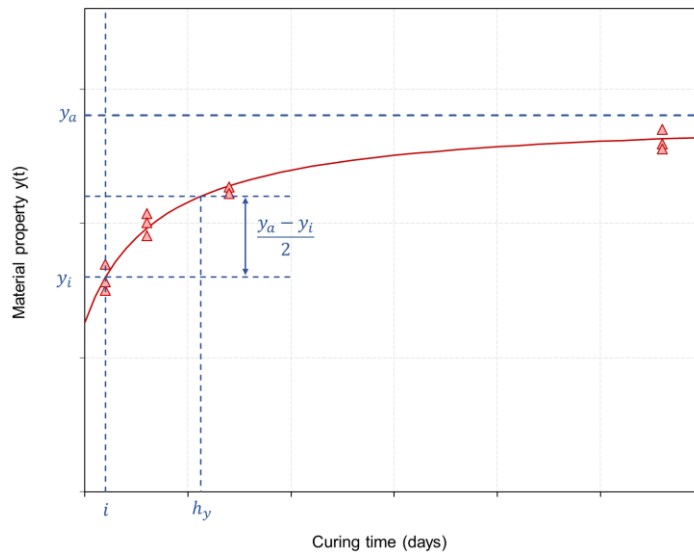


Figure 2.10. Modified Michaelis Menten model representation (Equation (2.2))

2.1.4. Viscoelastic properties of CBE materials

Because of the presence of bitumen, CBE materials, analogously to all the bituminous materials, are characterised by a behaviour that depends on the temperature, frequency and amplitude of the applied load. According to the amplitude of the applied strain and the number of loading cycles, four main types of behaviour should be considered when modelling the response of bituminous materials response (Di Benedetto *et al.* 2001, 2007, Olard *et al.* 2005):

- Stiffness and stiffness evolution with time in the linear domain;
- Fatigue and damage evolution;
- Accumulation of permanent deformation
- Crack and crack propagation, in particular at low temperature.

Figure 2.11 reports the four domains of the behaviour of bituminous materials. At very small strain amplitudes and small number of load cycles, the material has a linear viscoelastic (LVE) behaviour. The three other domains cause the major pavement distresses: when the strain amplitude is small, but the number of cycles is high, fatigue damage happens. At higher strain amplitude, rutting or crack propagation occur.

In the LVE domain, the material has a behaviour halfway between those of an elastic and viscous material. Two limits can be identified: at high frequencies, or very low temperatures, the bituminous material can be considered perfectly elastic, whereas, at very low frequencies or high temperatures, it is considered perfectly viscous.

Complex modulus $E^*(\omega)$ measurement is used for characterising the LVE behaviour of bituminous materials. $E^*(\omega)$ allows, indeed, evaluating the elastic modulus, E of the material, also considering its frequency dependency. The complex modulus $E^*(\omega)$ can be measured by applying a sinusoidal stress σ which causes a sinusoidal response of the strain ε :

$$\sigma = \sigma_0 \sin \omega t = \sigma_0 \exp[j(\omega t)] \quad (2.3)$$

$$\varepsilon = \varepsilon_0 \sin(\omega t - \varphi(\omega)) = \varepsilon_0 \exp[j(\omega t - \varphi(\omega))] \quad (2.4)$$

where j is the imaginary unit, $\omega = 2\pi f$ is the angular frequency (f is the testing frequency in Hz), σ_0 and ε_0 are the steady-state amplitudes of the measured stress and strain signals, respectively. The strain is delayed with respect to the stress by the phase angle, $\varphi(\omega)$ (**Figure 2.12a**). $\varphi(\omega)$ ranges between 0° , value that defines a perfectly elastic material and 90° in the case of perfectly viscous material.

Chapter 2
Literature Review

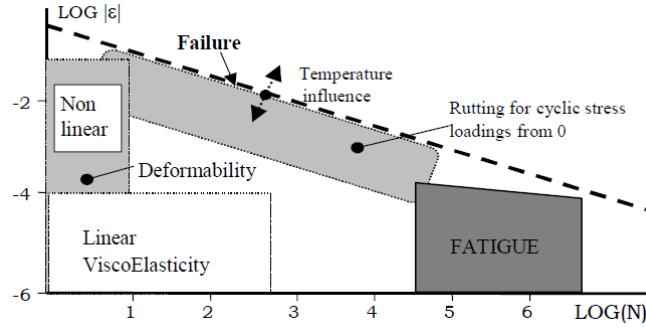


Figure 2.11. Domains of behaviour for bituminous mixtures, (strain amplitude as a function of the number of cycles) (Olard *et al.* 2005)

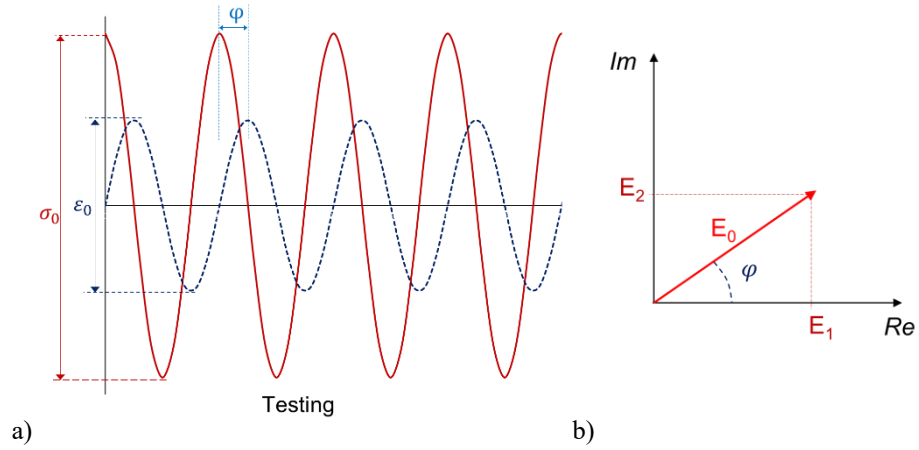


Figure 2.12. Complex modulus test: a) stress and strain trends, b) complex plan representation

E^* is obtained as ratio between σ and ε :

$$E^*(\omega) = \frac{\sigma_0}{\varepsilon_0} \exp[j\varphi(\omega)] = E_0(\omega) \exp[j\varphi(\omega)] = E_1 + jE_2 \quad (2.5)$$

where E_1 and E_2 are respectively, the real and imaginary part of E^* , and are called storage and loss moduli (**Figure 2.12b**). In particular:

$$E_0(\omega) = \sqrt{E_1^2 + E_2^2} \quad (2.6)$$

where $E_0(\omega) = |E^*|$ is the norm of the complex modulus, the stiffness modulus.

Chapter 2

Literature Review

The stiffness modulus $E_0(\omega)$ and phase angle $\varphi(\omega)$ are dependent on the temperature and load frequency. In general, when sinusoidal stress is applied, $E_0(\omega)$ decreases, increasing the temperature and decreasing frequency while the phase angle increases.

The complete characterisation of the rheological behaviour of bituminous materials would require a broad range of frequencies to be tested, from very low to very high. Such need collides with some technical and laboratory constraint, like equipment or time limits. However, if the material is thermo-rheologically simple, the effects of temperature and loading rate are interconnected based on the validity of the time-temperature superposition principle (TTSP). Therefore, they can be considered into a unique and simpler function. The principle is considered valid if the experimental data draws unique curves in the Cole-Cole plan, i.e. loss modulus as a function of storage modulus and in the Black diagram, i.e. stiffness modulus depicted as a function of the phase angle. As bituminous materials are generally thermo-rheologically simple, their LVE behaviour can be characterised by testing a limited range of frequencies at various testing temperatures. Master curves of $E_0(\omega)$ or $\varphi(\omega)$, describing the LVE response at a reference temperature T_{ref} as a function of the frequency, can thus be constructed applying the TTSP. The data measured at each temperature T are horizontally shifted and aligned to those obtained at T_{ref} :

$$f_r = f \cdot a_{T_{ref}}(T) \quad (2.7)$$

where f is the testing frequency, f_r is the shifted frequency, usually called reduced frequency and $a_{T_{ref}}(T)$ is the shift factor needed to superpose the data measured at T and T_{ref} (**Figure 2.13a**). Shift factors $a_{T_{ref}}$ are commonly manually determined shifting the response function segments along the logarithmic time-scale. The determination of $a_{T_{ref}}$ thereby becomes merely subjective and greatly dependant on the experience of the operator. An alternative mathematical procedure was proposed to remove ambiguity related to the shifting procedure: the closed-form shifting (CFS) algorithm. The CFS consists of minimising the overlapping between two successive isothermal curves (Gergesova *et al.* 2011) (**Figure 2.13b**).

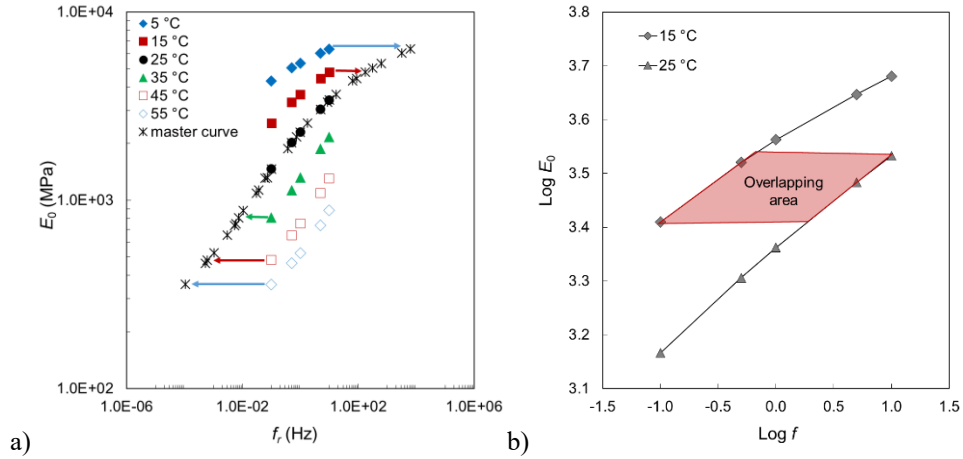


Figure 2.13. Construction of the stiffness modulus master curve: a) horizontal shifting ($T_{ref} = 25 \text{ }^\circ\text{C}$), b) CFS algorithm application

2.1.4.1. Measuring the complex modulus of cold mixtures

Recent studies used experimental protocols and mathematical models, originally developed for HMA, for characterizing the LVE behaviour of CM and CRM (Schwartz and Khosravifar 2013, Stimilli *et al.* 2013, Cardone *et al.* 2015, Schwartz *et al.* 2017, Dolzycki *et al.* 2017, Gandi *et al.* 2017a, Lin *et al.* 2017, Buczyński and Iwański 2018, Godenzoni *et al.* 2018, Kuchiishi *et al.* 2019, Ferrotti, Grilli, *et al.* 2020, Graziani, Mignini, *et al.* 2020, Graziani, Raschia, *et al.* 2020). **Table 2.5** provides an overview of the results of a literature review of the past nine years, focused on laboratory measurements of complex modulus E^* and the dynamic modulus E_0 , performed with cyclic axial tests on cylindrical specimens. The review considers CRM produced in the laboratory or cored from the field, containing RA aggregate quantities between 30 and 100%. Not only bitumen emulsion but also foamed bitumen were considered as the main binder. The emulsion and foamed bitumen dosages ranged between 2 and 6% and 2 to 3%, respectively. Cement was often used, either as a secondary stabilising agent/active filler or as a co-binder. The curing periods considered were extremely variable, ranging from few days to several years. The range of temperature investigated is numerous as well. The frequency and temperatures adopted are those normally used for testing HMA. Usually, AASHTO Standards were considered (AASHTO TP 62, AASHTO TP 79, AASHTO T 342). Many times, the strain level was not specified by the Authors. In these cases, the target strain level was likely about $100 \cdot 10^{-6}$ m/m. Other Authors specified the strain level, considering that the linearity limit of CRM could be lower than those of HMA.

Chapter 2

Literature Review

Cold materials were characterised by an LVE behaviour similar to those of HMA. Stiffness modulus decreased, and phase angle increased when temperature increased (and frequency decreases). Generally, cold materials were thermo-rheologically simple, and TTSP was applied (Cardone *et al.* 2015, Godenzoni, Graziani, *et al.* 2017, Lin *et al.* 2017, Raschia, Perraton, *et al.* 2021). Generally, due to the presence of the cementitious binder, CRM were characterised by a reduced thermo-sensitivity compared to HMA and exhibited a reduced viscous response (Stimilli *et al.* 2013, Cardone *et al.* 2015, Lin *et al.* 2017, Graziani, Mignini, *et al.* 2020). This translated into a lower reduction of the stiffness modulus at high temperatures (low frequencies). Also, the higher void content generally led to a reduction in the stiffness modulus. CRM had lower phase angle values at all temperatures and frequencies than HMA, probably due to the presence of the cementitious bonds (Stimilli *et al.* 2013, Ferrotti, Grilli, *et al.* 2020, Graziani, Mignini, *et al.* 2020). Curing time generally led to an increase of stiffness modulus and a reduction of phase angle (Stimilli *et al.* 2013, Graziani, Raschia, *et al.* 2020). Foamed bitumen caused slightly stiffer mixtures at higher temperatures, whereas emulsion may have resulted in slightly stiffer mixtures at lower temperatures (Schwartz and Khosravifar 2013, Kuchiishi *et al.* 2019).

The rheological response of cold materials strongly depends on their composition in terms of dosage of bituminous and cementitious binders, rheological behaviour of the bituminous binder and its ageing. Also, void content, RA content and type, as well as curing had significant effects (Dolzycki *et al.* 2017, Godenzoni, Graziani, *et al.* 2017, Godenzoni *et al.* 2018, Graziani, Mignini, *et al.* 2020, Graziani, Raschia, *et al.* 2020, Raschia, Moghaddam, *et al.* 2021, Raschia, Perraton, *et al.* 2021).

2.1.4.2. Modelling the viscoelastic behaviour of cold mixtures

The behaviour of bituminous materials can be simulated using rheological analogical LVE models. These are obtained by combining a number of springs, describing elastic elements, and linear dashpots representing Newtonian viscous elements (Ferry 1980). A great number of combinations between these elements was proposed. The simplest ones are the Kelvin-Voigt model (**Figure 2.14a**) and the Maxwell model (**Figure 2.15a**). Kelvin-Voigt model consists of a spring and a dashpot connected in parallel and represents a viscoelastic solid. The Maxwell model considers the spring and the dashpot in a series arrangement and is used for viscoelastic liquids. However, these models are too simple for describing the behaviour of bituminous materials. Therefore, they are generally used as basic elements to define models with higher complexity, such as the generalised Kelvin-Voigt (**Figure 2.14b**) and the generalised Maxwell models (**Figure 2.15b**). They consist, respectively, of a number of Kelvin-Voigt elements in series, possibly with one spring and one linear dashpot in series, and a number of Maxwell elements in parallel, possibly with a spring and a linear dashpot in parallel.

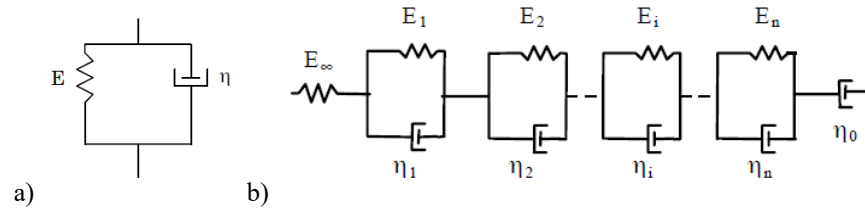


Figure 2.14. Analogical LVE models: a) Kelvin-Voigt, b) generalised Kelvin-Voigt

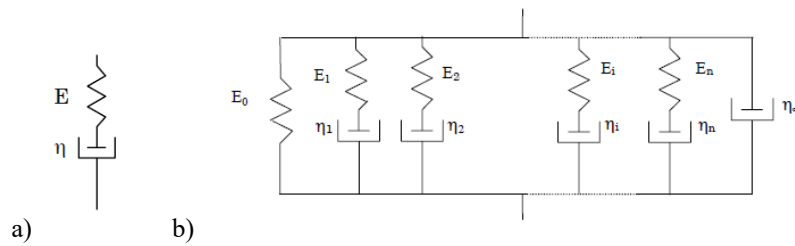


Figure 2.15. Analogical LVE models: a) Maxwell, b) generalised Maxwell

Other models, characterised by higher complexity, were proposed to describe the LVE behaviour of bituminous materials better. Among them there is the Huet-Sayegh (HS) model, proposed for bituminous mixtures (Sayegh 1967). The model consists of a linear spring put in parallel with the series arrangement of a linear spring and two fractional derivative elements (FDE) also called parabolic dashpots (**Figure 2.16a**), introduced instead of the linear dashpot used in Kelvin-Voigt and Maxwell models. The complex modulus is described with the HS model as:

$$E_{H-s}^*(j\omega) = E_e + \frac{E_g - E_e}{1 + \delta(j\omega\tau)^{-k} + (j\omega\tau)^{-h}} \quad (2.8)$$

where E_e , E_g are the equilibrium and glass moduli, respectively. δ , h and k are dimensionless model parameters, and τ is the characteristic time. E_e and E_g define the response of the springs, whereas k and h are linked to the FDE elements. E_e represents the value of E^* when $\omega\tau \rightarrow 0$, defining the purely elastic material response when the bituminous binder becomes liquid (high temperature/low frequency). In HMA mixtures, this value is ascribed to the interlock between aggregate particles (Di Benedetto *et al.* 2004). In CM and CRM, it also includes the effect of cementitious bonds (Ferrotti, Grilli, *et al.* 2020, Graziani, Raschia, *et al.* 2020). E_g is the value of E^* when $\omega\tau \rightarrow \infty$ and describes the purely elastic material response when the bitumen is a glassy solid (low temperature/high frequency). Its value mostly depends on the volumetric properties of the mixture (Olard and Di Benedetto 2003).

Chapter 2
Literature Review

The dimensionless parameters k , δ and h affect the shape of the model at low, intermediate and high temperatures (Mangiafico *et al.* 2013). Higher values of h and k signal the presence of a higher viscous dissipation component (the value one indicates the purely viscous response). Lower values of h and k represent a more elastic material behaviour (zero represents the purely elastic response). In general, $0 < k < h < 1$, with k characterising the low temperature/high frequency behaviour and h the high temperature/low frequency behaviour. τ is a function of the testing temperature T :

$$\tau(T) = a(T)\tau_0 \quad (2.9)$$

where $a(T)$ are the temperature shift factors, and τ_0 is the characteristic time at the reference temperature. τ is a frequency multiplier, and consequently, it only affects the position of the master curve along the frequency axes without any effect on its shape. Increasing the value of τ translates into a shifting of the stiffness modulus master curve to the left. This indicates a lower relaxation ability of the material. In general, higher values of τ are related to higher bitumen ageing and higher RA content in both hot and cold mixtures (Mangiafico *et al.* 2013, 2014, Godenzoni, Graziani, *et al.* 2017, Graziani, Mignini, *et al.* 2020).

Olard and Di Benedetto (2003) observed that the HS model does not properly describe the low frequencies (high temperatures) behaviour of binders. Therefore, they proposed an upgrade of the HS model, adding a linear dashpot. The 2S2P1D (2 springs, 2 parabolic elements, 1 dashpot) model, depicted in **Figure 2.16b**, describes E^* as:

$$E_{2S2P1D}^*(j\omega) = E_e + \frac{E_g - E_e}{1 + \delta(j\omega\tau)^{-k} + (j\omega\tau)^{-h} + (j\omega\beta\tau)^{-1}} \quad (2.10)$$

Introducing a Newtonian viscosity $\eta = (E_g - E_e) \beta\tau$ with the linear dashpot The model parameter β is dimensionless and it is linked to the dashpot viscosity. β is affected mainly by the ageing of the binder (Delaporte *et al.* 2007). In general, its value is lower in HMA than in CRM (Olard and Perraton 2010, Gandi *et al.* 2017b).

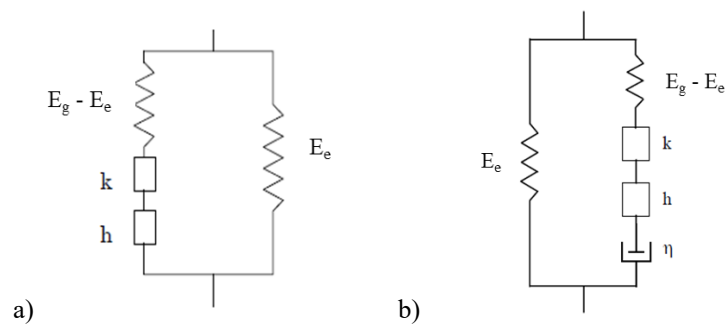


Figure 2.16. Analogical LVE model: a) Huet-Sayegh (HS), b) 2S2P1D

Chapter 2

Literature Review

HS and 2S2P1D models were found satisfactory describing the LVE behaviour of HMA and CRM (Gandi *et al.* 2017b, Godenzoni *et al.* 2018). However, even if the models fit well the master curve of the stiffness modulus, some issues regarding the modelling of the phase angle master curve of CRM were found. Specifically, these models underestimated the phase angle of the experimental data. The gap was quite constant regardless of the frequency (or temperature) considered. Graziani, Mignini, *et al.* (2020) proposed adopting a modified HS model to overcome this issue by considering a hysteretic part. The model, abbreviated HS-HY, describes E^* as:

$$E_{HS-HY}^*(\omega) = E_{HS}^*(\omega) \exp(j\varphi_0) \quad (2.11)$$

where $E_{HS}^*(\omega)$ represents the HS model, and $\exp(j\varphi_0)$ is a correction term that adds a constant phase angle φ_0 . The term $\exp(j\varphi_0)$ practically results in a rotation in the complex plane (**Figure 2.17**). Physically, the phase angle φ_0 describes time-independent (non-viscous) and temperature-independent dissipation phenomena, which are present during cyclic loading (Ferrotti, Grilli, *et al.* 2020). The hysteretic term generally describes dissipation mechanisms that may be attributed to the cementitious bonds or internal friction phenomena (Ashmawy *et al.* 1995, Genta 2009).

For considering these dissipation mechanisms in cold materials the DBNPDSC (Di Benedetto-Neifar Plastic Dissipation for Small Cycles) model was also proposed (Attia 2020, Raschia, Moghaddam, *et al.* 2021, Raschia, Perraton, *et al.* 2021). This model is based on the DBN (Di Benedetto-Neifar) model. DBN model is very versatile, allowing the study of LVE and elastic response but also introducing non-linearity, permanent deformation or fatigue (Di Benedetto *et al.* 2007). The non-linearity is considered using elasto-plastic (EP) bodies connected in series with viscous dashpots (**Figure 2.18**). EP bodies represent non-viscous behaviour and are typically used for representing non-cohesive granular materials, which can exhibit non-viscous dissipation. The higher is the number of elements selected, the higher is the model accuracy. If only viscous dissipation is present, EP bodies are replaced with springs, obtaining the generalised Kelvin-Voigt model. In case the DBN model is used for representing plasticity phenomena at small cycles number (and small strain domain), the model assumes a simplified form: DBNPDSC is obtained by the series arrangement of units consisting of a viscous and temperature-dependent dashpot in parallel with EP bodies. The same dissipation parameter characterises all dashpots. The phase angle is expressed as the total contribution of the viscous and non-viscous components.

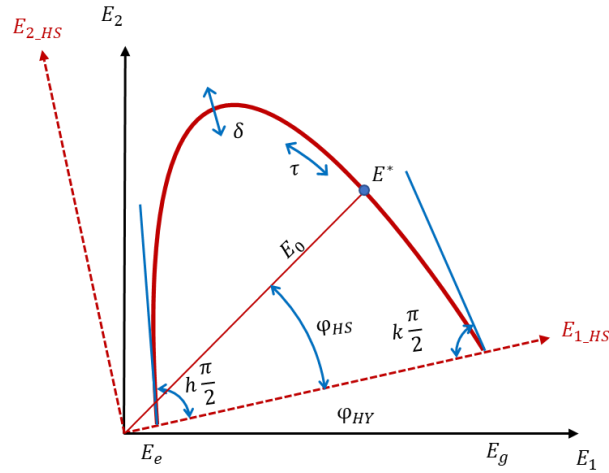


Figure 2.17. Comparison between the Huet–Sayegh (HS) and HS-HY models

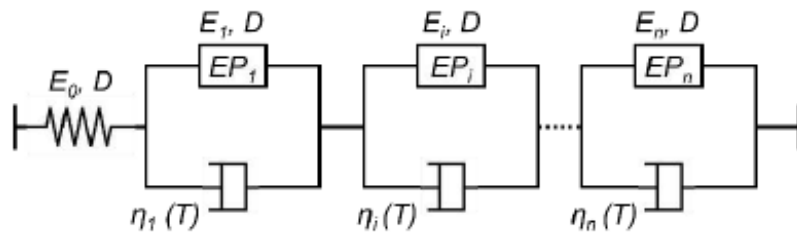


Figure 2.18. Analogical DBN model

As an alternative to analogical rheological models, analytical expressions, such as sigmoidal models, are used to simulate the rheological behaviour of bituminous mixtures. These models are more straightforward as they use mathematical formulas to fit the experimental data and need a lower number of fitting parameters. However, differently to analogical models, they do not have a physical meaning. They generally need at least four or five parameters, such in the case of the Richards model (Richards 1959, Rowe *et al.* 2009):

$$\log E_o(\omega) = \delta + \frac{\alpha}{[1 + \exp(\beta + \gamma \log f_r)]^{\frac{1}{\lambda}}} \quad (2.12)$$

where δ is the lower asymptote, corresponding to the purely viscous stiffness modulus (i.e. E_e) and α is the upper asymptote, with $\delta + \alpha$ corresponding to the purely elastic stiffness modulus (i.e. E_g). f_r is the reduced frequency, and β and λ are shape parameters.

Chapter 2
Literature Review

Other analytical models describe functions with a shape different from the sigmoidal model, e.g. the modified Christensen-Anderson-Marasteanu (CAM) model (Zeng *et al.* 2001):

$$E_{CAM}^* = E_e^* + \frac{E_g^* - E_e^*}{\left[1 + \left(\frac{f_c}{f'}\right)^k\right]^{\frac{m_c}{k}}} \quad (2.13)$$

where E_e^* and E_g^* are the complex modulus at equilibrium state when f approaches 0 (or at high temperature) and the complex modulus at glassy state when f approaches ∞ (or at low temperature), f_c is the limit of elasticity, a location parameter indicating the frequency at which the elastic component is approximately equal to the viscous component, f' is conversion frequency, k and m_c are shape indexes.

The last column of **Table 2.5** lists the models that have been used to simulate thermo-rheological behaviour of CRM. It is highlighted that sigmoidal models were traditionally applied only to real-valued stiffness modulus data, although the expression describing the shape of the phase angle can be then derived on the basis of on the Booiij and Thoone approximation developed for linear viscoelastic materials (Booiij and Thoone 1982). Complex-valued analogical rheological models, such as the HS, 2S2P1D, HS-HY and DBNPDS, can simultaneously simulate the stiffness modulus and phase angle.

Chapter 2
Literature Review

Multiscale Approach for Characterising the Behaviour of Cold Bitumen Emulsion Materials

Table 2.5. Summary of CRM properties and thermo-rheological characterization approaches based on cyclic axial tests on cylindrical specimens

Reference	RAP content	Stabilizing/Recycling agents	Specimen preparation	Curing	Test Temperatures	Testing Frequency	Target axial Strain	Rheological model
Stimilli <i>et al.</i> (2013)	90%	4% Emulsion + 2% Cement	Field cores and Gyratory compactor	1 to 6 months	0 - 40 °C	0.3 to 20 Hz	50 10 ⁻⁶ m/m	4-parameters sigmoidal
Schwartz and Khosravifar (2013)	40% and 100%	2.8-2.2% Foam	Field cores and Gyratory compactor	4-6 months (cores); 3 days at 40 °C (GC specimens)	5 - 35 °C	0.1 - 20 Hz	AASHTO T P62	4-parameters sigmoidal
Cardone <i>et al.</i> (2015b)	50%	3% Emulsion + 1-2% Cement	Gyratory compactor	28 days at 20°C	5 - 50 °C	0.1 - 20 Hz	15 10 ⁻⁶ m/m	4-parameters sigmoidal
Godenzoni, Graziani, <i>et al.</i> (2017)	50% and 70%	3% Foam + 2% Cement	Slab compactor	14 days at 40°C	-20 - 55 °C	0.03 - 10 Hz	30-50 10 ⁻⁶ m/m	Huet-Sayegh
Gandi <i>et al.</i> (2017)	50% to 100%	3% Emulsion + 1% Cement	Gyratory compactor	10 days at 38°C	-20 - 25 °C	0.01 - 3 Hz	30-50 10 ⁻⁶ m/m	2S2P1D
Dolzycki <i>et al.</i> (2017)	70%	2-6% Emulsion + 2-6% Cement	Gyratory compactor	28 days and 1 year at 20 °C	4 - 40 °C	0.01 - 25 Hz	AASHTO T P62	4-parameters sigmoidal
Lin <i>et al.</i> (2017)	100%	3% Emulsion + 2% Cement	Gyratory compactor	7, 14 and 28 days at 20 °C	-10 to 50 °C	0.01 - 25 Hz	AASHTO T 342	5-parameters sigmoidal (CAM)

Chapter 2
Literature Review

Multiscale Approach for Characterising the Behaviour of Cold Bitumen Emulsion Materials

Schwartz <i>et al.</i> (2017)	27 projects (6 FDR, 15 CIR, 3 CCPR)	Emulsion (20 projects); Foam (7 projects); Cement and Lime used as additives	Field cores	12-24 months	4.4 - 37.8 °C	0.01 - 25 Hz	AASHTO TP79	4-parameters sigmoidal
Godenzoni <i>et al.</i> (2018)	33%	3% Emulsion + 2% Cement; 3% Foam + 1.75% Cement	Field cores	7 years	0 - 50 °C	0.1 - 20 Hz	30 10 ⁻⁶ m/m	Huet-Sayegh
Buczyński and Iwański (2018)	20 to 80%	2.5% Foam + 2% Cement	Gyratory compactor	28 days at 20 °C	-7 - 40 °C	0.1 - 20 Hz	25-50 10 ⁻⁶ m/m	5-parameters sigmoidal (Richards)
Kuchiishi <i>et al.</i> (2019)	68%	5% Emulsion + 2% Cement 3% Foam + 2% Cement	Proctor compactor	6 days at 60 àC	4.4 – 54 °C	0.1 – 25 Hz	AASHTO T342-11	4-parameters sigmoidal
Graziani, Mignini, <i>et al.</i> (2020)	33%	3% Emulsion + 2% Cement; 3% Foam + 1.75% Cement	Field cores	7 years	0 - 50 °C	0.1 - 20 Hz	30 10 ⁻⁶ m/m	Huet-Sayegh - HY
Graziani, Raschia, <i>et al.</i> (2020)	94%	5% Emulsion + 1.5% Cement	Gyratory compactor	14 days at 25 °C and 14 days at 25 °C + days at 40 °C	0 - 40 °C	0.1 - 10 Hz	30 10 ⁻⁶ m/m	Huet-Sayegh - HY
Ferrotti, Grilli, <i>et al.</i> (2020)	88%	4.5% Emulsion + 2% Cement	Field cores	23 days in field + 171 at 20°C	0 - 50 °C	0.1 - 10 Hz	30 10 ⁻⁶ m/m	Huet-Sayegh - HY
Raschia, Moghaddam, <i>et al.</i> (2021)	90%	5% Emulsion	Gyratory compactor	14 days at 25 °C + days at 40 °C	-20 - 40 °C	0.1 - 10 Hz	40 10 ⁻⁶ m/m	DBNPDSC
Raschia, Perraton, <i>et al.</i> (2021)	94%	5% Emulsion + 1.5% Cement	Gyratory compactor	14 days at 25 °C, 14 days at 40 °C and 330 days at 25 °c	-20 - 40 °C	0.1 - 10 Hz	50 10 ⁻⁶ m/m	DBNPDSC

2.2. The multiscale approach

Bituminous mixtures are multiphase materials and, at different length scales, can be described as composites consisting of a homogeneous interconnected region, also called matrix, with particulate inclusions (Gibson 2016). Looking at materials used in road paving, it can be observed that many scales of observation exist, basically connected to the geometry of the material that is added to the bituminous binder (Underwood 2015, Allen *et al.* 2017). In the case of HMA, other than bitumen, four further scales of interest are commonly identified (**Figure 2.19**): mastic, fine aggregate matrix (FAM) mortar, mixture and pavement (Pichler *et al.* 2012, Underwood 2015, Allen *et al.* 2017):

- The bitumen is a semisolid binding material with viscous to viscoelastic properties and a length scale ranging between 10^{-6} and 10^{-5} m. Its study is mainly related to the rheological properties which can influence the properties of larger scales;
- The mastic is composed of a bitumen matrix with filler sized particle inclusions, with a maximum size smaller than $1.25 \cdot 10^{-4}$ m. At this scale, the interactions that occur at the interface of bitumen and aggregate are magnified thanks to the relatively large specific surface of the filler particles. Moreover, this scale can be considered the actual binding matrix of the mixture, and thus largely influencing the aggregate coating and the bitumen spreading into the mixture (Hesami *et al.* 2012, Sefidmazgi *et al.* 2013);
- The FAM mortar consists of a homogeneous mastic matrix with sand-size particles acting as inclusions. Its length scale is around 10^{-3} m. The study of this scale is interesting because FAM mortars are only one scale smaller than mixtures. FAM mortar is the material that exists between the coarse aggregate particles in the mixture. Thus, it is the material that deforms under high-temperature loading and that shows visible cracking under repeated loading at intermediate temperatures;
- The mixture is composed of a FAM mortar homogeneous matrix with coarse aggregate inclusions and length scale ranging between 10^{-2} and 10^{-1} m;
- The pavement, the macroscale, ranging between 10^{-1} and 10^3 m. It is the scale of the structural application. In this case, the mixtures are continuous and characterised by mechanical properties such as elastic modulus, Poisson ratio etc..

Starting from the binder, in a downscaling process, the smallest scales can be investigated, focusing on the chemical properties considering the bitumen a composite of different elements, e.g. hydrocarbons.

Multiscale studies are intended to help understand the physical and chemical mechanisms happening in the bituminous materials, investigating the scales where those mechanisms prevail. Moreover, the mechanisms individuated at different scales can be integrated into comprehensive analytical or computational elaborations. Therefore,

multiscale investigations can be effective tools for deducing cause-and-effect relationships when applied in the upscaling direction. The downscaling process can help to improve the properties and performances of bituminous mixtures by aiding decision about their composition and manufacture (Underwood, 2015a).

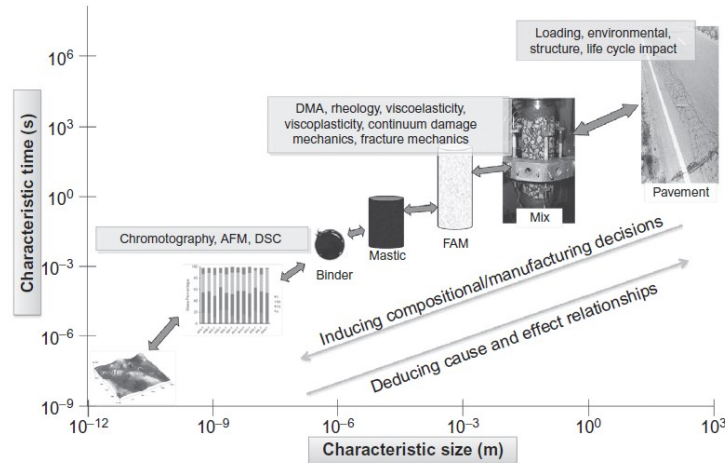


Figure 2.19. Scales involved in the multiscale investigation of bituminous mixtures (Underwood 2015)

Compared to HMA, for which multiscale approaches are a widespread tool, their application to cold materials is rather new, with few research studies carried out about this topic so far. This is mainly due to the relatively new introduction of these materials in road paving application compared to HMA materials. To this is added the generally higher level of complexity of cold materials, linked to the presence of water and a second binder, and their evolutive nature. The present section reports an overview of the multiscale studies of cold materials, focusing on FAM mortars and fresh mastics, which, together with mixtures, are the main focus of this thesis.

2.2.1. Study of FAM mortars

Several studies have shown that HMA FAM properties affect the viscoelastic, fatigue and fracture behaviour of mixtures (Izadi *et al.* 2011, Sousa *et al.* 2013, Underwood and Kim 2013a, 2013b, Aragão *et al.* 2017, Freire *et al.* 2017, Fakhari Tehrani *et al.* 2018, Le *et al.* 2018, Fadil *et al.* 2019), as well as their moisture damage resistance (Caro *et al.* 2008). It was also shown that healing, oxidation and ageing occur in the FAM phase (Izadi *et al.* 2011, Gundla *et al.* 2017, Zhang and Leng 2017). Besides, FAM mortars have been used to predict the overall behaviour of the mixtures using multiscale computational models (Aigner *et al.*

Chapter 2

Literature Review

2009, Eberhardsteiner *et al.* 2016, Neumann *et al.* 2017, Fakhari Tehrani *et al.* 2018, Le *et al.* 2018). Despite this, a common agreement about the composition of HMA FAM mortars does not exist. **Table 2.6** summarises the main approaches for defining the FAM mortar composition in terms of nominal maximum aggregate size (NMAS), grading curve, bitumen dosage and air voids content.

Compared to HMA, relatively few works investigated the composition of cold FAM mortars and related their behaviour to cold mixtures. FAM mortars were used in fine element models to evaluate the behaviour of mixtures. In these models, coarse aggregates were identified by a minimum dimension of 2 mm. The mortar matrix included mastic and fine particles, and air voids were considered as a separate phase in the mixture (Fu *et al.* 2015, 2018). Recent studies applied the FAM mortar concept in the study of the mechanical properties of CBE mixtures. The FAM mortars had NMAS of 2 mm and were produced using all the bitumen emulsion and cement content of the mixture (the residual bitumen to cement ratio was 2.0). The authors found that FAM mortars including about 80% of mixture water and 17% of mixture air voids could to predict the stiffness of mixtures throughout the curing process and their LVE behaviour (Graziani, Raschia, *et al.* 2020).

Cold bituminous mortars were also proposed as a model system for characterising bitumen emulsion (Miljković and Radenberg 2014, Miljković *et al.* 2017). This approach was inspired by the common practice for characterising the strength of cementitious binders (EN 196-1, ASTM C109 / C109M). The authors selected the same upper sieve size, 2 mm, and a similar grading distribution (Miljković and Radenberg 2015, 2016). Since those studies focused on the bitumen emulsion, the mortars had a bitumen-dominated behaviour with a B/C ratio ranging between 3 and 7. Cold bituminous mortars were also employed for evaluating the effect of mineral additions on the failure properties using a B/C ratio between 1 and 4.8 (Miljković and Radenberg 2015, Miljković *et al.* 2019). The mortar concept is also applied with a similar purpose within the RILEM TC-280 on the multiphase characterisation of CBE materials. Task group 1, “Emulsions and emulsion-based composites”, is currently running an interlaboratory test to develop a scientific framework for studying the link between the intrinsic interphase relations and macroscopic physicommechanical behaviour of CBE composites (Miljković *et al.* 2020). Other researchers also used mortars prepared with natural sand (upper sieve size was 0.5 mm) to compare the influence of different mineral additions (Portland cement, calcium carbonate and hydrated lime). They used the same content of residual bitumen and cement (10%) and total water content between 8% and 9% (Godenzoni *et al.* 2016).

The literature review suggests that testing CBE mortars rather than CBE mixtures offer attractive perspectives. Mortars may be used as model systems to predict mixture behaviour (saving laboratory time and materials with respect to CBE mixtures) or to study bitumen emulsion properties and interaction between bitumen emulsion cementitious materials eliminating inhomogeneities due to large aggregate particles. Moreover, a detailed

Chapter 2
Literature Review

study of the mortar phase properties can support the development of more realistic computational models for CBE mixtures, for example, in finite element modelling.

Table 2.6. Summary of the approaches proposed for defining HMA FAM composition

FAM property	Value/selected approach	Reference
NMAAS	1.18 mm	Kim (2003), Izadi <i>et al.</i> (2011), Sousa <i>et al.</i> (2013)
	2.00 mm	Pichler <i>et al.</i> (2012), Neumann <i>et al.</i> (2017)
	2.36 mm	Dai <i>et al.</i> (2005), Underwood and Kim (2013b, 2013a)
	Bailey method (primary control sieve)	Underwood and Kim (2013b, 2013a)
Grading distribution	Same gradation of the mixture	Izadi <i>et al.</i> (2011), Sousa <i>et al.</i> (2013)
	Same gradation of the mixture, excluding the fraction of filler-sized particles in the mastic	Underwood and Kim (2013b)
Bitumen content	Bitumen of the mixture, subtracting the bitumen absorbed by the coarse aggregate	Izadi <i>et al.</i> (2011)
	Bitumen of the mixture, subtracting the fraction of bitumen in the mastic	Underwood and Kim (2013b)
	FAM obtained by mechanical sieving of the mixture (Experimental procedure)	Sousa <i>et al.</i> (2013)
Air voids content	50-70% of the total air voids of the mixture	Underwood and Kim (2013b)
	2.5%-3.5% (at the end of the compaction)	Sousa <i>et al.</i> (2013)
Compaction method	Gyratory compactor	Izadi <i>et al.</i> (2011), Sousa <i>et al.</i> (2013)

Chapter 2

Literature Review

2.2.2. Viscosity of fresh mastics: CBE slurries

Studies on CBE mastics have been proposed for assessing the effect of mineral additions and their interaction with the bitumen emulsion on their rheological and fatigue behaviour (Godenzoni, Bocci, *et al.* 2017, Garilli *et al.* 2019, Al-Mohammedawi and Mollenhauer 2020). CBE mastics are also widely used for assessing the physical and mechanical properties of CBE mortars used in the construction of non-ballast tracks (Peng *et al.* 2014, Ouyang, Li, *et al.* 2017).

Most of the researches on CBE materials focuses on the study at the cured state or the curing process. Nevertheless, the awareness about CBE materials properties at the fresh state is fundamental. The workability and compactability of fresh CBE materials directly affect the volumetric and mechanical properties at the cured state. Workability represents the response of the material to being mixed and laid. Compactability represents its aptitude to being compacted (Raschia, Mignini, *et al.* 2019). Therefore, a material characterised by good workability will have more homogeneity and a better coating level. A good compactability will guarantee improved volumetric properties. In CBE materials, various factors contribute to workability and compactability: water content, emulsion dosage and type, presence of a cementitious co-binder, aggregate gradation. Water affects workability and compactability lubricating the aggregate, consequently reducing the shear strength (Kuchiishi *et al.* 2019). It favours the aggregates coating helping the spreading of the bitumen droplets. The effect of bitumen emulsion dosage is similar to the effect of water. In contrast, its type (cationic or anionic) and its breaking behaviour (SS, MS or RS), both related to the emulsifier type and dosage, influence the interaction with the aggregate and the cementitious binder, affecting the breaking kinetics (Ziyani *et al.* 2014, Miljković *et al.* 2017). Aggregate gradation may also affect workability and compactability: it was found that by increasing the filler content, the first is enhanced, whereas the latter can be hindered (Raschia, Mignini, *et al.* 2019). All these factors may also affect the coating of the CBE mixtures (Swiertz *et al.* 2012).

Direct measurement of the workability of mixtures is challenging (Hesami *et al.* 2012). Some researchers measured the torque needed to rotate a paddle in the mixtures at a certain speed (Gudimettla *et al.* 2004). Multiscale approaches can be applied to overcome these difficulties. The workability of HMA mixtures is generally linked to its mastic or bitumen phase (Hesami *et al.* 2012, Sefidmazgi *et al.* 2013). Analogously, the workability at the scale of CBE mortars and mixtures can be considered directly related to the rheological properties of the fresh mastic scale (Zhang *et al.* 2012). Because of that, the study of CBE slurries (or pastes), defined as the mastic at the fresh state, is gaining attention.

CBE slurries are complex fluids composed of an aqueous phase, in which different solid particles, i.e. bitumen droplets and mineral additions, are suspended. Solid particles may have different dimensions: bitumen droplets range between 0.001 and 0.02 mm (James 2006), whereas the mineral additions are ten times larger, ranging between 0.01 and 0.1 mm. The densities of the materials also differ significantly, as water and bitumen are about three

Chapter 2

Literature Review

times less dense than mineral additions. Mixing mineral additions to the bitumen emulsion leads to changes in its rheological response. Viscosity increases not only because of the presence of additional phases but also because of the beginning of phenomena such as emulsion breaking and cement hydration (Wang and Sha 2010, Wang *et al.* 2013, Tan *et al.* 2014).

Rheological studies for measuring the viscosity of complex fluids are a topic of interest in many industries, including road engineering and bituminous industry. A standard setup used for measuring the viscosity of bituminous materials is the rotational viscometer in coaxial cylinder configuration, e.g. Brookfield viscometer. In complex fluids, this instrument may not provide reliable measurements (Lo Presti *et al.* 2014). The difference in density of the components of the system and the eventual presence of processes altering the material structure (e.g. emulsion breaking and cement hydration in CBE slurries or swelling in crumb rubber modified bitumen) leads to a lack of sample stability, phase separation and tendency to sedimentation (Giancontieri *et al.* 2020). Therefore, the material can show a non-Newtonian behaviour, with shear-rate-dependency and time-dependency, that may affect viscosity measurements. For the reasons stated above, additional impellers have been proposed and developed for assisting the correct measurement of viscosity. Helical ribbon impellers were found to be the most suitable tool in the mixing of both high viscosity Newtonian and non-Newtonian fluids (Patterson *et al.* 1979, Yap *et al.* 1979). They have a pumping effect that helps to maintain particles in suspension and confer a high shear deformation, improving the homogeneity of the system. On that basis, dual helical ribbon (DHR) impellers have been successfully developed for measuring the viscosity of crumb rubber modified binders and mastics (Astolfi *et al.* 2019, Medina *et al.* 2020). DHR allowed continuous measurement of the viscosity guaranteeing the stability of the sample.

Despite the increasing interest in the rheological characterisation of CBE slurries, standards for their mixing and viscosity measurement are not available. A large number of procedures have been proposed in the literature (**Table 2.7**). Mixing can be performed either through a mechanical mixer or hand-stirring. The mixing phase duration was generally limited to prevent the starting of the emulsion breaking and the cement hydration processes. Some Authors proposed an initial pre-mixing phase only of water and mineral additions. This was intended to allow water to form a film around the surface of mineral additions to hinder the instability of the emulsion and its premature breaking (Ouyang and Tan 2015, Godenzoni, Bocci, *et al.* 2017). The most common equipment for measuring the viscosity was the rheometer in coaxial cylinders configuration, although the parallel plate configuration was also used. Tests were generally carried out at ambient temperature, but also the effect of the temperature changes was assessed (Zhang *et al.* 2012). Time zero of the testing was variable: it was considered the first contact of water with cement (Fang, Garcia-Hernandez, Winnefeld, *et al.* 2016), or the instant immediately after the end of the mixing (Tan *et al.* 2014, Ouyang and Tan 2015). In some studies, time zero was fixed at a selected time after the end of the mixing (Zhang *et al.* 2012, Godenzoni, Bocci, *et al.* 2017). In some experimental studies,

Chapter 2

Literature Review

before testing, a pre-shear mixing was applied to obtain a breakdown in the slurry structure and get uniform conditions (Tan *et al.* 2014, Ouyang and Tan 2015). Some testing procedures involved rest periods or hysteresis cycles. These cycles allowed uniform testing conditions to be achieved, thereby breaking the possible thixotropic structure to get more consistent measurements (Tan *et al.* 2014). Adopted shear rates were mainly linked to the equipment limits.

Viscosity measurement showed that CBE slurries have a non-Newtonian behaviour, generally showing a shear-thinning response (Peng *et al.* 2014, Fang, Garcia-Hernandez, Winnefeld, *et al.* 2016), although in some cases, it is followed by a shear-thickening response, suggesting a minimum flocculation shear rate (Ouyang *et al.* 2015). Different rheological behaviours were observed considering anionic or cationic emulsion. The anionic bitumen emulsion showed higher adsorption onto the surface of cement grains. This reduced the yield stress of the slurry and delayed the cement hydration process (Zhang *et al.* 2012). Slurries with plain emulsion had lower yield stress to resist segregation than emulsion modified by viscosity modifying agent (Tan *et al.* 2014). Good stability of the emulsion helped to reduce the coalescence of bitumen droplets diminishing the viscosity (Tan *et al.* 2014). The nature of the mineral addition had a definite effect on the viscosity of CBE slurries. The addition of cement significantly increased the viscosity compared to the impact of limestone filler (Fang, Garcia-Hernandez, Winnefeld, *et al.* 2016, Ouyang, Li, *et al.* 2017) or calcium carbonate (Godenzoni, Bocci, *et al.* 2017). The breaking behaviour of the emulsion changed as a function of the mineral filler. In particular, using limestone filler, the main process was the bitumen droplets coalescence. Differently, when cement was added, a direct adhesion of the droplets on the surface of the cement occurred due to its high adsorption ability (Ouyang *et al.* 2018). Moreover, the addition of cement highlighted a time-dependency starting within the first thirty testing minutes, which was not observed when cement was replaced with the limestone filler (Fang, Garcia-Hernandez, Winnefeld, *et al.* 2016). The volumetric concentration also affected the rheological behaviour of CBE slurries: high solid particles volume fraction lead to a higher viscosity and yield stress (Zhang *et al.* 2012). Water to cement ratio, emulsion to cement ratio and particle sizes significantly influenced the viscosity of the slurries (Tan *et al.* 2014, Ouyang and Tan 2015, Garilli *et al.* 2016).

Chapter 2
Literature Review

Multiscale Approach for Characterising the Behaviour of Cold Bitumen Emulsion Materials

Table 2.7. Summary of the procedures proposed for mixing and viscosity testing of CBE slurries

Reference	Mixing procedure	Viscosity measurement	
		Equipment	Procedure
Zhang <i>et al.</i> (2012)	Water and emulsion added into the mixer. Cement gradually introduced within 2 min at 62 rpm. 10 s stop interval and mixing for 2 min at 125 rpm	Brookfield viscometer	Tested at different temperatures and times after mixing. Before testing slurry kept in a mixing bowl covered with a soaked towel, then remixed at 62 rpm for 30 s.
Peng <i>et al.</i> (2014)	Water and emulsion stirred into a mixer for 1 min at 62 rpm. Cement introduced within 0.5 min at 62 rpm. Mixing for 2 min at 125 rpm and 0.5 min at 62 rpm	Rotary rheometer in coaxial cylinder configuration	Tested 5 min after mixing. Shear rate 1 - 300 s ⁻¹ . Up-curve/constant/down curve (down curve considered for the analysis).
Tan <i>et al.</i> (2014)	n.a.*	Parallel plate rheometer	Immediately tested. Pre-shear at 50 s ⁻¹ for 60 s. Linear decreasing shear rate from 50 - 0 s ⁻¹ for 10 s. 60 s or 300 s of rest. Two hysteresis cycles within 2 min, 0-50 s ⁻¹ (up curves of the second cycle considered in the analysis).
Ouyang <i>et al.</i> (2015)	n.a.*	Parallel plate rheometer	Immediately tested at 20 s ⁻¹ . Before each test, additional hand-stirring. Increasing shear rates from 2 to 50 s ⁻¹ within 60 s. Each step lasted 30 s. Test at 20 s ⁻¹ until the loss of fluidity.
Ouyang and Tan (2015), Ouyang <i>et al.</i> (2016)	Hand-stirring. Cement and water stirred firstly for 2 min, then emulsion added and continually stirred for 2 min.	Rheometer in coaxial cylinder geometry	Sample immediately loaded (within 1 min from mixing). 2 min pre-shear at 300 s ⁻¹ and 2 min of rest. Then strain rate increased gradually over 1 min to a final value of 100 s ⁻¹ .
Garilli <i>et al.</i> (2016)	Water and cement and stirred for 1 min. Emulsion added and stirred for 2 min.	Rheometer in coaxial cylinder configuration	Linear shear stress ramp from 0 to 50 Pa, 5 s duration of each stress step. Time zero: 10 min after water addition. Test every 15 min until the loss of fluidity.
Fang, Garcia-Hernandez,	Filler and cement premixed. Addition of emulsion, mixing at 60 rpm for 1 min.	Brookfield viscometer, spindle S27	Sample poured into the container and tested immediately. Time zero: coincident with the cement addition.

Chapter 2

Literature Review

Multiscale Approach for Characterising the Behaviour of Cold Bitumen Emulsion Materials

Winnefeld,
et al. (2016)

Ouyang, Li, <i>et al.</i> (2017)a	n.a.*	Rheometer in coaxial cylinder geometry	Immediately testing. 2 min pre-shear at 300 s ⁻¹ . 2 min rest. Shear rate is decreased from 100 s ⁻¹ to 1 s ⁻¹ .
Ouyang, Tan, <i>et al.</i> (2017), Ouyang <i>et al.</i> (2018)	Same used in: Ouyang and Tan (2015), Ouyang <i>et al.</i> (2016)	Rheometer in coaxial cylinder geometry	Immediately sheared. Up/down/up curve, linearly increasing shear rate from 0 to 100 s ⁻¹ , each curve within 1 min (second up curve considered in the analysis).
Godenzoni, Bocci, <i>et al.</i> (2017)	Mixing of mineral filler and water. Addition of emulsion and hand-stirring. Mixing at 489 rpm with a high-shear mixer.	Brookfield viscometer, spindle S21	Test after 15, 45 and 60 min from the beginning of the mechanical mixing. Shear rate from 50 up to 200 s ⁻¹

* information about the procedure not available

Chapter 3.

Research Description and Objectives

3.1. Introduction

The concerns over the environmental and economic impact and future sustainability make greener road paving solutions necessary and no longer postponable. In this context, CM and CRM can represent an effective solution. However, these materials have generally low performances compared to the traditional asphalt mixtures due to the lower bitumen content and the higher voids. CM and CRM are evolutive and need a certain curing period before being opened to traffic and reaching their long-term properties. They are relatively new materials, and their mix-design, physical and mechanical characterisation procedures, and the study of the curing effects, are still open-ended questions. The number of variables connected to the constituents is huge: different RA sources, aggregate mineralogy, bituminous and cementitious binders can lead to mixtures with different characteristics and performances. Also, the interaction between the different constituents can have a key role. In particular, in the case of CBE materials, the breaking behaviour of the emulsion can be affected by the mineralogy of the aggregate, the reactivity of RA and the type and dosage of filler and co-binder. A significant amount of interest exists in promoting the use of CBE materials. Nevertheless, in light of the issues stated above, several aspects need to be deepened:

- The assessment of the influence of the constituents and their interaction in the curing behaviour and the mechanical response of CBE materials;
- The development or validation of robust testing procedures to characterise the fresh state properties, the curing behaviour, and the long-term properties of CBE materials.

Much of the research on these issues focused on the characterisation of CBE materials at the mixture scale. However, considering the composite nature of bituminous materials, some phenomena or mechanisms of interaction are more easily discernible at smaller (mortar, mastic or binders) or larger scale of observation (pavement).

3.2. Objective Statement

The research presented herein aims to develop and validate a multiscale approach for characterising CBE materials. Such an approach is intended to help in deepening the knowledge on CBE materials properties, especially about the interaction between their different components. This could help promote the use of CBE materials, helping their composition optimisation and, therefore, enhancing their mechanical response. The multiscale approach could also support multiscale modelling, which is becoming a popular tool, especially in the HMA study. Additionally, testing methods traditionally used for bituminous materials are upgraded for considering the complex nature of CBE materials and properly characterise them.

The research is organised in several parts, each of them considering specific objectives:

- Identify the composition of CBE FAM mortars that closely describes the fine matrix of CBE mixtures (Chapter 5 - Mixture to FAM mortar Downscaling);
- Compare the curing behaviour of mixtures and FAM mortars, and evaluate the predictive potential of FAM mortars (Chapter 6 – Curing Behaviour of CBE Materials);
- Compare the rheological behaviour of mixtures and FAM mortars, and validate the predictive potential of FAM mortars (Chapter 7 - Linear Viscoelastic Study of CBE materials);
- Characterise the rheological properties of CBE slurries in terms of viscosity (Chapter 8 - Rheological Characterisation of CBE Slurries).

3.3. Methodology: the multiscale approach

In this research study, CBE mixtures were considered a composite multiphase material, and various scales of observation were identified (**Figure 3.1**). Starting from the mixture scale and moving in the downscaling direction, three further scales of engineering interest were considered:

- The FAM mortar, the binding matrix of the mixture obtained by removing coarse aggregate from the mixture. In this research, the FAM mortar has NMA of 2 mm, selected following the prevailing practice for FAM (see Section 2.2.1);
- The mastic (at the cured state) or slurry (at the fresh state), the FAM mortar binding matrix, obtained by removing fine aggregate and voids. The CBE mastic is composed of residual bitumen and mineral additions, i.e. filler and cementitious binder. In the present investigation, filler particles had NMA equal to 0.125 mm;

Chapter 3

Research Description and Objectives

Multiscale Approach for Characterising the Behaviour of Cold Bitumen Emulsion Materials

- The bitumen emulsion, the binding agent of CBE materials, along with the eventual cementitious binder. Bitumen emulsion is a composite material itself as the bitumen droplets are dispersed in water.

The research activities were carried out in the Department of Civil and Building Engineering and Architecture of the *Università Politecnica delle Marche* (Ancona, Italy). Part of the experimental programme presented in this dissertation and focusing on CBE slurries was developed in collaboration with the Nottingham Transportation Engineering Centre – University of Nottingham (Nottingham, UK) during a visiting period of three months (November 2018-December 2018, February 2019-March 2019).

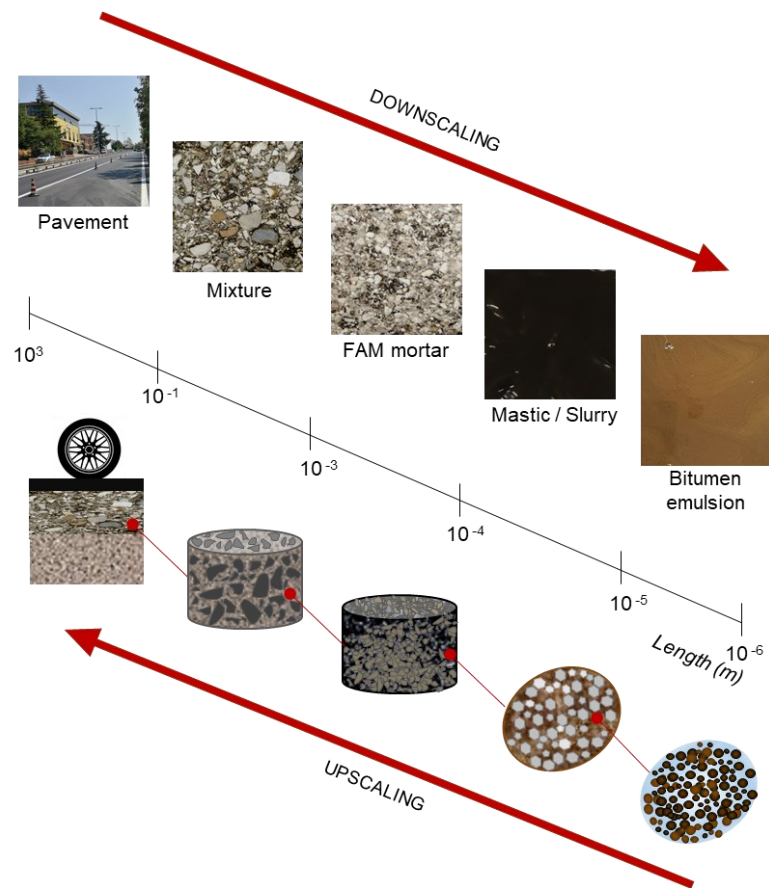


Figure 3.1. Schematic diagram showing the general definition of the various scale of observation of CBE materials

3.4. Outline of the dissertation

To accomplish the objectives, the investigation started from the study of CBE mixtures and, then, was developed considering two further primary branches: the investigation of FAM mortars and slurries (**Figure 3.2**). The present dissertation is organised according to the research study structure.

- Chapter 4 – Materials and Methods summarises the materials and the samples preparation methods. It also describes the approach adopted for the volumetric analysis of CBE materials. The composition of the investigated CBE mixtures, FAM mortars and slurries is then summarised. Finally, testing methods followed for the physical and mechanical characterisation of CBE materials are detailed;
- Chapter 5 – Mixture to FAM Mortar Downscaling focuses on the definition of the FAM mortar concept and describes the methodology adopted for the definition of its composition;
- Chapter 6 – Curing Behaviour of CBE Materials focuses on evaluating the curing behaviour of mixtures and FAM mortars in terms of water loss by evaporation, stiffness and strength. Finally, the ability of FAM mortars in predicting the evolution of the mechanical properties of CBE mixtures was validated;
- Chapter 7 – Linear Viscoelastic Study of CBE Materials focuses on characterising the long-term rheological properties of mixtures and FAM mortars in terms of complex modulus. Finally, the ability of FAM mortars in predicting the LVE response of CBE mixtures was evaluated;
- Chapter 8 – Rheological Characterisation of CBE Slurries focuses on the viscosity of slurries.
- Chapter 9 – Conclusions summarises the main research findings and proposes some recommendation for future investigations.

Appendixes describe the results of investigations preliminary carried out to characterise and design CBE materials or focusing on a specific length scale without any specific link to the other scales. They are organised as follows:

- Appendix A – Properties of Materials Employed summarises the main properties of the materials used in the investigation;
- Appendix B – Mixing procedures for CBE Mixtures and FAM Mortars details the mixing procedures for mixtures and mortars;
- Appendix C – Study of the Composition of CBE Mixtures with Different Cements for Base Courses details the definition of the composition of CBE mixtures investigated within Chapter 5 and Chapter 6;
- Appendix D – Effect of Curing on the Indirect Tensile Failure Energy of CBE Mixtures focuses on the effect of curing RH on the indirect tensile failure energy of the mixtures investigated in Chapter 5 and Chapter 6;

Chapter 3

Research Description and Objectives

Multiscale Approach for Characterising the Behaviour of Cold Bitumen Emulsion Materials

- Appendix E – Effect of Grading Distribution on the Volumetric Properties of CBE Mixtures for Binder Courses investigates the influence of several grading distributions on CBE mixtures volumetric properties. Some of these mixtures were investigated in Chapter 6 and Chapter 7;
- Appendix F – Study of the Composition of CBE Mixtures with High Strength Cements for Binder Courses focuses on optimising the composition of advanced high-performance mixtures for the application in binder courses. Some of these mixtures were investigated in Chapter 6 and Chapter 7.
- Appendix G – Fatigue Behaviour of CBE Mixtures for Binder Courses Produced with High Strength Cements focuses on the laboratory characterisation of the fatigue response of CBE mixtures;
- Appendix H – Cracking resistance of CBE FAM mortars focuses on characterising the cracking resistance of mortars whose curing behaviour was investigated within Chapter 6;
- Appendix I – Graphic Representation of the Results For Complex Modulus Test reports the complex modulus obtained by modelling CBE composites LVE behaviour (Chapter 7).

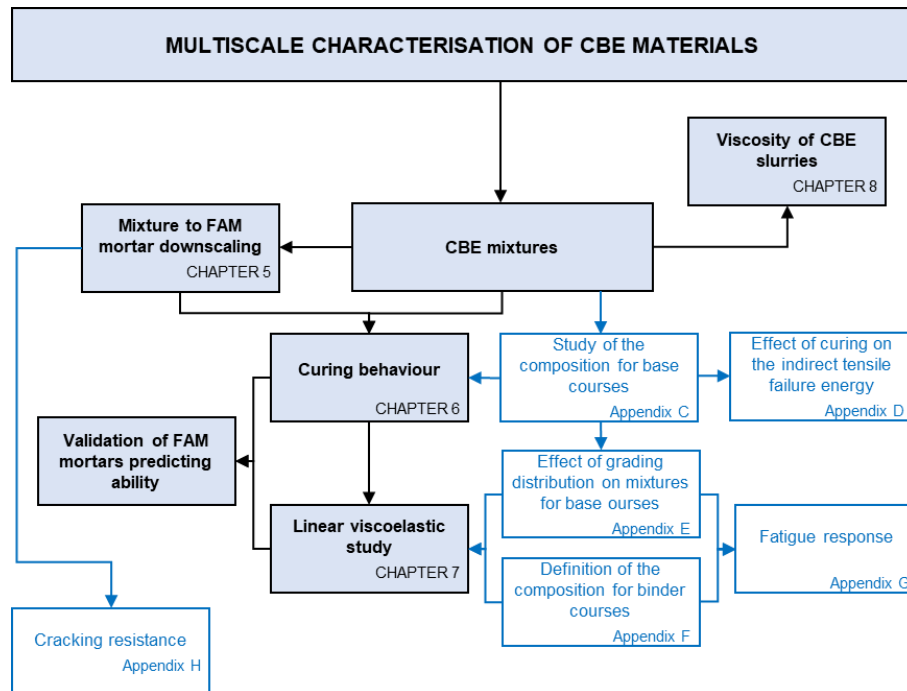


Figure 3.2. Scheme of the dissertation

Chapter 4.

Materials and Methods

4.1. Materials

CBE mixtures, FAM mortars and slurries were obtained using a set of materials comprising unique RA and natural aggregate sources and different types of cement and bitumen emulsions. The materials were adopted at each stage of the investigation based on the specific aim of each section.

The RA aggregate was supplied by Società Cooperativa Braccianti Riminese, from the San Leo mixing plant (Rimini, Italy). At the production plant, RA aggregate had been initially crushed and screened to eliminate the largest lumps and obtain a material with a nominal maximum dimension of 16 mm (RA 0/16). Laboratory sieving operations allowed obtaining two further fractions characterised by:

- a nominal maximum dimension of 2 mm (RA 0/2);
- a nominal maximum dimension of 16 mm and retained on the 2 mm sieve (RA 2/16).

The fine natural aggregate was crushed limestone sand with a nominal maximum dimension of 2 mm, and the filler was finely ground limestone powder. **Figure 4.1** depicts the grading distribution of the various aggregate sources.

Two commercial cationic over-stabilised bitumen emulsions were employed, both supplied by Valli Zabban S.p.A. (Bologna, Italy):

- B - produced using plain bitumen, classified C60B10 (EN 13808);
- BP - produced with SBS modified bitumen mixed with a small amount of SBS latex, classified C60BP10 (EN 13808).

The emulsions were slow setting, specifically designed for cold recycling applications. The residual bitumen content was 60%, and their base bitumen penetration grade was 70/100. Cationic emulsions were selected because they are much widespread in Europe for the production of CBE mixtures (Section 2.1.2).

Four cementitious binders, supplied by Italcementi S.p.A. (Bergamo, Italy), were selected to provide an extensive overview of the effect of cement on the mechanical properties of CBE mixtures:

- C1 - Portland limestone cement type II/B-LL with strength class 32.5R (EN 197-1);

- C2 - Sulfoaluminous cement (not standardised within the European standards framework);
- C3 - Portland-slag cement type II/B-S with strength class 52.5N (EN 197-1);
- C4 - Hydraulic binder for non-structural applications type HB3.0 (EN 15368).

C1 was selected as the reference cementitious binder because it is commonly used in CR applications in Italy (Autostrade per l'Italia 2013, Provincia Autonoma di Bolzano 2016). C2 has rapid setting and hardening and very high 28 days strength. Moreover, C2 has a lower pH compared to conventional Portland-based cements. C3 has ordinary early strength but a high 28 days strength. C4 is commonly used in Italy for mortars for non-structural masonry or rendering and plastering applications. C4 has low values of both early and long-term strength, and it is characterised by high water retention at the fresh state. The various cementitious binders were selected because they are representative of a wide range of strengths. The non-Portland cement, i.e. C2, was also chosen for assessing the potential effect of its different nature and the lower pH on the microstructure of the CBE materials and if this leads to a different mechanical response. Appendix A reports the main properties of the material employed.

Water was added for helping the workability and compactability of mixtures. Then, the total water content of CBE materials w_t included both emulsion water and additional external water. A fraction of the additional water is absorbed by the aggregate permeable voids w_{abs} , while the remaining fraction, along with the emulsion water, was identified as intergranular water w_i .

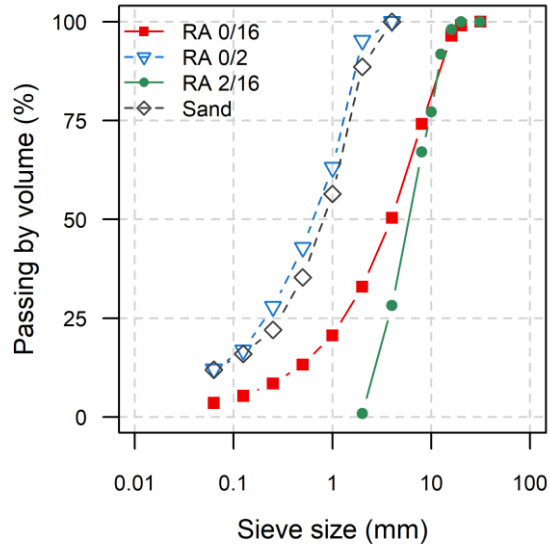


Figure 4.1. Aggregates grading distributions

4.2. Sample preparation

4.2.1. Mixing

4.2.1.1. Mixtures and FAM mortars

The mixing procedures of mixtures and FAM mortars were developed based on the experience on CBE materials of the research group at *Università Politecnica delle Marche*. The mixing of both CBE materials was performed in two stages using mechanical mixers to guarantee a good particle coating. First, aggregates were dried until reaching constant mass, at (105 ± 2) °C for natural aggregate and (40 ± 2) °C for RA. A water amount related to the aggregate absorption was added to the dry aggregate blend. The wet samples were stored in a sealed plastic bag for at least 12 h at room temperature to let aggregate reaching saturated surface dry (SSD) conditions. Then, the cementitious binder, water and bitumen emulsion were added step by step and mixed with the SSD aggregate blend. Water was added after 8 minutes, bitumen emulsion after 11 minutes. The whole process required about 15 minutes. At the end of the mixing, its effectiveness was checked by visual examination. Appendix B describes the detailed procedures adopted for mixing mixtures and mortars.

4.2.1.2. Slurries

The mixing of slurries was carried out directly inside the Brookfield viscometer container, both manually and mechanically. Firstly, water and mineral additions were stirred by hand for 10 s. The emulsion was then added and hand-stirred for 20 s. Finally, mechanical mixing was directly carried out with the Brookfield viscometer at 100 rpm for 120 s using the impeller.

4.2.2. Compaction

Compaction of mixtures and mortar specimens started immediately after the mixing end and was performed using a Superpave gyratory compactor (SGC). The adopted protocol required constant pressure of 600 kPa, gyration speed of 30 rpm and an inclination angle of 1.25° . Moulds with a diameter of 150 mm and 100 mm were employed to compact mixtures and mortars, respectively. The height of the specimens was measured at each gyration, allowing monitoring of the volumetric properties of CBE materials. To control the volumetric properties of the specimens, compaction was performed in fixed height mode. To check possible material loss during compaction, the mass of the mould containing the loose material before compaction was compared with the mass of the mould containing the compacted specimen.

4.2.3. Curing

The curing of mixtures and mortars specimens was carried out in climate chambers at controlled temperature and RH. Curing temperatures of (25 ± 2) °C was mainly adopted. Two curing environmental humidity conditions were considered: unsealed specimens (free evaporation) and sealed specimens inside plastic bags (coded as S). In the first curing condition, the process occurs at the RH of the climatic chamber, i.e. $(70 \pm 5)\%$. In this case, the free water evaporation promotes emulsion breaking. On the contrary, RH is close to 100% for the sealed specimens. In such a case, cement hydration is favoured, and water evaporation is not noteworthy. Accordingly, it was presumed that bituminous bonds were more developed in unsealed specimens, whereas cementitious bonds were more developed in sealed specimens (Appendix D). The two conditions investigated were chosen to represent two limiting field conditions: the former reproduced the situation in which the water is free to evaporate. The latter reproduced the application of a protection sheet or the placing of a new layer above the CBE mixture layer. In some cases, the curing temperature of (40 ± 2) °C and $(30 \pm 5)\%$ RH were used to carry out accelerated curing.

According to the objective of each section, several curing times, temperatures and RH were considered to get an overall frame of CBE materials curing behaviour. The specific curing protocol is specified at the beginning of each section. The curing process was modelled over time using the modified version of the Michaelis-Menten model (Equation (2.2) detailed in Section 2.1.3.1).

CBE slurries study focused on their fresh state behaviour. Therefore, no curing protocols were adopted.

4.3. Volumetric analysis

The volumetric properties of CBE mixtures and mortars are generally defined by applying the approach used for CTM, based on the dry bulk density of the material ρ_d . Such an approach does not suit CBE materials satisfactory because the presence of the bitumen is not considered properly. The volumetric analysis adopted in this thesis comes from the standard procedure adopted for the mix design of HMA mixtures (EN 12697-08). This approach takes into account:

- The air void content, i.e. the volume occupied by air respect of the bulk volume of the compacted specimen, calculated as a percentage of the total volume;
- The voids in the mineral aggregate, i.e. the volume of intergranular voids in the HMA compacted specimen. They involve both air voids and bitumen volume, calculated as a percentage of the total volume;
- The voids in the mineral aggregate filled with bitumen.

The approach can be used for CBE materials with some adjustment (Grilli *et al.* 2012, 2016). Indeed, if the volumetric properties at the cured state of CBE materials can be obtained using the same relation adopted for HMA, some additional assumption must be introduced in the fresh-state analysis because of the presence of the water bitumen emulsion and cement.

4.3.1. Fresh state CBE mixtures and mortars

The volumetric analysis of CBE mixtures and mortars in the fresh-state refers to the mixing and compaction phase. Thus, it can be assumed that no significant water evaporation occurs.

As mixing and compaction take place at ambient temperature, residual bitumen droplets are solid and cannot be absorbed by the aggregate, which is already in SSD condition. Moreover, in the common cold mixing practices, aggregates are not dried or heated, and thus, their pores are saturated by water yet. However, bitumen droplets are dispersed in water and consequently are considered part of the liquids for the purpose of analysing. Because of the mixing temperature, RA aggregate is assumed to act as a black rock (Section 2.1.2.3).

It is necessary to make a few considerations also about the water. As previously explained (Section 4.1), intergranular water includes both the emulsion water and the part of the additional water. The remaining part, which is absorbed by the aggregate, must be considered in the volume of the aggregate itself. Then, for what concerns the aggregates, the particle SSD density ρ_{ssd} is considered.

Figure 4.2 shows the typical composition of a specimen of CBE mixture or mortar. The mass (volume) of the solids M_s (v_s) is given by the sum of the mass (volume) of the SSD aggregate M_{ag} (v_{ag}), filler M_f (v_f) and unhydrated cement $M_{c,u}$ ($v_{c,u}$). The liquid part is formed by the mass (volume) of the residual bitumen of the emulsion M_B (v_B) and the mass of the intergranular water $M_{w,i}$ ($v_{w,i}$). Besides, $v_{w,i}$ and the volume occupied by the air voids v_A forms the non-structural part of the specimen.

By analogy to the volumetric approach used for HMA, for the volumetric characterisation of fresh CBE mixtures and mortars can be introduced:

- the Voids in the Mixture V_m , representing the volume fraction that is occupied by air and intergranular water:

$$V_m = \frac{v_A + v_{w,i}}{v} \cdot 100 = \frac{v - (v_s + v_B)}{v} \cdot 100 \quad (4.1)$$

- the Voids Filled with Liquids VFL , representing the fraction of voids occupied by residual bitumen and intergranular water:

$$VFL = \frac{v_B + v_{w,i}}{v_A + v_B + v_{w,i}} \cdot 100 = \frac{v_B + v_{w,i}}{v - v_s} \cdot 100 \quad (4.2)$$

During compaction, V_m decreases, whereas VFL increases (**Figure 4.3a**). When the value of VFL is 100%, the specimen reaches its theoretical saturation condition. However, previous

studies proved that when the value of VFL is about 85 - 90%, a loss of material (water, bitumen droplets and fines) occurs from the mould (**Figure 4.3b**). Such observation denotes that there is always a small amount of entrapped air due to the not interconnected voids. Consequently, for a correct design of CBE mixtures and mortars, the practical saturation limit of $VFL = 85-90\%$ must be considered to avoid altering their composition in the compaction process. (Graziani *et al.* 2016, Grilli *et al.* 2016).

In this study, the number of gyrations and a minimum V_m corresponding to $VFL = 85 - 90\%$ (N_{des} and $V_{m,min}$) were considered the practical compaction limit for a given specimen composition (**Figure 4.3a**). In this way, the specimen did not show any water leakage at the end of the compaction (**Figure 4.3c**). The material loss (Section 4.2.2) during compaction was lower than 0.5%, which is considered a practical limit for the specimen composition alteration (Graziani *et al.* 2016).

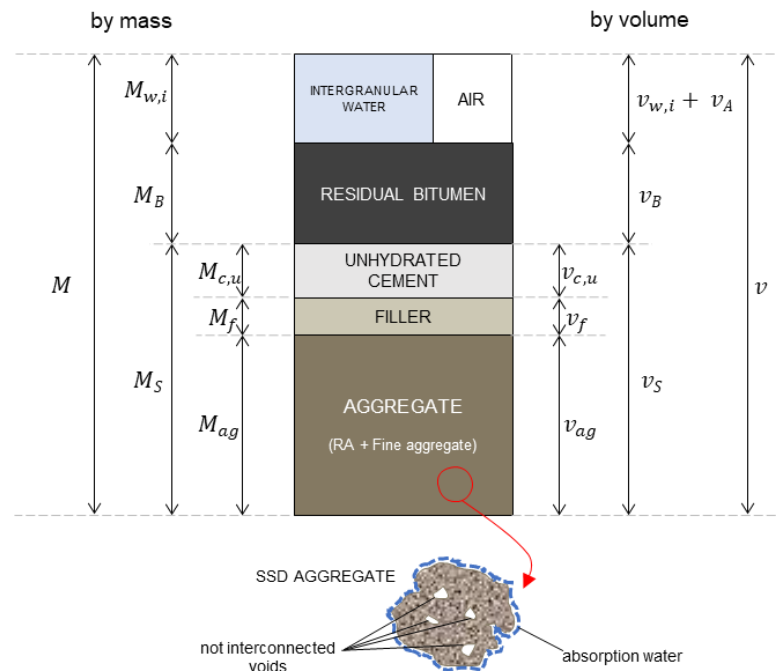


Figure 4.2. CBE mixtures and mortars composition at the fresh state (by mass and by volume)

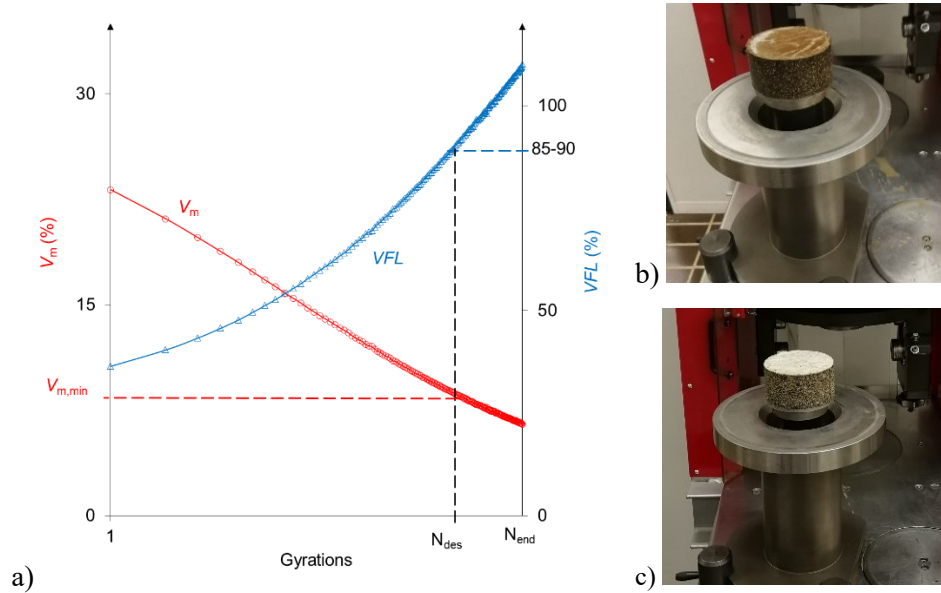


Figure 4.3. Volumetric analysis of fresh CBE materials: a) volumetric properties progress during compaction (Equations (4.1) and (4.2)), b) specimen aspect right after compaction with $VFL > 90\%$, c) specimen aspect right after compaction with $VFL < 90\%$

4.4. CBE materials composition

4.4.1. Mixtures

The composition of the mixtures investigated within this thesis was based on the typical composition adopted in Italy for CBE mixtures suitable for base and binder layers (Autostrade per l'Italia 2013, Provincia autonoma di Bolzano 2016, Ferrotti, Grilli, *et al.* 2020).

In the present work, three aggregate blends were considered, all obtained by using a high RA amount (>70%):

- CC: a continuous curve, i.e. dense graded, with NMAS 16 mm, derived from the Fuller-Thompson reference distribution;
- GG: a gap-graded distribution with NMAS 16 mm, derived from specifications for stone mastic asphalt. Its coarse fraction was constituted by RA 2/16, whereas the fine fraction was natural aggregate;

- GGallRA: a gap-graded distribution with NMAS 16 mm, and both coarse and sand fraction constituted by RA aggregate.

The CC distribution was adopted as a reference because it fits the grading envelopes suggested by the Italian technical guidelines (Autostrade per l'Italia 2013, Provincia Autonoma di Bolzano 2016). The GG distribution was considered because it was found that an increase in the filler dosage could enhance the workability and compactability of the loose mixture and the consequent improvement of its physical properties (i.e. lower voids) (Raschia, Mignini, *et al.* 2019). The GGallRA distribution was considered to evaluate the potential effect on the rheological response of a higher content of aged bitumen. Appendix E discusses the effect of different gradings on the physical and mechanical response of CBE mixtures. **Table 4.1** reports the compositions of the aggregate blends investigated. **Figure 4.4** depicts the three grading distributions.

Several mixtures were investigated depending on the specific aim of the investigation. **Table 4.2** summarises their gravimetric composition, as well as their volumetric properties. Apart from the cementitious binder type, the mixture MIX1b (MIX2b) differed from MIX1a (MIX2a) only for the total water dosage. MIX1a, MIX1b, MIX2a, MIX2b are suitable for base courses in low-medium traffic roads and subbase courses in high traffic roads because of their binders dosage. Appendix C deals with the study for establishing their composition in terms of water and air voids content. Mixtures from MIX3 to MIX5 had higher binder dosages and are intended to be also used as binder courses in low-high traffic roads and base layers in very high traffic roads. Details about selecting the composition of mixtures MIX3 and MIX4 can be found in Appendix E and Appendix F. Nevertheless, all the mixtures had a B/C ratio ranging between 0.8 and 1.3, indicating a balance between the two co-binders. Thus, the investigated mixtures characteristics are halfway between those of HMA mixtures and cement-treated mixtures. According to the classification described in Section 2.1.1.2, all the mixtures investigated were CBTM.

CBE mixtures were coded using an alphanumeric code:

- Mixture composition (MIX_i, with $i = 1a, 1b, \dots, 5$);
- Type of cement (C_i, with i from 1 to 4).

For example, the code MIX2b-C4 identifies the mixture obtained considering the CC grading distribution, 2.5% of cement C4, 3.3% of emulsion B (B/C = 0.8), 3.7% of total water and $V_m = 11\%$.

Chapter 4
Materials and Methods

Multiscale Approach for Characterising the Behaviour of Cold Bitumen Emulsion Materials

Table 4.1. Gravimetric composition of the aggregate blends of the mixtures

ID	Type	Composition
CC	Continuous curve	80% RA0/16, 17% sand, 3% filler
GG	Gap graded	70% RA2/16, 20% sand, 10% filler
GGallRA	Gap graded	70% RA2/16, 25% RA 0/2, 5% filler

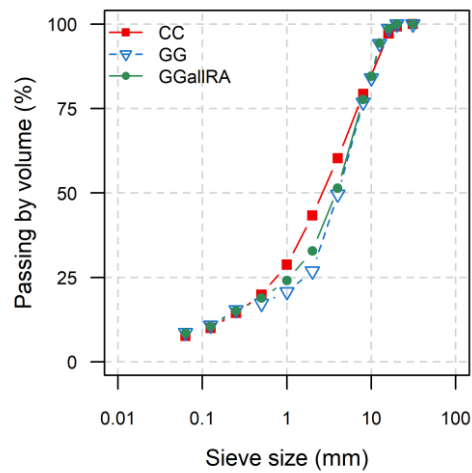


Figure 4.4. Mixtures grading distributions

Chapter 4
Materials and Methods

Multiscale Approach for Characterising the Behaviour of Cold Bitumen Emulsion Materials

Table 4.2. Composition of mixtures investigated within the thesis

ID	Grading (-)	Cement		Emulsion (Residual bitumen)		B/C (-)	w_t^* (%)	V_m (%)
		Type (-)	Dosage* (%)	Type (-)	Dosage* (%)			
MIX1a	CC	C1, C2	1.5	B	3.3 (2.0)	1.3	4.7	11.0
MIX1b	CC	C3,C4	1.5	B	3.3 (2.0)	1.3	3.7	11.0
MIX2a	CC	C1, C2	2.5	B	3.3 (2.0)	0.8	4.7	11.0
MIX2b	CC	C3,C4	2.5	B	3.3 (2.0)	0.8	3.7	11.0
MIX3	CC	C2, C3	2.5	BP	5.0 (3.0)	1.2	4.5	9.5
MIX4	GG	C2,C3	2.5	BP	5.0 (3.0)	1.2	4.0	9.5
MIX5	GGallRA	C2,C3	2.5	BP	5.0 (3.0)	1.2	4.0	9.0

*by dry aggregate mass

4.4.2. FAM mortars

FAM mortar composition was derived from the mixture composition for being representative of the real FAM existing in the mixture. The FAM mortar aggregate blend was simply obtained by removing the coarse aggregate (here assumed particles larger than 2 mm). **Table 4.3** and **Figure 4.5** report the composition of the mortars aggregate blends and their grading distributions, respectively. The study of mortar composition in terms of binders, water and air voids content, was one of the objectives of the present investigation and thus, it is discussed in Chapter 5. From the investigation, the design mortar compositions summarised in **Table 4.4** were derived.

The CBE mortars were coded using an alphanumeric code:

- Mortar composition (FAM_i, with i = 1a, 1b, ...5);
- Type of cement (C_i, with i from 1 to 4).

For example, the code FAM4-C2 identifies the mortar derived from the mixture MIX4-C2 considering the GG grading distribution, 2.5% of cement C2 by mass (9.5% in the FAM), 5.0% of emulsion BP by mass (19% in the FAM, B/C = 1.2), 4.7% of total water by mass (9.1% in the FAM) and voids of the FAM $V_m = 18.4\%$.

Chapter 4

Materials and Methods

Multiscale Approach for Characterising the Behaviour of Cold Bitumen Emulsion Materials

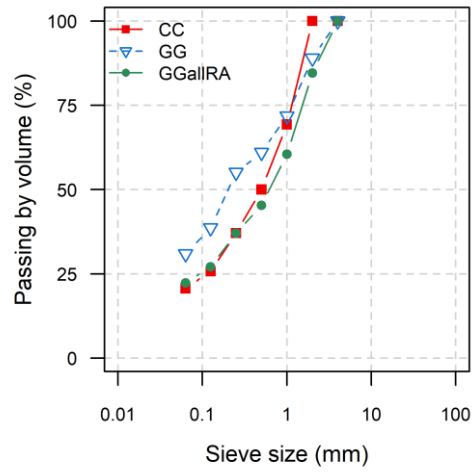


Figure 4.5. FAM mortars grading distributions

Table 4.3. Gravimetric composition of the aggregate blends of FAM mortars

ID	Type	Composition
CC	Continuous curve	61% RA0/2, 32% sand, 7% filler
GG	Gap graded	63% sand, 37% filler
GGallRA	Gap graded	83% RA 0/2, 17% filler

Chapter 4
Materials and Methods

Multiscale Approach for Characterising the Behaviour of Cold Bitumen Emulsion Materials

Table 4.4. Composition of FAM mortars investigated within the thesis

ID	Grading (-)	Cement		Emulsion (Residual bitumen)		B/C (-)	w_t^* (%)	V_m (%)
		Type (-)	Dosage* (%)	Type (-)	Dosage* (%)			
FAM1a	CC	C1, C2	3.5	B	7.8 (4.7)	1.3	6.9	14.1
FAM1b	CC	C3,C4	3.5	B	7.8 (4.7)	1.3	6.9	15.8
FAM2a	CC	C1, C2	5.9	B	7.8 (4.7)	0.8	6.9	14.1
FAM2b	CC	C3,C4	5.9	B	7.8 (4.7)	0.8	6.9	15.8
FAM3	CC	C2, C3	5.9	BP	11.8 (7.1)	1.2	6.5	13.2
FAM4	GG	C2,C3	9.5	BP	19.0 (11.4)	1.2	9.1	18.4
FAM5	GGallRA	C2,C3	8.3	BP	16.7 (10.0)	1.2	8.4	16.3

*by dry aggregate mass

4.4.3. Slurries

CBE slurries composition was derived starting from the typical compositions of CBE mixtures which are summarised in **Table 4.5** in terms of bitumen, mineral additions and water content by mass of dry aggregates (Bocci *et al.* 2011, Fang, Garcia-Hernandez, Winnefeld, *et al.* 2016, Dolzycki *et al.* 2017). The corresponding values of the mass ratios are also reported. Both emulsions B and BP were used during the investigation, whereas only cement C1 was considered. For each emulsion, a total of 26 dispersions were investigated to enclose the ranges of CBE mixtures composition shown in **Table 4.5**. Four types of dispersions were considered:

- Bitumen emulsion and bitumen emulsion diluted with water;
- Bitumen emulsion diluted with water plus limestone filler;
- Bitumen emulsion diluted with water plus Portland cement;
- Bitumen emulsion diluted with water plus limestone filler and Portland cement.

Table 4.6 reports the composition of all dispersions studied in term of mass ratio and volume fraction. The volume fraction of each component was obtained as the ratio between the volume of the component and the total volume of the dispersion. For this study, bitumen droplets were considered among the solids and thus, concurred in calculating the solid particles volume fractions φ_s jointly with the mineral additions. All the slurries investigated were produced from the same liquid phase. The selected dilution of emulsion and water was

Chapter 4
Materials and Methods

Multiscale Approach for Characterising the Behaviour of Cold Bitumen Emulsion Materials

characterised by the water/residual bitumen (W/B) ratio of 1.3. Such value was adopted because it is intermediate among the possible ratios.

The CBE dispersions were coded using a two-section alphanumeric code. The first section designates the components of the dispersion:

- Type of bitumen emulsion (B = plain, BP = modified);
- Dilution of water (W);
- Type of additions (F = limestone filler, C = Portland cement).

The second section defines the volume fraction of solid particles. For example, the code BPWFC_615 identifies a CBE slurry obtained by mixing modified bitumen emulsion water, filler and cement with a concentration of the solid particles phase equal to 0.615.

Table 4.5. Typical compositions of CBE mixtures derived from scientific literature

<i>CBE mixtures typical composition</i>		
Component	Lower limit By mass (%)	Upper limit By Mass (%)
Residual bitumen (B)	1.8	3.0
Cement (C)	0.0	6.0
Filler (F)	5.0	10.0
Water (W)	3.0	6.0
<i>CBE mixtures typical mass ratios</i>		
Ratios	Lower limit Mass ratio	Upper limit Mass ratio
Residual bitumen/Cement (B/C)	0.3	
Residual bitumen/Filler (B/F)	0.18	0.60
Cement/Filler (C/F)	0	0.60
Water/Residual bitumen (W/B)	0.56	1.67
Water/Cement (W/C)	1.00	
Water/Filler (W/F)	0.30	1.00

Table 4.6. Composition by mass and volumetric fractions of the CBE dispersions (bitumen emulsions and slurries)

Mass ratio					Volume fraction				Density	
B/F	B/C	W/B	W/F	W/C	W	B	F	C	φ_s	(Mg/m ³)
<i>Emulsion + Water</i>										
		0.7			0.404	0.596	0.000	0.000	0.596	1.008
		1.3			0.575	0.425	0.000	0.000	0.425	1.005
		2.0			0.671	0.329	0.000	0.000	0.329	1.003
		2.7			0.730	0.270	0.000	0.000	0.270	1.002
<i>Emulsion + Water + Limestone filler</i>										
0.9		1.3	1.2		0.489	0.361	0.150	0.000	0.511	1.252
0.6		1.3	0.8		0.450	0.332	0.218	0.000	0.550	1.363
0.4		1.3	0.6		0.420	0.309	0.271	0.000	0.580	1.450
0.4		1.3	0.5		0.400	0.295	0.305	0.000	0.600	1.506
0.3		1.3	0.4		0.385	0.284	0.331	0.000	0.615	1.549
0.3		1.3	0.4		0.370	0.273	0.357	0.000	0.630	1.592
0.3		1.3	0.4		0.360	0.265	0.375	0.000	0.640	1.621
0.3		1.3	0.3		0.350	0.258	0.392	0.000	0.650	1.650
0.2		1.3	0.3		0.335	0.247	0.418	0.000	0.665	1.692
0.2		1.3	0.3		0.320	0.235	0.445	0.000	0.680	1.737
0.2		1.3	0.2		0.300	0.221	0.479	0.000	0.700	1.792
<i>Emulsion + Water + Portland cement</i>										
	6.4	1.3		8.5	0.563	0.415	0.000	0.022	0.437	1.049
	2.4	1.3		3.2	0.544	0.400	0.000	0.056	0.456	1.117
	1.5	1.3		2.0	0.525	0.387	0.000	0.088	0.475	1.182
	1.1	1.3		1.4	0.507	0.374	0.000	0.119	0.493	1.244
	0.8	1.3		1.1	0.489	0.360	0.000	0.150	0.511	1.307
	0.5	1.3		0.7	0.450	0.332	0.000	0.218	0.550	1.444
<i>Emulsion + Water + Limestone filler + Portland cement</i>										
1.1	5.4	1.3	1.4	7.2	0.489	0.360	0.128	0.022	0.511	1.261
0.7	3.4	1.3	0.9	4.6	0.450	0.332	0.186	0.033	0.550	1.376
0.5	2.6	1.3	0.7	3.4	0.420	0.310	0.230	0.040	0.580	1.464
0.4	1.9	1.3	0.5	2.6	0.385	0.284	0.281	0.049	0.615	1.567
0.3	1.6	1.3	0.4	2.1	0.360	0.265	0.318	0.056	0.640	1.641

4.5. Test methods

4.5.1. Water loss by evaporation

The water loss by evaporation (DW) of each mixture and mortar specimen was determined by weighing the specimens:

$$DW = \frac{M_0 - M_i}{M_W} \cdot 100 \quad (4.3)$$

where M_0 is the specimen mass right after the end of the compaction, M_i is the specimen mass after i curing days, and M_W is the total mass of water in the specimen (obtained from its gravimetric composition).

4.5.2. Indirect Tensile Stiffness Modulus

Quick measurements of the stiffness of mixtures and mortars were obtained by measuring the indirect tensile stiffness modulus ($ITSM$). $ITSM$ was measured using a servo-pneumatic machine, according to EN 12697-26 (Appendix C) (**Figure 4.6a**). Repeated load pulses, having haversine waveform, were applied. The rise time was 124 ms and the pulse repetition period was 3.0 s. The peak load was adjusted using a closed-loop control system to achieve a target peak horizontal deformation. The specimen horizontal diametral deformation due to the application of the load pulse was measured using two Linear Variable Differential Transducers (LVDT). Before the test, the system applied ten conditioning pulses for regulating the load magnitude and duration to give the target horizontal deformation and rise time.

For each specimen, the test was repeated along two diameters, and the average $ITSM$ value was calculated:

$$ITSM = \frac{F \cdot (v + 0.27)}{z \cdot h} \quad (4.4)$$

where F is the peak load of the applied repeated pulse, z is the amplitude of the horizontal deformation, h is the mean thickness of the specimen and v is the Poisson ratio

In this investigation, the target peak horizontal deformation was fixed as 2 microns, v was assumed to be 0.35 or 0.30 depending on the material investigated. The testing temperature was 25 °C.

4.5.3. Indirect Tensile Strength

The strength of mixtures and mortars was obtained by measuring the indirect tensile strength (ITS). The ITS was measured using a servo-hydraulic testing machine according to EN 12697-23 (**Figure 4.6b**). A constant rate of deformation of (50 ± 2) mm/min was applied

along the two generatrices of the cylindrical specimen until failure. Assuming that the stress has a constant distribution across the vertical load application plane and that the load applied is continuous, *ITS* value was calculated:

$$ITS = \frac{2 \cdot P}{\pi \cdot D \cdot h} \quad (4.5)$$

where P is the maximum load, D is the specimen diameter, and h is its mean thickness. The testing temperature was 25 °C.



Figure 4.6. CBE mixtures and mortars mechanical testing: a) *ITSM* test, b) *ITS* test

4.5.4. Complex modulus

The stiffness of mixtures and mortars and their temperature-frequency dependence were evaluated by measuring the complex modulus $E^*(\omega)$ through cyclic uniaxial compression tests. $E^*(\omega)$ was measured using an AMPT PRO system (**Figure 4.7c**). Tested specimens had 75 mm in diameter (**Figure 4.7a**). These were obtained by coring 150 and 100 mm SGC specimens of mixtures and mortars, respectively, after long-term curing (**Figure 4.7b**). The equipment measured the axial stress with a load cell. Three LVDT placed 120° apart

measured the axial strain in the middle part of the specimen, considering a measuring base of 70 mm (**Figure 4.7d**). A haversine compression loading was applied to obtain the target strain amplitude (Section 2.1.4).

The testing temperatures were 5, 15, 25, 35, 45 and 55 °C. The testing frequencies were 10, 5, 1, 0.5, 0.1 Hz and the target strain amplitude was $30 \cdot 10^{-6}$ mm/mm. 20 loading cycles were applied at each test frequency.

4.5.4.1. Data analysis: construction of the master curves and rheological modelling

As CBE materials were found thermo-rheologically simple, the TTSP was applied for obtaining the master curves of $E_0(\omega)$ or $\delta(\omega)$, describing the LVE response at a reference temperature T_{ref} (see Section 2.1.4). The data measured at each temperature T were horizontally shifted according to Equation (2.9). In this study, for $E_0(\omega)$ master curve construction, $T_{ref} = 25$ °C was considered, and the values of the shift factors at each temperature $a_{T_{ref}}(T)$ (function of T and T_{ref}) were determined using the CFS algorithm, when applicable (see section 2.1.4.1). The manual procedure was applied only when the experimental data did not overlap, and thus the CFS could not be applied. The master curves of $\varphi(\omega)$ were then obtained using the same shift factors values calculated for $E_0(\omega)$.

The temperature dependency of the obtained a_T was modelled using the Williams-Landel-Ferry (WLF) model:

$$\log(a_{T_{ref}}) = -\frac{C_1(T - T_{ref})}{C_2 + T - T_{ref}} \quad (4.6)$$

where C_1, C_2 are constants obtained by least-squares fitting (Ferry 1980).

The complex modulus data were fitted using a modified version of the rheological 2S2P1D model (2.1.4.2) which will be discussed in Chapter 7.

Chapter 4
Materials and Methods



Figure 4.7. Complex modulus testing: a) mixtures specimens, b) FAM mortar specimen coring, c) AMPT PRO device, d) testing configuration detail

4.5.5. Viscosity

The viscosity η of CBE slurries and emulsions was measured using two Brookfield DV-II PRO Digital Viscometers: a low torque (LV model) and high torque (HA model) viscometers (**Figure 4.8a**). The LV model allows for testing low viscosity fluids (100% torque = 0.00006737 N m). The HA model is designed for medium-high viscous fluids (100% torque = 0.0014374 N m). The viscosity measurement accuracy, specified by the manufacturer, is 1% of the full-scale range.

η quantifies the resistance to the flow of a material. It is defined as the ratio between the shear stress τ and shear rate $\dot{\gamma}$:

$$\eta = \frac{\tau}{\dot{\gamma}} \quad (4.7)$$

If η is measured using a rotational viscometer in co-axial cylinder configuration, $\dot{\gamma}$ is different in each point of the testing vessel. For a cylindrical geometry:

$$\dot{\gamma} = \frac{2 \omega R_c^2 R_s^2}{\chi^2 (R_c^2 - R_s^2)} \quad (4.8)$$

$$\tau = \frac{T}{2\pi R_s^2 L} \quad (4.9)$$

where ω is the angular velocity of the impeller, R_c and R_s are the radii of the container and the impeller, respectively, T is the torque measured by the viscometer, χ is the radius at which $\dot{\gamma}$ is measured, and L is the effective length of the impeller.

When different geometries are adopted, Equations (4.8) and (4.9) lose their validity. To overcome this issue, Brookfield suggests to adopt an alternative method for obtaining an average value of $\dot{\gamma}$ based on the Metzner and Otto method (Lo Presti *et al.* 2014):

$$\dot{\gamma} = \text{SRC} \cdot N = \text{SRC} \left(\frac{60}{2\pi} \right) \omega \quad (4.10)$$

where N is the rotational speed, and SRC is the shear rate constant, linked to the impeller geometry. Therefore, the apparent viscosity can be obtained as follows:

$$\eta = \frac{0.1}{N} T\% \cdot \text{SMC} \cdot \text{TK} \omega \quad (4.11)$$

where $T\%$ is the percentage of the maximum torque bearable by the viscometer. SMC is the spindle multiplier constant (function of the impeller geometry), and TK is the torque constant, depending on the viscometer type (0.09373 and 2 for LV and HA model, respectively).

Two DHR impellers (DHR_2 and DHR_3), developed at the University of Nottingham (Medina *et al.* 2020), were used to measure the apparent viscosity of the dispersions. The standard spindle S27 (**Figure 4.8b**) was used as well, and its results were

Chapter 4

Materials and Methods

Multiscale Approach for Characterising the Behaviour of Cold Bitumen Emulsion Materials

compared with those obtained using the novel DHR impellers. The SRC value (Equation (4.10)) is 0.34 for both impellers (Giancontieri *et al.* 2020). The SMC values (Equation (4.11)) are 11.5 and 9.5 for DHR_2 and DHR_3, respectively, and 25 for S27.

Measurements in controlled shear rate test modality were carried out at room temperature. Three replicate specimens were tested for each dispersion. The definition of the testing procedure was an object of investigation within this thesis and will be detailed in Chapter 8.

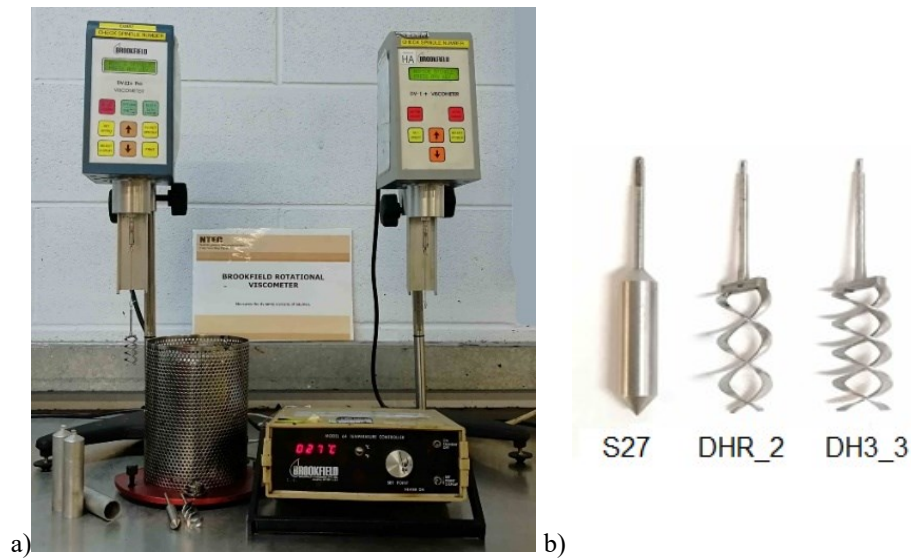


Figure 4.8. CBE slurries viscosity testing equipment a) Brookfield viscometers employed in the experimental study: LV model (on the left) and HA model (on the right) b) impellers used within the experimental study

Chapter 5.

Mixture to FAM Mortar Downscaling

5.1. Introduction

As noted in the literature review, a common agreement about the FAM mortars composition does not exist either for HMA and cold materials. However, it is crucial to properly define mortar composition, as it greatly influences its final properties. This Chapter introduces a methodology for downscaling from CBE mixtures to the correspondent FAM mortars. The composition of FAM mortars was defined based on observations about the impact of the volumetric properties on their early-age mechanical response.

5.2. Objectives

The objective of this part of the thesis was to identify a methodology for defining the composition of CBE FAM mortars that closely describes the fine matrix of CBE mixtures. Eight CBE mixture compositions, obtained with four types and two cement dosages, were considered for this aim. For each mixture, nine potential FAM mortar compositions were proposed and investigated. The focus was on the effect of water and air voids on their early-age strength. Finally, the design mortars compositions were selected. Such obtained FAM mortars were used for evaluating their potential predicting ability of curing behaviour and LVE properties of CBE mixtures (Chapter 6 and Chapter 7).

5.3. Methodology

The composition of the FAM mortars was obtained by considering the mixture as a three-phase composite (**Figure 5.1**), consisting of:

- FAM mortar (Phase I);
- Coarse aggregate inclusions (Phase II);
- External voids (Phase III).

The FAM mortar was considered the continuous binding phase of the composite and was conceptually obtained by removing the coarse aggregate from the mixture. It had a NMAS

of 2 mm and included all the bituminous and cementitious binders of the mixture. **Figure 4.5** reports the FAM grading distributions. The voids of the mixture (i.e. air and intergranular water) were divided in two parts: those that were part of the FAM and those that constituted the Phase III, here called external voids (**Figure 5.1**).

Figure 5.2 describes the experimental programme organisation. Starting from the gradation and composition of eight mixtures, i.e. MIX1a, MIX1b, MIX2a, MIX2b (reported in **Table 4.1** and **Table 4.2**), the derived cement dosages were 3.5% and 5.9%. Under the assumption that all binders are contained in the FAM mortar, the emulsion dosage was 7.8% (corresponding to 4.7% of residual bitumen). Therefore, FAM mortars had the same B/C ratios as the corresponding mixtures: 1.3 and 0.8.

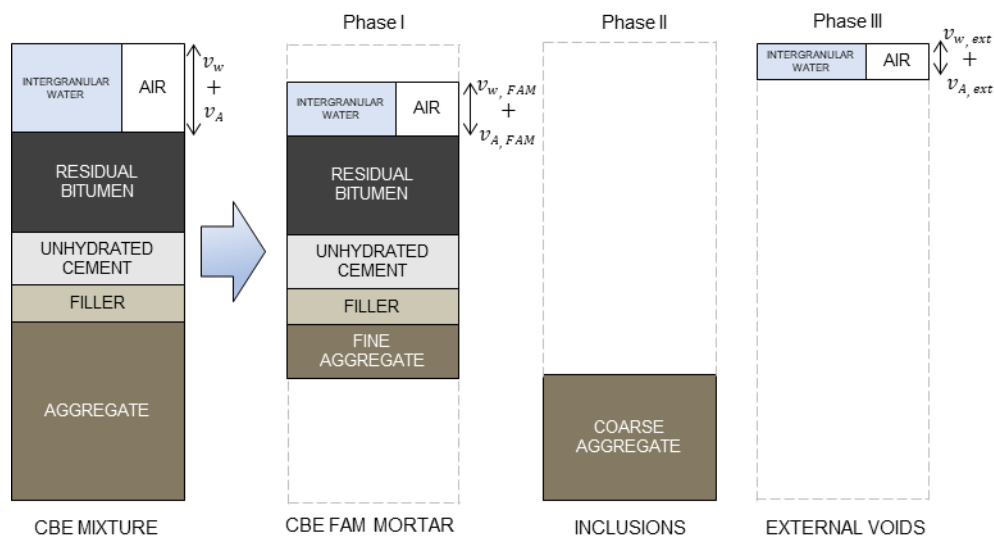


Figure 5.1. CBM mixture and FAM mortar volumetric composition model (fresh state)

To investigate the influence of the voids content on the FAM properties, nine mortars were produced and tested for each mixture. Each mortar composition was characterised by different water and air voids fractions (**Table 5.1**). The mortars characterised by $v_{w, FAM} / v_{w, mixture} = 1.00$ and $v_{a, FAM} / v_{a, mixture} = 1.00$ contained all the water and all the air voids of the mixture. According to the mixture general model depicted in **Figure 5.1**, in this case, Phase III would not be present, and the mixture would be a two-phase composite. On the other hand, mortars characterised by $v_{a, FAM} / v_{a, mixture} = 0$ were compacted, trying to remove all the air voids and reach saturation. In this case, all the air of the mixture would be included in Phase III. As explained in Section 4.3.1, the latter condition was impossible to obtain in practice, and thus a small amount of entrapped air voids was always included

in the FAM mortar specimens. Other limits came from practical issues. Indeed, during production, FAM mortars produced only with the emulsion water were too dry, resulting in difficulty to mix. As a consequence, additional water was always used. Specifically, for mortars produced with binders C1 and C2, the minimum gravimetric water content was 6.9% (corresponding to $v_{W,FAM} / v_{W,mixture} = 0.77$). For mortars produced with C3 and C4, the minimum gravimetric water content was 5.8% (corresponding to $v_{W,FAM} / v_{W,mixture} = 0.84$).

The *ITS* was measured on all materials after 1 day of unsealed curing at 25 °C and, based on the volumetric and mechanical properties, a final representative FAM mortar composition for each mixture was selected.

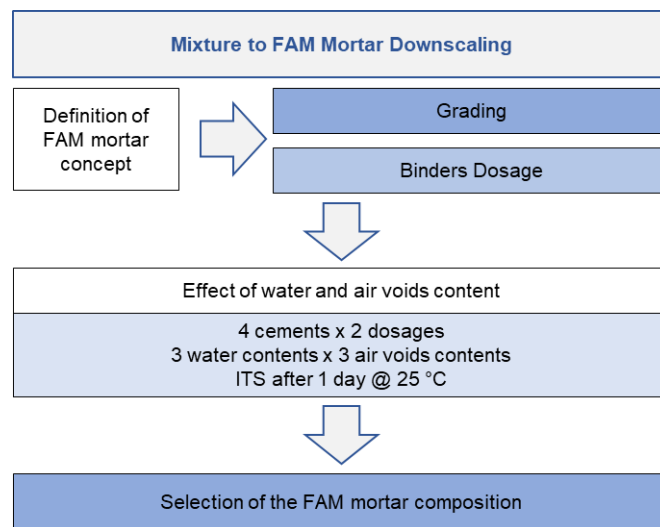


Figure 5.2. Mixture to FAM mortar downscaling: experimental programme organisation

Table 5.1. Water and air voids fractions adopted for the trial FAM mortar compositions

C1 – C2			C3 – C4		
w_t^* (%)	$v_{W,FAM} / v_{W,mixture}$	$v_{A,FAM} / v_{A,mixture}$	w_t^* (%)	$v_{W,FAM} / v_{W,mixture}$	$v_{A,FAM} / v_{A,mixture}$
9.4	1.00	1.00	7.1	1.00	1.00
		0.50			0.50
		0.00			0.00
8.2	0.89	1.00	6.5	0.93	1.00
		0.50			0.50
		0.00			0.00
6.9	0.77	1.00	5.8	0.84	1.00
		0.50			0.50
		0.00			0.00

*) dosage by dry aggregate mass

5.4. Analysis of the Results

Figure 5.3 and **Figure 5.4** show the *ITS* values obtained after 1 day of curing on the nine trial mortars (**Table 5.1**) produced starting from each mixture. The ratio between the *ITS* of FAM mortar and mixture ($ITS_{FAM} / ITS_{mixture}$) is reported as a function of the air voids fraction contained in the FAM mortar ($v_{A,FAM} / v_{A,mixture}$).

Figure 5.3 depicts the results for the mortars produced using all the water contained in the mixtures ($v_{W,FAM} / v_{W,mixture} = 1.00$). When the mortars included all the air voids of the mixture ($v_{A,FAM} / v_{A,mixture} = 1.00$), the *ITS* ratios ranged between 0.47 and 0.71. With this FAM mortar composition, the mixture would be a two-phase composite, and thus *ITS* ratios highlight the reinforcing effect of the coarse aggregate. Reducing the air voids fraction contained in the mortar, the ratio $ITS_{FAM} / ITS_{mixture}$ increased. In fact, decreasing $v_{A,FAM} / v_{A,mixture}$ implies that a fraction of air is subtracted from Phase I (FAM) and added to Phase III (external voids). This led to an increase in ITS_{FAM} , whereas $ITS_{mixture}$ was constant because the mixture composition is always the same. In **Figure 5.3**, it can be noticed that FAM mortars produced with binders C3 and C4 had higher *ITS* ratios than those produced with binders C1 and C2 when the air void volume was reduced. To explain this result, one should bear in mind that mixtures with the cements C1 and C2 had higher water content and, since V_m of the mixtures was fixed, the volume of air voids was lower (**Table 4.2**). As a consequence, the corresponding mortars also had higher water content than those produced with binders C3 and C4. Since the water volume is not a structural component, the latter FAM mortars will be more resistant compared to the corresponding mixture. Besides,

reducing air voids in FAM mortars with C3 and C4 was relatively higher, leading to a lower V_m value and consequently enhanced mechanical response. These considerations are valid for both B/C ratios.

Figure 5.4 shows the results obtained on the FAM mortars produced with binders C2 and C3 and B/C=1.3. The reduction of the water fraction in the FAM mortars $v_{W,FAM} / v_{W,mixture}$ always led to an increase in the ITS ratio. As explained above, decreasing $v_{W,FAM} / v_{W,mixture}$ implies that a fraction of water is subtracted from Phase I (FAM) and added to Phase III (external voids). Therefore, ITS_{FAM} increased, whereas $ITS_{mixture}$ was constant because the mixture composition does not change.

Figure 5.3 and **Figure 5.4** outline the effect of water and air voids content on the FAM mortars properties after 1 day of curing. Based on these results, a univocal FAM mortar composition to investigate the curing process and the LVE behaviour was selected: the grading distribution was obtained considering all the aggregate passing the 2 mm sieve, all the bitumen emulsion and all cement were contained in the FAM mortar. As regards the air voids content, there were two limiting options: $v_{A,FAM} / v_{A,mixture} = 0.00$ and $v_{A,FAM} / v_{A,mixture} = 1.00$. The first would imply that the FAM is a saturated mortar, and thus, all the mixture air voids, even the smallest ones, are part of the external voids (Phase III). The second would imply that all the mixture air voids, even the largest ones, are part of the FAM. Since both these conditions may be unrealistic, the intermediate configuration was chosen: $v_{A,FAM} / v_{A,mixture} = 0.50$. As regards the water content, the option $v_{W,FAM} / v_{W,mixture} = 1.00$, i.e. all the water in the mixture is part of the FAM, was excluded for the same reason given above for air voids. To avoid the effect of different water content highlighted in **Figure 5.3**, all the FAM mortars were manufactured with the same gravimetric water dosage of 6.90%. This corresponds to values of $v_{W,FAM} / v_{W,mixture} = 0.77$ for C1 or C2 and $v_{W,FAM} / v_{W,mixture} = 0.97$ for C3 or C4. Such a choice allowed the production of mortars with good workability.

In summary, for the study of curing behaviour (Chapter 6), FAM mortars with binders C1 and C2 had $V_m = 14.1\%$ (of which 4.0% is air, and the remaining 10.1% is water). In contrast, FAM mortars with binders C3 and C4 had $V_m = 15.8\%$ (6.0% and 9.8% air and water, respectively). These values correspond to 61% and 70% of the mixture V_m and are in agreement with the voids content of FAM of conventional HMA mixtures (Underwood and Kim 2013b).

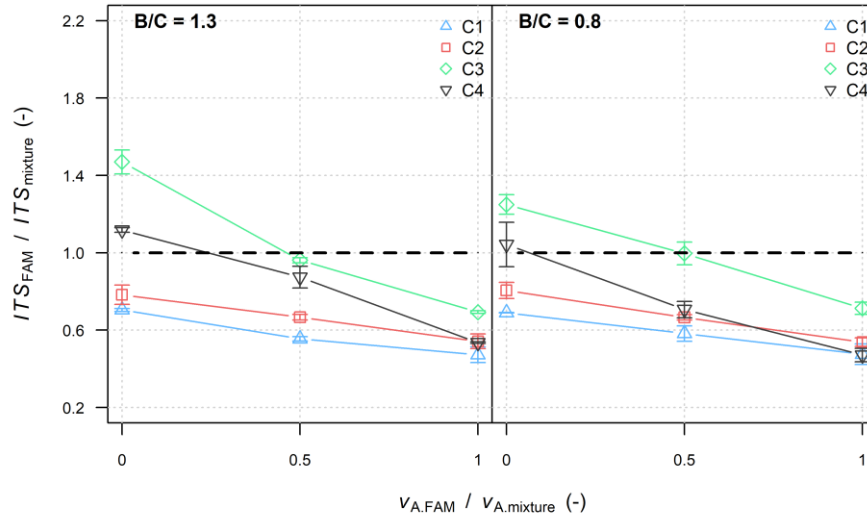


Figure 5.3. FAM mortar-to-mixture *ITS* ratio as a function of FAM mortar-to-mixture air voids content ratio obtained with $v_{W,FAM} / v_{W,mixture} = 1.00$

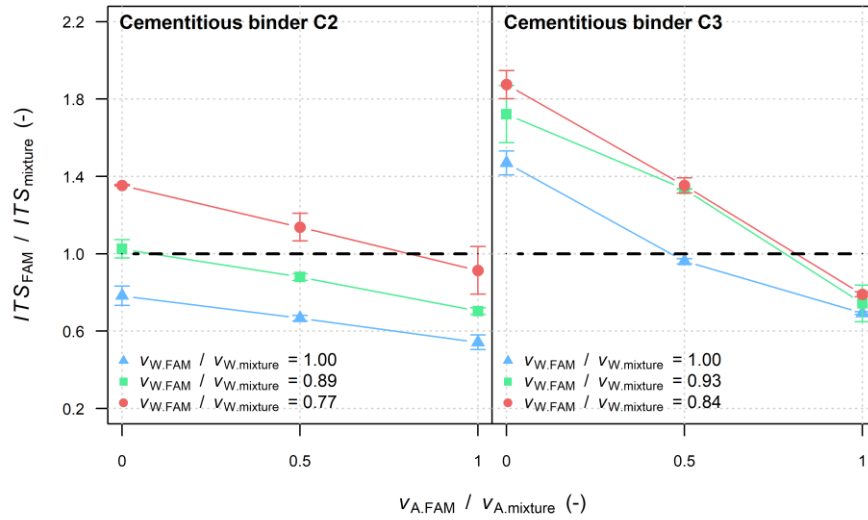


Figure 5.4. FAM mortar-to-mixture *ITS* ratio as a function of FAM mortar-to-mixture air voids content ratio obtained for CBE produced with cement C2 and C3, $B/C=1.3$

5.5. Summary

This Chapter deals with the definition of the CBE FAM mortars concept. Starting from eight CBE mixtures, a methodology for defining the composition of corresponding FAM mortars was developed. The aim was to find a mortar composition that closely describes the fine matrix of the CBE mixture. The focus was on the effect of the voids content, i.e. water and air voids, on the FAM mechanical response. Thus, nine mortars composition were defined for each mixture, varying the water and the air voids contents. The mortars were tested after one day of curing. Their strength was compared to those of the corresponding mixtures under the same curing conditions.

The main findings are as follows:

- The mortars were assumed to have a NMAS of 2 mm and contain all the bituminous and cementitious binders of the corresponding mixtures. Thus the B/C ratio was the same for the CBE materials;
- Mortars containing all the water and air voids of the mixtures showed the lower mechanical properties among the nine mortars tested. This composition corresponds to considering the mixture a perfect two-phase composite;
- Reducing mortars water or air void contents, thus considering the mixture as a three-phase composite, led to an improvement of the strength;
- Mortars containing only the water coming from the emulsion or without air voids were not considered realistic or feasible;
- Mortars containing about 60 - 70% of the mixture voids were selected for assessing their potential ability to predict mixtures behaviour.

Chapter 6.

Curing Behaviour of CBE Materials

6.1. Introduction

Curing is a characteristic feature of CBE materials and must be well characterised for having an actual awareness about the material performances and potential its applications in the real field. This Chapter focuses on studying the evolutive behaviour of CBE mixtures and the corresponding FAM mortars and on defining the potential relationship between the two scales.

6.2. Objectives

This part of the thesis aimed at measuring the evolution of physical and mechanical properties of CBE mixtures and FAM mortars throughout the curing process. The objectives were to compare the effect of different cement types and to evaluate the predictive potential of FAM mortars. The impact of different curing conditions, grading distributions and binders dosages were also evaluated.

6.3. Methodology

The procedures described in Appendix C and Chapter 5 allowed the definition of eight mixture compositions and the corresponding eight FAM mortar compositions, respectively:

- MIX1a, MIX1b produced with both C1 and C2 and MIX2a, MIX2b produced with both C3 and C4;
- FAM1a, FAM1b produced with both C1 and C2 and FAM2a, FAM2b produced with both C3 and C4.

These CBE composites were tested to evaluate and compare the evolution of DW , $ITSM$ and ITS throughout the curing process. **Figure 6.1** depicts the experimental programme organisation. The mixture and FAM mortar specimens were cured in a climatic chamber at $(25 \pm 2)^\circ\text{C}$ and $(70 \pm 5)\%$ RH in unsealed condition. Additional series of specimens, produced only with cementitious binders C1 and C2, were cured inside sealed plastic bags (identified with “S”) (Section 4.2.3). Five curing periods were considered:

Chapter 6

Curing Behaviour of CBE Materials

Multiscale Approach for Characterising the Behaviour of Cold Bitumen Emulsion Materials

- 1, 3, 7, 28 and 90 days for the mixtures;
- 6 hours, 1, 3, 7 and 28 days for the FAM mortars.

In the *ITSM* test, ν equal to 0.35 was assumed. For each curing condition and period, two and three replicate specimens were tested for measuring the *ITSM* and *ITS*, respectively.

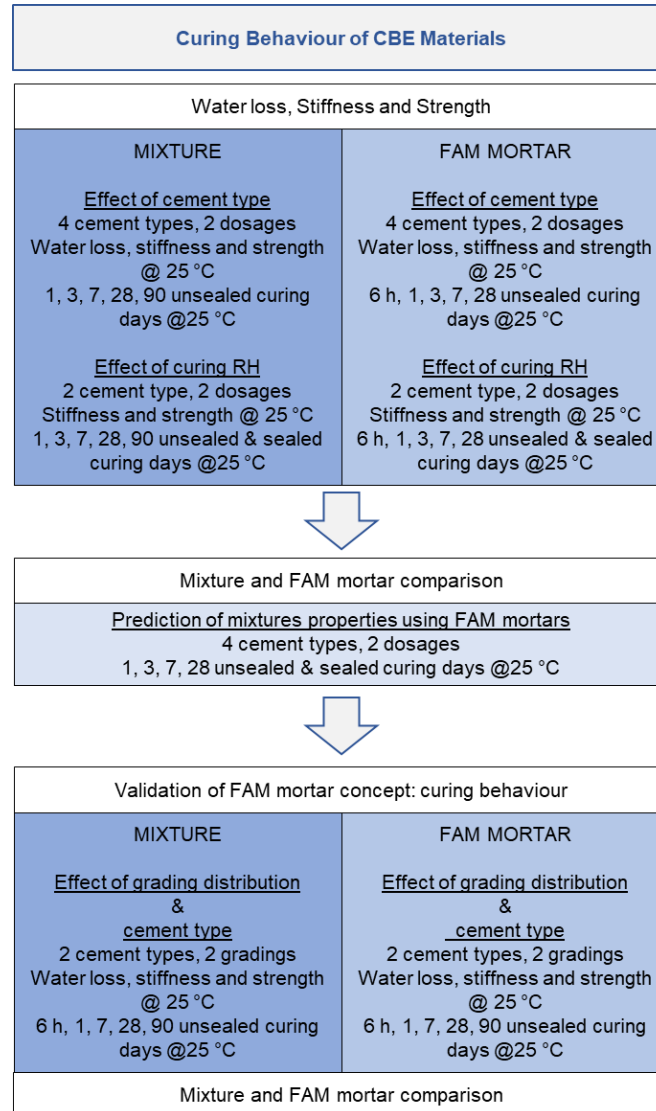


Figure 6.1. Study of CBE materials curing behaviour: experimental programme organisation

6.4. Analysis of the Results

In this section, the curing behaviours of the eight mixtures and the corresponding eight FAM mortars are analysed. The measured values of DW , $ITSM$ and ITS are plotted as a function of the logarithmic scale of time. The curves representing the fitted modified MM curing model (Equation (2.2)) are also depicted.

6.4.1. Water loss by evaporation

Figure 6.2 shows the evolution of DW for mixtures and FAM mortars produced with binders C1 and C4 in unsealed conditions. DW of specimens cured in sealed conditions was negligible, and therefore, it is not considered. For all materials, DW was higher than 50% after the first three curing days. Afterwards, the evaporation rate decreased, and DW showed an asymptotic trend. In the long-term, the higher cement dosage ($B/C = 0.8$) always led to lower DW due to the lower availability of evaporable water. In fact, the water chemically bonded by the cement could not evaporate. The amount of evaporated water was related to the cement type (Lura *et al.* 2017). Considering only the mixtures with $B/C = 0.8$, the average DW after 90 days was 82.1%, 69.1%, 77.5% and 88.5%, for mixtures produced with binders C1, C2, C3 and C4, respectively. Assuming that all the cementitious binder had the same degree of hydration (very close to 1), the results highlight the different amount of water bonded by the four types of cement. As expected, the highest amount of water was bonded by C2, the lowest by C4.

Figure 6.3 compares the average DW of mixtures and FAM mortars, from 1 day to 28 days. The FAM mortars provided an excellent prediction of the mixture DW except for the short term DW of the materials produced with binder C3. This confirmed that the selected mortar composition could represent an effective model of the FAM.

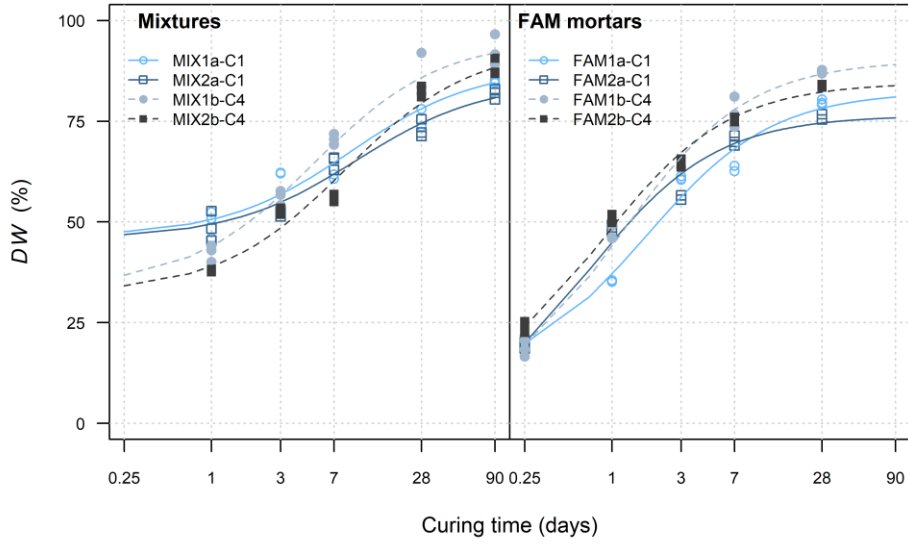


Figure 6.2. Evolution of DW for mixtures and FAM mortars produced with binders C1 and C4. Experimental data and modified MM model (Equation (2.2))

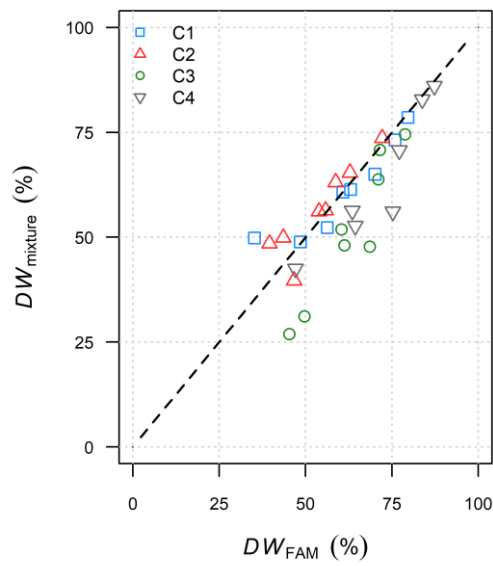


Figure 6.3. Comparison of DW of mixtures and FAM mortars (from 1 day to 28 days)

6.4.2. Stiffness and strength

Figure 6.4 shows the *ITSM* evolution for mixtures and FAM mortars produced with binders C1 and C3. All the investigated CBE materials had similar evolutive behaviours in terms of stiffness. **Figure 6.5** summarises the model parameters $ITSM_1$ (*ITSM* after 1 day) and $ITSM_a$ (asymptotic value of *ITSM*) for all mixtures. The *ITSM* increased rapidly in the first curing days and then tended towards an asymptotic value. The binder C2 led to the highest short-term stiffness. $ITSM_1$ was 4741 MPa and 7529 MPa, for mixtures with B/C ratios 1.3 (MIX1a-C2) and 0.8 (MIX2a-C2), respectively. These values were 50% and 109% higher than those obtained using the reference binder C1. $ITSM_1$ of mixtures produced with binders C1, C3 and C4 was comparable. Using C3 and C4, the stiffness was on average respectively 18% higher and 5% lower than the *ITSM* of mixtures with C1. In the long-term ($ITSM_a$), the highest stiffness was obtained with cementitious binders C2 and C3: the average increase with respect to cement C1 was between 42% and 56%. Cement C4 did not lead to a significant change in the stiffness: compared to mixtures with C1, $ITSM_a$ increased on average of about 8%. For all the cementitious binders, increasing the dosage from 1.5% to 2.5% caused an increase in mixtures stiffness at all curing times. The highest increase in $ITSM_a$ linked to the cement dosage was obtained with binder C2 (35.3%), the lowest with C3 (14.3%). Finally, at the same curing, mixtures were generally stiffer than the corresponding FAM mortars (**Figure 6.4**).

Figure 6.6 shows the *ITS* evolution for mixtures and FAM mortars produced with binders C1 and C3. The evolutive behaviours of all the materials investigated were similar. **Figure 6.7** summarises the model parameters ITS_1 (*ITS* after 1 day) and ITS_a (asymptotic value of *ITS*) for all mixtures. The binder C2 led to the highest short-term strength. ITS_1 was 0.35 MPa and 0.48 MPa, for mixtures with B/C ratios equal to 1.3 and 0.8, respectively. These values were 30% and 71% higher than those obtained using C1. Differently, using cements C3 and C4, the short term strength was slightly lower (11% and 23%, respectively) than that obtained using C1. For all the materials investigated, the *ITS* reached 50% of the long-term strength within the first three days. For all the mixtures, the *ITS* increase continued after 28 days, highlighting the long-term contribution of cement hydration and probably also ageing of residual bitumen from the emulsion. C2 also led to the highest long-term strength; ITS_a was 0.68 MPa and 0.83 MPa for MIX1a-C2 and MIX2a-C2, respectively, with an average increase of 35% than the strength of the mixtures produced with C1. Compared to mixtures with C1, the *ITS* increase using C3 was about 22%, whereas, with C4, ITS_a was 4% lower, an average. Increasing cement content from 1.5% to 2.5% resulted in higher *ITS* at all curing times and for mixtures. The gain in strength was limited (about 2% in the long-term) for binder C1, whereas using the other binders, the average increase of *ITS* was about 21%. Finally, at the same curing, the strength of mixtures was generally lower than the strength of FAM mortars (**Figure 6.6**).

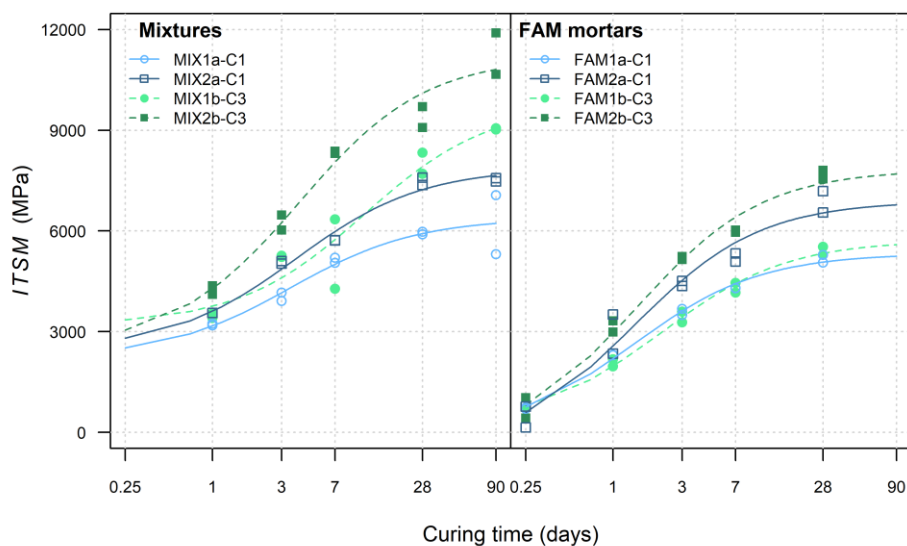


Figure 6.4. Evolution of $ITSM$ for mixtures and FAM mortars produced with cementitious binders C1 and C3. Experimental data and modified MM model (Equation (2.2))

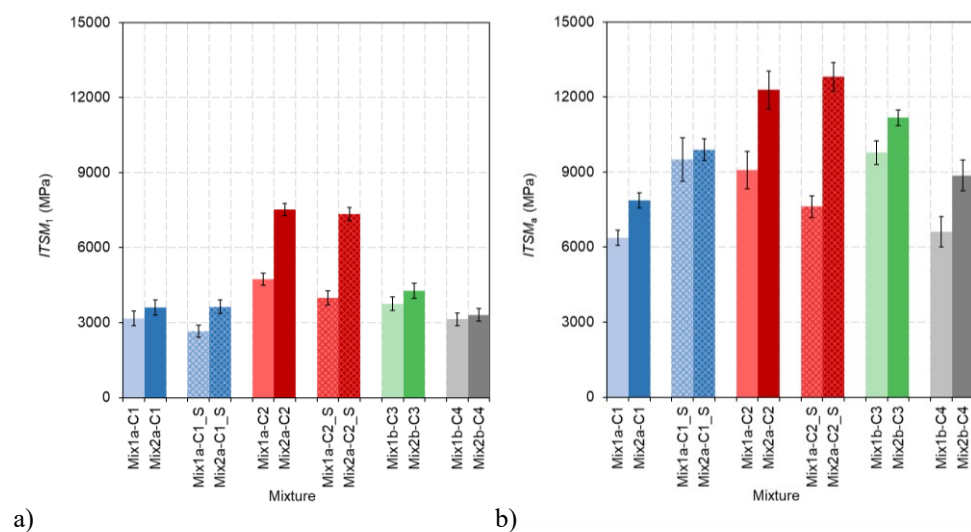


Figure 6.5. Regression parameters of the curing model (Equation (2.2)) for the $ITSM$ of mixtures a) $ITSM_1$, b) $ITSM_a$

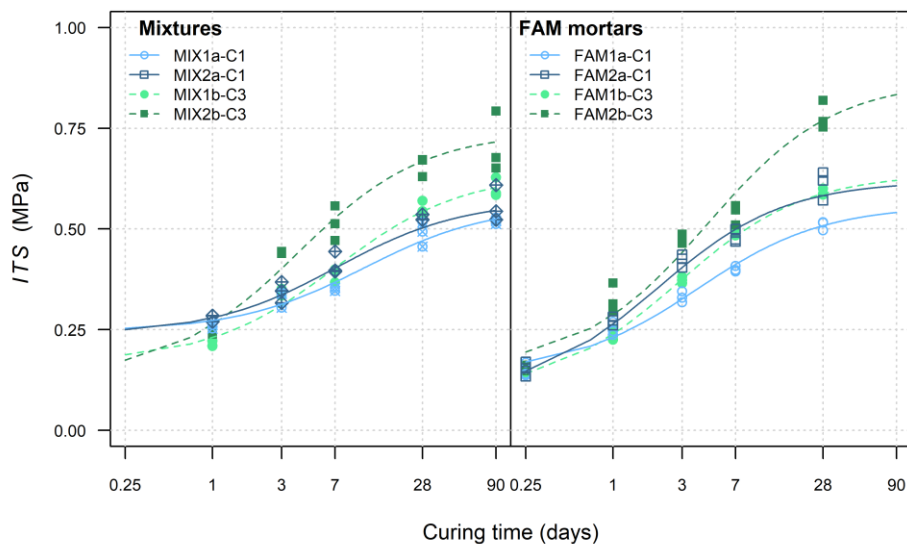


Figure 6.6. Evolution of ITS for mixtures and FAM mortars produced with cementitious binders C1 and C3. Experimental data and modified MM model (Equation (2.2))

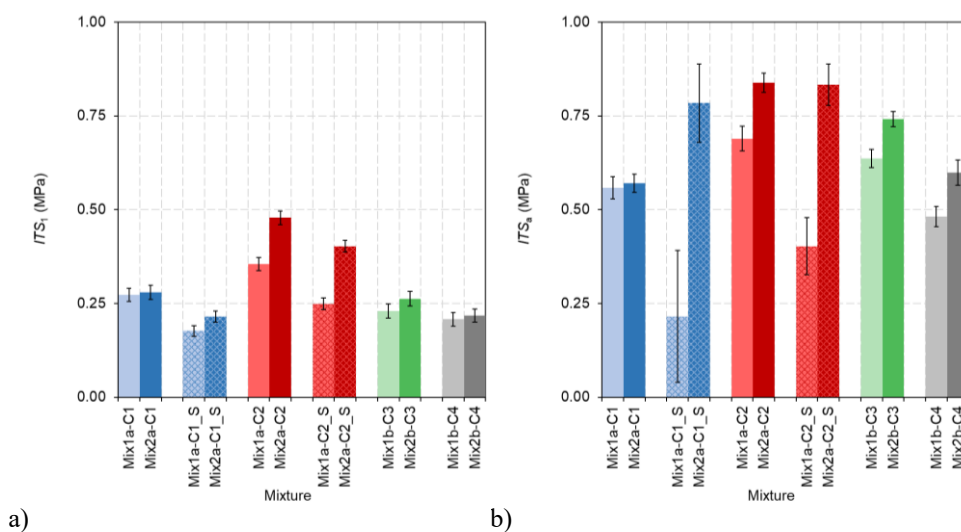


Figure 6.7. Regression parameters of the curing model (Equation (2.2)) for the ITS of mixtures a) ITS_1 , b) ITS_a

6.4.3. Effect of sealed curing conditions

The effect of sealed curing conditions (“S”) was evaluated on CBE mixtures produced with cementitious binders C1 and C2. **Figure 6.8** and **Figure 6.9** show, respectively, the evolution of *ITSM* and *ITS* for mixtures and FAM mortars produced with C2. The *ITSM* and *ITS* regression parameters for all mixtures are summarised in **Figure 6.5** and **Figure 6.7**, respectively.

Although *DW* was negligible with sealed curing, *ITSM* and *ITS* increased following trends similar to those observed in unsealed curing. **Figure 6.8** shows that sealed curing led to an increased *ITSM* at the higher cement content (MIX2a and MIX2b). Considering all the mixtures, **Figure 6.5** clearly shows that the effect of the cement content on the stiffness prevailed on the effect of sealed curing. On the other hand, **Figure 6.9** shows that sealed curing always led to a decrease in the *ITS*. This is confirmed by the model parameters shown in **Figure 6.7**. The adverse effect of sealed curing is particularly evident in the short-term strength (*ITS*₁).

In summary, curing conditions with restricted water evaporation had a limited effect on stiffness but penalised the strength. Since restricted water evaporation delays emulsion breaking, it can be stated that stiffness, i.e. the small-strain behaviour, was mainly affected by the cementitious bonds. On the other hand, strength, i.e. the large-strain behaviour, depended on the development of both bituminous and cementitious bonds. The critical role of restricted water evaporation on the development of mechanical properties is confirmed by **Figure 6.10**, which shows the correlation between *ITS* and *ITSM* for all the tested mixtures and FAM mortars. As can be observed, unique linear relationships relate the measured stiffness and strength, provided that the same curing condition is considered. For fixed values of stiffness, specimens cured in sealed condition were characterised by lower strength. On the other hand, for fixed values of strength, specimens cured in sealed condition were characterised by higher stiffness. Therefore, unsealed curing led to a better overall material performance: higher resistance with lower stiffness, resulting in a less prone-cracking material.

Figure 6.10a also suggests that the cement types did not lead to different microstructures forming within the CBE mixtures. Being fixed the curing RH, the influence of cements characterised by various strengths and natures is comparable to the effect of curing time and binders dosage. Indeed, all these resulted in a translation of the experimental data along the direction drawn by the linear relationships proposed. FAM mortars, scale in which the interaction mechanisms between the CBE materials components should be magnified, showed similar results confirming the outcome (**Figure 6.10b**).

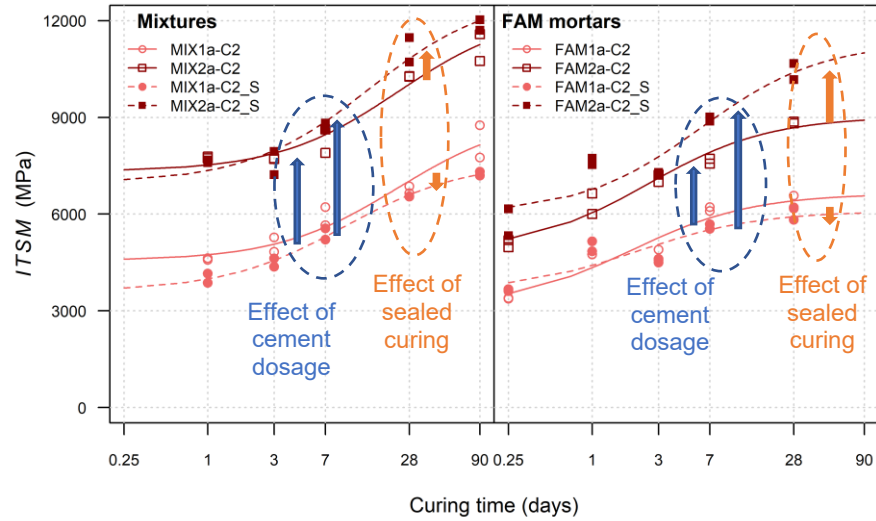


Figure 6.8. Evolution of *ITSM* as a function of curing time of CBE mixtures and FAM mortars produced with cement C2 (unsealed and sealed “S” curing conditions)

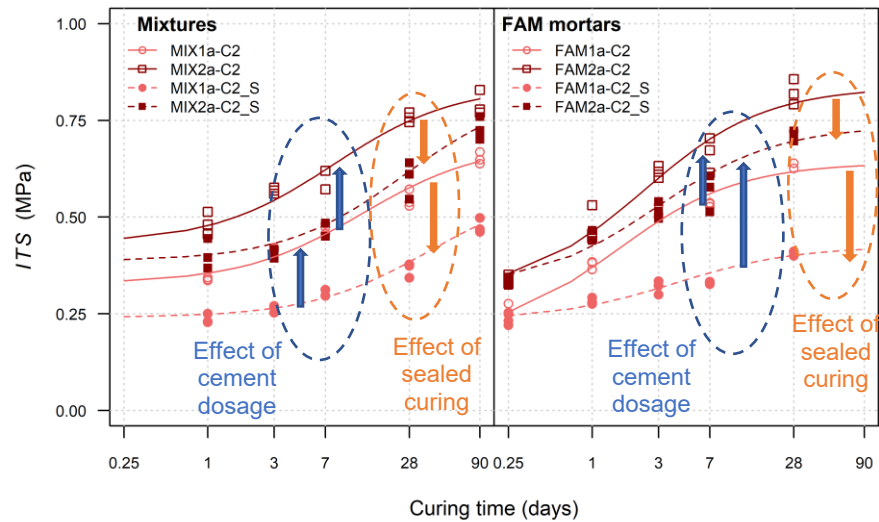


Figure 6.9. Evolution of *ITS* as a function of curing time of CBE mixtures and FAM mortars produced with cement C2 (unsealed and sealed “S” curing conditions)

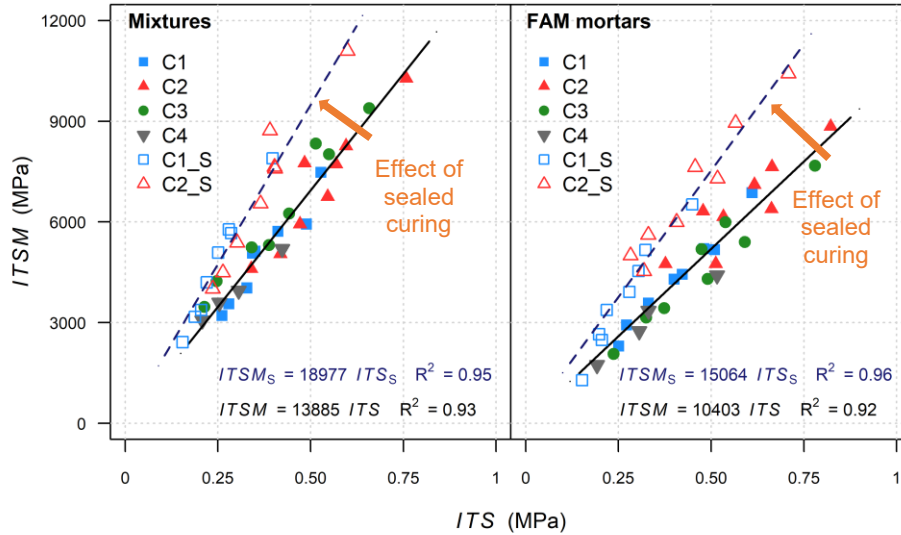


Figure 6.10. Correlation between *ITSM* and *ITS* in unsealed and sealed (“S”) curing conditions

6.4.4. Relationship between CBE mixtures and mortars properties

Figure 6.11 shows the correlation between the mechanical properties of mixtures and FAM mortars measured at the same curing time (i.e. 1, 3, 7 and 28 days) considering the same curing RH.

In general, the mixtures were stiffer than mortars (**Figure 6.11a**), with a few exceptions represented by specimens produced with cement C2. This indicates that the coarse aggregate acts as a reinforcement. The Hirsch model was used to simulate the relationship between the stiffness of the mixtures and the mortars (Ahmed and Jones 1990, Christensen *et al.* 2003). The model, originally developed for modelling cement concrete two-phase systems and later applied also to HMA mixtures, combines series and parallel elements (**Figure 6.12a**):

$$E_{mixture} = x(E_{CA}V_{CA} + E_{FAM}V_{FAM}) + (1 - x) \left(\frac{V_{CA}}{E_{CA}} + \frac{V_{FAM}}{E_{FAM}} \right)^{-1} \quad (6.1)$$

where V_{CA} and V_{FAM} are the volume fractions of coarse aggregate and FAM mortar (here 0.483 and 0.473, respectively). $E_{mixture}$ and E_{FAM} are the *ITSM* measured respectively for mixtures and mortars, whereas E_{CA} and x are fitting parameters. E_{CA} represents the relative

stiffness of the whole coarse aggregate volume in the composite system. The parameter x and its complementary, $(1 - x)$, express proportions of material structure in the parallel and series arrangement, respectively.

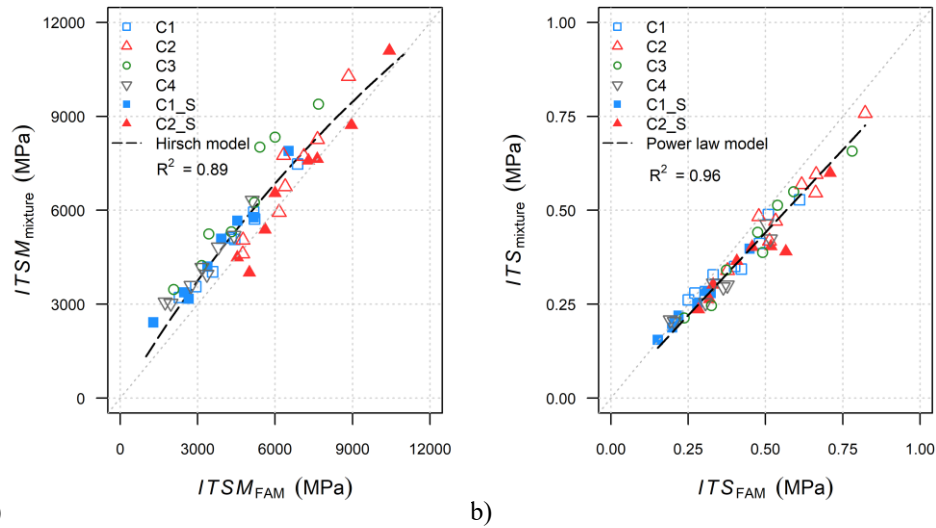


Figure 6.11. Mechanical properties of CBE mixtures as a function of mechanical properties of FAM mortars: a) $ITSM$, b) ITS

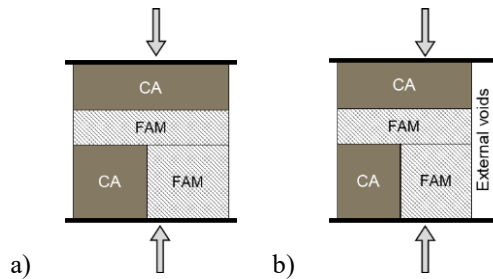


Figure 6.12. Schematic 1D representation of modulus composite models: a) original Hirsch model b) modified Hirsch model

In composite materials, the series arrangement (i.e. equal stress) indicates uniform stress and poor bonding. The parallel arrangement (i.e. equal strain) stands for perfect bonding between the matrix and the inclusions (Ahmed and Jones 1990). For cement concrete, the x value was found around 0.5 (Ahmed and Jones 1990, Christensen *et al.* 2003). The original model was adjusted (Figure 6.12b) to take into account the external voids phase (Phase III)

assumed in the CBE mixture conceptual model (**Figure 5.1**) (Graziani, Raschia, *et al.* 2020). Least squares error minimization provided a satisfactory fitting of the whole experimental data regardless of cementitious binder type, B/C ratio and curing conditions. The estimated model parameters were $E_{CA} = 29511$ MPa and $x = 0.339$. The x value indicates a medium-low bonding between the FAM mortar and the coarse aggregate.

Figure 6.11b displays that the mortar strength was equal or greater than the mixture one throughout the curing. This outcome may be linked to a scale effect due to the geometry of the specimens adopted and the dimension of pores that could accelerate the FAM curing process. Additional studies to better understand these finding must be carried out. The power law theory was adopted to modelling the relation between the *ITS* of the mixtures and the mortars (Ahmed and Jones 1990):

$$ITS_{mixture} = ITS_{FAM}(1 - aV_{CA}^n) \quad (6.2)$$

where a and n are model parameters function of shape and organisation of the inclusions. The model was proposed to model the strength of particulate composite characterised by poor bonding between the inclusion and the matrix, consequently considering no stress concentration at their interface. Using the least square minimization, an excellent fitting was obtained, with $a = 0.368$ and $n = 1.567$.

The existence of unique relationships between the mechanical properties of the two CBE composites scales, regardless of cement type, B/C ratio and curing, confirms that mixtures and mortars showed similar sensitivity in terms of strength and stiffness evolution. Therefore, correctly designed FAM mortars can be potentially used to predict mixtures mechanical behaviour over all the curing time regardless of their constituents. Further studies are though needed to assess the prediction ability of FAM mortars considering a wider range of CBE compositions and types of components.

Because the RA aggregate is considered a black rock (Section 2.1.2.3), the coarse RA aggregate particles are assumed as perfect inclusions submerged in the FAM. The mortar composition was obtained by removing from the mixture the coarse RA aggregate and part of the voids (air and water) (Chapter 5). Considering those assumptions, it can be likely stated that the evolutive behaviour of the mixture may be attributed to the FAM mortar properties evolution and that the contribution of the coarse aggregate to the mixture mechanical properties is nearly constant. For each CBE material investigated, the ratios $ITSM_{FAM} / ITSM_{mixture}$ and $ITS_{FAM} / ITS_{mixture}$ were indeed almost constant after three days of curing. This suggests that the structure of CBE is already developed after the first curing days. Emulsion breaking and cement hydration processes are nearly completed, and bituminous and cementitious bonds are mostly formed. Therefore, the increase in mechanical properties over time can be attributed to the consolidation and strengthening of the existing matrix bonds and eventual ageing effects.

6.5. Validation of the FAM mortar concept

The procedure described in Chapter 5 for establishing the composition of FAM mortars successfully defined mortars able to predict the evolution of mixtures stiffness and strength during curing. In this section, the developed FAM mortar concept is validated by applying it at four additional mixtures, i.e. MIX3 and MIX 4 produced with both cementitious binders C2 and C3 (**Table 4.2**). These mixtures are characterised by a higher binder dosage and lower voids than those discussed above. Besides, the modified emulsion was used instead of the traditional one. These mixtures have been developed for being suitable for pavement upper courses (Appendix E and Appendix F). However, the B/C was 1.2, a value similar to those of the mixture investigated above.

Results presented in Section 6.4.4 indicated that FAM mortars with NMAS of 2 mm, containing all the binders of the mixture, and about 60%-70% of V_m , were able to predict the evolution of the stiffness and the strength of CBE mixtures during curing. In particular, FAM mortars contained (**Figure 6.13**):

- 77% (FAM1a and FAM2a) and 97% (FAM1b and FAM2b) of the total volume of water of the mixtures, corresponding to 4.8% of the mixture total volume v_{mix} ;
- 50% of the air voids volume corresponding respectively to 1.9% and 2.9% of MIX1a, MIX2a and MIX1b, MIX2b v_{mix} .

A recent study used the methodology described in Chapter 5 for defining FAM mortars composition to characterise the stiffness evolution and the rheological behaviour of mixtures having B/C = 2.0 and $V_m = 15\%$. The Authors selected a mortar containing 81% of the mixture total water and 17% of its air voids (Graziani, Raschia, *et al.* 2020). The mortar included 4.7% and 1.5% of water and air with respect to v_{mix} (**Figure 6.13**). Results showed that the thermo-rheological behaviour and stiffness evolution of the mixture and the corresponding mortar were very similar.

In light of that, at this stage of the investigation, instead of studying several mortar compositions for defining the proper one, FAM mortars containing 4.5% of water and 2% of air voids respect of v_{mix} , were considered (**Figure 6.13**). The aggregate blends and mortars compositions of FAM3 and FAM4 mortars, corresponding to mixtures MIX3 and MIX4, respectively, are summarised in **Table 4.3** and **Table 4.4**.

Analogously to the experimental programme discussed above, the four mixtures and the corresponding four FAM mortars were tested to measure and compare the evolution of DW , $ITSM$ and ITS during curing. The specimens were cured in a climatic chamber at $(25 \pm 2)^\circ\text{C}$ and $(70 \pm 5)\%$ RH in unsealed conditions. Five curing periods were considered for DW and ITS : 6 hours, 1, 7, 28 and 90 days for both mixtures and mortars. The $ITSM$ was measured at 1, 7, 28 and 90 days. In the $ITSM$ test, v was assumed to equal 0.30. For each material and curing period, two replicate specimens were tested (**Figure 6.1**).

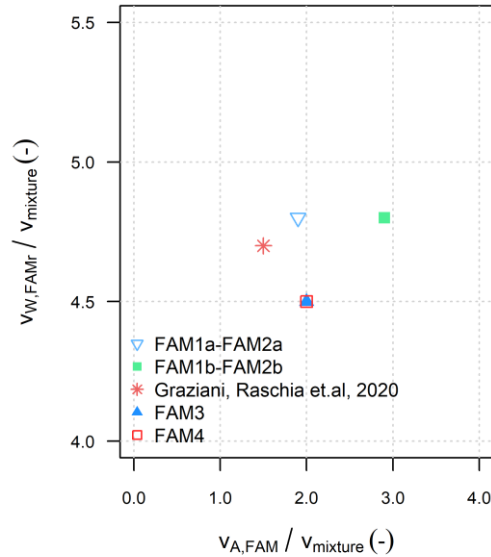


Figure 6.13. FAM mortars composition in terms of volume of water and air respect of the total mixture volume

6.5.1.1. Relationship between CBE mixtures and FAM mortars

Coherently with what was observed in the previous Sections, CBE mixtures and FAM mortars showed similar trends in the evolution of DW , $ITSM$ and ITS . **Table 6.1** and **Table 6.2** lists the regression parameters of the curing model (Equation (2.2)) obtained for mixtures and mortars.

Considering the results of mixtures (**Table 6.1**), the influence of the cementitious binder type is similar to those observed for MIX1 and MIX2:

- In the long-term, cement C2 bound a higher water amount than C3 (thus, the asymptotic value DW_a is lower);
- Being equal the grading distribution, mixtures produced with cement C2 had higher stiffness and strength than mixtures with C3, both in the early-age and long-term. Indeed, in the early-age (y_1), the increase in $ITSM$ and ITS was, on average, 92% and 30%, respectively. In the long-term (y_a), the stiffness and strength gain was, on average, 31% and 17%, respectively.

Considering the same cementitious binder type, the grading GG (MIX4) allowed obtaining a significant enhancement in the $ITSM$ with respect to CC (MIX3). The stiffness increased averagely of 67% and 53% in the early-age and long-term, respectively. The impact of the

grading on the strength was limited, and concerned especially the long-term strength: ITS_a was on average 13% higher for the mixtures MIX4 than those of mixtures MIX3.

The comparison between the model regression parameters (i.e. y_1 and y_a) of mixtures MIX1, MIX2 (**Figure 6.5** and **Figure 6.7**) and MIX3 (**Table 6.1**) shows that, although V_m was lower, the increase of the binders dosage and the use of the modified emulsion generally led to a reduction of the stiffness, both in the early-age and long-term curing, being equal the grading distribution. MIX3 had higher ITS than MIX1, although the B/C ratio was similar (1.2 and 1.3, respectively). On the other hand, in general, the mixtures MIX2, having a lower B/C ratio (i.e. 0.8), had higher ITS . However, one should bear in mind that MIX4 had lower V_m than MIX1 and MIX2. Thus the effect on the composition is not well clear. Similar trends were observed for FAM mortars (**Table 6.2**).

Figure 6.14 reports the correlation between the DW of mixtures and FAM mortars measured at the same curing times (i.e. 6 hours, 1, 7, 28 and 90 days). The CBE materials are here identified as a function of their grading distribution (CC and GG) and cement type (C2 and C3). For example, the code CC-C3 identifies the pair of materials produced with continuous grading (MIX3 and FAM3) and cementitious binder C3. Even in this case, FAM mortars satisfactorily predicted the mixture DW .

Table 6.1. Regression parameters of the curing model for MIX3 and MIX4

Mixture	y_1	y_a	h_y	R^2
<i>DW</i>	(%)	(%)	(days)	(-)
MIX3-C2	38.2	74.0	5.4	0.96
MIX3-C3	30.2	86.5	6.9	0.87
MIX4-C2	33.8	65.5	2.9	0.99
MIX4-C3	42.6	71.8	2.4	0.96
<i>ITSM</i>	(MPa)	(MPa)	(days)	(-)
MIX3-C2	4268	9701	16.2	0.95
MIX3-C3	2349	7198	4.1	0.99
MIX4-C2	7480	14405	30.1	0.94
MIX4-C3	3711	11287	6.4	1.00
<i>ITS</i>	(MPa)	(MPa)	(days)	(-)
MIX3-C2	0.372	0.775	6.4	0.94
MIX3-C3	0.308	0.678	3.7	0.98
MIX4-C2	0.403	0.897	3.8	0.93
MIX4-C3	0.291	0.749	3.6	0.99

Chapter 6

Curing Behaviour of CBE Materials

Multiscale Approach for Characterising the Behaviour of Cold Bitumen Emulsion Materials

Table 6.2. Regression parameters of the curing model for FAM3 and FAM4

FAM mortar	y_1	y_a	h_y	R^2
<i>DW</i>	(%)	(%)	(days)	(-)
FAM3-C2	38.1	59.5	3.2	0.98
FAM3-C3	45.1	76.6	4.4	0.99
FAM4-C2	33.1	50.0	3.0	0.98
FAM4-C3	49.9	72.4	2.6	0.99
<i>ITSM</i>	(MPa)	(MPa)	(days)	(-)
FAM3-C2	3655	6837	5.7	0.90
FAM3-C3	2199	5774	5.0	0.98
FAM4-C2	6615	9340	2.4	0.91
FAM4-C3	3106	7640	3.8	0.98
<i>ITS</i>	(MPa)	(MPa)	(days)	(-)
FAM3-C2	0.476	1.124	7.7	0.95
FAM3-C3	0.311	0.927	5.6	0.99
FAM4-C2	0.498	1.059	3.7	0.97
FAM4-C3	0.314	0.851	3.7	0.99

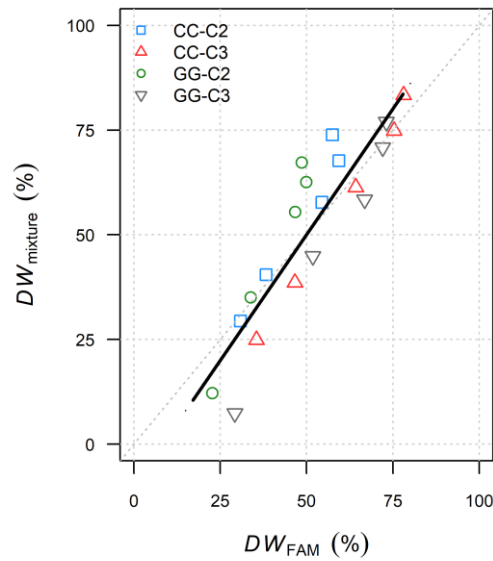


Figure 6.14. Comparison of *DW* of mixtures (MIX3 and MIX 4) and FAM mortars (FAM3 and FAM4) from 6 hours to 90 days

Figure 6.15 shows the correlation between the mechanical properties of mixtures and FAM mortars measured at the same curing time (i.e. 6 hours, 1, 7, 28 and 90 days).

Generally, the mixtures had always higher stiffness (**Figure 6.15a**) and lower strength (**Figure 6.15b**) than the FAM mortars, confirming what previously observed. The modified Hirsch model (Equation (6.1)) and the Power law model (Equation (6.2)) can be applied satisfactorily for predicting the stiffness and the strength of mixtures throughout curing, respectively, regardless of the constituent materials. **Table 6.3** lists the regression parameters of the models relating MIX3 and MIX4 with FAM3 and FAM4, respectively. This outcome confirms the possibility of applying the FAM mortar concept developed in Chapter 5 for characterising the curing behaviour of CBE mixtures. However, it is worth noting that the model parameters are strictly related to the composition of the mixture. Thus, even though FAM mortars containing 68% of the mixtures voids have been proved to have a good predicting ability of the mixtures mechanical properties evolution, the goodness of the proposed approach should be validated by applying it to a wider number of CBE mixtures compositions and types of constituent materials.

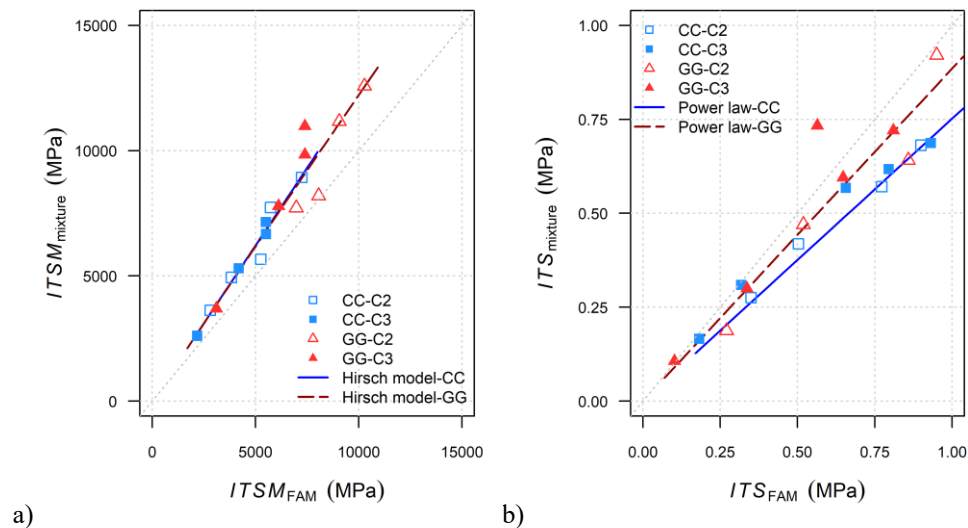


Figure 6.15. Mechanical properties of MIX3 (CC) and MIX4 (GG) as a function of mechanical properties of FAM3 and FAM4: a) *ITSM*, b) *ITS*

Table 6.3. Model parameters (Equations (6.1 and (6.2) and regression parameters for relating *ITSM* and *ITS* of FAM3 and FAM 4 with MIX3 and MIX4 (CC and GG, respectively)

Model parameters	CC	GG
V_{CA}	0.477	0.618
V_{FAM}	0.493	0.352
<i>modified Hirsch model</i>		
E_{CA} (MPa)	28912114	851914
x	0.387	0.560
R^2	0.95	0.85
<i>Power law</i>		
a	0.417	0.172
n	0.704	0.839
R^2	0.93	0.84

6.6. Summary

The present Chapter deals with the curing behaviour of CBE mixtures and FAM mortars. Their evolution is assessed to evaluate the effect of four types and two dosages of cementitious binders, two types and two dosages of emulsions. In total, twelve mixtures compositions and three B/C ratios were considered. The effect of two curing conditions (i.e. unsealed and sealed curing) and different grading distributions were also investigated. Finally, the predictive ability of properly designed FAM mortars was evaluated, relating their mechanical behaviour to those of the mixtures investigated.

The main findings are as follows:

- The use of CSA cement C2 improved the mechanical properties of CBE materials in the early-stage of curing;
- CSA (C2) and Portland-slag high strength cements (C3) allowed enhancing the mechanical properties of CBE materials in the long-term;
- Unsealed curing improved material performances resulting in higher strength and lower stiffness;
- Gap graded distribution (GG) increased the stiffness and the strength of CBE mixtures compared to the continuous grading (CC);
- The increase in the binders dosage and use of the modified emulsion (MIX3) resulted in a general reduction of the stiffness;

Chapter 6

Curing Behaviour of CBE Materials

Multiscale Approach for Characterising the Behaviour of Cold Bitumen Emulsion Materials

- The influence of higher binders dosages and modified emulsion on the strength is not fully clear;
- FAM mortars showed a similar sensitivity in terms of stiffness and strength evolution compared to mixtures;
- The evolutive behaviours of stiffness and strength of mixtures and mortars were compared using the Hirsch model and the Power law model, respectively;
- Properly designed mortars showed a satisfactory potential ability to predict mixtures behaviour, regardless of curing conditions, grading distribution, binders type and dosages.

It is worth highlighting that such results could be related to the composition of mixtures examined. Further studies should be carried out, including a larger variety of compositions and types of components.

Chapter 7.

Linear Viscoelastic Study of CBE Materials

7.1. Introduction

The characterisation of the LVE response of bituminous materials is fundamental in modelling road pavement behaviour, and it is an essential input in the design of flexible pavements. Therefore, this Chapter focuses on the small strain characterisation of CBE mixtures and the corresponding FAM mortars and their relationship.

7.2. Objectives

The objective of this part of the thesis was to characterise the long-term LVE response of CBE mixtures and FAM mortars by measuring the complex modulus E^* . The final goal was to evaluate the potential relationship between the small strain behaviour of mixtures and mortars. The impacts of different cement types and grading distributions were also evaluated.

7.3. Methodology

The experimental study investigated six mixtures and the corresponding six FAM mortars:

- MIX3, MIX4 and MIX5 produced with both C2 and C3
- FAM3, FAM4 and FAM5 produced with both C2 and C3.

Table 4.2 and **Table 4.4** report the composition of mixtures and FAM mortars, respectively. In particular, FAM mortar compositions were obtained assuming that they contained 4.5% of water and 2% of air voids with respect to the total volume of the correspondent mixtures (see Section 6.5).

Figure 7.1 summarises the experimental programme organisation. The mixture and FAM mortar specimens, with a 150 mm and 100 mm diameter, were produced using the SGC. Specimens were cured in a climatic chamber in unsealed condition for 15 days at $(25 \pm 2)^\circ\text{C}$ and $(70 \pm 5)\%$ RH. This was followed by 10 days of accelerated curing at $(40 \pm 2)^\circ\text{C}$ and $(30 \pm 5)\%$ RH. After these curing periods, the samples were cored to obtain

the specimens with a diameter of 75 mm. The curing was then extended for more than 90 days at $(25 \pm 2)^\circ\text{C}$ and $(70 \pm 5)\%$ RH. Based on the results reported in Appendix F it was likely possible to assume that the evolutive process of the CBE materials properties was almost completed at the testing time. Hence, its influence was considered negligible. Testing details are provided in Section 4.5.4. Two replicates (labelled R1 and R2) for each CBE material were tested. Rheological modelling of the experimental data was then carried out. Finally, mixtures and FAM mortars LVE behaviours have been compared.

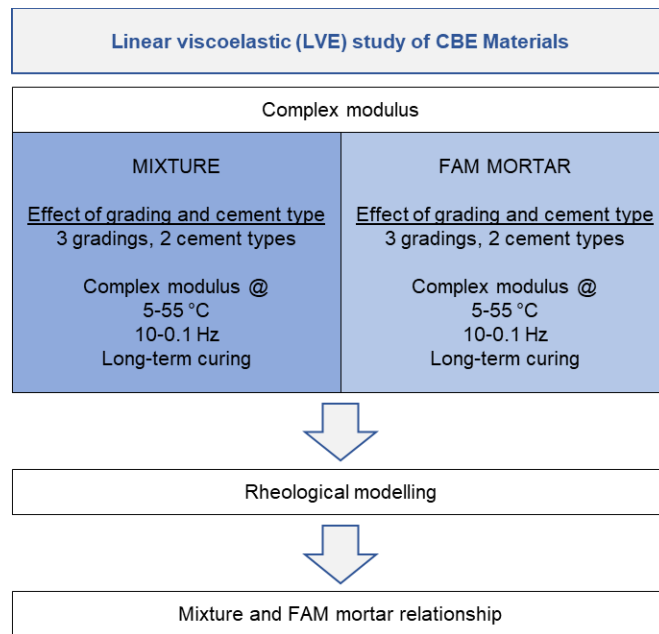


Figure 7.1. Study of CBE materials LVE behaviour: experimental programme organisation

7.4. Analysis of the Results

7.4.1. Complex modulus results

Figure 7.2 reports, as an example, E_0 and φ experimental data, i.e. isothermal curves, obtained testing a mixture specimen and a FAM mortar specimen (MIX3-C3_R1 and FAM3-C3_R1, respectively). The overall mixtures behaviour was similar for all the tested specimens. The higher stiffness moduli were obtained at the lowest temperatures and highest frequencies (i.e. 5 °C and 10 Hz, respectively). Therefore, the temperature increase and the frequency reduction resulted in the E_0 decrease. In parallel, φ decreased, reaching its maximum at the higher temperatures (45 °C or 55°C) and then dropped. Such a behaviour is typical of bituminous materials and hence, is similar to that observed for typical HMA. However, the frequency and temperature susceptibility of the CBE mixture are due to two distinct bituminous components: the fresh emulsion residual bitumen (EB) and the aged binder coating the RA, the recycled binder (RB).

Figure 7.3a and **Figure 7.3b** depict the measured data of stiffness modulus and phase angle in the Black diagram for the six CBE mixtures. **Figure 7.4a** and **Figure 7.4b** show the same results in terms of loss and storage moduli (Cole-Cole plan). As can be observed, for CBE mixtures, the E_0 variability did not exceed one order of magnitude. At the same time, the maximum φ , about 25 °, was lower than typical HMA values (Kim, 2009). This was due to the reduced frequency and thermal sensitivity of CBE mixtures lent by the cementitious binder. Similar behaviours were observed in Dolzycki *et al.* (2017), Schwartz *et al.* (2017), Kuchiishi *et al.* (2019), Ferrotti, Grilli, *et al.* (2020), Graziani, Mignini, *et al.* (2020), Graziani, Raschia, *et al.* (2020). **Figure 7.3c** and **Figure 7.3d** depict the measured data in the Black diagram for the six FAM mortars. **Figure 7.4c** and **Figure 7.4d** depict the same results in the Cole-Cole plan. The general behaviour of mortars was similar to that observed for mixtures. However, the differences observed due to grading distribution and cement type were more pronounced.

Figure 7.3 and **Figure 7.4** show that the (E_0, φ) and the (E_1, E_2) pairs described single curves for all tested specimens in the Black diagram and Cole-Cole plan, respectively. This means that the TTSP was applicable.

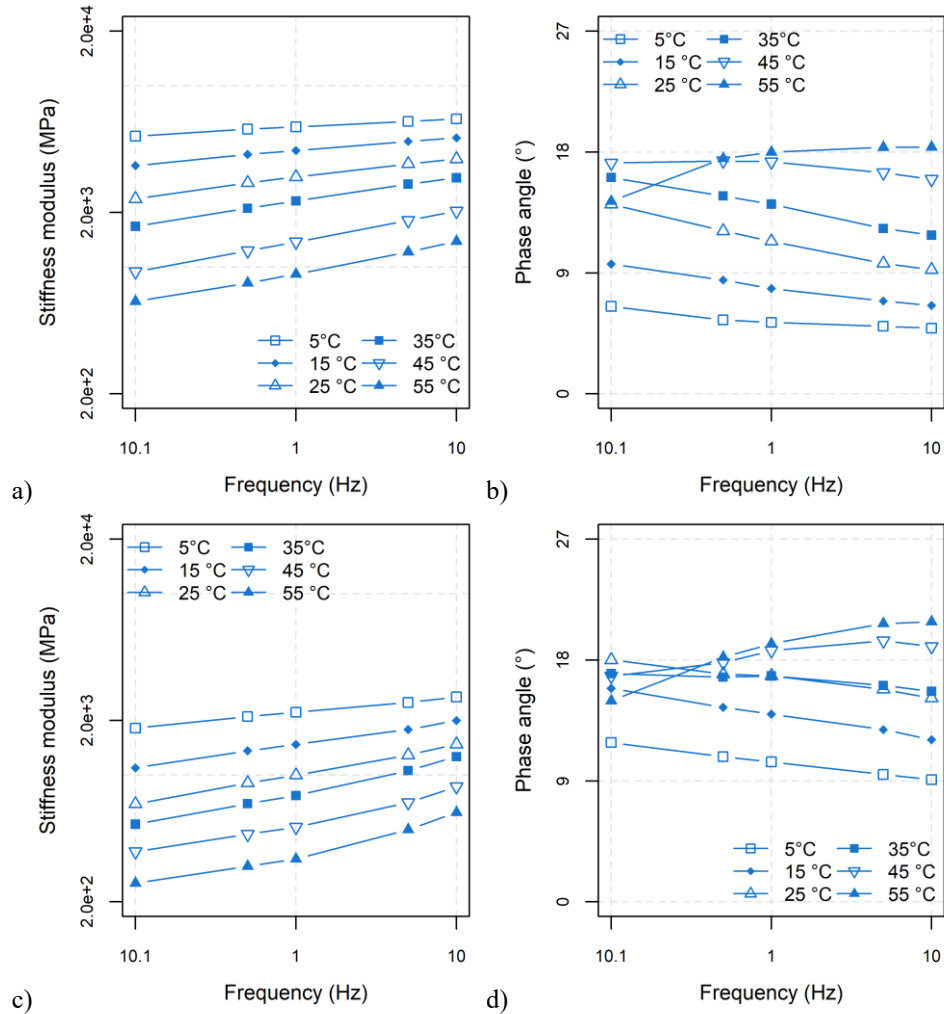


Figure 7.2. Isothermal curves: a) E_0 of MIX3-C3_R1, b) ϕ of MIX3-C3_R1, c) E_0 of FAM3-C3_R1 and d) ϕ of FAM3-C3_R1

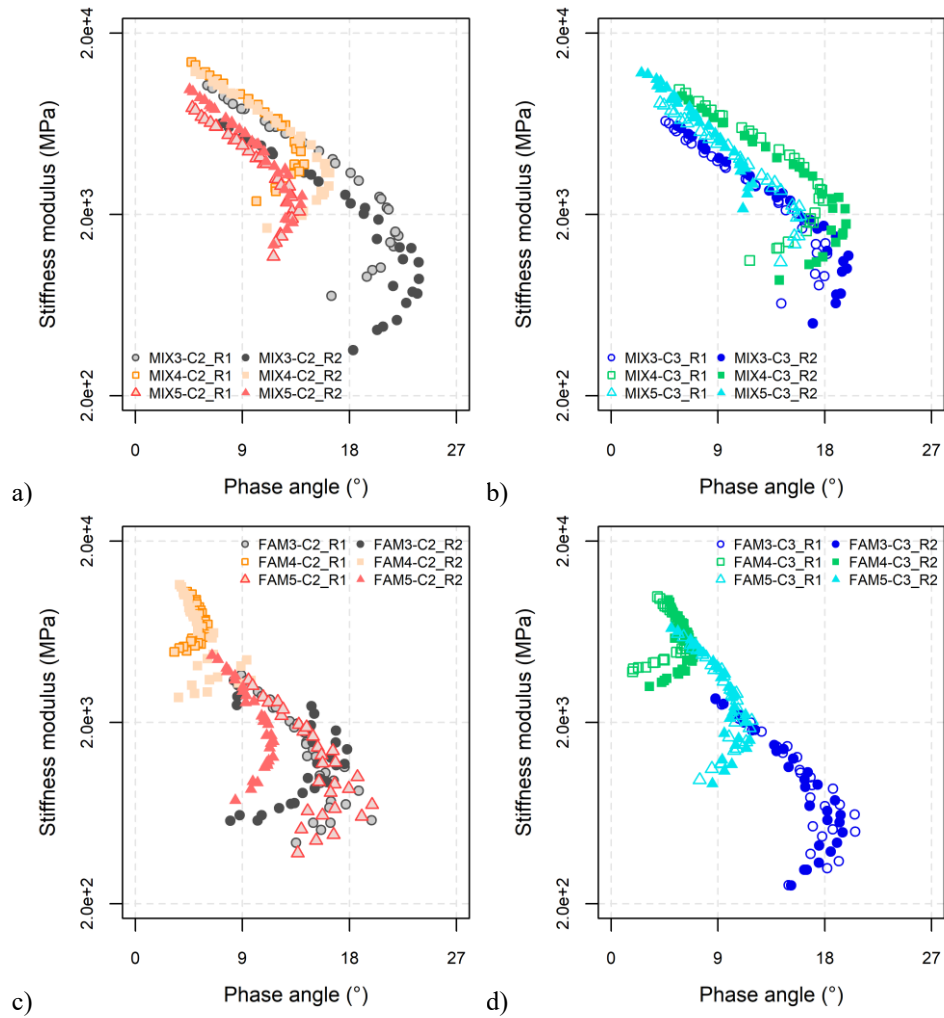


Figure 7.3. Stiffness modulus and phase angle data, plotted in the Black diagram, a) mixtures with cement C2, b) mixtures with cement C3, c) FAM mortars with cement C2 and d) FAM mortars with cement C3

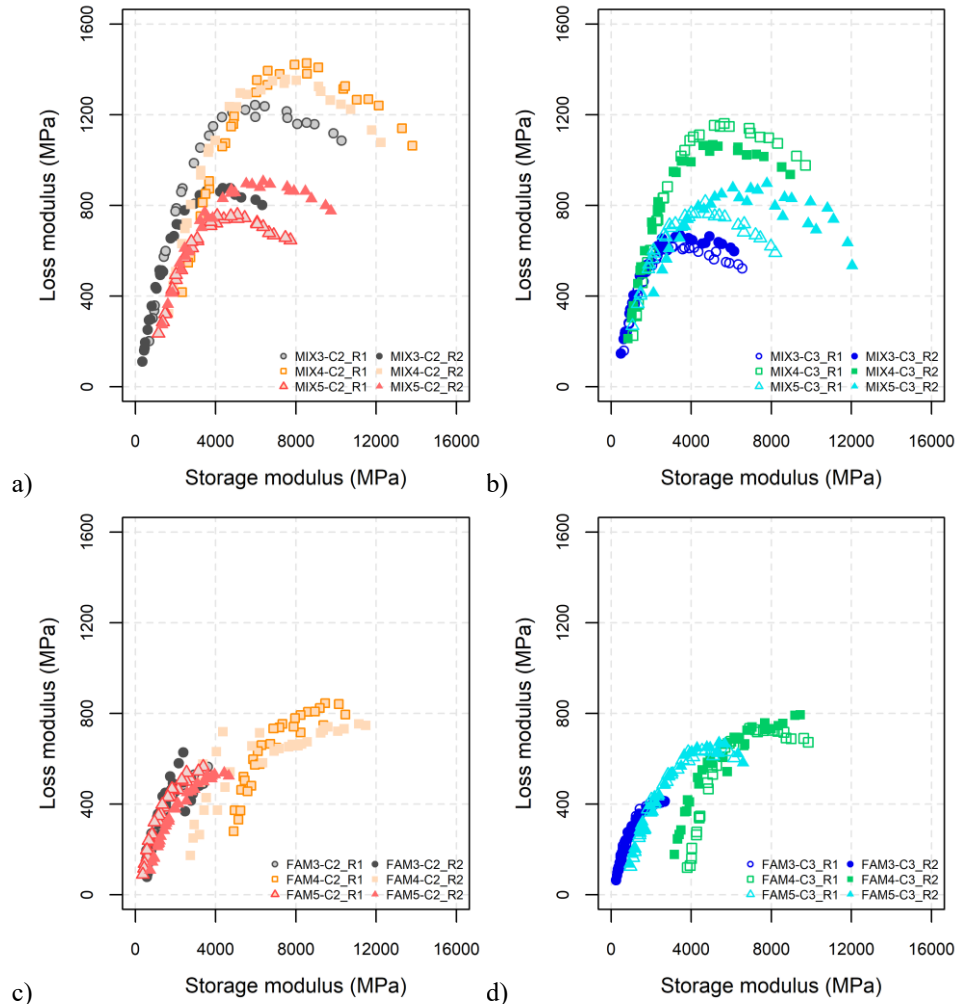


Figure 7.4. Loss modulus and storage modulus data plotted in the Cole-Cole diagram, a) mixtures with cement C2, b) mixtures with cement C3, c) FAM mortars with cement C2 and d) FAM mortars with cement C3

7.4.2. Thermo-rheological modelling

The master curves of the twelve CBE mixtures specimens and twelve corresponding FAM mortars specimens were obtained for the reference temperature ($T_{ref} = 25 \text{ }^\circ\text{C}$). **Figure 7.5** shows the calculated shift factors as a function of the temperature. The WLF constants, C_1

and C_2 , obtained by least-squares fitting, are reported in **Table 7.1** and **Table 7.2** for CBE mixtures and FAM mortars. It can be observed that MIX3 and MIX5 had similar C_1 and C_2 , and MIX4 showed slightly smaller values of the WLF constants. On the contrary, the variability in C_1 and C_2 of FAM mortars was greater. This means that the mixtures had comparable temperature dependency (and consequently, shift factors). Vice versa, mortars had a much different temperature dependency. These results may be linked to the CBE materials composition in terms of contents of RB, EB, and total bitumen (EB+RB), as well as to the value of the recycled binder ratio, $RBR = RB/(EB+RB)$, as shown in **Table 7.3**.

Table 7.1. CBE mixtures parameters of the 2S2P1D-HY model (Equation (7.1)) and WLF model (Equation (4.6)), $T_{ref} = 25$ °C

ID	E_e (MPa)	E_g (MPa)	k (-)	h (-)	δ (-)	β (-)	$Log \tau$ (-)	φ_0 (°)	C_1 (-)	C_2 (-)
<i>MIX3</i>										
C2_R1	490	14990	0.12	0.38	1.75	1905	-0.70	2.7	18.0	132.4
C2_R2	263	11150	0.12	0.38	1.95	1905	-1.62	2.4	18.0	132.4
C3_R1	450	9310	0.12	0.38	2.09	1230	-0.15	1.5	18.0	132.4
C3_R2	370	9096	0.12	0.38	2.05	851	-0.63	2.2	18.0	132.4
<i>MIX4</i>										
C2_R1	1995	18324	0.13	0.40	1.68	488	-0.53	1.8	14.3	116.6
C2_R2	1407	16872	0.13	0.40	1.68	424	-0.74	2.0	14.3	116.6
C3_R1	895	14309	0.13	0.40	1.66	722	-1.02	1.8	14.3	116.6
C3_R2	750	13264	0.13	0.40	1.78	302	-1.05	2.2	14.3	116.6
<i>MIX5</i>										
C2_R1	750	10323	0.12	0.33	1.72	4259	0.07	1.7	19.5	139.7
C2_R2	799	14110	0.12	0.33	1.99	3802	0.05	0.9	19.5	139.7
C3_R1	560	10571	0.12	0.33	1.64	5012	0.12	1.6	19.5	139.7
C3_R2	1200	14923	0.12	0.33	2.07	4677	1.50	0.5	19.5	139.7

Table 7.2. FAM mortars parameters of the 2S2P1D-HY model (Equation (7.1)) and WLF model (Equation (4.6)), $T_{ref} = 25$ °C

ID	E_e (MPa)	E_g (MPa)	k (-)	h (-)	δ (-)	β (-)	$\text{Log } \tau$ (-)	φ_0 (°)	C_1 (-)	C_2 (-)
<i>FAM3</i>										
C2_R1	370	9505	0.12	0.35	3.13	547	-2.23	2.1	8.6	78.4
C2_R2	555	8690	0.12	0.35	1.80	1879	-3.05	2.9	8.6	78.4
C3_R1	225	5946	0.12	0.35	2.50	488	-2.03	2.7	8.6	78.4
C3_R2	206	5994	0.12	0.35	2.47	1226	-2.20	2.6	8.6	78.4
<i>FAM4</i>										
C2_R1	4569	16122	0.14	0.41	2.76	363	-0.58	0.7	21.7	179.0
C2_R2	2870	13891	0.14	0.41	2.35	586	0.52	0.4	21.7	179.0
C3_R1	3782	14595	0.14	0.41	2.33	204	-0.87	0.1	21.7	179.0
C3_R2	3130	15098	0.14	0.41	4.04	114	0.01	0.8	21.7	179.0
<i>FAM5</i>										
C2_R1	276	8006	0.13	0.32	2.81	6448	-1.99	2.3	26.3	210.5
C2_R2	550	9235	0.13	0.32	2.86	5623	-1.16	0.6	26.3	210.5
C3_R1	762	10310	0.13	0.32	2.18	4964	-0.83	0.6	26.3	210.5
C3_R2	702	10941	0.13	0.32	2.49	5265	-0.62	0.6	26.3	210.5

Table 7.3. CBE materials compositions in terms of binders

ID	B^* (%)	RB^* (%)	$EB+RB^*$ (%)	RBR (-)	$Cement^*$ (%)	B/C (-)	$(EB+RB)/C$ (-)
<i>Mixture</i>							
MIX3	2.7	3.7	6.4	0.57	2.3	1.2	2.8
MIX4	2.7	2.1	4.8	0.43	2.3	1.2	2.1
MIX5	2.7	4.0	6.7	0.59	2.3	1.2	2.9
<i>FAM mortar</i>							
FAM3	5.9	4.2	10.2	0.42	4.9	1.2	2.1
FAM4	8.8	0	8.8	0.00	7.3	1.2	1.2
FAM5	7.9	5.4	13.3	0.41	6.6	1.2	2.0

* by the total mass of CBE materials

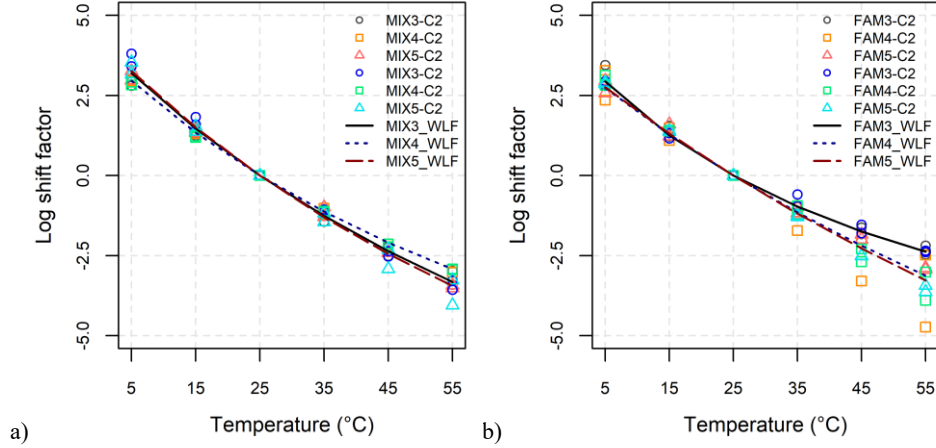


Figure 7.5. Shift factors and WLF models ($T_{ref} = 25$ °C): a) CBE mixtures b) FAM mortars

The complex modulus data were fitted using a modified version of the 2S2P1D model (Section 2.1.4.2), considering 2 springs, 2 parabolic elements, 1 dashpot and a hysteretic element. The model, here shortened 2S2P1D-HY, is described by the equation:

$$E_{2S2P1D-HY}^*(\omega) = E_{2S2P1D}^*(\omega) \exp(j\varphi_0) \quad (7.1)$$

where $E_{2S2P1D}^*(\omega)$ represents the 2S2P1D model and $\exp(j\varphi_0)$ is a correction term which adds a temperature- and frequency-independent, phase angle φ_0 . This term describes dissipation mechanisms connected to internal friction phenomena. The correction of the model is equivalent to those previously applied in the HS-HY model, and it is detailed in Section 2.1.4.2. **Table 7.1** and **Table 7.2** list the eight parameters of the 2S2P1D-HY model obtained for mixtures and mortars, respectively:

- The equilibrium modulus E_e ;
- The glass modulus E_g ;
- The three dimensionless parameters h , k and δ ;
- The characteristic time, τ ;
- The dimensionless parameter β ;
- The phase correction φ_0 .

Figure 7.6 depicts the complex modulus tests experimental data and the fitted 2S2P1D-HY model. In particular, **Figure 7.6c** and **Figure 7.6d** report the master curves of the investigated mixtures obtained by applying the estimated $a_{T_{ref}}$. The accuracy of the prediction of the model was calculated as follows:

$$Error_{E_0} = \frac{E_0 - E_{2S2P1D-HY}}{E_{2S2P1D-HY}} \cdot 100 \quad (7.2)$$

$$Error_{\varphi} = \varphi - \varphi_{2S2P1D-HY} \quad (7.3)$$

where $E_{2S2P1D-HY}$ and $\varphi_{2S2P1D-HY}$ are the values of stiffness modulus and phase angle obtained by applying the model. The model provided a good fitting of both E_0 and φ , as $Error_{E_0}$ was always lower than $\pm 10\%$, and $Error_{\varphi}$ was between -2° and $+2^\circ$ (**Figure 7.7**).

From the analysis of the model parameters of CBE mixtures (**Table 7.1**), it can be noticed that cement type mainly influenced the stiffness asymptotic values E_e and E_g . In general, being equal the grading distribution, mixtures with cement C2 were stiffer than those with C3. Simultaneously, mixtures with C2 also had lower phase angle, except MIX3 mixes, for which φ values obtained with the two cements were comparable. However, it must be noted that the range of variability of the phase angle was too small to identify significant effects of the cement type clearly. The grading distribution had a greater impact on the stiffness of CBE mixtures. Considering the same cement type and low frequencies (E_e), mixtures MIX4 had higher modulus than mixtures MIX5 and MIX3. Mixtures MIX4 were also stiffer at high frequencies (E_g), whereas MIX5 and MIX3 E_g values were comparable. One should bear in mind that the V_m of MIX5 was 0.5% lower than the V_m of MIX3 and MIX4 (**Table 4.2**). Therefore, the level of voids within the different mixtures could also have had some small secondary effects in the values of E_e and E_g , in addition to the primary effects coming from the cement type and grading distribution. A slight heterogeneity could explain the variation of E_e and E_g from one replicate to another of the same mixture. Indeed, the specimens may have had slightly different aggregate skeletons.

The parameters related to the viscous part of the model h , k and δ did not depend on the cement type. On the contrary, they showed some variability linked to the mixture grading. As the mixtures were produced using the same emulsion, this may confirm that RB also contributed to the viscous response of CBE mixtures. Similar values of h and k were found by other researchers using similar rheological models, i.e. HS-HY and 2S2P1D (Gandi *et al.* 2017b, Graziani, Mignini, *et al.* 2020, Graziani, Raschia, *et al.* 2020). The values of h and k were generally lower than those commonly used for describing the LVE behaviour of HMA using 2S2P1D (Olard and Di Benedetto 2003, Di Benedetto *et al.* 2004). Such an outcome suggests that CBE materials have a lower viscous response than HMA.

The different viscous response of the investigated CBE mixtures is also confirmed by the values of the characteristic time τ . The dimensionless parameter β was lower for mixtures MIX4, whereas it had the highest values for mixtures MIX5. As β is directly linked to the Newtonian viscosity of the binder and increases with ageing, the result could be linked to the content of RB in the mixtures (**Table 7.3**).

The hysteretic correction φ_0 ranged between 0.5 and 2.7. Such variability could be ascribed to the heterogeneity of the specimens and the different organisation in the aggregate skeleton.

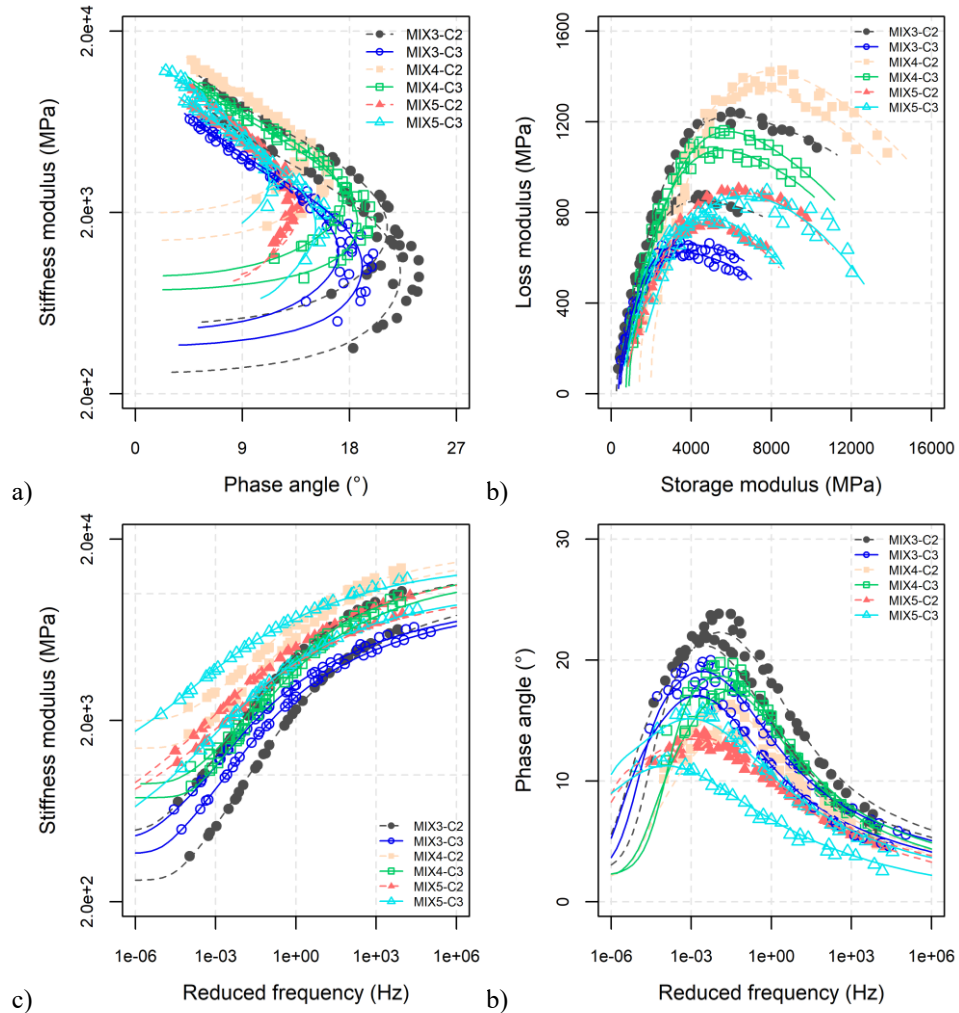


Figure 7.6. CBE mixtures experimental data and 2S2P1D-HY model a) Black diagram, b) Cole-Cole plan, c) stiffness modulus master curves ($T_{ref} = 25 \text{ }^\circ\text{C}$) and d) phase angle master curves ($T_{ref} = 25 \text{ }^\circ\text{C}$)

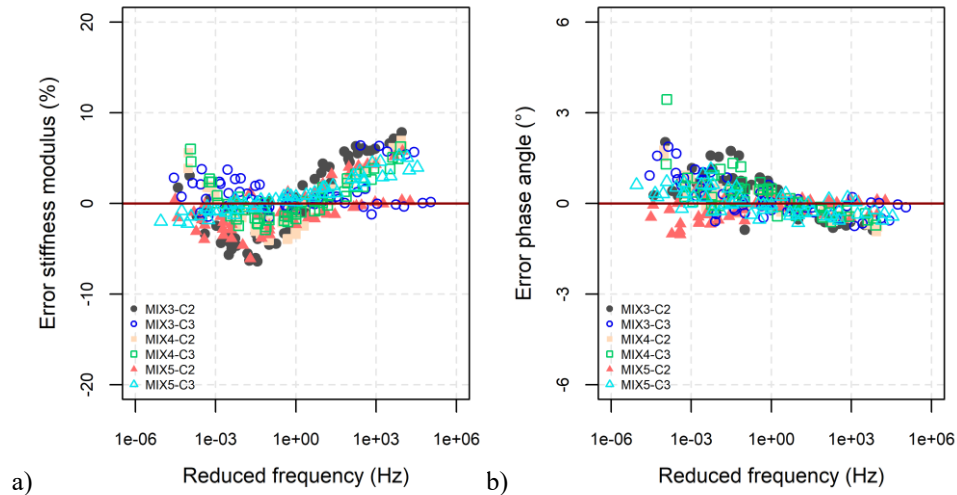


Figure 7.7. Accuracy of 2S2P1D-HY model prediction (Equations (7.2) and (7.3)) for CBE mixtures: a) stiffness modulus, b) phase angle

Figure 7.8 shows the FAM mortars complex modulus tests experimental data and the fitted 2S2P1D-HY model. Also for the mortars, the model provided a good fitting of both E_0 and φ . Indeed, $Error_{E_0}$ and $Error_{\varphi}$ were generally between $\pm 10\%$ and $\pm 3^\circ$, respectively. (**Figure 7.9**).

FAM mortars stiffness asymptotic values (**Table 7.2**) depended on the cement type being equal the grading distributions. However, the greater variability was due to the grading distribution type. The lower values of E_e and E_g were obtained for FAM3, whereas FAM4 had the highest E_e and E_g . As shown in **Table 7.3**, the highest the cement content (and lowest (B+RB)/C ratio), the highest the stiffness asymptotic values. In general, for bituminous mixtures, the lowest the voids, the stiffer are bituminous materials. Despite that, FAM mortars with the higher V_m content had also higher E_e and E_g . This may indicate that in the FAM mortar LVE behaviour, the effect of the cement prevailed on the effect of V_m . Also, in this case, the variability of E_e and E_g between the different replicates could be ascribed by the heterogeneity of the specimens.

The parameters related to the viscous part of the model h , k and δ showed that FAM mortars FAM5 and FAM3 were less viscous than FAM4. The τ values also confirmed the result. The higher viscous response of FAM4 may depend on the lack of RB in FAM4 (**Table 7.3**). FAM5 and FAM3 also had higher β values than FAM4, confirming the relationship between the parameter and the RB content (**Table 7.3**).

The hysteretic correction φ_0 ranged between 0.1° and 2.9° . Such variability could be due to the heterogeneity of the specimens skeleton.

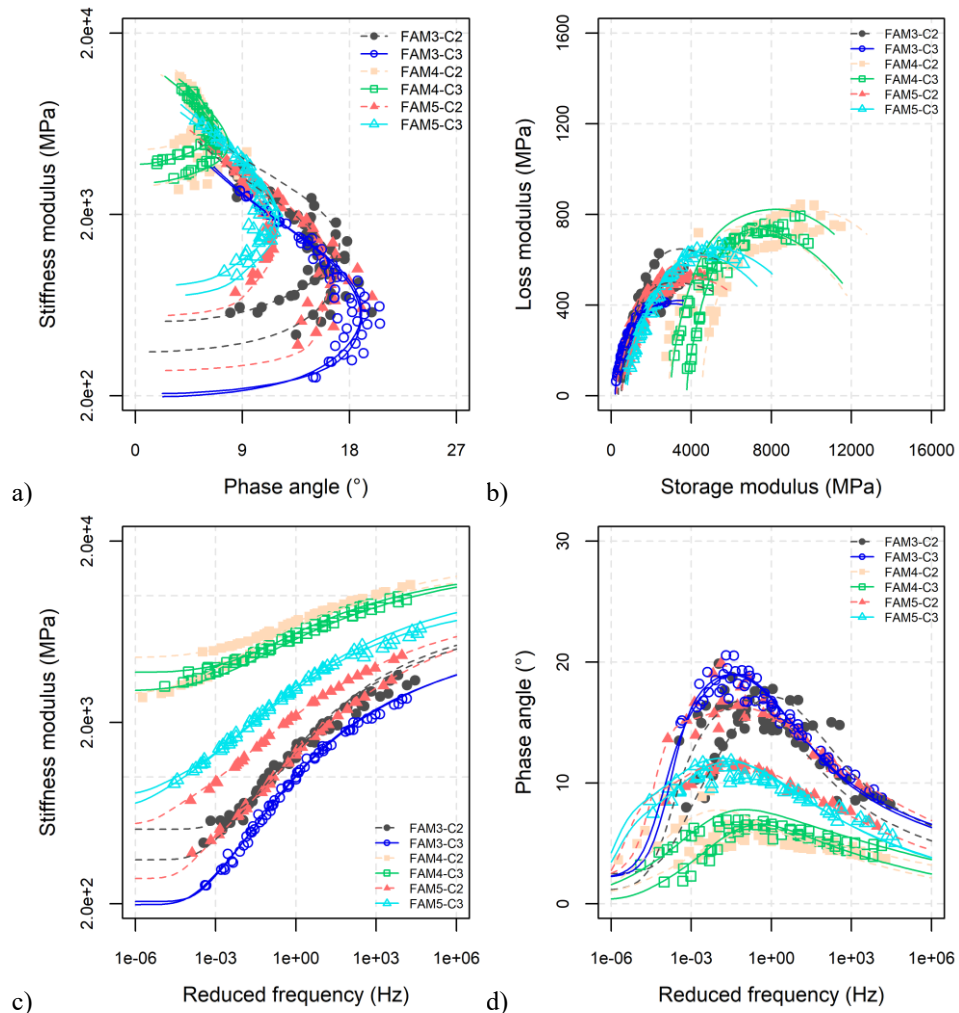


Figure 7.8. FAM mortars experimental data and 2S2P1D-HY model a) Black diagram, b) Cole-Cole plan, c) stiffness modulus master curves ($T_{ref} = 25$ °C) d) phase angle master curves ($T_{ref} = 25$ °C)

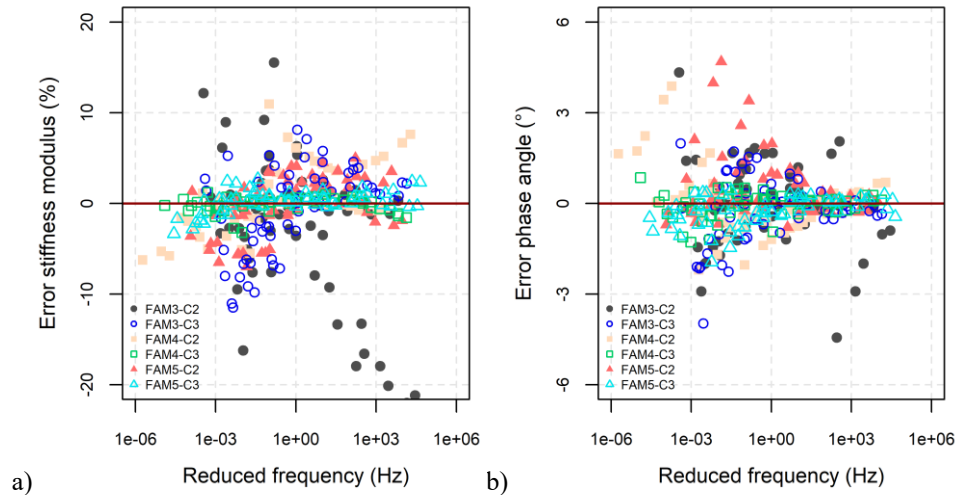


Figure 7.9. Accuracy of 2S2P1D-HY model prediction (Equations (7.2) and (7.3) for FAM mortars: a) stiffness modulus, b) phase angle

7.4.3. Relationship between CBE mixtures and FAM mortars

Figure 7.10 compares the average asymptotic stiffness values of mixtures and FAM mortars, obtained for CBE materials produced with the same cement type and grading distribution. Mixtures had generally higher E_e and E_g . However, the E_g of FAM4 was about double those of MIX4 (GG grading distribution).

The rheological behaviour of the mixtures and FAM mortars was compared using normalised complex modulus curves (Di Benedetto et al., 2004). The normalisation was applied only to the LVE part of the behaviour, i.e. $E^* \exp(-j\varphi_0)$:

$$E_{normalised}^* = \frac{E^* \exp(-j\varphi_0) - E_e}{E_g - E_e} \quad (7.4)$$

The normalised Black diagrams and Cole-Cole plans obtained are depicted in **Figure 7.11** for MIX3 and the corresponding FAM3, in **Figure 7.12** for MIX4 and FAM4, and in **Figure 7.13** for MIX5 and FAM5. As can be observed, the normalised curves obtained with different cements were almost superposed, confirming that only the bituminous binder controls the viscous response of CBE materials. Differently, normalised data of CBE mixtures and FAM mortars were slightly detached, indicating that they had different viscous responses. The gap is more evident for CBE materials obtained from GG grading (**Figure 7.12**). This suggests that also the RB in the coarse aggregate skeleton contributed to the LVE response of CBE mixtures.

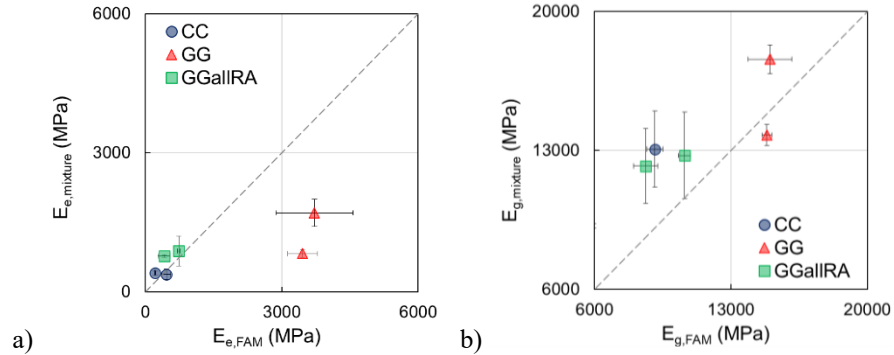


Figure 7.10. Comparison of CBE mixtures and FAM mortars 2S2P1D-HY model parameters a) E_e , b) E_g . Error bars represent the variability of the parameters

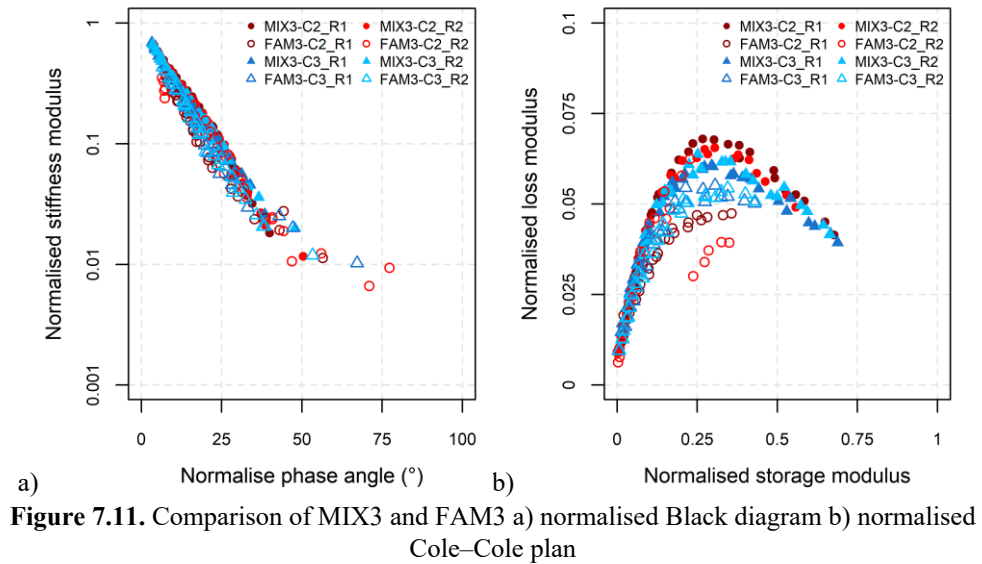


Figure 7.11. Comparison of MIX3 and FAM3 a) normalised Black diagram b) normalised Cole–Cole plan

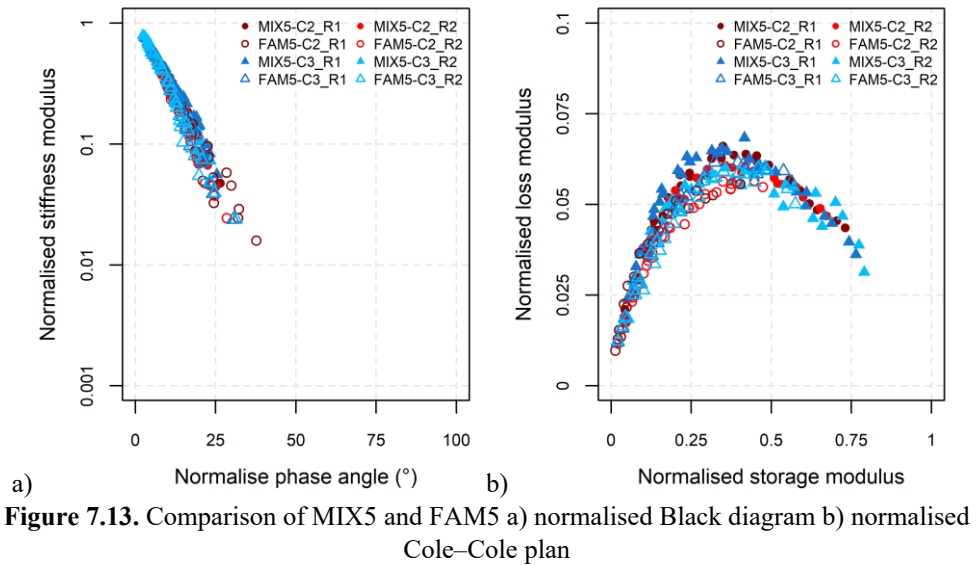
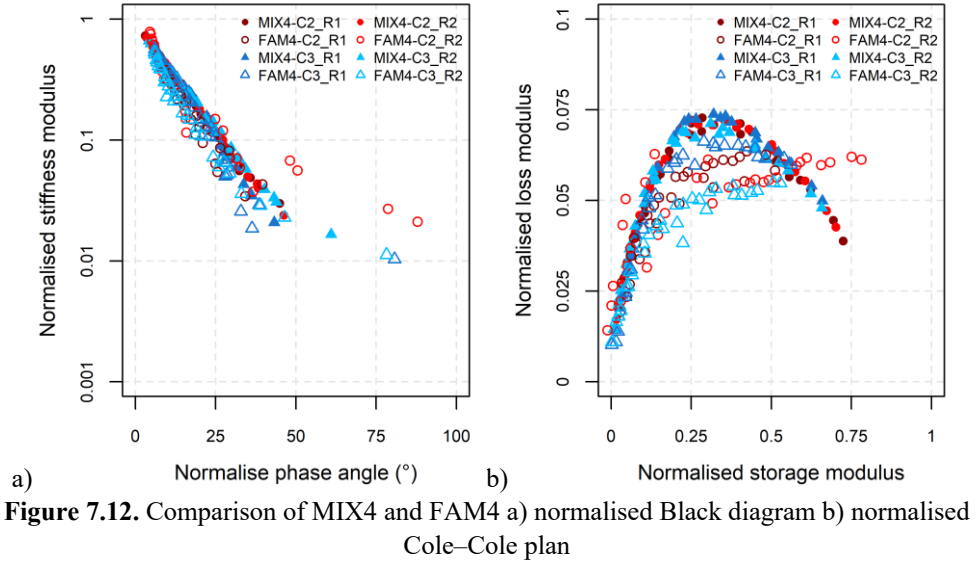


Figure 7.14 relates the remaining six model average parameters of CBE mixtures and mortars produced with the same cement type and grading distribution.

The values of k and h of mixtures and the corresponding mortars were almost the same (**Figure 7.14a** and **Figure 7.14b**). The δ values of FAM mortars were always lower than those used for fitting the LVE behaviour of mixtures (**Figure 7.14c**). τ of mixtures MIX3 and MIX5 (characterised by CC and GGallRA grading, respectively) was higher than those of the corresponding mortars FAM3 and FAM5, suggesting a reduced viscous response of mixtures. An opposite behaviour was observed for CBE materials obtained starting from the GG grading: MIX4 had lower τ than FAM4, and consequently, higher viscous response (**Figure 7.14d**). This may be attributed to the lack of RB in FAM4 (**Table 7.3**). The pairs $(\beta_{FAM}, \beta_{mixtures})$ were close to the equality line. On the contrary, the relationship between the parameter φ_0 of mixtures and FAM mortars was not clear, probably because it mainly depends on differences among the aggregate skeletons of the tested specimens.

The results showed that CBE mixtures and FAM mortars had similar sensitivities in the small strain domain. However, the LVE response of the two CBE composites was not the same as it was also influenced by the RB coating the coarse aggregate skeleton. Therefore, from a rheological point of view, RA cannot be considered a black rock. Besides, the individual compositions of mixtures and FAM mortars may have affected the LVE behaviour of CBE composites.

Chapter 6 demonstrated that FAM mortars predict the curing behaviour of mixtures since they totally contain the components affecting the curing, i.e. emulsion and cement. On the contrary, as the LVE behaviour of bituminous materials is strongly dependent on the bituminous binder, the relationship between mixtures and mortars cannot disregard the presence of the aged recycled binder coating the coarse RA skeleton.

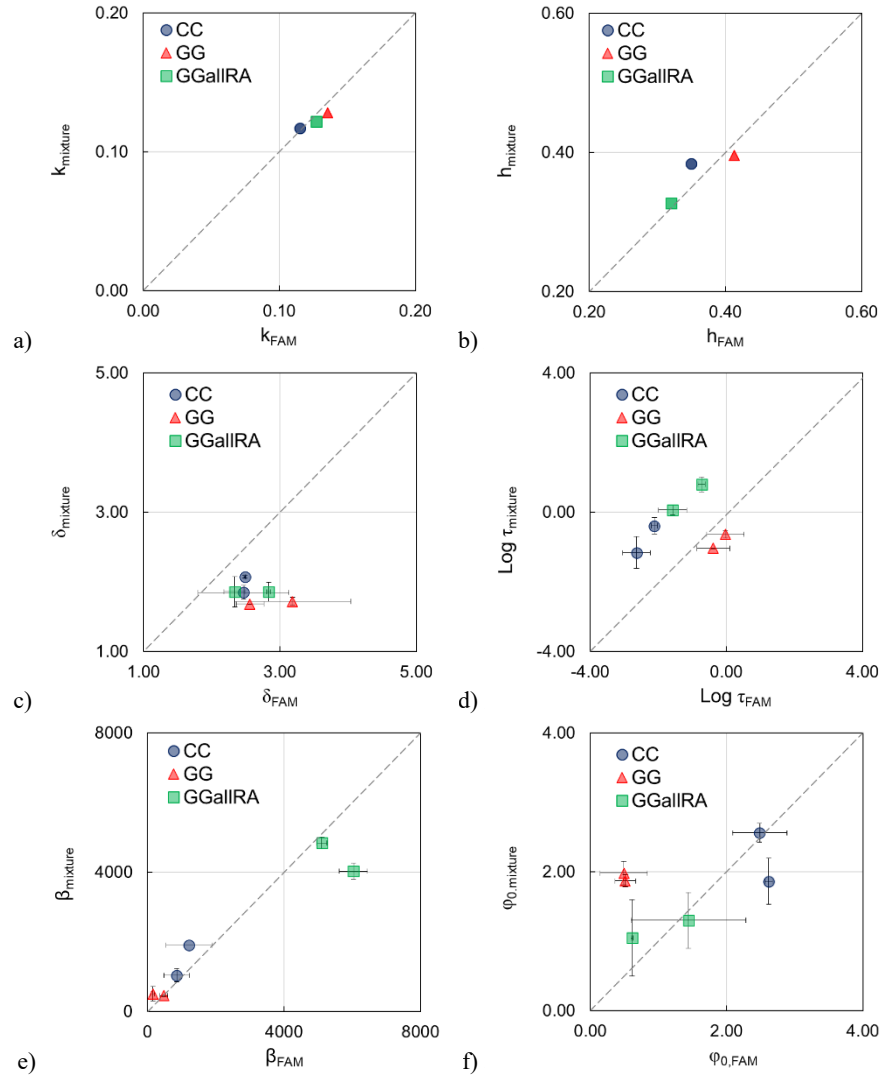


Figure 7.14. Comparison of CBE mixtures and FAM mortars 2S2P1D-HY model parameters a) k , b) h , c) δ , d) $\text{Log } \tau$, e) β and f) φ_0 . Error bars represent the variability of the parameters

7.4.3.1. CBE composites modelling: influence of the coarse aggregate

The complex modulus test results suggested that both the FAM mortar and the RA coarse aggregate skeleton contribute to the LVE behaviour of CBE mixtures. Therefore, this section describes a simple methodology to upscale the small strain response of the mortar for predicting the small-strain response of the mixture (**Figure 7.15**). The basic hypothesis is that the mortar and the coarse aggregate are perfectly bonded, and thus when an external load is applied to the mixture, a uniform strain is assumed in the two phases. This corresponds to the simple parallel arrangement shown in **Figure 7.16**.

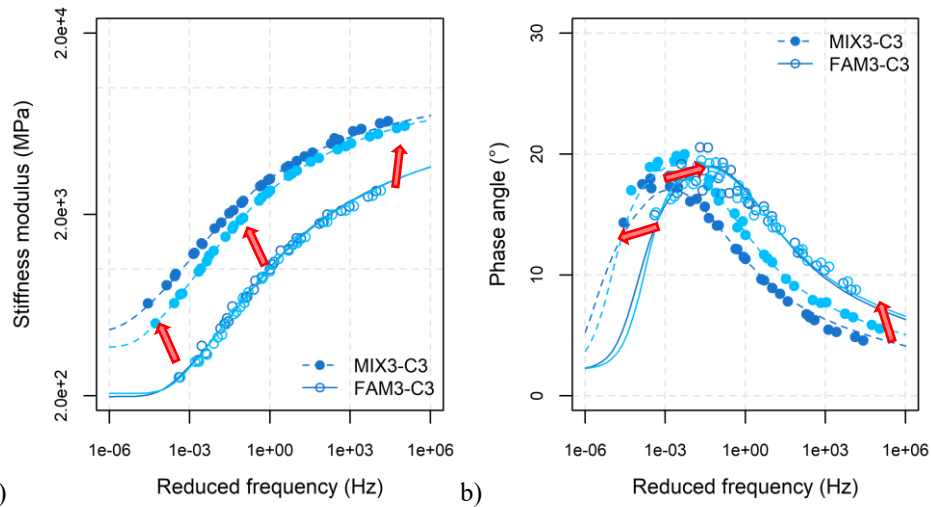


Figure 7.15. FAM3-C3 to MIX3-C3 master curves upscaling a) stiffness modulus, b) phase angle

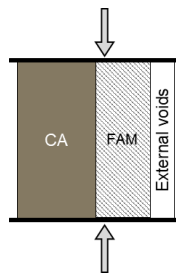


Figure 7.16. 1D schematic representation of CBE mixture in parallel arrangement

Considering the simple model depicted in **Figure 7.16**, the asymptotic stiffness moduli of the mixture, i.e. $E_{e,mixture}$ and $E_{g,mixture}$, can be expressed as:

$$E_{e,mixture} = E_{e,CA}V_{CA} + E_{e,FAM}V_{FAM} \quad (7.5)$$

$$E_{g,mixture} = E_{g,CA}V_{CA} + E_{g,FAM}V_{FAM} \quad (7.6)$$

where V_{CA} and V_{FAM} are the volume fractions of coarse aggregate and FAM mortar. $E_{e,FAM}$ and $E_{g,FAM}$ are mortar equilibrium and glass moduli, respectively. $E_{e,CA}$ and $E_{g,CA}$ are fitting parameters representing the relative stiffness of the coarse aggregate volume at low and high frequencies.

Using the average values obtained for mixtures and mortars of E_e and E_g (**Table 7.1** and **Table 7.2**), the coarse aggregate asymptotic moduli $E_{e,CA}$ and $E_{g,CA}$ were determined. **Table 7.4** reports the input parameters used in Equations (7.5) and (7.6) and the model parameters $E_{e,CA}$ and $E_{g,CA}$. The simple schematic model allowed obtaining the stiffness modulus of the coarse aggregate skeleton at both low and high frequencies. The only exception was for the pair MIX4-C3 and FAM4-C3, for which the value of $E_{e,CA}$ was unrealistic. This is probably due to the dispersion of the experimental data in the high-temperature range.

The parallel arrangement was then applied to the real and imaginary part of the complex moduli of mixtures and mortars obtained at the same testing temperature and frequency. Therefore, the values of E_1 and E_2 of the coarse aggregate skeletons were derived, and the data have been fitted using the 2S2P1D-HY model. **Table 7.4** reports the model parameters. **Figure 7.17** and **Figure 7.18** depict the obtained results for CBE materials produced with CC grading and cement C3 and with GG grading and C2, respectively. The remaining results are shown in Appendix I. It must be noted that the complex modulus E_{CA}^* does not represent the actual coarse aggregate LVE response, as the coarse aggregate is a granular material dispersed in the mortar matrix. It rather represents an “*equivalent*” modulus, whose contribution in the LVE response of CBE mixtures is strictly linked to that of the mortar phase. Indeed, for mixtures with CC or GGallRA gradings (**Figure 7.17** and Appendix I), the coarse aggregate was always stiffer than mixtures and FAM mortars. On the contrary, in the case of GG distribution, the stiffer phase of the CBE mixture composite is represented by the mortar (**Figure 7.18**). The coarse aggregate skeletons contributions were fitted with similar values of the viscous parameters h , k , δ and β . This may indicate a good homogeneity of the RA source.

Table 7.4. Parallel arrangement and 2S2P1D-HY model average parameters ($T_{ref}=25\text{ }^{\circ}\text{C}$) obtained in the study of the influence of coarse aggregate

ID	V (-)	E _e (MPa)	E _g (MPa)	k (-)	h (-)	δ (-)	β (-)	Log τ (-)	φ ₀ (°)
<i>Mixtures</i> ⁺									
MIX3-C2*	1	490	15000	0.12	0.38	1.75	1905	-0.700	2.70
MIX3-C3	1	400	9000	0.12	0.38	2.07	1041	-0.390	1.86
MIX4-C2	1	1700	17600	0.13	0.40	1.68	456	-0.635	1.87
MIX4-C3	1	800	13800	0.13	0.40	1.72	512	-1.036	1.98
MIX5-C2	1	800	12000	0.12	0.33	1.86	4031	0.063	1.30
MIX5-C3	1	900	13000	0.12	0.33	1.86	4845	0.805	1.05
<i>FAM mortars</i> ⁺									
FAM3-C2	0.493	400	8400	0.12	0.35	2.47	5147	-2.442	2.48
FAM3-C3	0.493	200	6000	0.12	0.35	2.49	857	0.008	2.62
FAM4-C2	0.352	3700	15000	0.14	0.41	2.56	474	-0.033	0.51
FAM4-C3	0.352	3500	15000	0.14	0.41	3.19	159	-0.384	0.49
FAM5-C2	0.399	400	8600	0.13	0.32	2.84	6035	-1.576	1.44
FAM5-C3	0.399	730	10600	0.13	0.32	2.34	5114	-0.728	0.61
<i>Coarse aggregate</i>									
CA3-C2	0.477	550	22153	0.14	0.42	1.89	1E+10	-1.009	1.00
CA3-C3	0.477	632	12671	0.14	0.39	1.74	1E+10	0.198	1.59
CA4-C2	0.618	641	19938	0.14	0.39	1.18	1E+10	-1.104	1.40
CA4-C3	0.618	-702	3500						
CA5-C2	0.578	1111	14861	0.18	0.40	3.18	1E+10	1.346	0.82
CA5-C3	0.578	1056	15212	0.14	0.39	1.92	1E+10	1.527	0.44

* only sample R1 considered, ⁺ mixtures and mortars parameters were obtained as average of the two replicates

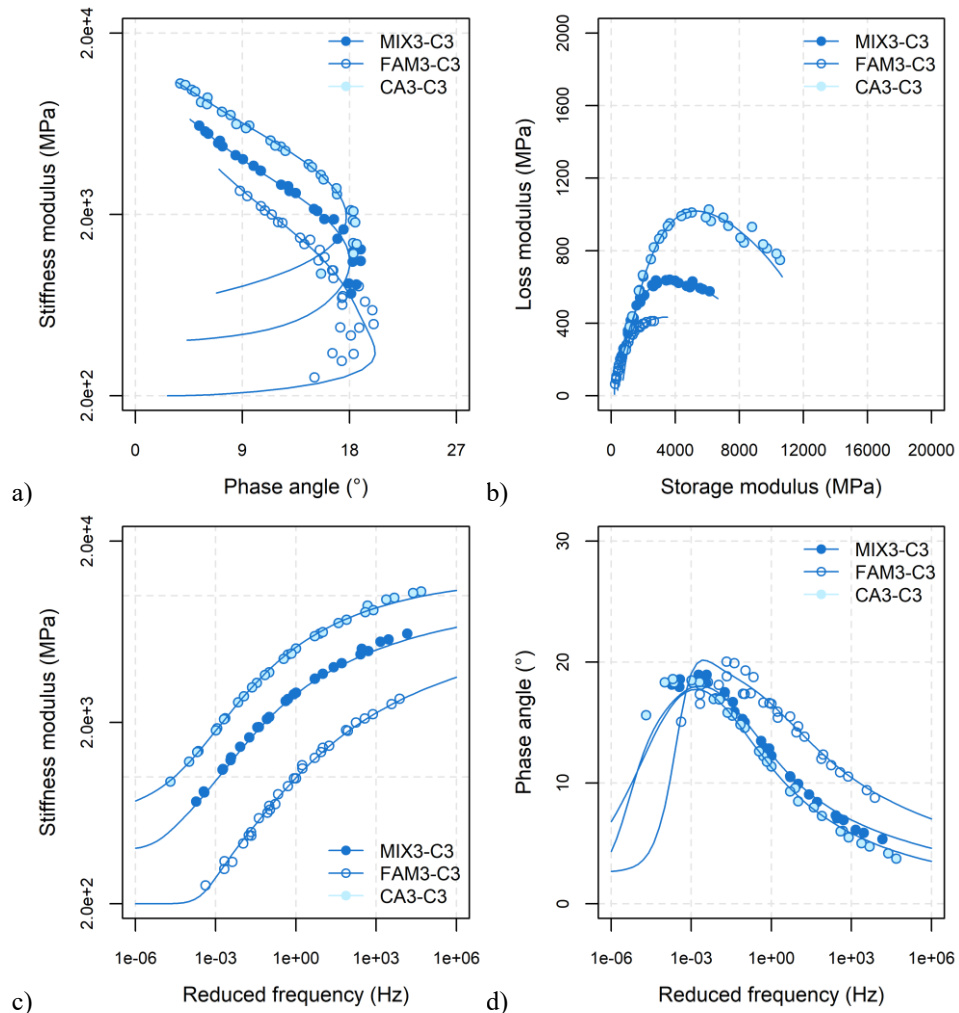


Figure 7.17. Average complex modulus results and fitted 2S2P1D-HY obtained for CBE materials with grading CC and cement C3 a) Black diagram, b) Cole-Cole plan, c) stiffness modulus master curves ($T_{ref} = 25 \text{ }^\circ\text{C}$) and d) phase angle master curves ($T_{ref} = 25 \text{ }^\circ\text{C}$)

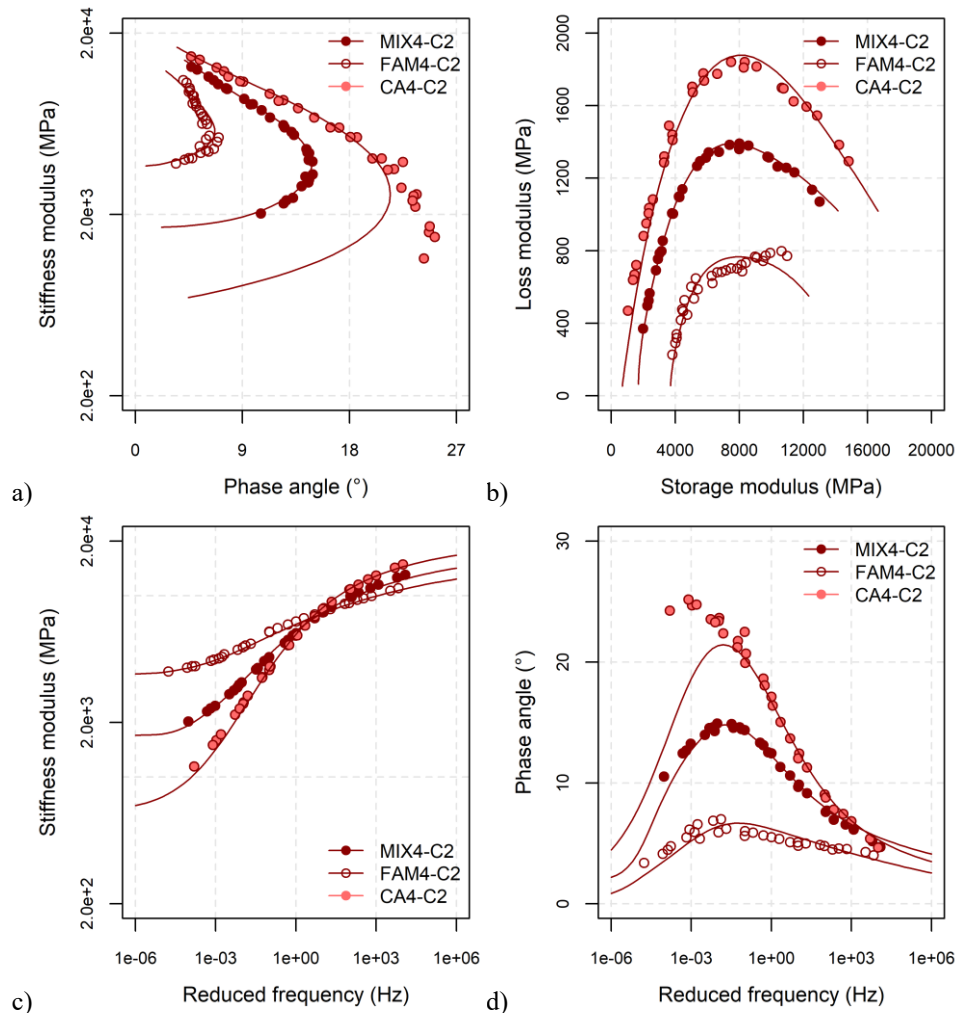


Figure 7.18. Average complex modulus results and fitted 2S2P1D-HY obtained for CBE materials with grading GG and cement C2 a) Black diagram, b) Cole-Cole plan, c) stiffness modulus master curves ($T_{ref} = 25 \text{ }^\circ\text{C}$) and d) phase angle master curves ($T_{ref} = 25 \text{ }^\circ\text{C}$)

7.5. Summary

The present Chapter deals with the LVE response of CBE mixtures and FAM mortars. This was evaluated measuring the complex modulus after long-term curing of mixtures produced considering three grading distribution, two high strength cements and modified bitumen emulsion. Complex modulus was measured on the six corresponding FAM mortars as well. The experimental results were modelled using analogical rheological models.

The main findings are as follows:

- Mixtures and FAM mortars were thermo-rheologically simple materials, i.e. the TTSP was valid;
- The effect of cement type was mainly linked to the elastic component of the CBE materials. In particular, C2 generally led to materials having higher stiffness modulus and lower phase angle at all frequencies and temperatures;
- The grading distribution affected the elastic response of CBE materials;
- Mixtures and FAM mortars showed similar sensitivity in the LVE response. However, the differences due to the material composition were more pronounced at the FAM mortar scale;
- CBE materials LVE behaviour can be satisfactorily modelled using a modified version of the 2S2PID model, which considers dissipation mechanisms ascribed to internal friction phenomena and the presence of cementitious bonds;
- Mixtures and FAM mortars were modelled using viscous parameters of the new model slightly different. This indicates that not only the mortar matrix controlled the LVE response of CBE mixtures and that also the aged bitumen coating the RA coarse aggregate particles contributed to it;
- A simple model was proposed for estimating the RA coarse aggregate contribution to the CBE mixture LVE response.

FAM mortars were found an interesting tool for characterising the LVE behaviour of CBE mixtures. Their ability to predict the mixture behaviour is strongly linked to their composition. However, an additional complication rises from the presence of the aged bitumen coating to coarse aggregate particles which contributes to the LVE response of the mixture. Additional studies are needed to investigate the influence of FAM mortar composition on its predicting ability of mixture behaviour. Besides, the effect on the LVE response of CBE materials of the bituminous binder nature, i.e. aged and new bitumen, is worth being further investigated.

Chapter 8.

Rheological Characterisation of CBE Slurries

8.1. Introduction

As observed in the literature review, a proper evaluation of the rheological properties of CBE slurries is fundamental because of its close link with the workability of CBE mixtures. This Chapter deals with the study of the viscosity of CBE slurries. The investigation was carried out in collaboration with the Nottingham Transportation Engineering Centre (University of Nottingham).

8.2. Objectives

This part of the thesis focused on the rheological characterisation of CBE slurries in terms of viscosity. The Brookfield viscometer was selected because of its user-friendliness, cost-effectiveness and good reliability. The experimental study was organised in two parts. The first focused on the definition of the testing procedure. The objective was to select the most accurate methodology to investigate the viscosity of CBE slurries. Tests to define a simple testing procedure were carried out. In particular, the effect of using a traditional spindle and innovative DHR impellers (Giancontieri *et al.* 2020) was assessed. The second part of the study focused on the effect of CBE slurries composition on the viscosity. A wide number of slurries was investigated to study and model the influence of bitumen emulsion and mineral additions. The study aims to provide useful information that can act as guidelines for defining the most effective CBE mixtures composition for obtaining a good balance between their fresh properties, i.e. workability and compactability, and their mechanical properties.

8.3. Methodology

Figure 8.1 shows the organisation of the experimental programme.

Part 1, which considered the influence of both types of impellers (spindle and DHR), was organised in tasks. Part 1A focused on evaluating the possible changes in the viscosity

due to emulsion breaking or cement hydration. The task aimed to ensure that the testing time scale is shorter than the structure-alteration time scale. During Part 1A, the viscosity of a selected number of slurries was measured at the constant speed of 100 rpm for 600 s, with a reading interval of 20 s (**Figure 8.2a**). Because CBE slurries are non-Newtonian materials, the measurement of the viscosity at different shear rates is crucial. Therefore, Part 1B focused on the effect of speed changes on the viscosity. As a starting point, the procedures suggested for bitumen and bitumen emulsion in EN 13302 and AASHTO T 316 were considered. In particular, EN 13302 considers a stabilising period before reading of 30 s, whereas the reading period required by AASHTO 316 is 180 s. Procedures used in previous studies were considered, as well (**Table 2.7**). **Figure 8.2b** depicts the testing procedure followed during Part 1B. Starting from the mixing speed of 100 rpm, the test speed was changed every 180 s, and the torque was registered every 20 s. The task aimed at establishing an appropriate time for maintaining each test speed. This time must be long enough to allow the material stabilisation.

Only the DHR impellers were used in Part 2. The selected stabilising period was 60 s. Thus, speed was changed once per 60 s, and the torque was recorded immediately before the speed switching. The first torque reading (time zero) was taken 180 s after the start of mechanical mixing (120 s of mixing + 60 s of stabilising period) at 100 rpm ($\dot{\gamma} = 34 \text{ s}^{-1}$). The procedures, depicted in **Figure 8.2c** and **Figure 8.2d**, had some slight differences between the LV and HA viscometer because of the different sets of speeds available. When the LV model viscometer was used (**Figure 8.2c**), the test speed was gradually increased up to 200 rpm ($\dot{\gamma} = 68 \text{ s}^{-1}$) and then decreased until reaching 50 rpm. For the HA model viscometer, the maximum speed is 100 rpm, and the set of testing speeds is reduced. Thus, after the first reading at 100 rpm, the speed was decreased until 50 rpm and, then, increased and decreased a second time (**Figure 8.2d**).

The composition of the investigated CBE slurries is reported in **Table 4.6**.

Chapter 8

Rheological Characterisation of CBE Slurries

Multiscale Approach for Characterising the Behaviour of Cold Bitumen Emulsion Materials

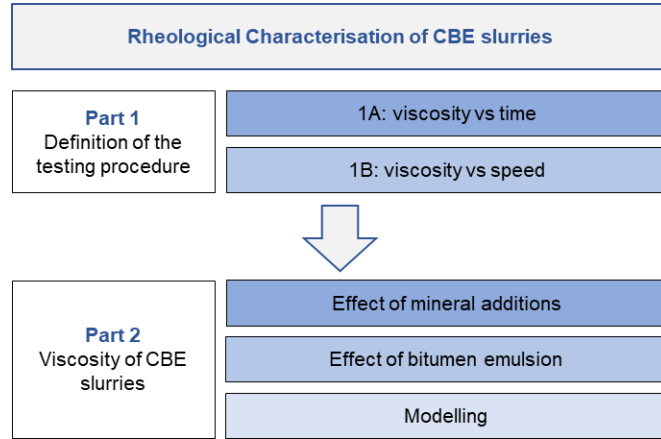


Figure 8.1. Viscosity of CBE slurries: experimental programme organisation

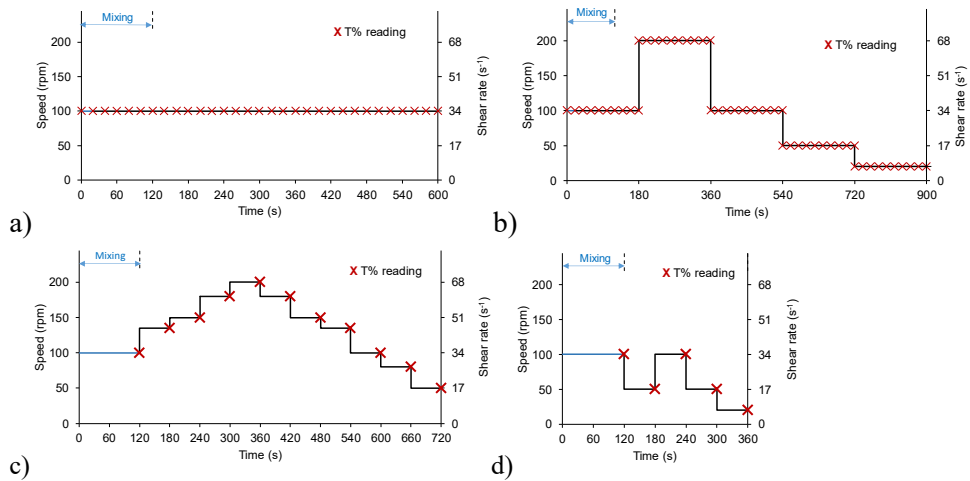


Figure 8.2. Test procedure followed during the experimental study a) Part 1A, b) Part 1B, c) Part 2 - LV model viscometer, d) Part 2 - HA model viscometer

8.4. Analysis of the Results

8.4.1. Part 1: Definition of the testing procedure

The present section analyses the results obtained during the first part of the investigation. **Figure 8.3** displays the results of Part 1A of the study. The curves of the average viscosity as a function of testing time were obtained at $\dot{\gamma} = 34 \text{ s}^{-1}$ (100 rpm) with both types of impellers. Time zero in the x-axis coincides with the beginning of the mechanical mixing in the viscometer. The viscosity of the plain bitumen emulsion (B_596) measured with both S27 and DHR was almost constant within 600 s. Besides, the viscosity obtained using different impellers was similar: the difference in the measured values was always lower than 10%. The outcome confirms that the SRC of S27 and DHR is the same from a practical point of view (Equation (4.10)).

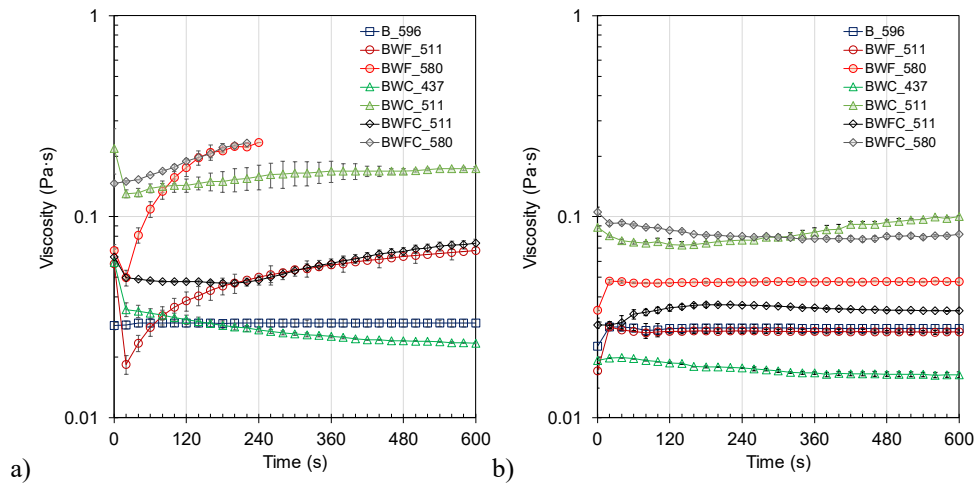


Figure 8.3. Viscosity changes over time of bitumen emulsion and CBE slurries measured using a) S27, b) DHR. Error bars represent the standard deviation of the experimental data

The results obtained for systems characterised by a higher level of complexity, such as CBE slurries, highlighted some more variability. Some differences due to the type of impeller have been observed. The viscosity values measured with S27 (**Figure 8.3a**) showed some reliability issues in terms of repeatability (e.g. BWF_511 and BWC_511) and sample stability. Using S27, the viscosity of slurries increased with time when the filler was used. Also, for BWF_580 and BWFC_580, the test had to stop after 240 s because the torque was too high. Differently, when equipped with the DHR (**Figure 8.3b**), the viscometer was able to measure the viscosity of these slurries over 600 s. This behaviour suggests that sedimentation and phase separation happened when the standard spindle was used.

After the end of the first 120 s of measurement (mixing time, see Section 4.2.1.2), the viscosity of slurries measured with the DHR can be considered constant: the variation in the viscosity between the measurement taken at 120 s and 600 s was lower than 15%. The only exception was for BWC_511, for which an increase of η of about 27% was measured. It is worth highlighting that the volumetric concentration of cement in this slurry is relatively high (0.150), and some change in the structure could have occurred, and the emulsion breaking process could have been accelerated. Indeed, cement concentration is crucial and can dramatically accelerate the breaking process. For example, after mixing a slurry characterised by cement volume fraction equal to 0.270 (BWC_580), sudden emulsion breaking occurred, as displayed in **Figure 8.4a**.

Results showed that, in general, in the first minutes after the mixing, there was no evidence of variation in viscosity due to the emulsion breaking or cement hydration. The viscosity change measured using S27 is ascribable to the instability of the sample and not to structural changes. Therefore, tests can be performed after a reasonable time after the mixing with no significant changes in the viscosity.

Figure 8.5 reports the results of the tests carried out in Part 1B of the investigation. The average viscosity curves obtained using both S27 and DHR are depicted as a function of time and shear rate ($\dot{\gamma} = 6.8 - 68 \text{ s}^{-1}$). The x-axis zero (time zero) coincides with the start of the mechanical mixing. Results confirm that after the first 120 s, i.e. mixing time, the viscosity can be considered stabilised. S27 and DHR provided the same viscosity values for the plain bitumen emulsion, B_596 (**Figure 8.5a**). Also in this case, the viscosity measurement with the S27 of slurries containing filler appeared less stable than those obtained with the DHR, showing a higher variability with time (**Figure 8.5b** and **Figure 8.5d**).

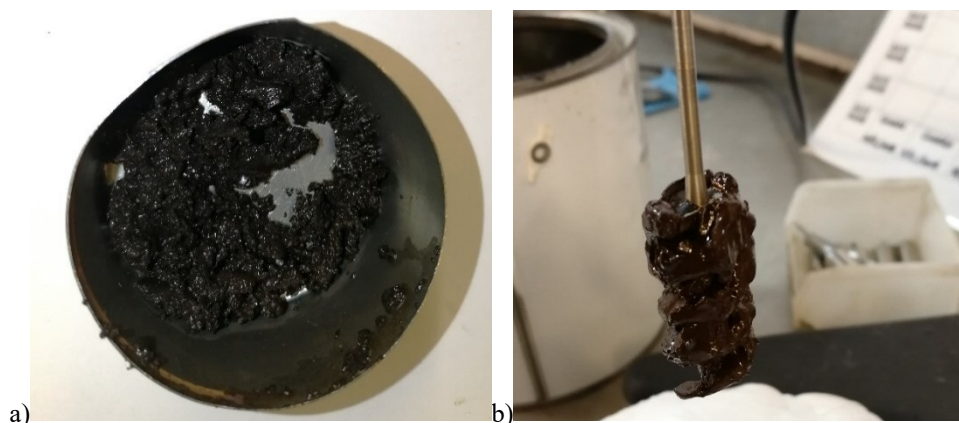


Figure 8.4. . CBE slurries appearance: a) BWC_580 immediately after the hand-stirring (emulsion breaking), b) BPWF_680 right after the lowering of the impeller

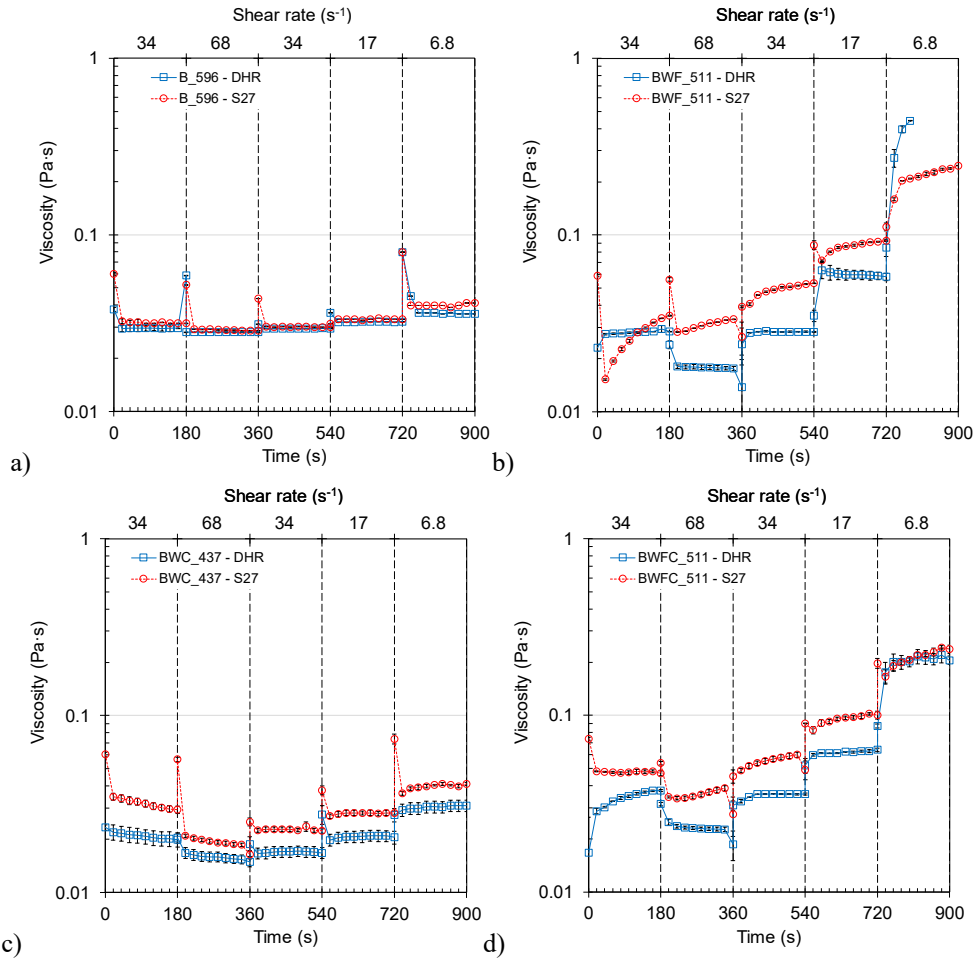


Figure 8.5. Viscosity measured during Phase 1B a) B_596 (emulsion), b) BWF_511, c) BWC_437, d) BWFC_511. Error bars represent the standard deviation of the experimental data

After the change of speed (and consequently of $\dot{\gamma}$), the viscosities of emulsion and CBE slurries were stabilised immediately with the DHR. When they were measured with S27, the stabilisation was slightly delayed. However, the viscosities measured after 60 s and 180 s were similar (difference lower than 10%). This suggests that the viscosity can be measured by recording the torque percentage after 60 s from the speed change to reduce the total duration of the test.

Tests carried out at $\dot{\gamma} = 6.8 \text{ s}^{-1}$ (20 rpm) were not reliable. The speed was too low to avoid the sedimentation of the filler sized particles. Therefore, it is suggested that the viscosity measurement should be carried out at high shear rates (equal to or greater than 17 s^{-1}).

8.4.2. Part 2: Viscosity of CBE slurries

The present section displays the results obtained during Part 2 of the experimental programme using only the DHR impellers (DHR_2 and DHR_3). The choice to use DHR_2 or DHR_3 was made as a function of the predicted system viscosity. A narrower pitch indeed characterises DHR_3, and it allows measuring lower viscosities, ranging between 0.01 Pa·s and 0.5 Pa·s. The viscosity range measurable by DHR_2 is 0.1 – 1 Pa·s. When both DHR_2 and BHR_3 could be used, the two impellers allowed obtaining the same viscosity values. In particular, **Figure 8.6** reports some examples of the hysteresis curves of the viscosity as a function of the shear rate. The “up” curves were obtained by increasing $\dot{\gamma}$ from 34 to 68 s^{-1} (from 100 to 200 rpm), whereas the “down” curves were measured after a successive decreasing of $\dot{\gamma}$ from 68 to 34 s^{-1} . The results obtained during the speed rising and decreasing phase of measurement were very close under the same speed. The viscosity difference was always lower than 10% for $\dot{\gamma}$, ranging between 46 and 68 s^{-1} . When $\dot{\gamma}$ is smaller (34 s^{-1}), the difference was higher, reaching 64% for BWF_511. The outcome could be due to some homogenisation of the material structure. This may result from an additional mixing resulting from the enhanced pumping effect obtained at the higher shear rates. In the analysis of the rheological behaviour, the down curves will be considered.

Figure 8.7 reports the average viscosity flow curves measured with the DHR impellers for dispersions produced with the modified bitumen emulsion (BP). Results on dispersions produced with the plain bitumen emulsion (B) are not displayed as they were similar to those obtained with BP.

In the adopted shear rate range, emulsion and its simple dilution with water had a Newtonian behaviour. This can be due to the small range of shear rate considered since the addition of a dispersed phase, i.e. bitumen, in a Newtonian fluid generally leads to a non-Newtonian behaviour. Differently, all the tested slurries were shear-thinning, indicating non-Newtonian behaviour.

The dilution of the emulsion with water reduced the viscosity significantly. Passing from $W/B = 0.7$ (BP_596) to 1.3 (BPW_425), η was about 250% lower.

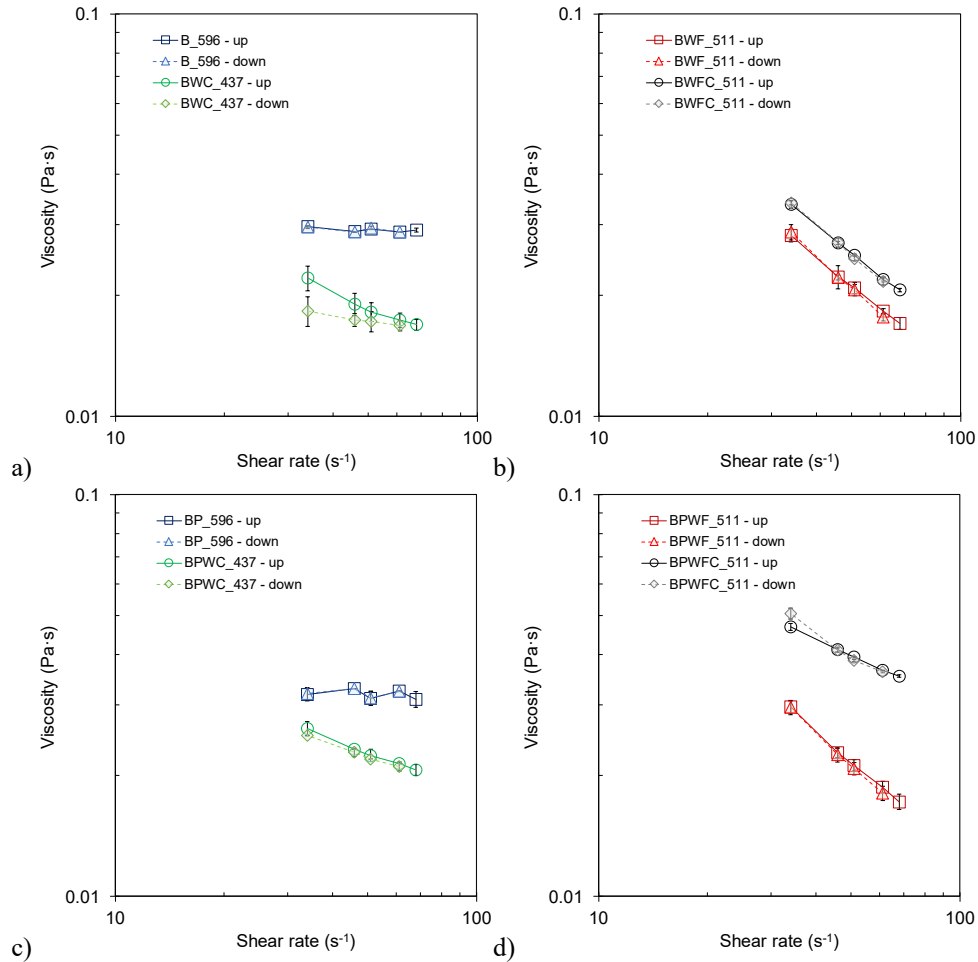


Figure 8.6. Viscosity as a function of shear rate measured during the rising phase of speed (up) and decreasing phase of speed (down) for a) B_596 and BWC_437, b) BWF_511 and BWFC_511, c) BP_596 and BPWC_437, d) BPWF_511 and BPWFC_511. Error bars represent the standard deviation of the experimental data.

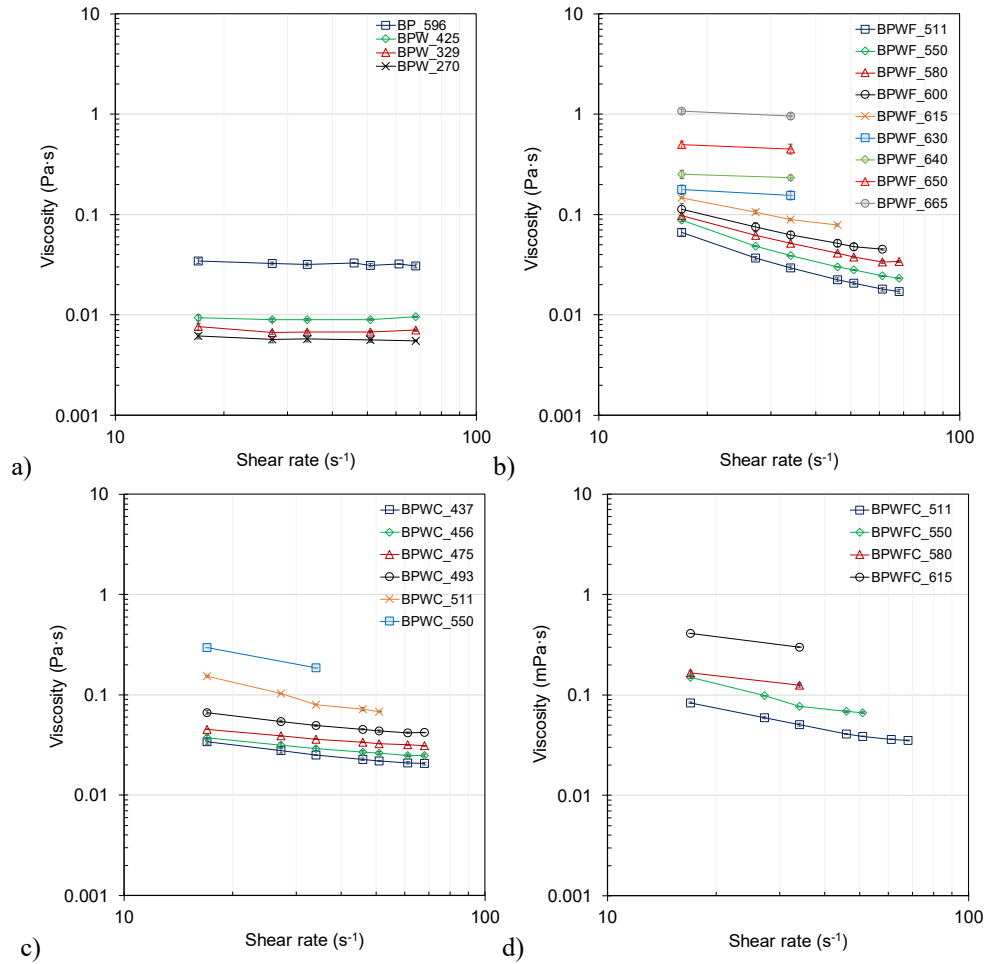


Figure 8.7. Viscosity versus shear rate for a) BPW, b) BPWF, c) BPWC, d) BPWFC. Error bars represent the standard deviation of the experimental data

Considering slurries produced with the same mineral addition, increasing its dosage, and consequently the solid particles volume fraction, the viscosity always increased. The addition of cement increased the viscosity substantially compared to slurries with the same total solid particles volume fraction and only filler (e.g. $\phi_s = 0.511$).

BPWF_680 and BWF_700 (Table 4.6) were impossible to test. Figure 8.4b shows BPWF_680 immediately after the hand stirring and the lowering of the impeller, which resulted in testing being unfeasible. The slurries had a very low level of fluidity with a doughy aspect. No impeller was able to measure the viscosity as the torque always exceeded 100%.

Figure 8.8 compares the viscosity measured in slurries with the same ϕ_s produced with the two emulsion types (B and BP). Results show that modified bitumen emulsion generally resulted in slurries with a slightly higher viscosity compared to plain bitumen emulsion, especially at high ϕ_s . Such a could be the result of the presence of the SBS latex droplets in the modified emulsion that introduce an additional solid phase in the dispersion, and consequently, the actual value of ϕ_s is slightly higher.

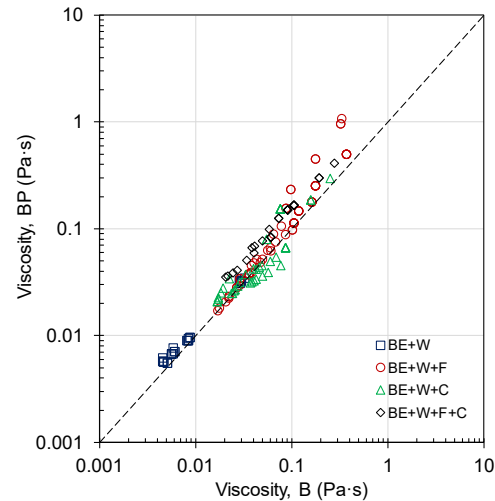


Figure 8.8. Effect of bitumen emulsion type on the viscosity of bitumen emulsion dispersions and CBE slurries

Figure 8.9 reports the results of the viscosity measured in function of the solid particles volume fraction at $\dot{\gamma} = 34 \text{ s}^{-1}$. Such a shear rate value was selected because it is achievable using both the viscometers adopted and, at the same time, high enough to exclude particles sedimentation effects. The viscosity depends on the solid particle volume fraction: η grew as solid particles are added. This behaviour is typical of suspensions: at low concentrations, particles can move freely, and the suspension will be in a fluid, viscous state. Increasing the concentration of the solid particles, thus their volume fraction, the suspensions will develop

an ever more packaged structure, and the suspension will become a solid elastic (Mason 1999, Willenbacher and Georgieva 2013). Starting from the Einstein model developed for suspensions of low volume fractions of spheres (diluted suspensions), a number of models were proposed to describe the dependence of the viscosity on the solid particles volume fraction over the years (Barnes *et al.* 1989, Mueller *et al.* 2010, Willenbacher and Georgieva 2013). For concentrated suspensions, the relationship between the viscosity and the volume fraction must consider the maximum packing volume fraction φ_m . The latter represents the value at which the viscosity rises to infinite because a high level of particles packing is reached, such that the flow is impossible. Its value is connected to the particle size distribution and the particle shape, as well as to the inter-particle forces.

In this study, the Krieger-Dougherty model (Krieger and Dougherty 1959) is considered for fitting the experimental data:

$$\eta = \eta_s \left(1 - \frac{\varphi_s}{\varphi_m}\right)^{-\eta_0 \varphi_m} \quad (8.1)$$

where η_s is the viscosity of the suspending medium and η_0 is the intrinsic viscosity (also called Einstein coefficient). Curved lines in **Figure 8.9** represents the fitted model, whereas **Table 8.1** reports the model parameters.

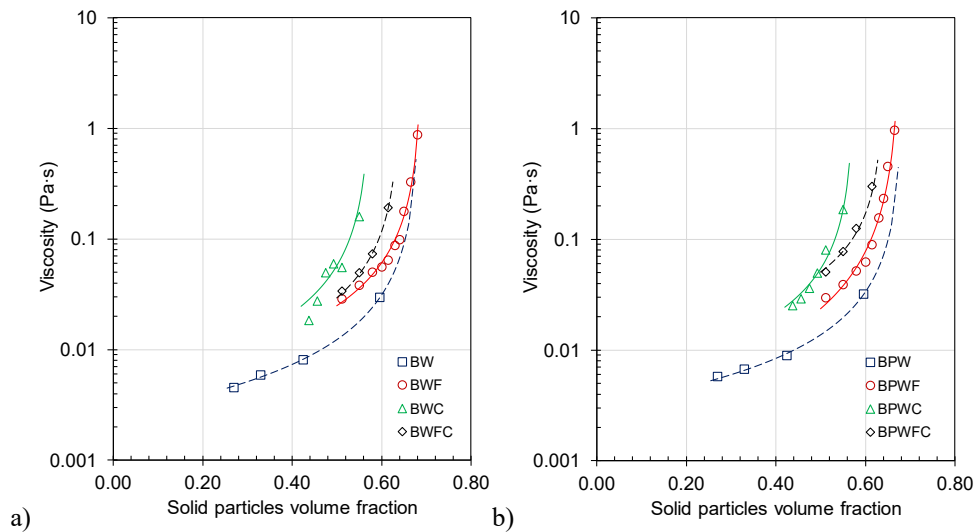


Figure 8.9. Viscosity versus solid particles volume fraction a) B, b) BP ($\dot{\gamma} = 34 \text{ s}^{-1}$)

The values of φ_m depended on bitumen emulsion and mineral additions type. Dispersions produced with the modified bitumen emulsion had slightly lower values of φ_m , confirming their higher viscosity compared to the viscosity of the dispersions with the plain bitumen

(**Figure 8.9**). Dispersions with only bitumen particles (i.e. BW and BPW) and those with only filler added (BWF and BPWF) had similar values of φ_m (from 0.678 to 0.690). When only cement is added (BWC and BPWC), φ_m diminished drastically (0.576 and 0.574). In contrast, the values of dispersions produced with both types of mineral additions (BWFC and BPWFC) were characterised by intermediate values (0.642 and 0.641). This effect could mainly be attributed to a different reactivity of the additions that can affect their interaction with the emulsion and the establishment of varying inter-particle forces. It could also be due to the different size and size distribution of the mineral addition and their packability highlighted by differing Rigden voids, i.e. 23.8% and 33.2% for filler and cement, respectively (see Appendix A). Additionally, cement could have had a faster effect on the emulsion breaking leading to a change in the bitumen droplets dimension. Further studies are necessary to establish the contribution of the different phenomena. The obtained value of φ_m can explain why BWF_700 and BPWF_680 (**Table 4.6**) were impossible to be tested. Indeed, the two selected φ_s are very close to the value of φ_m .

The η_s values showed a slight variation and were always higher with respect to the viscosity of the water at ambient temperature (about 0.001 Pa·s). This could be related to the choice of a too simple model considering the complexity of the system. Nevertheless, the model allowed a good fitting even for suspension characterised by multiple solid particles types (i.e. bitumen, filler and cement) to be obtained.

The product ($\eta_0 \varphi_m$), describing the growth rate of the viscosity, ranged between 0.973 and 1.446. Although slightly variable, its values are comprised in the range generally proposed in the rheology of suspensions (Barnes *et al.* 1989).

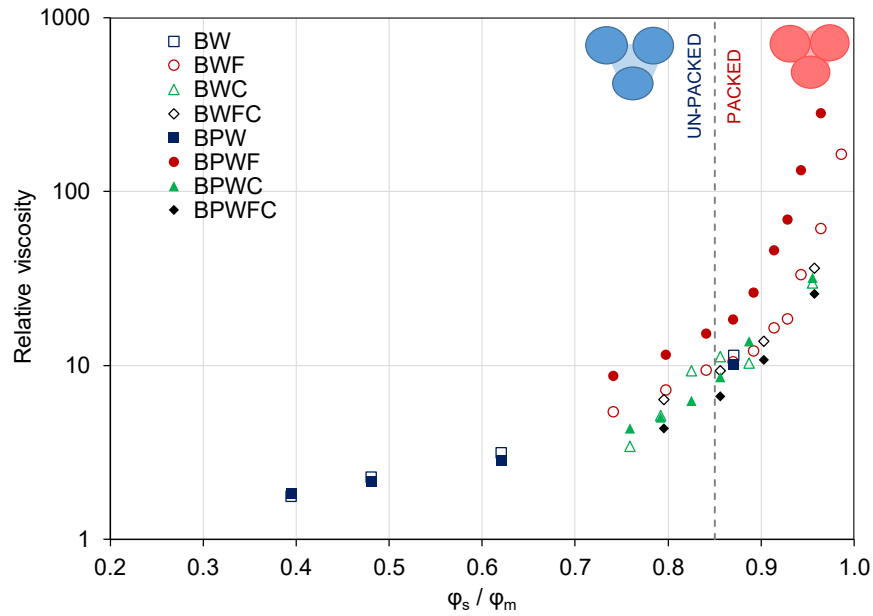
Figure 8.10 shows the relative viscosity ($\eta_r = \eta/\eta_s$) obtained by normalizing the viscosity experimental data with respect to the intrinsic viscosity obtained using the Krieger-Dougherty model (Equation (8.1)). η_r is shown as a function of the ratio between the solid particle volume fraction and the maximum packing volume fraction (φ_s/φ_m). All the materials show a similar behaviour: such evidence is confirmed by the values of the model exponents, $\eta_0 \varphi_m$, that are comparable.

η_r increased when adding solid particles and, when a specific value of φ_s/φ_m was reached, it raised asymptotically. In general, the exponential increase started when φ_s/φ_m was between 0.85 and 0.95. When CBE materials reached these concentration range values, the solid particles did not flow freely anymore, and it could be assumed that a packed concentrated structure was formed (**Figure 8.10**).

It is worth highlighting that the viscosity growth could also be related to the starting of other phenomena due to the interaction of the two co-binders (i.e. emulsion breaking or cement hydration). Again, further studies are needed to provide a better explanation of such outcomes.

Table 8.1. Krieger-Dougherty model parameters (Equation (8.1)) obtained for all the tested dispersions

Dispersion	φ_m	η_0	η_s (Pa·s)	$\eta_0 \varphi_m$	R^2
BW	0.685	1.743	2.58E-03	1.194	0.999
BPW	0.681	1.637	3.14E-03	1.115	0.997
BWF	0.690	1.728	5.32E-03	1.192	0.994
BPWF	0.678	2.132	3.39E-03	1.446	0.967
BWC	0.576	2.037	5.32E-03	1.173	0.975
BPWC	0.574	1.905	5.81E-03	1.094	0.801
BWFC	0.642	1.768	5.32E-03	1.135	0.997
BPWFC	0.641	1.519	1.16E-02	0.973	0.905

**Figure 8.10.** Relative viscosity as a function of the ratio between solid particles volume fraction and maximum packing volume fraction

8.5. Summary

The present Chapter deals with developing a robust procedure for measuring the viscosity of CBE slurries using a rotational viscometer. The mixing and testing procedures were herein developed. The influence of using a standard spindle and a novel DHR impeller was evaluated. Finally, following the testing procedure developed, the study focused on evaluating the impact of different mineral addition and bitumen types on the viscosity of CBE slurries. Also, the influence of solid particles concentrations was evaluated to obtain useful information for CBE mixtures composition design.

The main findings are as follows:

- Measurements carried out using the DHR impeller and the standard spindle proved that the first one allowed more reliable results to be obtained, diminishing the phase separation and sedimentation effects;
- CBE slurries were non-Newtonian, showing a shear-thinning behaviour within the tested range of shear rate;
- A small difference was observed due to the bitumen emulsion type: with modified bitumen, the viscosity was slightly higher at the same solid particles volume fractions;
- The type of addition had a substantial effect on the viscosity. When only Portland cement was used, the viscosity was significantly higher than those of slurries produced with only limestone filler. Slurries produced with both additions exhibited an intermediate behaviour;
- Despite the high complexity of the system, the Krieger-Dougherty model provided a good fitting of the experimental data, allowing the identification of the maximum packing volume fraction;
- When 95% of the maximum packing volume fraction is reached, the viscosity starts rapidly increasing, suggesting the formation of a packed structure.

Overall, the use of rotational viscometry with DHR geometry demonstrated to be a promising approach for the fundamental rheological characterisation of cold bitumen emulsion slurries. Further studies are needed to assess the effectiveness of using the DHR, for example, investigating most significant ranges of shear rates. To this aim, the application of the DHR in Dynamic Shear Rheometers is currently under investigation. The study of the effect of mineral additions types, bitumen emulsion types and solid particles concentration merits being explored, as well as the impact of particle sizes and their distribution, should be evaluated. Additional studies are required to relate the viscosity of CBE slurries and the fresh properties of CBE mixtures to obtain a practical recommendation for accurately define the composition of the mixtures.

Chapter 9.

Conclusions

9.1. Concluding Remarks

This thesis aimed at developing a multiscale approach for characterising the behaviour of cold bitumen emulsion (CBE) materials. Although CBE materials have significant sustainability benefits, they commonly highlight some mechanical response weaknesses due to their composition. A multiscale approach is introduced within this thesis to deepen the understanding of interaction mechanisms between the different constituents and to evaluate their influence on the performances of CBE materials. An adequate knowledge of CBE materials will support their widespread implementation, enhance their performances, and overcome the issues connected to their application. Besides, for improving the mechanical behaviour of CBE materials, the present study considered the adoption of innovative materials, such as non-conventional cementitious binders and modified emulsion. The use of alternative compositions was investigated as well and considered, for example, the adoption of alternative grading distributions and higher binders dosages than those adopted in the common practice in Italy. Finally, the effectiveness of traditional testing methods used for bituminous materials in characterising CBE materials mechanical behaviour was evaluated.

9.1.1. Multiscale approach

The multiscale study considered four scales of observation: mixtures, fine aggregate matrix (FAM) mortars, slurries and emulsions.

The first part of the thesis focused on the development and validation of the FAM mortar concept. The FAM mortar composition was obtained starting from the mixture by removing the coarse aggregate volume. CBE mixtures are multiphase composite materials, constituted of a continuous matrix, the FAM mortar, in which coarse aggregate inclusions are dispersed and an external voids phase. All the binders, i.e. bitumen emulsion and cement, were contained in the mortar. Besides, FAM mortars contained about 60-70% of the mixtures voids.

The evolution of the physical (water loss by evaporation) and physical properties (stiffness and strength) during curing was measured on both CBE mixtures and FAM mortars. The latter showed a good ability to predict the evolution of the properties of the mixture through simple models with a good approximation, regardless of curing conditions, grading distribution, binders type and dosages.

The linear viscoelastic (LVE) properties of both mixtures and FAM mortars after long-term curing was evaluated by measuring the complex modulus. The LVE behaviour of CBE materials depended on both the fresh bitumen emulsion and the aged bitumen coating the RA aggregate. Although the two CBE composites showed a similar sensitivity in the LVE behaviour, the latter was strictly linked to the CBE materials composition. Not only the mortar matrix contributed to the LVE response of CBE mixtures, but also the aged binder in the coarse aggregate skeleton affected it indeed. Besides, the bituminous binder type and dosage, i.e. fresh or aged, in the mortars strongly affected their LVE behaviour and the relation with the mixtures one. Therefore, to adequately predict the mixture LVE response, FAM mortar composition should consider the effective binders composition of the mixtures.

Finally, the investigation focused on the rheological characterisation of CBE slurries and bitumen emulsions in terms of viscosity. The investigation showed that the viscosity was strongly linked to the type and concentration of the mineral additions, whereas the emulsion type influence was less noteworthy. Moreover, it was possible to find the theoretical composition that led to the formation of a packed structure within the slurry. Such observations should be considered in the mix design of CBE mixtures as they could help enhance their volumetric properties, and consequently, the mechanical response.

In conclusion, the use of the multiscale approach was found to be a promising tool for characterising the behaviour of CBE materials. Indeed, the study at the FAM mortar scale could be adopted for predicting the mixture behaviour. It can be used to deepen the study of mechanisms happening in the binding matrix of the mixtures, e.g. cracking or ageing. Moreover, FAM mortars properties can be used as input parameters in computational modelling. The study at the slurry scale could provide useful information for selecting CBE mixtures with optimised properties at the fresh state.

9.1.2. Impact of CBE materials constituents and compositions

The thesis investigated the influence of different materials constituents and compositions on the mechanical response of CBE materials.

The use of non-conventional cementitious binders and the modified emulsion was found advantageous. In particular, high strength cements allowed a significant enhancement of the mechanical response of CBE materials during curing. The benefits are even greater in adopting the Sulfoaluminous cement, which caused the improvement of the stiffness and the strength of the materials from the first curing hours. This is beneficial as it could allow the early opening of the road to the traffic. Moreover, the use of Sulfoaluminous cement instead of Portland cements could be beneficial in reducing the environmental footprint of CBE materials.

For enhancing the diffusion of CBE materials even in the higher pavement layers (e.g. binder courses) higher dosages of bitumen emulsion and cement and the adoption of modified emulsion and non-conventional cements are suggested. They allowed, indeed, obtaining a higher strength without leading to a significant increase in the stiffness.

Moreover, the adoption of grading distributions characterised by higher dosages of fines can provide better volumetric properties of CBE mixtures and the consequent improvement in the mechanical response. Such CBE mixtures, studied for being applied in binder courses, also showed a reduced thermal sensitivity and a satisfactory fatigue response than those of cold materials found in the literature and produced with traditional materials.

9.1.3. Testing methods and models for CBE materials

The study provided useful information about the application of traditional testing methods and models for characterising CBE materials.

In particular, the curing behaviour of CBE mixtures and mortars can be characterised using stiffness and strength tests in the indirect tensile configuration. The results can be modelled using the modified Michaelis-Menten model, which described with a good approximation the evolution of the properties of the materials with time.

CBE materials complex modulus can be measured using the procedures applied to HMA, but considering reduced strain levels for considering the impact of the reduced dosage of bitumen and the presence of cement on the linearity of the materials. The traditional rheological models applied for characterising the LVE behaviour of HMA showed some inadequacy in the modelling of the phase angle master curve. Therefore, the 2S2P1D-HY rheological model was proposed to consider the presence of dissipation phenomena connected to the presence of cementitious bonds or internal friction. The new model allowed satisfactory modelling of the LVE response of both CBE mixtures and mortars.

The study proposes a new procedure to study the CBE slurries viscosity using the rotational viscometer. A novel Dual Helical Ribbon (DHR) impeller effectively reduced the phase separation and sedimentation effects compared to traditional spindles. Besides, the viscosity dependency on the concentration of the solid particles can be easily modelled using the Krieger-Dougherty model originally developed for concentrated suspensions.

9.2. Recommendations

Even though the proposed multiscale approach showed encouraging results, this thesis represents a starting point. To continue the research effectively, some areas need further studies, including:

- The predicting ability of FAM mortars worth also being investigated in terms of cracking behaviour, considering the fatigue and permanent deformation phenomena;
- The influence of the mortar composition and aged binder contained in the coarse aggregate skeleton merits being further explored for a full understanding of CBE mixtures and mortars relationship;

Chapter 9

Conclusions

Multiscale Approach for Characterising the Behaviour of Cold Bitumen Emulsion Materials

- Additional studies are required to relate the viscosity of CBE slurries and fresh properties of mortars and mixtures to obtain practical recommendations for accurately define the composition of the mixtures;
- Life cycle assessments studies should be carried out for quantifying the benefits of the adoption of CBE materials, with a particular focus on the impact of the different types of constituents, i.e. cementitious binders, emulsion types, amounts of reclaimed asphalt.

References

- Ahmed, S. and Jones, F.R., 1990. A review of particulate reinforcement theories for polymer composites. *Journal of Materials Science*, 25 (12), 4933–4942.
- Aigner, E., Lackner, R., and Pichler, C., 2009. Multiscale prediction of viscoelastic properties of asphalt concrete. *Journal of Materials in Civil Engineering*, 21 (12), 771–780.
- AkzoNobel Surface Chemistry, 2017. Bitumen Emulsion, Technical Bulletin. *AkzoNobel*.
- Al-Hdabi, A., Al Nageim, H., and Seton, L., 2014a. Performance of gap graded cold asphalt containing cement treated filler. *Construction and Building Materials*, 69, 362–369.
- Al-Hdabi, A., Al Nageim, H., and Seton, L., 2014b. Superior cold rolled asphalt mixtures using supplementary cementations materials. *Construction and Building Materials*, 64, 95–102.
- Al-Mohammedawi, A. and Mollenhauer, K., 2020. A study on the influence of the chemical nature of fillers on rheological and fatigue behavior of bitumen emulsion mastic. *Materials*, 13 (20), 1–22.
- Allen, D.H., Little, D.N., Soares, R.F., and Berthelot, C., 2017. Multi-scale computational model for design of flexible pavement—part I: expanding multi-scaling. *International Journal of Pavement Engineering*.
- Alonso, M.C., García Calvo, J.L., Hidalgo, A., and Fernández Luco, L., 2010. Development and application of low-pH concretes for structural purposes in geological repository systems. In: *Geological Repository Systems for Safe Disposal of Spent Nuclear Fuels and Radioactive Waste*.
- Aragão, F.T.S., Badilla-Vargas, G.A., Hartmann, D.A., Oliveira, A.D. de, and Kim, Y.R., 2017. Characterization of temperature- and rate-dependent fracture properties of fine aggregate bituminous mixtures using an integrated numerical-experimental approach. *Engineering Fracture Mechanics*, 180, 195–212.
- ARRA, 2001. *Basic Asphalt Recycling Manual*. Asphalt Recycling and Reclaiming Association.
- Ashmawy, A.K., Salgado, R., Guha, S., and Drnevich, V.P., 1995. Soil Damping and Its Use in Dynamic Analyses. *Third International Conference on Recent Advances in Geotechnical Earthquake Engineering & Soil Dynamics-Session 1-Static and Dynamic Engineering Soil Parameters and Constitutive Relations of Soils*.

References

- Astolfi, A., Subhy, A., Praticò, F., and Lo Presti, D., 2019. Quality-control procedure for dry-process rubberised asphalt mastics. 560–567.
- Attia, T., 2020. Interfaces between pavement layers in bituminous mixtures. *École Nationale des Travaux Publics de l'État*.
- Autostrade per l'Italia, 2013. *Norme tecniche di appalto pavimentazioni*.
- Barnes, H.A., Hutton, J.F., and Walters, K., 1989. An introduction to rheology (Vol. 3). Elsevier. *Elsevier*.
- Di Benedetto, H., Olard, F., Sauzéat, C., and Delaporte, B., 2004. Linear viscoelastic behaviour of bituminous materials: From binders to mixes. *Road Materials and Pavement Design*, 5 (sup1), 163–202.
- Di Benedetto, H., Partl, M.N., Francken, L., and De La Roche Saint André, C., 2001. Stiffness testing for bituminous mixtures. *Materials and Structures/Materiaux et Constructions*.
- Di Benedetto, H., Sauzéat, C., Mondher, N., and Olard, F., 2007. Three-dimensional Thermo-viscoplastic Behaviour of Bituminous Materials: The DBN Model. *Road Materials and Pavement Design*.
- Bocci, E., Graziani, A., and Bocci, M., 2020. Cold in-place recycling for a base layer of an Italian high-traffic highway. *In: Lecture Notes in Civil Engineering*.
- Bocci, M., Grilli, A., Cardone, F., and Graziani, A., 2011. A study on the mechanical behaviour of cement-bitumen treated materials. *Construction and Building Materials*, 25 (2), 773–778.
- Booij, H.C. and Thoone, G.P.J.M., 1982. Generalization of Kramers-Kronig transforms and some approximations of relations between viscoelastic quantities. *Rheologica Acta*, 21 (1), 15–24.
- Brouwers, H.J.H., 2004. The work of Powers and Brownyard revisited: Part 1. *Cement and Concrete Research*, 34 (9), 1697–1716.
- Buczyński, P. and Iwański, M., 2018. Complex modulus change within the linear viscoelastic region of the mineral-cement mixture with foamed bitumen. *Construction and Building Materials*.
- Cardone, F., Grilli, A., Bocci, M., and Graziani, A., 2015. Curing and temperature sensitivity of cement-bitumen treated materials. *International Journal of Pavement Engineering*, 16 (10), 868–880.
- Del Carmen Rubio, M., Moreno, F., Martínez-Echevarría, M.J., Martínez, G., and Vázquez, J.M., 2013. Comparative analysis of emissions from the manufacture and use of hot and half-warm mix asphalt. *Journal of Cleaner Production*.
- Caro, S., Masad, E., Airey, G., Bhasin, A., and Little, D., 2008. Probabilistic analysis of

References

- fracture in asphalt mixtures caused by moisture damage. *Transportation Research Record*.
- Christensen, D.W., Pellinen, T., and Bonaquist, R.F., 2003. Hirsch model for estimating the modulus of asphalt concrete. In: *Asphalt Paving Technology: Association of Asphalt Paving Technologists-Proceedings of the Technical Sessions*.
- CRABforOERE, 2018. Cold Recycled Asphalt Bases for Optimised Energy & Resource Efficient Pavements [online]. Available from: <https://www.crabforoere.eu/> [Accessed 29 Nov 2020].
- Cross, S., Chesner, W., Justus, H., and Kearney, E., 2011. Life-cycle environmental analysis for evaluation of pavement rehabilitation options. *Transportation Research Record*.
- D'Angelo, J., Harm, E., Bartoszek, J., Baumgardner, G., Corrigan, M., Cowsert, J., Harman, T., Jamshidi, M., Jones, W., Newcomb, D., Prowell, B., Sines, R., and Yeaton, B., 2008. *Warm-mix asphalt: European practice*. Washington, DC, United States. No. FHWA-PL-08-007.
- Dai, Q., Sadd, M.H., Parameswaran, V., and Shukla, A., 2005. Prediction of Damage Behaviors in Asphalt Materials Using a Micromechanical Finite-Element Model and Image Analysis. *Journal of Engineering Mechanics*.
- Delaporte, B., Di Benedetto, H., Chaverot, P., and Gauthier, G., 2007. Linear viscoelastic properties of bituminous materials: From binders to mastics. In: *Asphalt Paving Technology: Association of Asphalt Paving Technologists-Proceedings of the Technical Sessions*.
- Diefenderfer, B.K., Bowers, B.F., Schwartz, C.W., Farzaneh, A., and Zhang, Z., 2016. Dynamic modulus of recycled pavement mixtures. *Transportation Research Record*.
- Dolzycki, B., Jaczewski, M., and Szydłowski, C., 2017. The long-term properties of mineral-cement-emulsion mixtures. *Construction and Building Materials*, 156, 799–808.
- Dolzycki, B., Szydłowski, C., and Jaczewski, M., 2020. The influence of combination of binding agents on fatigue properties of deep cold in-place recycled mixtures in Indirect Tensile Fatigue Test (ITFT). *Construction and Building Materials*.
- Doyle, T.A., McNally, C., Gibney, A., and Tabaković, A., 2013. Developing maturity methods for the assessment of cold-mix bituminous materials. *Construction and Building Materials*, 38, 524–529.
- Du, S., 2014. Interaction mechanism of cement and asphalt emulsion in asphalt emulsion mixtures. *Materials and Structures/Materiaux et Constructions*, 47 (7), 1149–1159.
- Du, S., 2018. Effect of curing conditions on properties of cement asphalt emulsion mixture. *Construction and Building Materials*, 164, 84–93.
- Dulaimi, A., Al Nageim, H., Ruddock, F., and Seton, L., 2017. High performance cold asphalt concrete mixture for binder course using alkali-activated binary blended

References

- cementitious filler. *Construction and Building Materials*, 141, 160–170.
- Eberhardsteiner, L., Hofko, B., and Blab, R., 2016. Prediction of hot mix asphalt stiffness behavior by means of multiscale modeling. *RILEM Bookseries*, 13, 33–38.
- European Commission, 2020. Circular economy action plan. *European Commission*.
- Fadil, H., Jelagin, D., Larsson, P.L., and Partl, M.N., 2019. Measurement of the viscoelastic properties of asphalt mortar and its components with indentation tests. *Road Materials and Pavement Design*, 20 (sup2), S797–S811.
- Fakhari Tehrani, F., Absi, J., Allou, F., and Petit, C., 2018. Micromechanical modelling of bituminous materials' complex modulus at different length scales. *International Journal of Pavement Engineering*, 19 (8), 685–696.
- Fang, X., Garcia-Hernandez, A., and Lura, P., 2016. Overview on cold cement bitumen emulsion asphalt. *RILEM Technical Letters*, 1 (December), 116.
- Fang, X., Garcia-Hernandez, A., Winnefeld, F., and Lura, P., 2016. Influence of cement on rheology and stability of rosin emulsified anionic bitumen emulsion. *Journal of Materials in Civil Engineering*, 28 (5), 1–12.
- Fang, X., Garcia, A., Winnefeld, F., Partl, M.N., and Lura, P., 2016. Impact of rapid-hardening cements on mechanical properties of cement bitumen emulsion asphalt. *Materials and Structures/Materiaux et Constructions*, 49 (1–2), 487–498.
- Fedrigo, W., Núñez, W.P., and Visser, A.T., 2020. A review of full-depth reclamation of pavements with Portland cement: Brazil and abroad. *Construction and Building Materials*, 262, 120540.
- Ferrotti, G., Canestrari, F., Xiaotian, J., and Cardone, F., 2020. Use of modified reclaimed asphalt in warm mixtures. *In: Proceedings of ISBM Lyon 2020*. RILEM Springer.
- Ferrotti, G., Grilli, A., Mignini, C., and Graziani, A., 2020. Comparing the Field and Laboratory Curing Behaviour of Cold Recycled Asphalt Mixtures for Binder Courses, 12–14.
- Ferry, J.D., 1980. *Viscoelastic properties of polymers*. Viscoelastic properties of polymers.
- Flores, G., Gallego, J., Miranda, L., and Marcobal, J.R., 2020. Cold asphalt mix with emulsion and 100% rap: Compaction energy and influence of emulsion and cement content. *Construction and Building Materials*.
- Freire, R.A., Babadopulos, L.F.A.L., Castelo Branco, V.T.F., and Bhasin, A., 2017. Aggregate maximum nominal sizes' influence on fatigue damage performance using different scales. *Journal of Materials in Civil Engineering*, 29 (8), 1–11.
- Fu, J., Yang, Y., Zhang, X., and Wang, F., 2018. Different strain distributions of cement-emulsified asphalt concrete pavement between the macro- and meso-scale. *Road Materials and Pavement Design*.

References

- Fu, J., Zhang, X., and Wang, F., 2015. The Meso structure and strain distribution analysis of cement emulsified asphalt concrete. *International Journal of Pavement Research and Technology*.
- Fu, P. and Harvey, J.T., 2007. Temperature sensitivity of foamed asphalt mix stiffness: Field and lab study. *International Journal of Pavement Engineering*.
- Galobardes, I., Cavalaro, S.H., Goodier, C.I., Austin, S., and Rueda, Á., 2015. Maturity method to predict the evolution of the properties of sprayed concrete. *Construction and Building Materials*.
- Gandi, A., Carter, A., and Singh, D., 2017a. Rheological behavior of cold recycled asphalt materials with different contents of recycled asphalt pavements. *Innovative Infrastructure Solutions*.
- Gandi, A., Carter, A., and Singh, D., 2017b. Rheological behavior of cold recycled asphalt materials with different contents of recycled asphalt pavements. *Innovative Infrastructure Solutions*, 2 (1), 1–9.
- García, A., Lura, P., Partl, M.N., and Jerjen, I., 2013. Influence of cement content and environmental humidity on asphalt emulsion and cement composites performance. *Materials and Structures/Materiaux et Constructions*, 46 (8), 1275–1289.
- Garilli, E., Autelitano, F., and Giuliani, F., 2019. Use of bending beam rheometer test for rheological analysis of asphalt emulsion-cement mastics in cold in-place recycling. *Construction and Building Materials*, 222, 484–492.
- Garilli, E., Autelitano, F., Godenzoni, C., Graziani, A., and Giuliani, F., 2016. Early age evolution of rheological properties of over-stabilized bitumen emulsion-cement pastes. *Construction and Building Materials*, 125, 352–360.
- Genta, G., 2009. *Vibration Dynamics and Control*. Noise Control Engineering Journal. Boston, MA: Springer US.
- Gergesova, M., Zupančič, B., Saprunov, I., and Emri, I., 2011. The closed form t-T-P shifting (CFS) algorithm. *Journal of Rheology*, 55 (1), 1–16.
- Giancontieri, G., Hargreaves, D., and Lo Presti, D., 2020. Are we correctly measuring the rotational viscosity of heterogeneous bituminous binders? *Road Materials and Pavement Design*, 0 (0), 1–20.
- Giani, M.I., Dotelli, G., Brandini, N., and Zampori, L., 2015. Comparative life cycle assessment of asphalt pavements using reclaimed asphalt, warm mix technology and cold in-place recycling. *Resources, Conservation and Recycling*.
- Gibson, R.F., 2016. *Principles of Composite Material Mechanics*. Principles of Composite Material Mechanics.
- Godenzoni, C., Bocci, M., and Graziani, A., 2017. Rheological characterization of cold bituminous mastics produced with different mineral additions. *Transport*

References

- Infrastructure and Systems - Proceedings of the AIIT International Congress on Transport Infrastructure and Systems, TIS 2017*, (2015), 185–191.
- Godenzoni, C., Graziani, A., Bocci, E., and Bocci, M., 2018. The evolution of the mechanical behaviour of cold recycled mixtures stabilised with cement and bitumen: field and laboratory study. *Road Materials and Pavement Design*.
- Godenzoni, C., Graziani, A., and Corinaldesi, V., 2016. The influence mineral additions on the failure properties of bitumen emulsion mortars. *RILEM Bookseries*.
- Godenzoni, C., Graziani, A., and Perraton, D., 2017. Complex modulus characterisation of cold-recycled mixtures with foamed bitumen and different contents of reclaimed asphalt. *Road Materials and Pavement Design*, 18 (1), 130–150.
- Graziani, A., Godenzoni, C., Cardone, F., Bocci, E., and Bocci, M., 2017. An application of the Michaelis–Menten model to analyze the curing process of cold recycled bituminous mixtures. *International Journal of Pavement Research and Technology*.
- Graziani, A., Godenzoni, C., Cardone, F., and Bocci, M., 2016. Effect of curing on the physical and mechanical properties of cold-recycled bituminous mixtures. *Materials and Design*, 95, 358–369.
- Graziani, A., Iafelice, C., Raschia, S., Perraton, D., and Carter, A., 2018. A procedure for characterizing the curing process of cold recycled bitumen emulsion mixtures. *Construction and Building Materials*, 173, 754–762.
- Graziani, A., Mignini, C., Bocci, E., and Bocci, M., 2020. Complex Modulus Testing and Rheological Modeling of Cold-Recycled Mixtures. *Journal of Testing and Evaluation*, 48 (1), 20180905.
- Graziani, A., Raschia, S., Mignini, C., and Carter, A., 2020. Use of fine aggregate matrix to analyze the rheological behavior of cold recycled materials. *Materials and Structures*, 7.
- Grilli, A., Graziani, A., Bocci, E., and Bocci, M., 2016. Volumetric properties and influence of water content on the compactability of cold recycled mixtures. *Materials and Structures/Materiaux et Constructions*, 49 (10), 4349–4362.
- Grilli, A., Graziani, A., and Bocci, M., 2012. Compactability and thermal sensitivity of cement – bitumen-treated materials, (May 2013), 37–41.
- Gu, F., Ma, W., West, R.C., Taylor, A.J., and Zhang, Y., 2019. Structural performance and sustainability assessment of cold central-plant and in-place recycled asphalt pavements: A case study. *Journal of Cleaner Production*.
- Gudimettla, J.M., Cooley, L.A., and Brown, E.R., 2004. Workability of hot-mix asphalt. In: *Transportation Research Record*.
- Gundla, A., Gudipudi, P., and Underwood, B.S., 2017. Evaluation of the sensitivity of asphalt concrete modulus to binder oxidation with a multiple length scale study. *Construction*

References

and Building Materials.

- Habert, G., 2013. Assessing the environmental impact of conventional and 'green' cement production. *In: Eco-Efficient Construction and Building Materials: Life Cycle Assessment (LCA), Eco-Labeling and Case Studies.*
- Hesami, E., Jelagin, D., Kringos, N., and Birgisson, B., 2012. An empirical framework for determining asphalt mastic viscosity as a function of mineral filler concentration. *Construction and Building Materials*, 35, 23–29.
- Israelachvili, J., 2011. *Intermolecular and Surface Forces*. Intermolecular and Surface Forces.
- Izadi, A., Motamed, A., and Bhasin, A., 2011. Designing Fine Aggregate Mixtures to Evaluate Fatigue Crack-Growth in Asphalt Mixtures Anoosha Izadi , Arash Motamed and Amit Bhasin Report 161022-1 Center for Transportation Research The University of Texas at Austin 1616 Guadalupe Street Austin , TX 787, 7 (1), 54.
- James, A., 2006. Overview of asphalt emulsion. *Transportation research circular*, 1–15.
- Jensen, O.M. and Hansen, P.F., 2001. Water-entrained cement-based materials - I. Principles and theoretical background. *Cement and Concrete Research*.
- Juenger, M.C.G., Winnefeld, F., Provis, J.L., and Ideker, J.H., 2011. Advances in alternative cementitious binders. *Cement and Concrete Research*, 41 (12), 1232–1243.
- Kavussi, A. and Modarres, A., 2010. Laboratory fatigue models for recycled mixes with bitumen emulsion and cement. *Construction and Building Materials*, 24 (10), 1920–1927.
- Khalid, H.A. and Monney, O.K., 2009. Moisture damage potential of cold asphalt. *International Journal of Pavement Engineering*.
- Kim, Y., Im, S., and Lee, H.D., 2011. Impacts of curing time and moisture content on engineering properties of cold in-place recycling mixtures using foamed or emulsified asphalt. *Journal of Materials in Civil Engineering*.
- Kim, Y.R., 2003. Mechanistic fatigue characterization and damage modeling of asphalt mixtures. Texas A&M University, College Station, TX.
- Kim, Y.R., 2009. *Modeling of Asphalt Concrete*.
- Krieger, I.M. and Dougherty, T.J., 1959. A Mechanism for Non-Newtonian Flow in Suspensions of Rigid Spheres. *Transactions of the Society of Rheology*.
- Kuchiishi, A.K., Vasconcelos, K., and Bariani Bernucci, L.L., 2019. Effect of mixture composition on the mechanical behaviour of cold recycled asphalt mixtures. *International Journal of Pavement Engineering*.
- Kuna, K., Airey, G., and Thom, N., 2017. Mix design considerations of foamed bitumen mixtures with reclaimed asphalt pavement material. *International Journal of Pavement*

References

- Engineering*, 18 (10), 902–915.
- Le, J.L., Hendrickson, R., Marasteanu, M.O., and Turos, M., 2018. Use of fine aggregate matrix for computational modeling of low temperature fracture of asphalt concrete. *Materials and Structures/Materiaux et Constructions*, 51 (6), 1–13.
- Leandri, P., Losa, M., and Di Natale, A., 2015. Field validation of recycled cold mixes viscoelastic properties. *Construction and Building Materials*.
- Lesueur, D. and Potti, J.J., 2004. Cold mix design: A rational approach based on the current understanding of the breaking of bituminous emulsions. *Road Materials and Pavement Design*, 5 (X), 65–87.
- Li, X.J. and Marasteanu, M.O., 2010. Using Semi Circular Bending Test to Evaluate Low Temperature Fracture Resistance for Asphalt Concrete. *Experimental Mechanics*.
- Lin, J., Hong, J., and Xiao, Y., 2017. Dynamic characteristics of 100% cold recycled asphalt mixture using asphalt emulsion and cement. *Journal of Cleaner Production*.
- Lin, J., Wei, T., Hong, J., Zhao, Y., and Liu, J., 2015. Research on development mechanism of early-stage strength for cold recycled asphalt mixture using emulsion asphalt. *Construction and Building Materials*.
- Lo Presti, D., Fecarotti, C., Clare, A.T., and Airey, G., 2014. Toward more realistic viscosity measurements of tyre rubber-bitumen blends. *Construction and Building Materials*, 67 (PART B), 270–278.
- Lo Presti, D., Vasconcelos, K., Orešković, M., Pires, G.M., and Bressi, S., 2020. On the degree of binder activity of reclaimed asphalt and degree of blending with recycling agents. *Road Materials and Pavement Design*.
- Lura, P., Van Breugel, K., and Maruyama, I., 2001. Effect of curing temperature and type of cement on early-age shrinkage of high-performance concrete. *Cement and Concrete Research*, 31 (12), 1867–1872.
- Lura, P., Winnefeld, F., and Fang, X., 2017. A simple method for determining the total amount of physically and chemically bound water of different cements. *Journal of Thermal Analysis and Calorimetry*, 130 (2), 653–660.
- Mangiafico, S., Di Benedetto, H., Sauzéat, C., Olard, F., Pouget, S., and Planque, L., 2013. Influence of reclaimed asphalt pavement content on complex modulus of asphalt binder blends and corresponding mixes: Experimental results and modelling. *Road Materials and Pavement Design*, 14 (SUPPL.1), 132–148.
- Mangiafico, S., Di Benedetto, H., Sauzéat, C., Olard, F., Pouget, S., and Planque, L., 2014. New method to obtain viscoelastic properties of bitumen blends from pure and reclaimed asphalt pavement binder constituents. *Road Materials and Pavement Design*, 15 (2), 312–329.
- Mason, T.G., 1999. New fundamental concepts in emulsion theology. *Current Opinion in*

References

- Colloid and Interface Science*, 4 (3), 231–238.
- Medina, J.G., Giancontieri, G., and Lo Presti, D., 2020. Quality control of manufacturing and hot storage of crumb rubber modified binders. *Construction and Building Materials*, 233, 117351.
- Michaelis, L., Menten, M.L., Goody, R.S., and Johnson, K.A., 1913. Die Kinetik der Invertinwirkung/ The kinetics of invertase action. *Biochemistry*.
- Miljković, M., Graziani, A., and Mignini, C., 2020. Interphase relations in the characterisation of bitumen emulsion-cement composites. In: *Proceedings of ISBM Lyon 2020*. RILEM.
- Miljković, M., Poulidakos, L., Piemontese, F., Shakoorioskooie, M., and Lura, P., 2019. Mechanical behaviour of bitumen emulsion-cement composites across the structural transition of the co-binder system. *Construction and Building Materials*, 215, 217–232.
- Miljković, M. and Radenberg, M., 2014. Fracture behaviour of bitumen emulsion mortar mixtures. *Construction and Building Materials*, 62, 126–134.
- Miljković, M. and Radenberg, M., 2015. Characterising the influence of bitumen emulsion on asphalt mixture performance. *Materials and Structures/Materiaux et Constructions*, 48 (7), 2195–2210.
- Miljković, M. and Radenberg, M., 2016. Effect of compaction energy on physical and mechanical performance of bitumen emulsion mortar. *Materials and Structures/Materiaux et Constructions*, 49 (1–2), 193–205.
- Miljković, M., Radenberg, M., Fang, X., and Lura, P., 2017. Influence of emulsifier content on cement hydration and mechanical performance of bitumen emulsion mortar. *Materials and Structures/Materiaux et Constructions*, 50 (3).
- Modarres, A., Nejad, F.M., Kavussi, A., Hassani, A., and Shabanzadeh, E., 2011. A parametric study on the laboratory fatigue characteristics of recycled mixes. *Construction and Building Materials*.
- Mollenhauer, K. and Simnofske, D., 2015. Tolerances for inhomogeneity of pavement structure for in-situ cold recycling. In: *Proceedings 3rd ISAP TC APE Asphalt Pavements and Environment Symposium, Sun City*.
- Montepara, A. and Giuliani, F., 2001. The role of cement in the recycling of asphalt pavement cold-stabilized with bituminous emulsions. In: *Second International Symposium on Maintenance and Rehabilitation of Pavements and Technological Control*. Alabama (USA).
- Mueller, S., Llewellyn, E.W., and Mader, H.M., 2010. The rheology of suspensions of solid particles. *Proceedings of the Royal Society A: Mathematical, Physical and Engineering Sciences*.
- Nassar, A.I., Mohammed, M.K., Thom, N., and Parry, T., 2016. Mechanical, durability and

References

- microstructure properties of Cold Asphalt Emulsion Mixtures with different types of filler. *Construction and Building Materials*, 114, 352–363.
- Nassar, A.I., Mohammed, M.K., Thom, N., and Parry, T., 2018. Characterisation of high-performance cold bitumen emulsion mixtures for surface courses. *International Journal of Pavement Engineering*.
- Needham, D., 1996. Developments in bitumen emulsion mixtures for roads. University of Nottingham.
- Needham, D., 2000. A study of cement modified bitumen emulsion mixtures. *Proceedings of the Association of Asphalt Paving Technologists*.
- Neumann, J., Simon, J.W., Mollenhauer, K., and Reese, S., 2017. A framework for 3D synthetic mesoscale models of hot mix asphalt for the finite element method. *Construction and Building Materials*, 148, 857–873.
- Niazi, Y. and Jalili, M., 2009. Effect of Portland cement and lime additives on properties of cold in-place recycled mixtures with asphalt emulsion. *Construction and Building Materials*, 23 (3), 1338–1343.
- Offenbacher, D., Saidi, A., Ali, A., Mehta, Y., Decarlo, C.J., and Lein, W., 2021. Economic and Environmental Cost Analysis of Cold In-Place Recycling. *Journal of Materials in Civil Engineering*, 33 (3).
- Olard, F. and Di Benedetto, H., 2003. General “2S2P1D” Model and Relation Between the Linear Viscoelastic Behaviours of Bituminous Binders and Mixes. *Road Materials and Pavement Design*, 4 (2), 185–224.
- Olard, F., Di Benedetto, H., Dony, A., and Vaniscote, J.C., 2005. Properties of bituminous mixtures at low temperatures and relations with binder characteristics. *Materials and Structures/Materiaux et Constructions*.
- Olard, F. and Perraton, D., 2010. On the optimization of the aggregate packing characteristics for the design of high-performance asphalt concretes. *Road Materials and Pavement Design*.
- Oruc, S., Celik, F., and Akpınar, M.V., 2007. Effect of cement on emulsified asphalt mixtures. *Journal of Materials Engineering and Performance*, 16 (5), 578–583.
- Ouyang, J., Hu, L., Li, H., and Han, B., 2018. Effect of cement on the demulsifying behavior of over-stabilized asphalt emulsion during mixing. *Construction and Building Materials*, 177, 252–260.
- Ouyang, J., Li, H., and Han, B., 2017. The rheological properties and mechanisms of cement asphalt emulsion paste with different charge types of emulsion. *Construction and Building Materials*, 147, 566–575.
- Ouyang, J. and Tan, Y., 2015. Rheology of fresh cement asphalt emulsion pastes. *Construction and Building Materials*, 80, 236–243.

References

- Ouyang, J., Tan, Y., Corr, D.J., and Shah, S.P., 2016. Investigation on the mixing stability of asphalt emulsion with cement through viscosity. *Journal of Materials in Civil Engineering*, 28 (12), 1–8.
- Ouyang, J., Tan, Y., Corr, D.J., and Shah, S.P., 2017. Viscosity prediction of fresh cement asphalt emulsion pastes. *Materials and Structures/Materiaux et Constructions*, 50 (1), 1–10.
- Ouyang, J., Tan, Y., Li, Y., and Zhao, J., 2015. Demulsification process of asphalt emulsion in fresh cement-asphalt emulsion paste. *Materials and Structures/Materiaux et Constructions*, 48 (12), 3875–3883.
- Ozer, H., Al-Qadi, I.L., Lambros, J., El-Khatib, A., Singhvi, P., and Doll, B., 2016. Development of the fracture-based flexibility index for asphalt concrete cracking potential using modified semi-circle bending test parameters. *Construction and Building Materials*.
- Ozer, H., Al-Qadi, I.L., Singhvi, P., Khan, T., Rivera-Perez, J., and El-Khatib, A., 2016. Fracture characterization of asphalt mixtures with high recycled content using Illinois semicircular bending test method and flexibility index. *Transportation Research Record*.
- Patterson, W.I., Carreau, P.J., and Yap, C.Y., 1979. Mixing with helical ribbon agitators: Part II. Newtonian Fluids. *AIChE Journal*.
- Peng, J., Deng, D., Liu, Z., Yuan, Q., and Ye, T., 2014. Rheological models for fresh cement asphalt paste. *Construction and Building Materials*, 71, 254–262.
- Perraton, D., Di Benedetto, H., Carter, A., and Proteau, M., 2019. Link between different bottom-up fatigue's law coefficients of mechanical-empirical pavement design software. *Construction and Building Materials*.
- Perraton, D., Tebaldi, G., Dave, E., Bilodeau, F., Giacomello, G., Grilli, A., Graziani, A., Bocci, M., Grenfell, J., Muraya, P., Pasetto, M., Kuna, K., Apeageyi, A., Lo Presti, D., Airey, G., Jenkins, K., Hajj, E., Hugener, M., and Marsac, P., 2016. Tests campaign analysis to evaluate the capability of fragmentation test to characterize recycled asphalt pavement (RAP) material. *RILEM Bookseries*.
- Phair, J.W., 2006. Green chemistry for sustainable cement production and use. *Green Chemistry*, 8 (9), 763–780.
- Pichler, C., Lackner, R., and Aigner, E., 2012. Generalized self-consistent scheme for upscaling of viscoelastic properties of highly-filled matrix-inclusion composites - Application in the context of multiscale modeling of bituminous mixtures. *Composites Part B: Engineering*.
- Pouliot, N., Marchand, J., and Pigeon, M., 2003. Hydration mechanisms, microstructure, and mechanical properties of mortars prepared with mixed binder cement slurry-asphalt emulsion. *Journal of Materials in Civil Engineering*, 15 (1), 54–59.

References

- Powers, T.C., 1958. Structure and Physical Properties of Hardened Portland Cement Paste. *Journal of the American Ceramic Society*.
- Preti, F., Gouveia, B.C.S., Rahmanbeiki, A., Romeo, E., Carter, A., and Tebaldi, G., 2019. Application and validation of the cohesion test to characterise reclaimed asphalt pavement. *Road Materials and Pavement Design*.
- Provincia Autonoma di Bolzano, 2016. *Capitolato speciale d'appalto opere stradali*.
- Raschia, S., Graziani, A., Carter, A., and Perraton, D., 2019. Laboratory mechanical characterisation of cold recycled mixtures produced with different RAP sources. *Road Materials and Pavement Design*.
- Raschia, S., Mignini, C., Graziani, A., Carter, A., Perraton, D., and Vaillancourt, M., 2019. Effect of gradation on volumetric and mechanical properties of cold recycled mixtures (CRM). *Road Materials and Pavement Design*, 20 (sup2), S740–S754.
- Raschia, S., Moghaddam, T.B., Perraton, D., Baaj, H., Carter, A., and Graziani, A., 2021. Effect of RAP Source on Compactability and Behavior of Cold-Recycled Mixtures in the Small Strain Domain. *Journal of Materials in Civil Engineering*, 33 (4), 04021030.
- Raschia, S., Perraton, D., Di Benedetto, H., Lamothe, S., Graziani, A., and Carter, A., 2021. Visco-Elasto-Plastic Characterization In The Small Strain Domain Of Cement-Bitumen Treated Materials Produced At Low Temperatures. *Journal of Materials in Civil Engineering*, 33 (4), 04021039.
- Raschia, S., Perraton, D., Graziani, A., and Carter, A., 2020. Influence of low production temperatures on compactability and mechanical properties of cold recycled mixtures. *Construction and Building Materials*.
- Richards, F.J., 1959. A flexible growth function for empirical use. *Journal of Experimental Botany*.
- Rowe, G.M., Khoei, S.H., Blankenship, P., and Mahboub, K.C., 2009. Evaluation of aspects of E* test by using hot-mix asphalt specimens with varying void contents. *Transportation Research Record*.
- Saadoon, T., Gómez-Meijide, B., and Garcia, A., 2018. Prediction of water evaporation and stability of cold asphalt mixtures containing different types of cement. *Construction and Building Materials*, 186, 751–761.
- Saha, G. and Biligiri, K.P., 2016. Fracture properties of asphalt mixtures using semi-circular bending test: A state-of-the-art review and future research. *Construction and Building Materials*.
- Sangiorgi, C., Tataranni, P., Simone, A., Vignali, V., Lantieri, C., and Dondi, G., 2017. A laboratory and field evaluation of Cold Recycled Mixture for base layer entirely made with Reclaimed Asphalt Pavement. *Construction and Building Materials*, 138, 232–239.

References

- Sayegh, G., 1967. Viscoelastic properties of bituminous mixtures. *2nd International Conference on the Structural Design of Asphalt Pavements. University of Michigan, Ann Arbor.*
- Schwartz, C.W., Diefenderfer, B.K., and Bowers, B.F., 2017. *Material Properties of Cold In-Place Recycled and Full-Depth Reclamation Asphalt Concrete.* Material Properties of Cold In-Place Recycled and Full-Depth Reclamation Asphalt Concrete.
- Schwartz, C.W. and Khosravifar, S., 2013. *Design and evaluation of foamed asphalt base materials,* " Report No. MD-13-SP909B4E. Maryland.
- Sefidmazgi, N.R., Teymourpour, P., and Bahia, H.U., 2013. Effect of particle mobility on aggregate structure formation in asphalt mixtures. *Road Materials and Pavement Design.*
- Serfass, J.P., Gaudefroy, V., Beghin, A., Odie, L., Verhee, F., de la Roche, C., and Wendling, L., 2012. A detailed assessment of grave-emulsion combining trial section monitoring and laboratory testing. *In: 5th Eurasphalt & Eurobitume Congress.* 11p.
- Sousa, P., Kassem, E., Masad, E., and Little, D., 2013. New design method of fine aggregates mixtures and automated method for analysis of dynamic mechanical characterization data. *Construction and Building Materials*, 41, 216–223.
- Stimilli, A., Ferrotti, G., Graziani, A., and Canestrari, F., 2013. Performance evaluation of a cold-recycled mixture containing high percentage of reclaimed asphalt. *Road Materials and Pavement Design.*
- Stimilli, A., Virgili, A., and Canestrari, F., 2015. New method to estimate the “re-activated” binder amount in recycled hot-mix asphalt. *Road Materials and Pavement Design.*
- Swiertz, D., Johannes, P., Tashman, L., and Bahia, H., 2012. Evaluation of laboratory coating and compaction procedures for cold mix asphalt. *Asphalt Paving Technology-Proceedings Association of Asphalt Technologists*, 81, 81.
- Tadros, T.F., 2013. Emulsion Formation, Stability, and Rheology. *In: Emulsion Formation and Stability.*
- Tan, Y., Ouyang, J., and Li, Y., 2014. Factors influencing rheological properties of fresh cement asphalt emulsion paste. *Construction and Building Materials*, 68, 611–617.
- Tan, Y., Ouyang, J., Lv, J., and Li, Y., 2013. Effect of emulsifier on cement hydration in cement asphalt mortar. *Construction and Building Materials*, 47, 159–164.
- Tapsoba, N., Sauzéat, C., and Benedetto, H. Di, 2013. Analysis of Fatigue Test for Bituminous Mixtures. *Journal of Materials in Civil Engineering.*
- Thanaya, I.N.A., Zoorob, S.E., and Forth, J.P., 2009. A laboratory study on cold-mix, cold-lay emulsion mixtures. *Proceedings of the Institution of Civil Engineers: Transport*, 162 (1), 47–55.

References

- Thenoux, G., González, Á., and Dowling, R., 2007. Energy consumption comparison for different asphalt pavements rehabilitation techniques used in Chile. *Resources, Conservation and Recycling*, 49 (4), 325–339.
- Thomas, T. and Kadrmas, A., 2002. Performance-Related Tests and Specifications for Cold In-Place Recycling : Lab and Field Experience. *Transportation Research Board 2003 Annual Meeting*.
- Timm, D.H., Diefenderfer, B.K., and Bowers, B.F., 2018. Cold Central Plant Recycled Asphalt Pavements in High Traffic Applications. *Transportation Research Record*.
- Underwood, B.S., 2015. Multiscale modeling approach for asphalt concrete and its implications on oxidative aging. In: *Advances in Asphalt Materials: Road and Pavement Construction*. 273–302.
- Underwood, B.S. and Kim, Y.R., 2013a. Effect of volumetric factors on the mechanical behavior of asphalt fine aggregate matrix and the relationship to asphalt mixture properties. *Construction and Building Materials*, 49, 672–681.
- Underwood, B.S. and Kim, Y.R., 2013b. Microstructural investigation of asphalt concrete for performing multiscale experimental studies. *International Journal of Pavement Engineering*.
- Valentin, J., Čížková, Z., Suda, J., Batista, F., Mollenhauer, K., and Simnofske, D., 2016. Stiffness Characterization of Cold Recycled Mixtures. *Transportation Research Procedia*, 14, 758–767.
- Wang, F., Liu, Y., and Hu, S., 2013. Effect of early cement hydration on the chemical stability of asphalt emulsion. *Construction and Building Materials*, 42, 146–151.
- Wang, F., Liu, Z., Wang, T., and Hu, S., 2008. A novel method to evaluate the setting process of cement and asphalt emulsion in CA mortar. *Materials and Structures/Materiaux et Constructions*.
- Wang, Z. and Sha, A., 2010. Micro hardness of interface between cement asphalt emulsion mastics and aggregates. *Materials and Structures/Materiaux et Constructions*, 43 (4), 453–461.
- Willenbacher, N. and Georgieva, K., 2013. Rheology of Disperse Systems. *Product Design and Engineering: Formulation of Gels and Pastes*, 7–49.
- Xiao, F., Yao, S., Wang, J., Li, X., and Amirhanian, S., 2018. A literature review on cold recycling technology of asphalt pavement. *Construction and Building Materials*, 180, 579–604.
- Xu, O., Wang, Z., and Wang, R., 2017. Effects of aggregate gradations and binder contents on engineering properties of cement emulsified asphalt mixtures. *Construction and Building Materials*.
- Yan, J., Ni, F., Yang, M., and Li, J., 2010. An experimental study on fatigue properties of

References

- emulsion and foam cold recycled mixes. *Construction and Building Materials*.
- Yap, C.Y., Patterson, W.I., and Carreau, P.J., 1979. Mixing with helical ribbon agitators: Part III. Non-Newtonian fluids. *AIChE Journal*.
- Zeng, M., Bahia, H.U., Zhai, H., Anderson, M.R., and Turner, P., 2001. Rheological modeling of modified asphalt binders and mixtures (with discussion). *Journal of the Association of Asphalt Paving Technologists*, 70.
- Zhang, Y., Kong, X., Hou, S., Liu, Y., and Han, S., 2012. Study on the rheological properties of fresh cement asphalt paste. *Construction and Building Materials*, 27 (1), 534–544.
- Zhang, Y. and Leng, Z., 2017. Quantification of bituminous mortar ageing and its application in ravelling evaluation of porous asphalt wearing courses. *Materials and Design*, 119, 1–11.
- Ziyani, L., Gaudefroy, V., Ferber, V., Deneele, D., and Hammoum, F., 2014. Chemical reactivity of mineral aggregates in aqueous solution: Relationship with bitumen emulsion breaking. *Journal of Materials Science*, 49 (6), 2465–2476.

Appendix A
Properties of the Materials Employed

Multiscale Approach for Characterising the Behaviour of Cold Bitumen Emulsion Materials

Appendix A

Properties of Materials Employed

A.1. Aggregates

Table A.1. Properties of RA 0/16 aggregate

Property	Standard	Symbol	Unit	Value
Upper aggregate size	EN 933-1	D	mm	16
Passing the 0.063	EN 933-1	f	%	5.6
Particle density	EN 1097-6	ρ_a	kg/m ³	2482
Water absorption	EN 1097-6	WA ₂₄	%	1.14
Flakiness index	EN 933-3	FI	%	7.3
Shape Index	EN 933-4	SI	%	5.7
Crushed aggregate particle	EN 933-5	C	%	100
Sand Equivalent	EN 933-8	SE	%	70.6
Resistance to fragmentation	UNI EN 1097-2	LA	%	17
Resistance to freezing and thawing	EN 1367-1	ΔLA	%	-1.4
Limit Liquid	UNI CEN ISO/TS 17892-12	W _L	%	ND
Plasticity index	UNI CEN ISO/TS 17892-12	IP	-	NP
Soluble binder content (with respect aggregates)	12697-1	S	%	5.0
Fragmentation test by Proctor (10/14)		PCS	%	6.8

Appendix A

Properties of the Materials Employed

Multiscale Approach for Characterising the Behaviour of Cold Bitumen Emulsion Materials

Table A.2. Main properties of RA 0/2 aggregate

Property	Standard	Symbol	Unit	Value
Upper aggregate size	EN 933-1	D	mm	2.0
Passing the 0.063	EN 933-1	f	%	16.9
Particle density	EN 1097-6	ρ_a	kg/m ³	2424
Water absorption	EN 1097-6	WA ₂₄	%	1.32
Soluble binder content (with respect aggregates)	12697-1	S	%	8.3

Table A.3. Main properties of RA 2/16 aggregate

Property	Standard	Symbol	Unit	Value
Upper aggregate size	EN 933-1	D	mm	16
Passing the 0.063	EN 933-1	f	%	0
Particle density	EN 1097-6	ρ_a	kg/m ³	2550
Water absorption	EN 1097-6	WA ₂₄	%	1.14
Soluble binder content (with respect aggregates)	12697-1	S	%	3.2

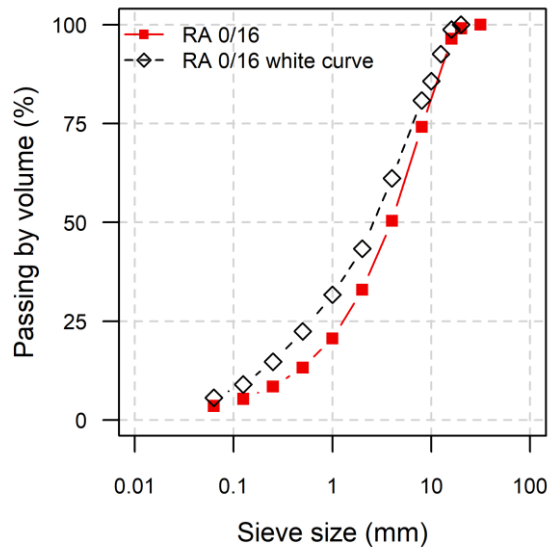


Figure A.1. RA 2/16 black curve and white curve (extracted aggregate)

Appendix A
Properties of the Materials Employed

Multiscale Approach for Characterising the Behaviour of Cold Bitumen Emulsion Materials

Table A.4. Main properties of the fine natural aggregate

Property	Standard	Symbol	Unit	Value
Upper aggregate size	EN 933-1	D	mm	2
Passing the 0.063	EN 933-1	f	%	12.2
Particle density	EN 1097-6	ρ_a	kg/m ³	2732
Water absorption	EN 1097-6	WA ₂₄	%	1.50

Table A.5. Main properties of the filler

Property	Standard	Symbol	Unit	Value
Upper aggregate size	EN 933-1	D	mm	0.125
Passing the 0.063	EN 933-1	f	%	45.3
Particle density	EN 1097-6	ρ_a	kg/m ³	2650
Rigden voids	EN 1097-4	v	%	23.8
Blaine finesses	EN 196-6	s	cm ² /g	3400

Appendix A
Properties of the Materials Employed

Multiscale Approach for Characterising the Behaviour of Cold Bitumen Emulsion Materials

A.2. Bitumen emulsions

Table A.6. Properties of the bitumen emulsion B

Property	Standard	Unit	Value
<i>Emulsion</i>			
Binder content	EN 1428	%	60
Density		kg/m ³	1015
pH value	EN 12850	-	2.2
Viscosity at 40 °C – efflux time	EN 12846-1	s	40
Adhesivity: water immersion test	EN 13614	%	90
Breaking behaviour: mineral filler method	EN 13075-1		190
Mixing stability with cement	EN 12848	%	< 2
<i>Residual bitumen</i>			
Penetration at 25 °C	EN 1426	dmm	100
Softening point	EN 1427	°C	43

Table A.7. Properties of the bitumen emulsion BP

Property	Standard	Unit	Value
Emulsion			
Binder content	EN 1428	%	60
Density		kg/m ³	1015
pH value	EN 12850	-	2.2
Viscosity at 40 °C – efflux time	EN 12846-1	s	40
Adhesivity: water immersion test	EN 13614	%	90
Breaking behaviour: mineral filler method	EN 13075-1		190
Mixing stability with cement	EN 12848	%	< 2
Residual bitumen			
Penetration at 25 °C	EN 1426	dmm	100
Softening point	EN 1427	°C	60

Appendix A
Properties of the Materials Employed

Multiscale Approach for Characterising the Behaviour of Cold Bitumen Emulsion Materials

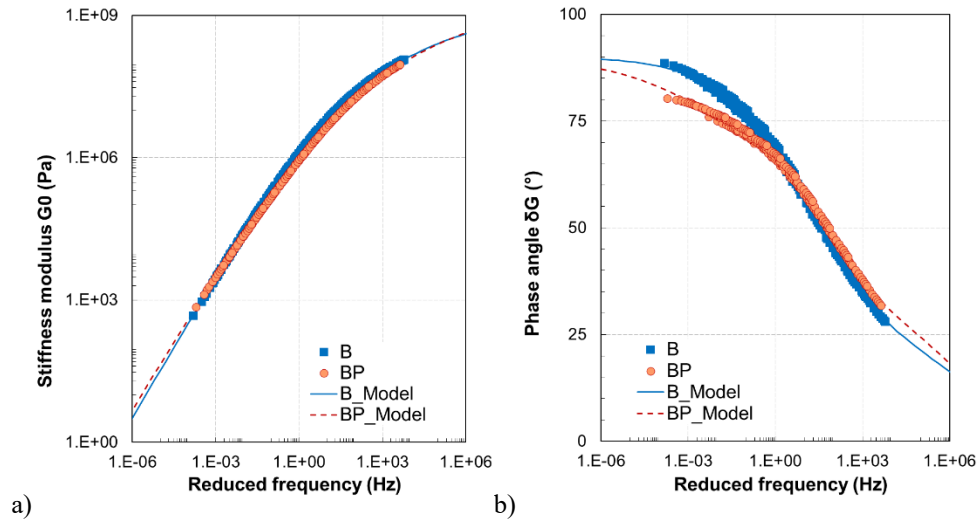


Figure A.2. Bitumen emulsions master curves and 2S2P1D fitted model a) stiffness modulus b) phase angle

Table A.8. Bitumen emulsions 2S2P1D model parameters

ID	E_e (MPa)	E_g (MPa)	k (-)	h (-)	δ (-)	β (-)	$\text{Log } \tau$ (-)	C_1 (-)	C_2 (-)
B	0	1.00E+09	0.29	0.68	5.85	29	-4.74	20	206
BP	0	1.00E+09	0.34	0.75	7.07	43	-4.71	21	220

Appendix A
Properties of the Materials Employed

Multiscale Approach for Characterising the Behaviour of Cold Bitumen Emulsion Materials

A.3. Cementitious binders

Table A.9. Properties of the cementitious binders

Property		C1	C2	C3	C4
Volumetric mass	g/cm ³	3.02±0.01	2.90±0.03	3.09±0.01	2.9±0.1
Blaine fineness	cm ² /g	3800±100	5700±200	4090±100	6100±350
Rigden voids	%	33.2	33.5	33.4	32.3
Cumulative <90µm	%	99.5	99.5	99.5	95
pH		12-13.5	11-12	12-13.5	12-13.5
Initial setting time*	min	170	15	180	180
Final setting time*	min	220	25	245	300
Compressive strength @2 days *	MPa	19±2	45±2	20±2	3±1
Compressive strength @28 days*	MPa	39±3	80±3	56±3	10±2

*Standard mortar

Table A.10. Cementitious binders composition

Component	C1	C2	C3	C4
CaO	60.00	40.00	55.54	53.00
Al ₂ O ₃	3.50	25.00	6.67	2.60
SiO ₂	14.50	7.00	25.64	12.25
Fe ₂ O ₃	2.90	1.20	2.26	1.40
MgO	1.28	3.50	4.28	0.80
Na ₂ O	0.50	0.50	0.36	1.34
K ₂ O	0.35	0.50	0.71	0.70
TiO ₂	0.28	0.30	0.44	0.11
P ₂ O ₅	0.06	0.08	0.07	0.05
Mn ₂ O ₃	0.05	0.15	n.c.	0.02
SrO	0.03	0.60	n.c.	0.03
SO ₃	2.75	20.30	2.49	2.42

Appendix B

Mixing procedures for CBE Mixtures and FAM Mortars

B.1. Mixtures

The following procedure was developed at *Università Politecnica delle Marche* for mixing CBE mixtures and was adopted for producing the materials investigated within this thesis. The procedure consists of mechanical mixing which allows obtaining a homogeneous blend. This is alternate with hand mixing to allow a better blending of fine particles.

The mixer allows obtaining 3 specimens (about 2800 g each) for each batch of mixed materials (**Figure B.1**).

First, aggregates are dried until reaching constant mass for having better control of the water content of the mixture, at the temperature of:

- (105 ± 2) °C for the natural aggregate
- (40 ± 2) °C for RA aggregate.

Before mixing, the aggregates are cooled down. The mixing is carried out at ambient temperature (20-25 °C). The mixing procedure is organised in two stages: the first stage (Phase 1) aims at preparing the aggregate blend to achieve the SSD condition, the second one (Phase 2) at adding the binders to the SSD aggregates.

Phase 1 consists of the following:

- Weighing of the required amounts of dry RA aggregate, dry sand and filler, and mix for 1 min;
- Addition of the amount of water needed to achieve the SSD conditions and mixing (**Figure B.1b**);
- Storing of the aggregate blend in a sealed plastic bag for at least 12 h at room temperature (**Figure B.1c**);

Phase 2 consists of the following:

- Remove the SSD aggregate from the plastic bag immediately before the second mixing phase, mechanical mix for 1 min + hand mixing;
- Add the required amount of cement (**Figure B.2a**), mechanical mixing for 1 min and hand mixing;
- Add the pre-wetting additional water (**Figure B.2b**), mechanical mixing for 1 min and hand mixing (**Figure B.2c**);

Appendix B

Mixing procedures for CBE Mixtures and FAM Mortars

Multiscale Approach for Characterising the Behaviour of Cold Bitumen Emulsion Materials

- Add about a half of the required amount of bitumen emulsion (**Figure B.2d**), mechanical mixing for 1 min and hand mixing;
 - Add the remaining amount of bitumen emulsion, mechanical mixing for 1 min and hand mixing;
 - Check the particle coating by visual examination (**Figure B.2e** and **Figure B.2f**).
- The compaction starts immediately after the end of the mixing. The mixing operations (phase 2) last 10-15 minutes. **Figure B.3** outlines the mixing procedure of CBE mixtures followed within the present study.



a)



b)



c)

Figure B.1 Mixing of CBE mixtures: a) mechanical mixer used at *Università Politecnica delle Marche*, b) Phase 1: preparation of the aggregate blend with the absorption water, c) sealed aggregate blend

Appendix B

Mixing procedures for CBE Mixtures and FAM Mortars

Multiscale Approach for Characterising the Behaviour of Cold Bitumen Emulsion Materials

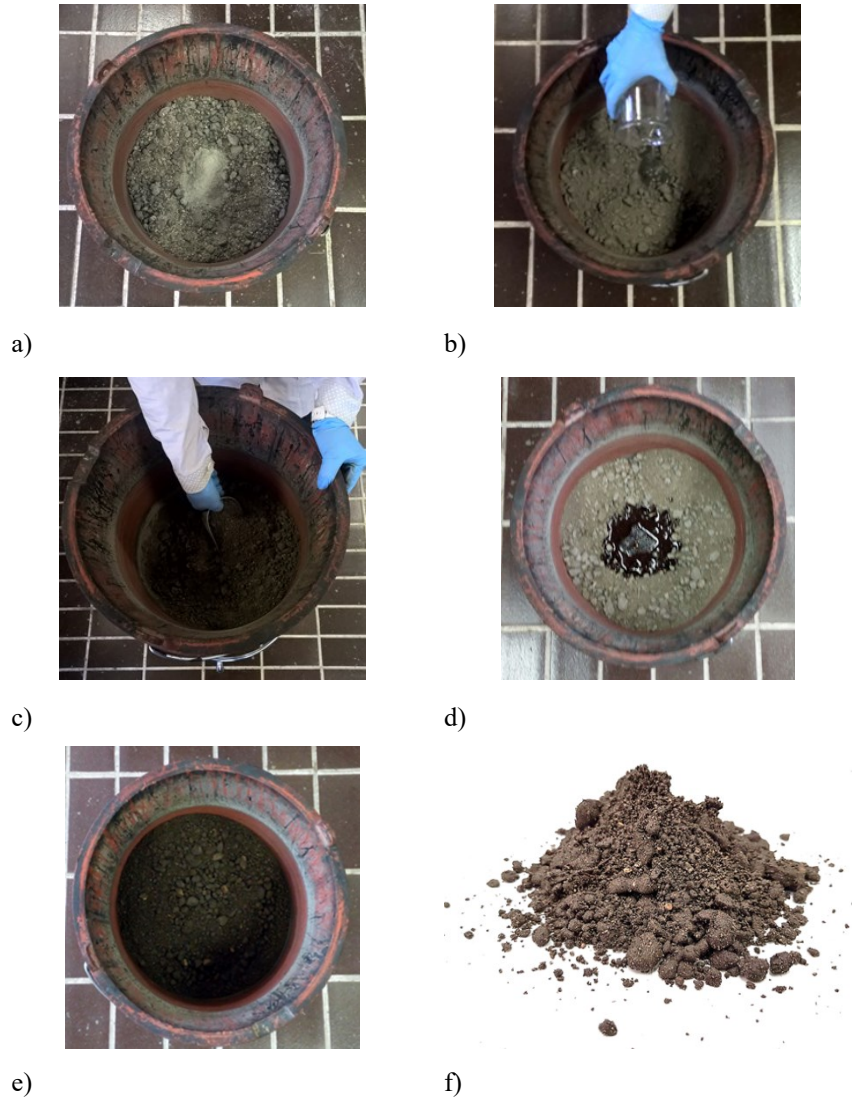


Figure B.2. CBE mixtures mixing Phase 2: a) addition of cement to the aggregate blend, b) addition of the pre-wetting water, c) hand mixing, d) addition of the first half of the emulsion, e) and f) mixture appearance after mixing

Appendix B

Mixing procedures for CBE Mixtures and FAM Mortars

Multiscale Approach for Characterising the Behaviour of Cold Bitumen Emulsion Materials

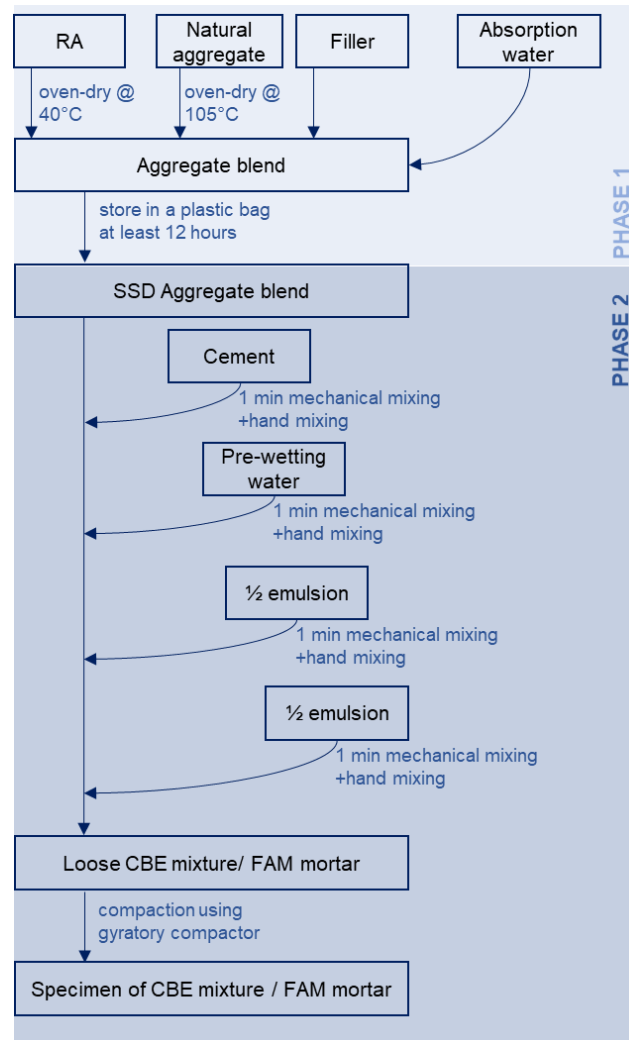


Figure B.3. Mixing of CBE mixtures and FAM mortars scheme

B.2. FAM mortars

The procedure for mixing FAM mortars was developed at *Università Politecnica delle Marche* following the one used for CBE mixtures. The procedure is also adopted within the interlaboratory testing of the RILEM TC 280-CBE (Multiphase characterisation of cold bitumen emulsion materials), Task Group 1 focusing on Emulsions and emulsion-based composites.

Appendix B

Mixing procedures for CBE Mixtures and FAM Mortars

Multiscale Approach for Characterising the Behaviour of Cold Bitumen Emulsion Materials

Mixing is carried out by means of a mechanical mixer (**Figure B.4a**) and by hand. The mixer allows obtaining three specimens (about 800 g) for each batch of mixed materials.

First, aggregates are first dried until reaching constant mass at

- (105 ± 2) °C for the natural aggregate
- (40 ± 2) °C for RA aggregate.

Before mixing, the aggregates are cooled down. The mixing is carried out at ambient temperature (20-25 °C). The mixing procedure is organised in two stages: the first stage (Phase 1) aims at preparing the fine aggregate blend to achieve the SSD condition, the second one (Phase 2) at adding the binders to the SSD aggregates.

Phase 1 consists of the following:

- Weighing the required amounts of dry sand and filler, and mix for 1 min (**Figure B.4b**)
- Add the amount of water to achieve the SSD condition and mix (**Figure B.4c**);
- Store the fine aggregate mixture in a sealed plastic bag for at least 12 h at room temperature (**Figure B.4d**);

Phase 2 consists of the following:

- Remove the SSD fine aggregate mixture from the plastic bag immediately before the mixing and mechanical mixing for 1 min and hand mixing
- Add the required amount of cement, mechanical mixing for 1 min and hand mixing (**Figure B.5a**);
- Add the required amount of pre-wetting water, mechanical mixing for 1 min and hand mixing (**Figure B.5b**);
- Add about a half of the required amount of bitumen emulsion (**Figure B.5c**), mechanical mixing for 1 min and hand mixing (**Figure B.5d**),
- Add the remaining amount of bitumen emulsion, mechanical mixing for 1 min and hand mixing (**Figure B.5e**);
- Check the particle coating by visual examination (**Figure B.5f**).

The compaction starts immediately after the end of the mixing. The mixing operations (phase 2) last 10-15 minutes. **Figure B.3** outlines the mixing procedure of CBE FAM mortars followed within the present study.

Appendix B

Mixing procedures for CBE Mixtures and FAM Mortars

Multiscale Approach for Characterising the Behaviour of Cold Bitumen Emulsion Materials



Figure B.4. Mixing of FAM mortars: a) mechanical mixer used at *Università Politecnica delle Marche*, b) Phase 1: preparation of the aggregate blend, c) addition of the absorption water, d) sealed aggregate blend

Appendix B

Mixing procedures for CBE Mixtures and FAM Mortars

Multiscale Approach for Characterising the Behaviour of Cold Bitumen Emulsion Materials

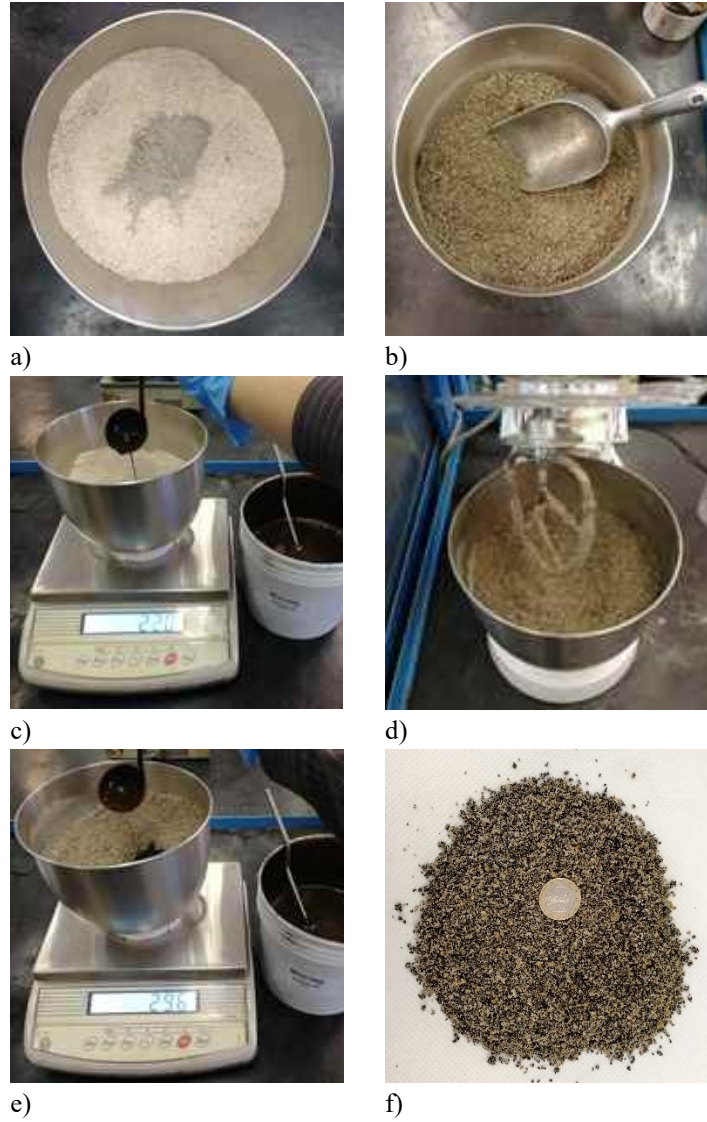


Figure B.5. FAM mortars mixing Phase 2 a) addition of cement to the aggregate blend, b) addition of the pre-wetting water; c) addition of the first half of the emulsion, d) hand mixing, e) addition of the second half of the emulsion, f) FAM mortar appearance after mixing

Appendix C

Study of the Composition of CBE Mixtures with Different Cements for Base Courses

C.1. Introduction

Enhanced performances of CBE mixtures can be obtained with an adequate design of their composition. Adopting non-conventional cementitious binders can be beneficial for the mechanical mixtures performances (Fang, Garcia, *et al.* 2016, Dulaimi *et al.* 2017, Nassar *et al.* 2018, Saadon *et al.* 2018). In a similar manner, the improvement of the volumetric properties improves the mechanical response of CBE materials. The present Appendix summarises the procedure carried out for establishing the composition of CBE mixtures suitable for being used in base courses. The use of traditional bitumen emulsion was considered, as well as the adoption of four different cementitious binder types. The aggregate blend and the dosages of the binders were fixed. The focus was on the CBE composition in terms of water and air voids content to meet the requirements given by the Italian main technical guidelines. The resulting eight mixtures compositions were used to define FAM mortars composition (Chapter 5) and study the curing behaviour study (Chapter 6).

C.2. Methodology

CBE mixtures aggregate blend consisted of RA 0/16, fine natural aggregate and filler. The grading distribution selected was close to the Fuller-Thompson grading distribution with NMAS = 16 mm. The composition of the aggregate blend was defined with the main intent of maximising the RA content. The composition of the grading, coded "CC", is reported in **Table 4.1**. As bituminous binder, the traditional bitumen emulsion was considered (B). As cementitious co-binders, four types of cement (C1, C2, C3 and C4) were adopted (see Section 4.1). The emulsion and cement dosages (by dry aggregate mass) were fixed at the beginning of the research, based on the Italian practice for cold recycled subbase and base courses (Provincia Autonoma di Bolzano 2016). Specifically, emulsion dosage was 3.3% (corresponding to 2.0% of residual bitumen), and cement dosages were 1.5% and 2.5%. The eight mixtures were identified using the codes MIX1a, MIX1b, MIX2a, MIX2b (**Table 4.2**). Mixing and compaction procedures are detailed in Appendix B and Section 4.2.2, respectively.

For the definition of the optimal water content, only four mixtures were considered, characterised by a cement dosage of 2%, which is halfway between the two design values. In this phase, mixtures were identified using the cement type (Mix C1, Mix C2, Mix C3 and Mix C4). The total water content was established by analysing the volumetric properties and the compactability of the four mixtures (Grilli *et al.* 2016, Raschia, Graziani, *et al.* 2019) using the volumetric approach described in Section 4.3. Trial mixtures were produced at four total water contents: 3.2%, 4.2%, 5.2% and 6.2%. The mixtures produced with binders C1 and C2 at the lowest water content (3.2%) were discarded because the material was too dry and not homogeneous. The mixtures produced with binders C3 and C4 at the highest water content (6.2%) were discarded because the material was too wet and the water drained out. From each batch of mixed loose material, three specimens were compacted at 180 gyrations. This allowed measuring the volumetric properties, i.e. V_m and VFL , as a function of the number of gyrations (Section 4.3.1). A common V_m value for all mixtures was chosen by analysing the compaction curves, and then the optimal water content for each mixture was selected. The final compositions of the mixture were tested to verify the mix design requirements set by Italian construction specifications (Autostrade per l'Italia 2013, Provincia Autonoma di Bolzano 2016). First, $ITSM$ and ITS were measured on specimens subjected to an accelerated curing regime of 3 days at 40 °C in unsealed condition. The $ITSR$ was then evaluated on two additional series of specimens that were first cured 28 days at 25 °C and then submerged in water at 40°C for 3 or 7 days. $ITSR$ was obtained as the ratio between the ITS of the material after the 28 curing days and the further period of soaking in water, and the ITS of the material after 28 curing days. Details about testing procedures are provided in Section 4.5 of the present thesis.

C.3. Analysis of the Results

Figure C.1a reports the average compaction curves obtained for mixture specimens with a total water content of 4.2%. As expected, V_m reduced, and VFL increased as compaction proceeded. The specimens produced with binders C3 and C4 showed lower voids with respect to the specimens produced with binders C1 and C2. **Figure C.1b** shows that, also for the other total water contents, the voids obtained with binders C3 and C4 were about 2% lower than those obtained with binders C1 and C2 at the same water content. This may be related to two kinds of phenomena. First, the cement type could alter the viscosity of the slurries obtained by mixing water, emulsion, filler and cement. That, in turn, may influence the lubrication ability of the mixture (Tan *et al.* 2014). Second, cement may affect the demulsifying behaviour of over-stabilised emulsion (Ouyang *et al.* 2015). Therefore, the effect of cement on the workability and compactability of the mixtures is extremely important, especially for field compaction, and should be considered in the mix design phase.

The increase in water content generally led to a decrease in V_m but, in some cases, also caused the loss of material from the mould and thus changed the specimen composition. Specimens whose indicator is below the $VFL = 90\%$ line (**Figure C.1b**), thus characterised

by *VFL* values higher than 90%, showed a mass loss greater than 0.5% at the end of the compaction, confirmed by an evident water ejection. This resulted in a remarkable change in their composition (Section 4.3).

To develop the FAM mortar concept and assess the curing behaviour (Chapter 5 and Chapter 6), the target voids value of $V_m = 11\%$ was selected for all the mixtures. Such a V_m value is considered possible to reach in the in situ compactions of CBE mixtures (Stimilli *et al.* 2013, Bocci *et al.* 2020). **Figure C.1c** and **Figure C.1d** show the average values of the compaction energy (number of gyrations) needed to reach $V_m = 11\%$ and the corresponding values of *VFL*. The total water content was selected based on these results: $w_{tot} = 4.7\%$ for the mixtures produced with binders C1 and C2 and $w_{tot} = 3.7\%$ for the mixtures produced with binders C3 and C4. With these compositions, it was possible to obtain the target voids value with similar compaction energy (between 80 and 100 gyrations) and *VFL* values well below the practical saturation limit.

Figure C.2a displays the average values of *ITSM* and *ITS* at 25 °C for the selected mixture compositions measured after 3 days of curing at 40 °C. The dashed line represents the minimum value of strength (*ITS* = 0.4 MPa) and stiffness (*ITSM* = 3000 MPa) required by the Italian technical specifications (Autostrade per l'Italia 2013, Provincia Autonoma di Bolzano 2016). The increase in the cement dosage always led to an improvement in the mechanical properties. The mixtures produced with high strength cements (C2 and C3) showed higher values of *ITS* and *ITSM* compared to the reference cement C1. In contrast, the mixtures produced with C4 showed lower mechanical properties (below the *ITS* acceptance limit).

Figure C.2b shows the average values of *ITS* and *ITSR* after 28 days of curing at 25 °C. The dashed line is the minimum value (*ITSR* = 70%) required by the Italian technical guidelines (Autostrade per l'Italia 2013, Provincia Autonoma di Bolzano 2016). All the mixtures highlighted an *ITSR* greater than 75% and thus a not-pronounced water sensitivity. Increasing the soaking time from 3 to 7 days generally led to an increase in the *ITSR*. This suggests that the additional curing time at the high temperature of soaking (i.e. 40 °C) improved the mechanical properties of the mixtures, counterbalancing the effect of the immersion in water.

The comparison between **Figure C.2a** and **Figure C.2b** shows that the *ITS* values obtained after 3 days of curing at 40 °C were always lower than those obtained after 28 days of curing at 25 °C. The reduction of strength in the case of the accelerated curing was a function of the type and dosage of cement and ranged between 0.3% (MIX1a-C2) and 44% (MIX1b-C4).

Appendix C

Study of the Composition of CBE Mixtures with Different Cements for Base Courses

Multiscale Approach for Characterising the Behaviour of Cold Bitumen Emulsion Materials

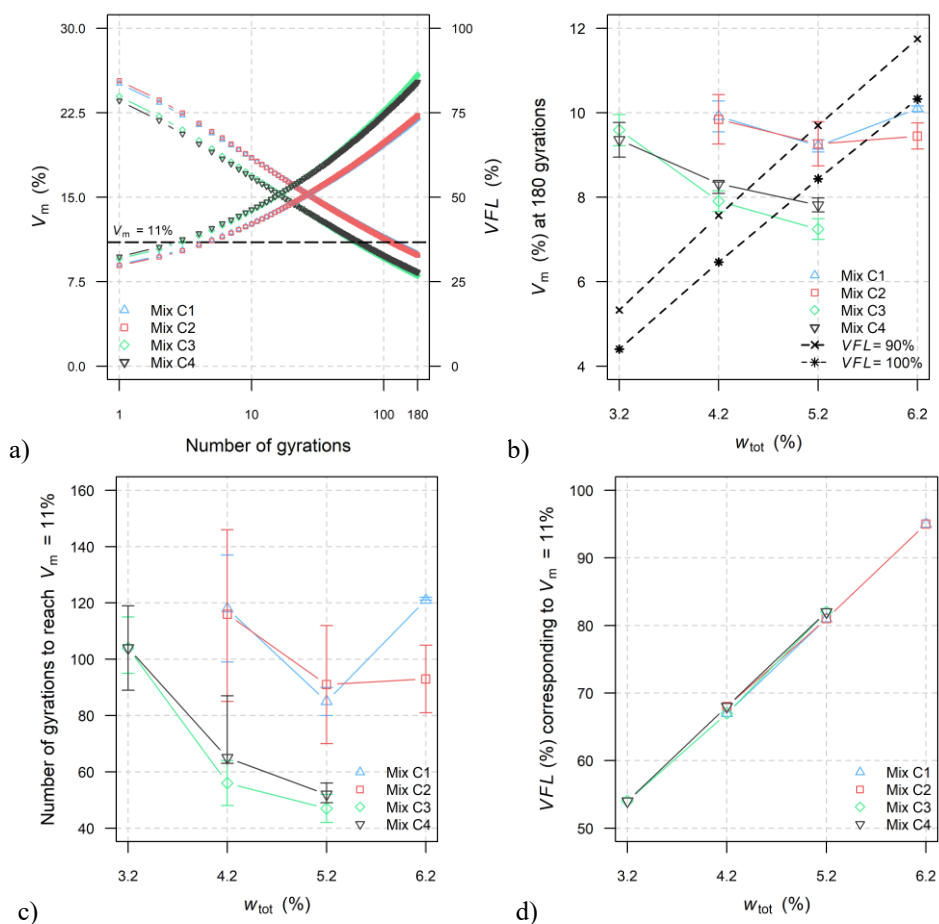


Figure C.1. Effect of total water content (w_{tot}) on the volumetric properties of CBE mixtures: a) compaction curves obtained with $w_{tot} = 4.2\%$, b) V_m at the end of the compaction c) number of gyrations to reach $V_m = 11\%$, d) VFL corresponding to $V_m = 11\%$

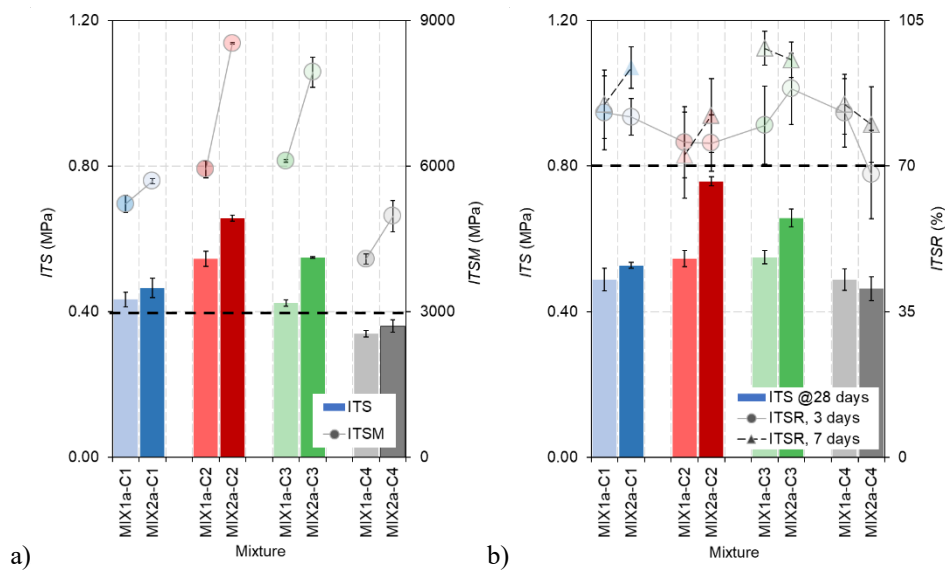


Figure C.2. Mechanical properties of CBE mixtures (25 °C): a) after 3 days of curing at 40 °C, b) water sensitivity

C.4. Summary

This Appendix deals with the definition of CBE mixtures compositions suitable for base courses. The use of different cementitious binder was considered. The focus of the investigation was the definition of the optimal total water content. The binders dosages were defined a priori based on the general Italian practices. A unique emulsion dosage was considered, whereas two cement dosages were selected. Three water content for each mixture were used.

The main findings are as follows:

- Cementitious binders C1 and C2 showed similar compactability, as well as C3 and C4;
- Specifically, C3 and C4 had lower voids at the same water content. Based on these findings, the water content selected were 4.7% and 3.7% for mixtures with C1 and C2, and mixtures with C3 and C4, respectively;
- With the selected water contents and the target volume of voids, all mixtures met the limits required by Italian technical specification, except those produced with C4, whose mechanical properties were slight below
- All mixtures showed a reduced water sensitivity. Besides, an increased soaking time seems to lead to additional curing counterbalancing the effect of water immersion.

Appendix D

Effect of Curing on the Indirect Tensile Failure Energy of CBE Mixtures

D.1. Introduction

The development of the CBE mixture physical and mechanical properties strongly depends on the curing process. With time, the CBE mixture changes its structure and enhances its performances. However, not only time contributes to these phenomena. Curing temperature and RH can play a key role, fastening or slowing down the processes or favouring the occurrence of certain mechanisms, hindering some other. This investigation focuses on evaluating the impact of curing time and RH on the indirect tensile failure energy of CBE mixtures suitable for base courses.

D.2. Methodology

The CBE mixture aggregate blend was composed of RA aggregate, fine natural aggregate and natural filler. The composition of the grading, coded “CC”, is reported in **Table 4.1**. As co-binders, traditional bitumen emulsion and cement C1 were used (Section 4.1). Emulsion dosage was 3.3% (corresponding to 2.0% of residual bitumen), and cement dosages were 1.5% and 2.5%. B/C ratios were 1.3 and 0.8. Therefore, mixtures MIX1a-C1 and MIX2a-C1 were here considered (**Table 4.2**). Mixing and compaction procedures are detailed in Appendix B and Section 4.2.2. The diameter of the specimens was 150 mm. The fixed height compaction mode was applied to reach selected target voids of the mixture V_m (**Table 4.2**). Curing started right after the end of the compaction. Specimens were cured at (25 ± 2) °C in unsealed and sealed conditions. As a consequence, two RH were considered: $(70 \pm 5)\%$ for unsealed specimens and about 100% for sealed ones (see Section 4.2.3). The specimens were cured for 1, 3, 7, 28, 90 days.

At the end of the curing, the *ITS* test was performed following the procedure described in 4.5.3 at 25 °C. During the tests, the horizontal deformation u of the specimens was measured using two transducers set at the horizontal diameter (**Figure 4.6b**). The horizontal stress σ and strain ε in the centre of the specimen can be computed as follows:

$$\sigma = \frac{2F}{\pi DH} \quad (\text{D.1})$$

$$\varepsilon = \frac{2u}{D} \frac{1 + 3\nu}{4 + \pi\nu - \pi} \quad (\text{D.2})$$

where F is the load and ν is the Poisson ratio (assumed equal to 0.2). D and h are the specimen diameter and its mean thickness, respectively.

D.3. Analysis of the Results

Figure D.1a compares the curves $\sigma - \varepsilon$ obtained for two specimens of MIX1a-C1, cured for 90 days in sealed and unsealed conditions. The two curves highlighted a similar behaviour: both were characterised by a first phase where the horizontal stress increased linearly with strain, followed by an evident non-linear phase until failure.

The curves in **Figure D.1a** stop at the peak value of the load (failure point). The post-peak behaviour was not represented because the fracture propagation was very fast for all the mixtures investigated, and the deformation measurements were not reliable. Thus, the failure energy E_{fail} was calculated as the area under the $\sigma - \varepsilon$ curve, up to the peak value (**Figure D.1b**). On the contrary, other researchers (Miljković and Radenberg 2014) analysed the post-peak behaviour. It is important to highlight that they investigated materials with a higher bitumen content and characterised by a B/C ratio equal to or greater than 4. Thus, their fracture propagation was governed principally by the bituminous matrix.

The maximum stress (corresponding to the *ITS*) as a function of the horizontal failure strain (ε_{fail}) is depicted in **Figure D.2**. After one day, all the mixtures showed the highest values of ε_{fail} . This is probably due to the low quantity of bonds (both cementitious and bituminous) developed in the first curing hours. The result confirms that at early-stage CM show a behaviour similar to granular materials (Thomas and Kadrmas 2002, Lin *et al.* 2015). For specimens of MIX1a-C1, ε_{fail} decreased until reaching the value of about 10000 microstrains with the progress of the curing process. Specimens of MIX2a-C1 showed different behaviour. In fact, after three days of curing, they showed a marked reduction of ε_{fail} . Then, ε_{fail} increased over time and stabilised at the value of about 10000 microstrains after 28 days of curing. Moreover, unsealed specimens had ε_{fail} slightly larger or equal to those of sealed specimens.

Differently to what observed for the *ITS* (Section 6.4.3), the effect of the different curing conditions on ε_{fail} was not as noticeable. There was no significant trend, and the difference between ε_{fail} of specimens cured in unsealed or sealed conditions was reduced. The results suggest that the long-term behaviour of CBE mixtures, in terms of horizontal failure strain, was similar, regardless of the B/C ratio and curing condition. In contrast, during the first stages of curing, the different amounts of bituminous and cementitious bonds had a significant effect on the horizontal strain at failure of the mixtures

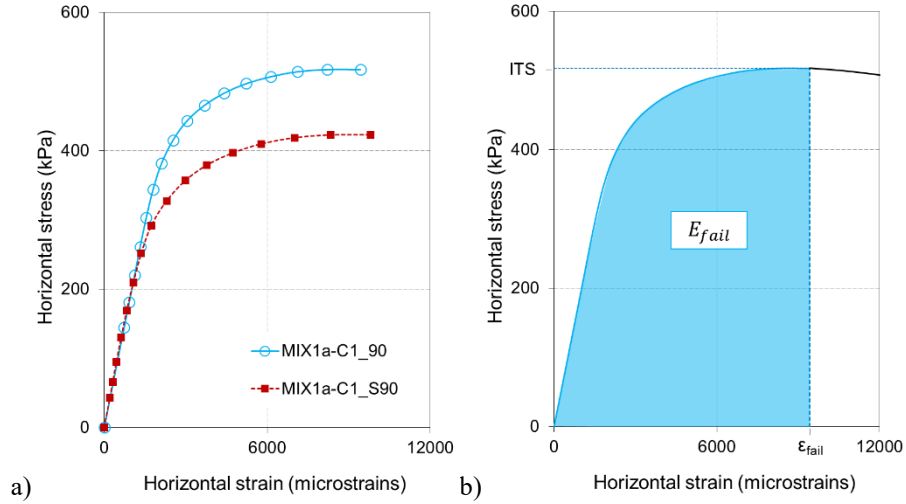


Figure D.1. $\sigma - \epsilon$ curves a) of the MIX1a-C1 specimens cured 90 days in unsealed and sealed (S) conditions, b) failure energy

Figure D.3a shows that, until 90 days, E_{fail} generally increased with curing time, especially in the medium and long-term. Moreover, specimens of MIX1a-C1 showed, in general, higher failure energy values compared to those of MIX2a-C1. The results confirm that a higher B/C ratio leads to a more ductile failure behaviour.

Figure D.3b shows the influence of curing conditions on E_{fail} . In particular, the graph depicts the relative failure energy variation, changing from sealed (E_{fail_S}) unsealed (E_{fail_U}) conditions:

$$\Delta E_{fail} = \frac{E_{fail_U} - E_{fail_S}}{E_{fail_S}} \cdot 100 \quad (D.3)$$

As can be observed, unsealed specimens were characterised by higher failure energy with respect to sealed specimens. The result suggests that bituminous bonds were more developed in unsealed conditions. However, at 90 days, the effect of curing conditions was less evident. This confirms that, even in sealed curing conditions, bituminous bonds contribute to the fracture behaviour of the mixtures.

Appendix D

Effect of Curing on the Indirect Tensile Failure Energy of CBE Mixtures

Multiscale Approach for Characterising the Behaviour of Cold Bitumen Emulsion Materials

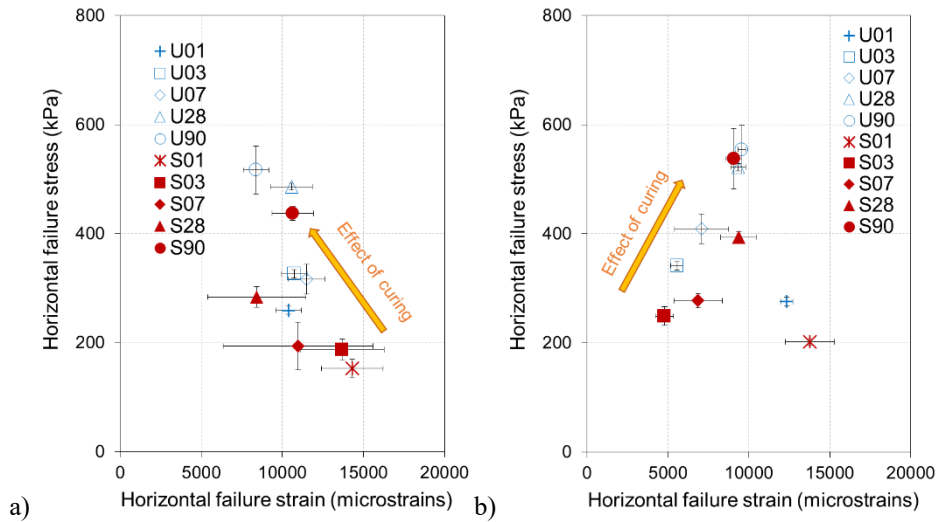


Figure D.2. Horizontal failure stress as a function of horizontal failure strain for a) MIX1a-C1, b) MIX2a-C1. Error bars represent the standard deviation

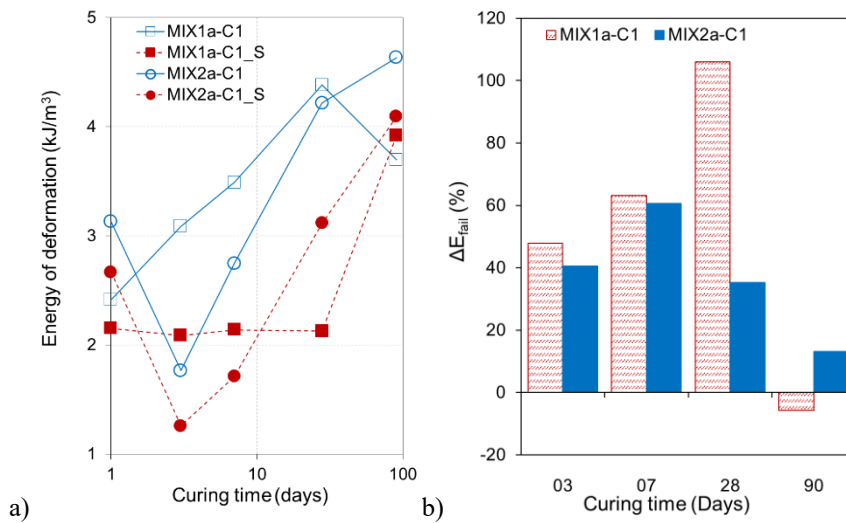


Figure D.3. Failure energy of CBE mixtures: a) over curing time, b) comparison between unsealed and sealed specimens

D.4. Summary

This Appendix deals with evaluating the influence of the development of bituminous and cementitious bonds on the curing of CBE mixtures. To this end, the effect of different curing RH i.e. unsealed and sealed condition, and the influence of different B/C ratios (i.e. 1.3 and 0.8), were investigated. Horizontal strain at failure and failure energy were considered.

The main findings are as follows:

- The curing RH did not significantly influence the horizontal strain at failure. Besides, the horizontal strain in the early stage depended on the cementitious and bituminous bonds, whereas in the long-term, it tended to the same value of 10000 microstrains regardless of B/C;
- Failure energy increased over curing time, especially in the medium and long-term;
- Curing conditions influenced failure energy. CBE specimens cured at the lower RH presented higher failure energy, suggesting that the bituminous bonds were more developed in this condition. However, in the long-term, the failure behaviour was similar regardless of the curing condition.

Appendix E

Effect of Grading Distribution on the Volumetric Properties of CBE Mixtures for Binder Courses

E.1. Introduction

To promote the use of cold mixtures in upper pavement layers, their mechanical properties should be improved. In general, continuously graded curves are adopted in cold mixtures production. However, recent studies attempted to assess the effect of different grading distributions on the mechanical properties of CRM (Xu *et al.* 2017, Raschia, Mignini, *et al.* 2019). Moreover, other researchers investigated the use of not conventional types of cements for improving the response of cold mixtures, e.g. supplementary blended cementitious fillers and rapid hardening cements (Dulaimi *et al.* 2017, Saadoon *et al.* 2018). The present Appendix focuses on evaluating the effect of different four distributions on the volumetric properties of CBE mixtures suitable for binder courses. The use of traditional and modified bitumen emulsions was considered, as well as the adoption of two high-strength cementitious binders. The volumetric properties of CBE mixtures were investigated both at the fresh and the cured state. The results obtained allowed selecting the CBE mixtures investigated in Chapter 6 and Chapter 7.

E.2. Methodology

CBE mixtures were produced in the laboratory using RA aggregate, fine natural aggregate and filler (see Section 4.1). Three gradations of RA aggregate were used, i.e. RA0/16, RA 2/16, RA0/2. Both the traditional and modified emulsion were employed, i.e. B and BP. The two high strength cements were here considered as co-binders: i.e. C2 and C3. Four grading distributions, labelled CC, CC-10, Fine-16, GG, were considered (**Table E.1**). The reference gradation (CC) was continuous, close to the Fuller-Thompson maximum density curve with exponent 0.45 and NMAAS 16 mm. The second (CC-10) was obtained reducing the NMAAS of the reference distribution to 10 mm, and the third (Fine-16) was obtained by adding 5% of filler to the reference distribution. The fourth grading distribution GG, was a gap-graded type, with NMAAS 16 mm. **Figure E.1** depicts the grading distribution considered. Emulsion dosage (with respect to aggregate mass) was 5.0%, whereas cement dosage was 2.5%. CC

Appendix E

Effect of Grading Distribution on the Volumetric Properties of CBE Mixtures for Binder Courses

Multiscale Approach for Characterising the Behaviour of Cold Bitumen Emulsion Materials

and GG are the same gradings adopted for producing MIX3 and MIX4 (**Table 4.1** and **Table 4.2**). Each of the 16 mixtures was produced considering three different intergranular water contents ranging between 2.0% and 4.0% (**Table E.2**).

The mixing procedure is described in Appendix A. Specimens were compacted with the SGC using 150 mm mould, fixing the energy of compaction (number of gyrations equal to 100) to study the influence of water content on the compactability of the mixtures (Section 4.2.2). Compactability was assessed using the volumetric analysis in terms of voids in the mixture at the fresh state $V_{m, fresh}$ (Equation (4.1)).

Table E.1. Grading distribution composition considered

ID	Type	NMAS	Composition
CC*	Continuous	16 mm	80% RA0/16, 17% sand, 3% filler
CC-10	continuous	10 mm	75% RA0/10, 17% sand, 8% filler
Fine-16	Continuous, high filler	16 mm	80% RA0/16, 20% filler
GG*	Gap graded	16 mm	70% RA2/16, 20% sand, 10% filler

*same grading distributions introduced in section 4.4.1

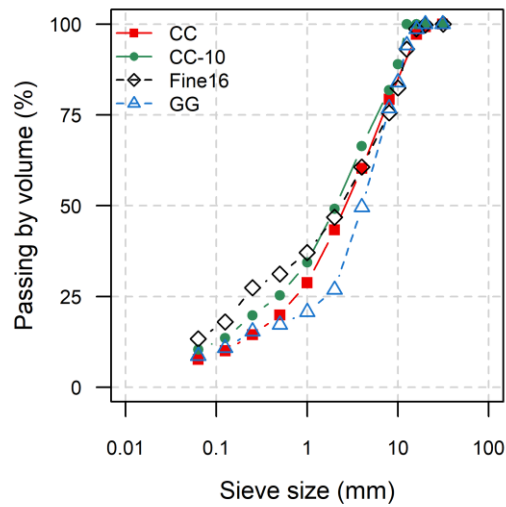


Figure E.1. Grading distributions considered in the study

Specimens were cured at 25 °C and RH = (7.0 ± 5)% for at least 90 days in unsealed conditions. During curing, specimens changed their volumetry. The hydrated cement (consisting of reacted cement and non-evaporable water) has a higher volume than the

Effect of Grading Distribution on the Volumetric Properties of CBE Mixtures for Binder Courses

Multiscale Approach for Characterising the Behaviour of Cold Bitumen Emulsion Materials

anhydrous one (see Sections 2.1.2.2 and 2.1.3). Therefore, if the amount of trapped water is negligible, the voids of the cured mixture are:

$$V_{m,cured} = \frac{v_{A,cured}}{v} \cdot 100 = \frac{v_A + v_{W,evaporated}}{v} \cdot 100 \quad (E.1)$$

where $v_{A,cured}$ is the volume of air obtained by summing the volume of air voids at the fresh state v_A and the volume of evaporated water $v_{W,evaporated}$. CBE mixtures will have different volumetric properties compared to those at fresh state, specifically $V_{m,cured} < V_{m,fresh}$. $V_{m,cured}$ was calculated according to EN 12697-8. The volume of non-evaporable water (bonded by the cement) was considered on par with the other solid components of CBE mixtures.

Table E.2. Intergranular water contents considered for each mixture

ID	Intergranular water dosage (%)			
	C2-B	C2-BP	C3-B	C3-BP
CC*	3.0 – 3.5 – 4.0	3.0 – 3.5 – 4.0	2.5 – 3.0 – 3.5	2.5 – 3.0 – 3.5
CC-10	3.0 – 3.5 – 4.0	3.0 – 3.5 – 4.0	2.5 – 3.0 – 3.5	2.5 – 3.0 – 3.5
Fine-16	3.0 – 3.5 – 4.0	3.0 – 3.5 – 4.0	2.5 – 3.0 – 3.5	2.5 – 3.0 – 3.5
GG*	2.5 – 3.0 – 3.5	2.5 – 3.0 – 3.5	2.0 – 2.5 – 3.0	2.0 – 2.5 – 3.0

*same grading distributions introduced in section 4.4.1

E.3. Analysis of the Results

Figure E.2 displays the mixtures voids at the fresh state $V_{m,fresh}$ as a function of the intergranular water content of the mixtures produced with BP. Mixtures with B exhibited similar behaviour. The adoption of grading distributions different from the reference one resulted in different $V_{m,fresh}$. Specifically, comparing the voids of the mixtures produced with the same intergranular water content (i.e. 3.0% for C2 and 2.5% mixtures for C3) and different grading distribution, better compactability was obtained with Fine-16 (average reduction of $V_{m,fresh}$ on the four mixtures equal to -1.4%) and GG (-0.9% on average). The influence of the decrease of the NMA from 16 mm to 10 mm was smaller (-0.4% on average). The effects of the type of cement and emulsion were less relevant.

Figure E.3 displays the reduction of the voids in the mixture due to the passage from fresh to cured state. Some differences may be highlighted among mixtures with different grading distributions. Nevertheless, the grading distribution effect was not well-clear and may fall in the variability of the test. Regarding the influence of the type of binders (i.e. cement and emulsion), C2 and C3 allowed reducing voids of averagely 1.4% and 1.7%,

Appendix E

Effect of Grading Distribution on the Volumetric Properties of CBE Mixtures for Binder Courses

Multiscale Approach for Characterising the Behaviour of Cold Bitumen Emulsion Materials

respectively. Therefore, hydrated C3 may have a higher volume compared to C2. However, the difference between the reduction measured for CBE mixtures produced with the two cements is not considered significant. It may be due to the variability of the experimental data. Further studies are needed to deepen this effect. The effect of the emulsion type was even more negligible (average reduction of 1.5% and 1.6% with B and BP, respectively). It can be stated that the improvement of CBE mixtures volumetric properties must be obtained at the fresh-state through a proper mix design and compaction. After curing, mixtures will always have lower voids than the fresh state, and the reduction of voids could be slightly related to the type of binders. Anyway, the effect of the type of binder is less significant than those obtained through the mix-design optimisation.

Based on the results, the distribution GG was selected for producing the CBE mixtures investigated in Chapter 6 and Chapter 7. This grading indeed allowed an improvement of the volumetric properties, and its mortar matrix was completely composed of natural aggregate. This enabled the comparison of the influence of the presence of aged binder at the FAM mortar scale.

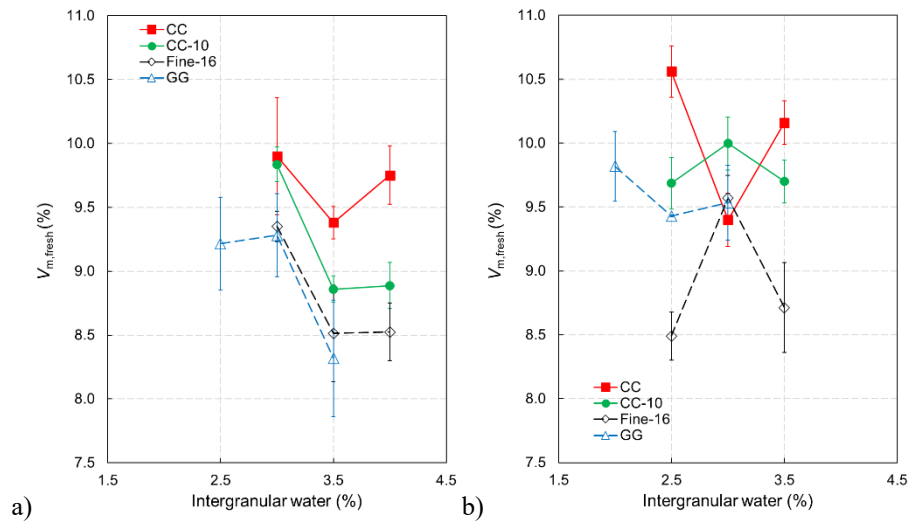


Figure E.2. V_m as a function of the intergranular water of CBE mixtures with modified emulsion and cement: a) C2, b) C3. Error bars represent the variability of the experimental data

Appendix E

Effect of Grading Distribution on the Volumetric Properties of CBE Mixtures for Binder Courses

Multiscale Approach for Characterising the Behaviour of Cold Bitumen Emulsion Materials

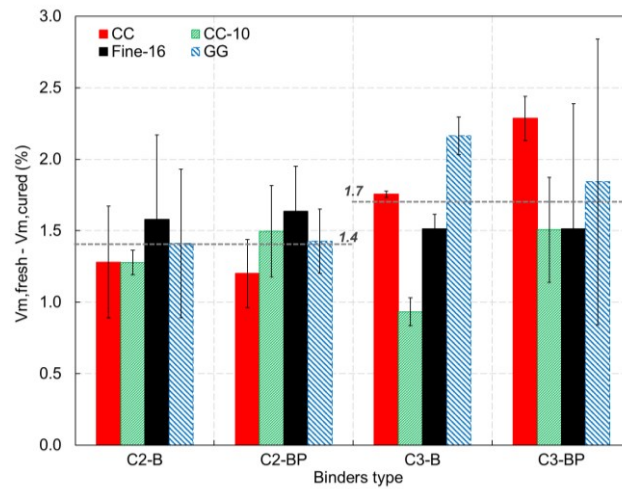


Figure E.3. Reduction of voids in the mixture after curing. Error bars represent the variability of the experimental data

E.4. Summary

This Appendix evaluates the effect of different grading distributions on the volumetric properties of CBE mixtures produced with bitumen emulsion and high strength cements.

The main findings are as follows:

- Continuous grading distributions did not confer better compactability to CBE mixtures;
- The increase of fines or a gap-graded distribution allowed the reduction of voids;
- At the end of curing, voids of mixtures were further reduced because of the increase in the cement volume. This reduction is mainly linked to the type of cement and the volume of its hydration products.

Appendix F

Study of the Composition of CBE Mixtures with High Strength Cements for Binder Courses

F.1. Introduction

A proper selection of bituminous and cementitious co-binders types, and their good proportioning, is crucial for improving the mechanical response of cold mixtures and, consequently, promoting their use in upper pavement layers. The present Appendix aims at identifying CBE mixture compositions suitable for binder courses. To this goal, the use of modified bitumen emulsion and two high strength cements was evaluated. The evolution of the physical (*DW*) and mechanical properties (*ITSM* and *ITS*) were assessed over a year of curing. Besides, *ITSM* was measured at different temperatures to evaluate the thermal sensitivity of the mixtures. The results obtained allowed selecting CBE mixtures investigated within Chapter 6 and Chapter 7.

F.2. Methodology

The CBE mixtures investigated were prepared using RA aggregate, fine natural aggregate, filler, bitumen emulsion, cement and water (see Section 4.1). The aggregate blend was CC (**Table 4.1**). Both the traditional and the modified bitumen emulsion were used, i.e. B and BP. As co-binders, the two high-strength cements, C2 and C3, were considered.

Eight CBE mixtures were obtained combining different types and dosages of co-binders. Two reference mixtures were produced using emulsion B, whereas the emulsion BP was adopted for the remaining six mixtures. The B/C ratio was equal to 1.0 and 1.2 to have a balance among the co-binders. **Table F.1** summarises the binder dosages (by dry aggregates mass). The total water dosage was 4.5% by dry aggregate mass.

Mixing and compaction procedures are detailed in Appendix B and Section 4.2.2, respectively. The diameter of the specimens was 100 mm. The fixed height compaction mode was applied to reach selected target voids of the mixture V_m . Two values of V_m were chosen: 8.5% for mixtures with B and 9.5% for the mixtures with BP.

Curing started right after the end of the compaction. Specimens were cured at (25 ± 2) °C and constant RH of $(70\pm 5)\%$ in unsealed conditions. The specimens were cured

Study of the Composition of CBE Mixtures with High Strength Cements for Binder Courses

Multiscale Approach for Characterising the Behaviour of Cold Bitumen Emulsion Materials

for 6 hours, 1, 3, 7, 28, 90, 365 days. To assess the thermal sensitivity, specimens were cured for 28 days (**Table F.1**).

Table F.1. Summary of the testing programme

ID	Cement		Bitumen emulsion		B/C ratio	Curing time	Thermal sensitivity (days)
	Type (-)	Dosage (%)	Type (-)	Dosage (%)		<i>DW</i> , <i>ITSM</i> , <i>ITS</i> (days)	
MIX3 ⁺	C2, C3	2.5	BP	5.0	1.2	6 h, 1, 3, 7, 28,	
MIX6 ⁺	C2, C3	2.5	B	5.0	1.2	90, 365	28
MIX7 ⁺	C2, C3	3.0	BP	5.0	1.0	1, 28, 90, 365	
MIX8	C2, C3	2.5	BP	4.2	1.0		

* mixtures investigated in Chapter 6 and Chapter 7, ⁺ mixtures investigated also in Appendix G

F.3. Analysis of the Results

The evolution of *DW*, from 6 hours to 1 year of curing, of CBE mixtures with B/C = 1.2 (MIX3 and MIX6) is shown in **Figure F.1a**. The *DW* rate of evolution was noticeably higher in the first week, when its average value was 55% and 59% for C2 and C3 mixtures, respectively. After that, the evaporation got slower, and it was negligible after 90 days. Although the type of emulsion did not influence *DW*, some differences due to the type of cement can be observed. After 6 hours, CBE mixtures with C2 lost a higher amount of water. In the long-term, C2 mixtures displayed a higher amount of non-evaporated water (about 25%) than C3 mixtures (20%). Even though a slight amount of non-evaporated water could be entrapped, such evidence points out that C2 bonded a higher amount of water during its hydration process (see Section 2.1.2.2). **Figure F.1b** depicts the average values of *DW* after 1, 28, 90, 365 days for mixtures with B/C = 1.0 (MIX7 and MIX8). Results are similar to the ones obtained when B/C = 1.2.

Figure F.2a shows the evolution of *ITSM* throughout curing when B/C = 1.2. CBE mixtures produced using the same cement highlighted a comparable behaviour. In the early stage of curing, *ITSM* developed rapidly using C2. After 6 hours, *ITSM* was about 3600 MPa. Differently, *ITSM* was about 700 MPa with C3. After the first days, the rate of *ITSM* evolution of C2 mixtures decreased. Despite that, mixtures produced with C3 exhibited a lower *ITSM* even in the long term. A significant effect related to the type of bitumen was not observed. One should bear in mind that CBE mixtures with B had lower V_m . Consequently, the effect of the modified bitumen could have counterbalanced the effect of the reduced V_m .

Figure F.2b depicts the evolution of *ITS* for CBE mixtures with B/C = 1.2. In the early stage of curing, *ITS* developed faster for mixtures with C2. After 6 hours, the strength

was about 0.30 MPa and 0.18 MPa for mixtures with C2 and C3, respectively. In the long-term, using C2, *ITS* was 20% and 12% higher with B and BP, respectively. *ITS* was comparable over all the curing for C3 mixtures, whereas it was slightly higher for the mixture with B and C2. The result can be related to the different V_m . The behaviour was comparable when the same type of cement was used.

Figure F.3 depicts the average values of the mechanical properties after 1, 28, 90 and 365 days of curing, measured for mixtures with B/C=1.0. Results were similar to the ones measured for the higher B/C ratio. Comparing the *ITSM* (**Figure F.3a** and **Figure F.2a**) of mixtures produced using BP (having equal V_m), it can be observed that the different binders combinations did not have an effective influence on the stiffness. After the first curing day, mixtures differed by up to 15% and 10% when C2 and C3 were used, respectively. After 1 year, the differences were always lower than 10%. The *ITS*, as well as *ITSM*, did not highlight a pronounced sensitivity to the binder dosage (**Figure F.3b** and **Figure F.2b**). For mixtures produced with BP, the differences due to the dosages of binders were up to 18% and 15% after 1 day and 365 days, respectively.

Figure F.4 shows the relationship between *ITSM* and *ITS* described by linear regression. The relationship was the same for all the mixtures, regardless of type and dosage of emulsion and cement. This outcome means that using a different cement influenced mainly the rate of development of the mechanical properties.

Figure F.5a shows the *ITSM* values at different temperatures obtained fixing the target horizontal deformation of $2 \cdot 10^{-6}$ mm/mm. The experimental data can be fitted using linear regression:

$$\log ITSM = -a \cdot T + b \quad (F.1)$$

where T is the temperature, and a and b are fitting parameters depending on CBE mixtures characteristics (reported in **Table F.2**). In particular, the slope of the regression line a defines the thermal sensitivity of the material. All the investigated mixtures highlighted a thermal sensitivity typical of bituminous materials: *ITSM* decreased while temperature increased. However, thanks to the cement, the thermal sensitivity of mixtures was less noticeable compared to HMA (Cardone *et al.* 2015). Observing the effect of the bitumen type, a was slightly higher for mixtures with B when cement type and dosage were the same. Mixtures with C2 had lower thermal sensitivity than mixtures with C2 and the same composition.

Figure F.5b quantifies the variation of the stiffness, $\Delta ITSM$ when the target horizontal deformation was $5 \cdot 10^{-6}$ mm/mm ($ITSM_5$) instead of $2 \cdot 10^{-6}$ mm/mm ($ITSM_2$):

$$\Delta ITSM = \frac{ITSM_2 - ITSM_5}{ITSM_2} \cdot 100 \quad (F.2)$$

The increase of the deformation always reduced the *ITSM*. The result can be attributed to non-linearity effects related to the horizontal deformation. Besides, the higher the temperature, the higher was $\Delta ITSM$.

Study of the Composition of CBE Mixtures with High Strength Cements for Binder Courses

Multiscale Approach for Characterising the Behaviour of Cold Bitumen Emulsion Materials

Based on the results, the binders composition used for MIX3, i.e. 5% emulsion and 2.5% cement, was selected for producing the CBE mixtures investigated in Chapter 6 and Chapter 7.

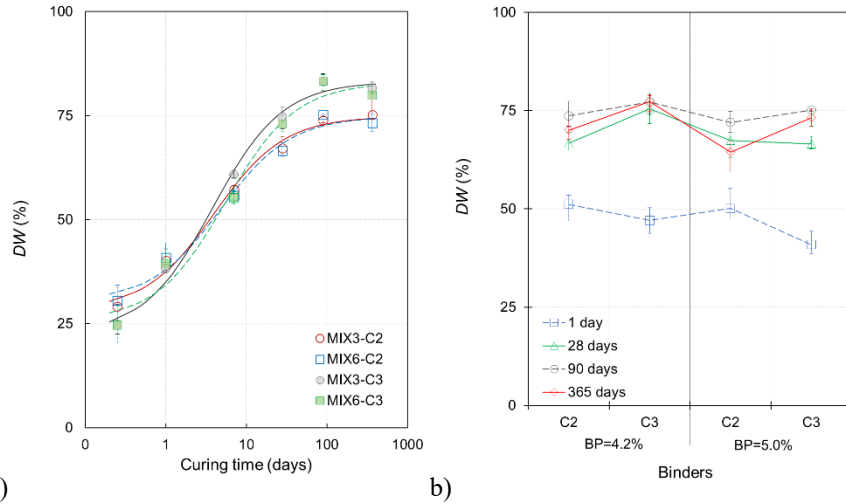


Figure F.1. Evolution of DW: a) as a function of curing time of mixtures with B/C = 1.2, b) with B/C = 1.0 after 1, 28, 90, 365 days. Error bars show the variability of the data

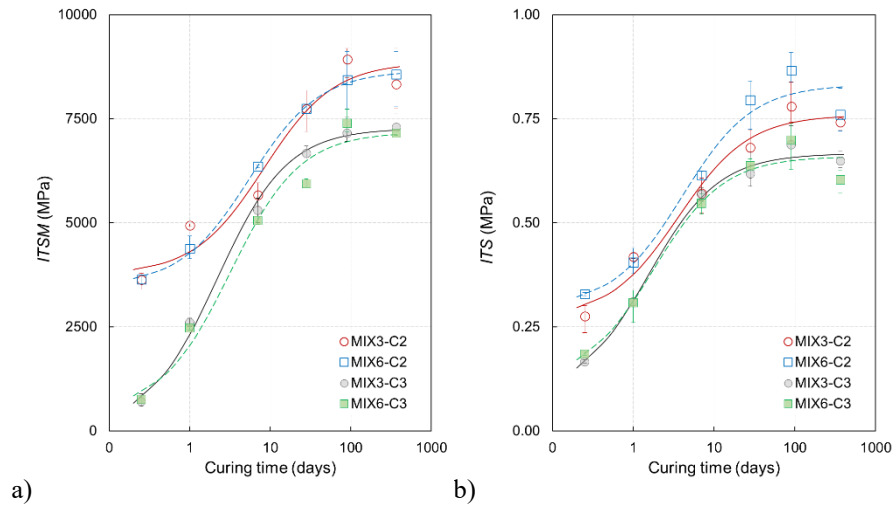


Figure F.2. Mechanical properties as a function of curing time of the mixtures with B/C = 1.2: a) *ITSM*, b) *ITS*. Error bars show the variability of the data

Appendix F

Study of the Composition of CBE Mixtures with High Strength Cements for Binder Courses

Multiscale Approach for Characterising the Behaviour of Cold Bitumen Emulsion Materials

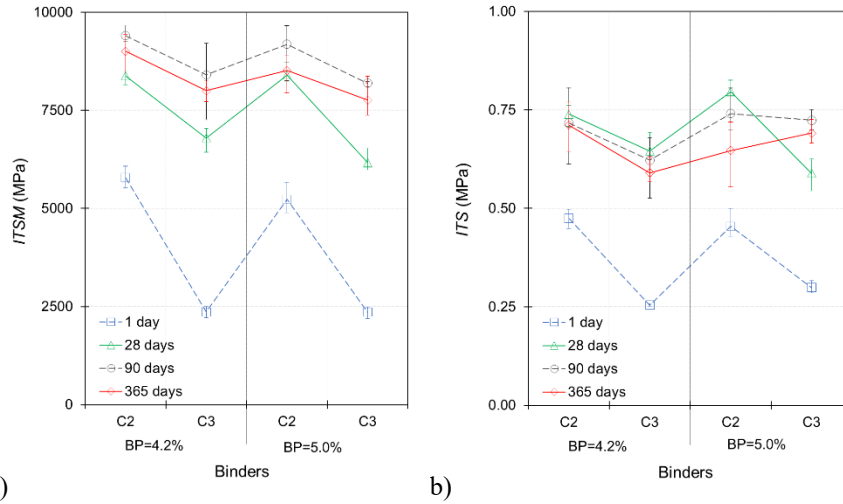


Figure F.3. Mechanical properties of CBE mixtures with B/C = 1.0 after 1 day, 28, 90, 365 days: a) *ITSM*, b) *ITS*. Error bars show the variability of the data

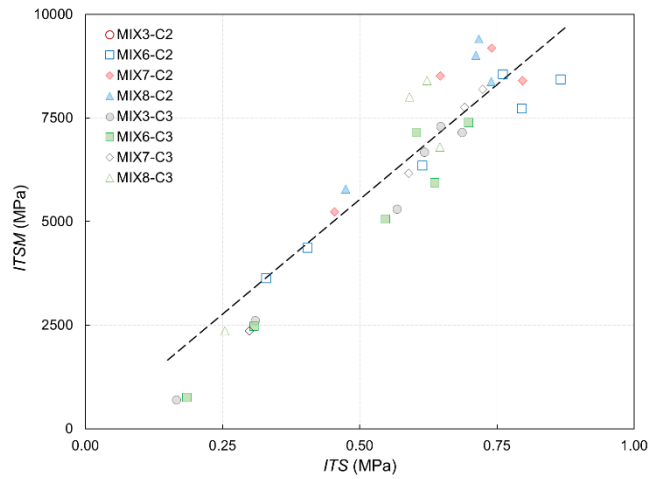


Figure F.4. Relationship between *ITSM* and *ITS*

Study of the Composition of CBE Mixtures with High Strength Cements for Binder Courses

Multiscale Approach for Characterising the Behaviour of Cold Bitumen Emulsion Materials

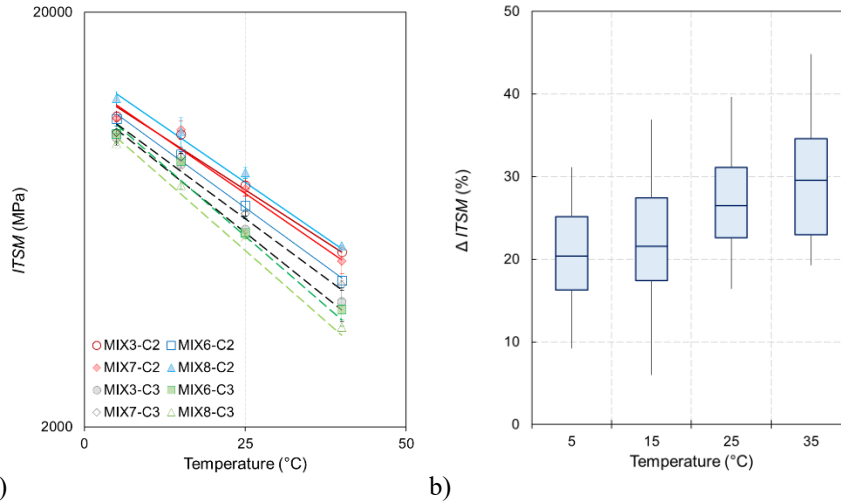


Figure F.5. CBE mixtures thermal sensitivity: a) *ITSM* as a function of temperature for all mixtures (horizontal deformation $2 \cdot 10^{-6}$ mm/mm), b) $\Delta ITSM$ due to the changing of the target horizontal deformation (Equation F.2)

Table F.2. Regression parameters for Equation (F.1)

Mixture	Hor. Def. = $2 \cdot 10^{-6}$ mm/mm			Hor. Def. = $5 \cdot 10^{-6}$ mm/mm		
	a	b	R ²	a	b	R ²
C2-2.5_B5.0	0.0113	4.112	0.98	0.0124	4.069	0.96
C3-2.5_B5.0	0.0126	4.093	0.97	0.0155	3.999	0.97
C2-2.5_BP5.0	0.0097	4.122	0.96	0.0118	4.036	0.96
C3-2.5_BP5.0	0.0118	4.077	0.96	0.0124	3.918	0.98
C2-2.5_BP4.2	0.0102	4.155	0.97	0.0115	4.074	0.96
C3-2.5_BP4.2	0.0127	4.062	0.99	0.0135	3.977	0.99
C2-3.0_BP5.0	0.0104	4.129	0.94	0.0123	4.089	0.98
C3-3.0_BP5.0	0.0109	4.087	0.98	0.0137	3.939	0.96

F.4. Summary

The investigation aimed at defining CBE mixtures composition whose mechanical properties are adequate for the application in binder courses. The influence of two types of high strength cement was evaluated, as well as the effect of traditional and modified bitumen emulsion.

The main findings are as follows:

- The use of cement C2 allowed the rate of evolution of the mechanical properties to be considerably increased in the early curing stage. Also, in the long-term, stiffness and strength reached satisfactory levels;
- The mechanical response of mixtures produced using the Portland slag cement resulted lower all over one curing year;
- No particular effects related to the type of bitumen emulsion were observed, albeit the level of compaction could hide this evidence;
- All mixtures investigated exhibited low thermal sensitivity thanks to the cement;
- Nonlinearity effects related to the deformation were found for all the mixtures investigated.

Appendix G

Fatigue Behaviour of CBE Mixtures for Binder Courses Produced with High Strength Cements

G.1. Introduction

Fatigue resistance is one of the main features of pavement materials, which are continuously subjected to repeated traffic loads. Fatigue is a fundamental input in the design of flexible pavements. The fatigue resistance of CM and CRM is a quite complex topic due to their evolutive nature and the presence of the cementitious co-binder. Different test configurations (e.g. Indirect Tensile Fatigue Test, *ITFT*, four-point bending), testing modes (i.e. controlled stress and controlled shear) and testing temperatures have been adopted for testing CM and CRM (Modarres *et al.* 2011, Dolzycki *et al.* 2020, Flores *et al.* 2020). Most frequently, *ITFT* configuration, controlled shear stress mode and 20 °C temperature are adopted (Modarres *et al.* 2011, Dolzycki *et al.* 2020, Flores *et al.* 2020). In general, CM have lower resistance to repeated loading, especially at high strain levels (Bocci *et al.* 2011, Stimilli *et al.* 2013, Leandri *et al.* 2015, Lin *et al.* 2017). This behaviour can be related to higher air void content and the lower bitumen content of CRM mixtures than HMA. However, introducing a thicker base layer of CRM can help increase the pavement life than a thinner HMA base layer (Lin *et al.* 2017). CBE mixtures have higher fatigue resistance than cold foam mixtures, probably thanks to the homogenous coating of aggregate particles achieved with the emulsion (Yan *et al.* 2010). The fatigue resistance of CM is strictly related to the dosages of the co-binders and their respective proportions. In general, increasing the bitumen dosages improves the fatigue resistance, whereas increasing the cement dosage can lead to better or worst responses in terms of fatigue life (Kavussi and Modarres 2010, Dolzycki *et al.* 2020, Flores *et al.* 2020). The effect of curing time is not well understood yet. Some investigations found that the curing time increase does not appear to significantly change the slope of fatigue lines (Kavussi and Modarres 2010, Modarres *et al.* 2011). On the other side, other studies showed that the fatigue life increases with the increase of curing time (Lin *et al.* 2017). Such a behaviour can be connected to the actual composition of the mixtures investigated in terms of co-binders dosages, as well as to other types of phenomena, e.g. ageing.

The present laboratory investigation focuses on the fatigue behaviour of CBE mixtures suitable for binder courses. CBE mixtures characterised by two gradings

distribution and produced using traditional and modified emulsion and two types of high strength cements were investigated to this goal. The *ITFT* was carried out at the long-term curing stage. Some of the investigated mixtures, i.e. MIX3 and MIX4, were also object of investigation of the curing and LVE behaviours (Chapter 6 and Chapter 7).

G.2. Methodology

The CBE mixtures investigated were prepared using RA aggregate, natural fine aggregate, limestone filler, bitumen emulsion, cement and water. Two aggregate blends were adopted: “CC” and “GG” (Table 4.1). Both the traditional and modified bitumen emulsion were used, i.e. B and BP. As co-binders, the high-strength cements C2 and C3 were considered. Materials properties are reported in Section 4.1 and Appendix A.

Ten CBE mixtures were investigated, six obtained using the grading distribution CC and four using GG. Different binders dosages were considered. Table G.1 reports the compositions of the mixtures. B/C ratio ranged between 1.0 and 1.2.

Mixing and compaction procedures are detailed in Appendix B and Section 4.2.2, respectively. The diameter of the specimens was 100 mm. The fixed height compaction mode was applied to reach selected target voids of the mixture V_m . Two values of V_m were chosen: 8.5% for mixtures with B and 9.5% for the mixtures with BP.

The long-term fatigue resistance was assessed: specimens were cured at $(25 \pm 2)^\circ\text{C}$ and constant RH of $(70 \pm 5)\%$ for at least 365 days. Fatigue resistance was measured using the *ITFT* configuration (EN 12697-24, Annex E). The test was carried out in controlled stress mode, applying a haversine repeatedly, with 0.1 s loading time and 0.4 s rest time. The testing temperature was 20°C . Hence the specimens were conditioned at least four hours before the testing. The minimum number of tested specimens was five for each mixture investigated.

The horizontal tensile strain ε_h of the specimen was measured using a LVDT:

$$\varepsilon_h = \frac{2,1 \cdot \Delta H}{D} \quad (\text{G.1})$$

where ΔH is the length variation of the specimen diameter, and D is the diameter. Increasing ε_h , the stiffness S_{mix} of the material decreases:

$$S_{mix} = \frac{\sigma_h}{\varepsilon_h} (1 + 3\nu) \quad (\text{G.2})$$

where ν is the Poisson ratio, σ_h is the horizontal stress applied in the middle of the specimen:

$$\sigma_h = \frac{2 \cdot F}{\pi \cdot D \cdot t} \quad (\text{G.3})$$

where F is the force applied and t is the thickness of the specimen.

The initial horizontal strain ε_0 and S_{mix} were calculated considering the average of the values measured in the first 115 loading cycles.

Appendix G

Fatigue Behaviour of CBE Mixtures for Binder Courses Produced with High Strength Cements

Multiscale Approach for Characterising the Behaviour of Cold Bitumen Emulsion Materials

For estimating the fatigue resistance of the specimen, two fatigue criteria were considered:

- The number of loads cycles needed to reach the complete failure of the specimen N_f ;
- The number of loads cycles corresponding to a stiffness decrease of 50% of the initial stiffness $N_{f,50}$.

The classical representation of the fatigue law, also known as Wöhler law, was used, considering the number of cycles to failure under the initial strain amplitude:

$$N = A \cdot \varepsilon_0^{-a_2} \quad (\text{G.4})$$

where N is the fatigue life, a_2 is the slope of the Wöhler curve associated with a straight line in the $\log N - \log \varepsilon_0$ domain, and A is a coefficient, function of the testing conditions.

The strain level that leads to fatigue life of 1 million cycles, ε_6 , used in the European standards to classify the fatigue resistance of bituminous mixtures, was also considered within this investigation:

$$\frac{N_f}{10^6} = \left(\frac{\varepsilon_0}{\varepsilon_6} \right)^{-a_2} \quad (\text{G.5})$$

Table G.1. Composition of CBE mixtures considered for the fatigue study

ID	Cement			Emulsion (Residual bitumen)		B/C	w_t^* (%)	V_m (%)
	Grading (-)	Type (-)	Dosage* (%)	Type (-)	Dosage* (%)			
MIX3 ^{a,b}	CC	C2, C3	2.5	BP	5.0 (3.0)	1.2	4.5	9.5
MIX4 ^a	GG	C2,C3	2.5	BP	5.0 (3.0)	1.2	4.0	9.5
MIX6 ^b	CC	C2, C3	2.5	B	5.0 (3.0)	1.2	4.5	8.5
MIX7 ^b	CC	C2,C3	3.0	BP	5.0 (3.0)	1.0	4.5	9.5
MIX9	GG	C2,C3	2.5	BP	4.2 (2.5)	1.0	4.5	9.5

*by dry aggregate mass, ^a mixtures investigated in Chapter 6 and Chapter 7, ^b mixtures investigated in Appendix F

G.3. Analysis of the Results

Figure G.1 shows the results of the *ITFT* tests in terms of $N_{f,50}$ as a function of ε_0 . Similar trends were obtained using the N_f criteria. Observing the different fatigue laws, it can be

observed that all the mixtures had similar behaviours, covering a similar range of the $N_{f,50} - \varepsilon_0$ domain. Considering the values of the slope a_2 , some slight differences are observed within the mixtures (**Figure G.2**). In general, the values of a_2 were higher when the failure criteria $N_{f,50}$ was used instead of N_f . As expected, the 50% stiffness reduction resulted in a fatigue life slightly lower than those obtained using the specimen failure criteria.

Considering the influence of the cement types, for mixtures MIX3, using cement C2 instead of C3 led to a value of a_2 slightly higher, i.e. 3.9% and 2.8% in the case of N_f and $N_{f,50}$, respectively. This increase was much higher for mixtures MIX4 and MIX5, respectively 26.9% and 51.3% considering as failure criteria $N_{f,50}$, and about 44% for both mixtures considering N_f . Mixtures with B/C = 1.0 showed an opposite trend when cement C3 was used instead of C2, with an average decrease of -10% and -11.4% considering N_f and $N_{f,50}$, respectively. This suggests that the effect of the cement type was not unique, and the emulsion dosage also influenced that. Observing mixtures having the same grading distribution and binder dosages but produced with different types of emulsions, i.e. MIX3 and MIX6, a_2 was higher passing from BP to B for mixtures with C2. In contrast, the parameter decreased when cement C3 was used. However, it must be pointed out that the diverse voids levels adopted for mixtures produced with BP and B could hide some possible different response of the materials. Also in this case, there was no clear effect related to the combination of binders used. Finally, comparing mixtures with the same binders dosages but different grading, i.e. MIX3 and MIX4, it was observed that the adoption of the gap graded distribution (MIX4) led to an increase of a_2 , and consequently to a reduction of the fatigue life.

The analysis of the only slope of the fatigue law curves does not allow considering the magnitude of the horizontal strain, which is a crucial parameter in pavement design. For this reason, it is useful to take into account ε_6 (**Figure G.3**). All the mixtures had values of ε_6 between 82 and 120 $\mu\text{m/m}$. These values are within the general interval covered by HMA, ranging between 60 and 150 $\mu\text{m/m}$ (Tapsoba *et al.* 2013, Perraton *et al.* 2019, Ferrotti, Canestrari, *et al.* 2020). The influence of the binders in terms of types of cement, type of emulsion and dosages, was reduced. Indeed, the percentage variation in the ε_6 values due to the different combinations of the composition always ranged between -11% and 11%. On the contrary, the grading distribution effect was more evident: the adoption of the gap graded distribution led to ε_6 reduction of about 23% and 33, for mixtures with cement C2 and C3, respectively.

Appendix G

Fatigue Behaviour of CBE Mixtures for Binder Courses Produced with High Strength Cements

Multiscale Approach for Characterising the Behaviour of Cold Bitumen Emulsion Materials

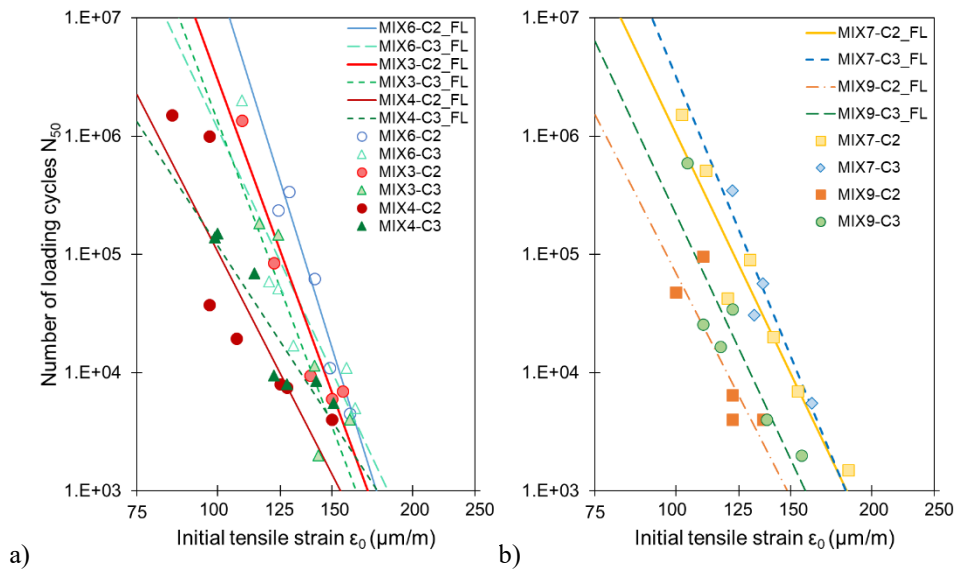


Figure G.1. ITFT experimental results and fatigue law (“FL”) obtained for all the mixtures tested a) B/C = 1.2, b) B/C = 1.0

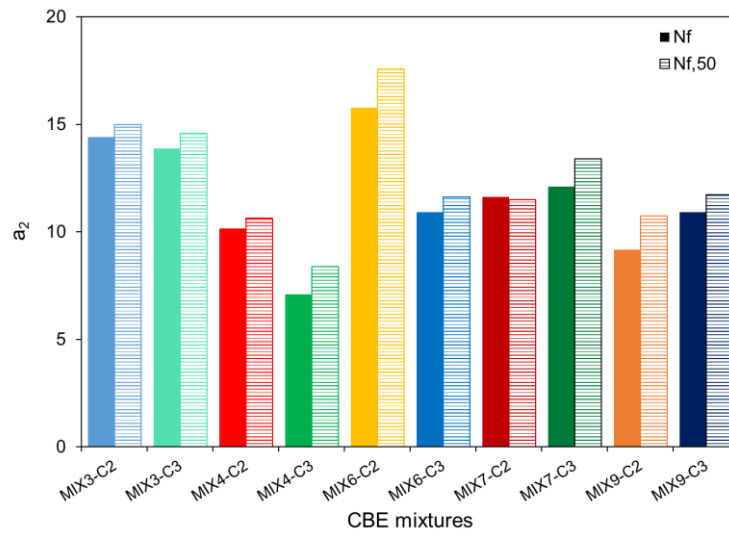


Figure G.2. Fatigue law parameter a_2 of the investigated mixtures obtained with both failure criteria, N_f and $N_{f,50}$

Fatigue Behaviour of CBE Mixtures for Binder Courses Produced with High Strength Cements

Multiscale Approach for Characterising the Behaviour of Cold Bitumen Emulsion Materials

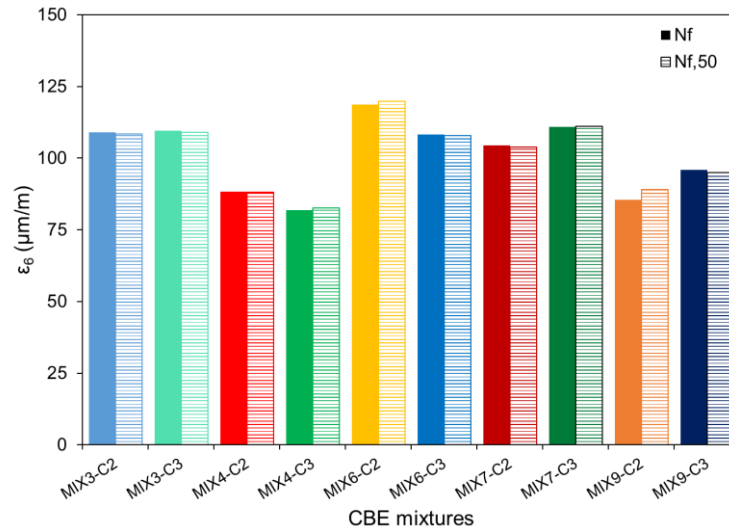


Figure G.3. Fatigue law parameter ε_6 of the investigated mixtures obtained with both failure criteria, N_f and $N_{f,50}$

Finally, **Figure G.4** compares the fatigue laws of the ten investigated mixtures to those of five mixtures found in the literature for cold mixtures. Their composition and testing methods are summarised in **Table G.2** (Bocci *et al.* 2011, Stimilli *et al.* 2013, Leandri *et al.* 2015, Dolzycki *et al.* 2020). These mixtures always had slopes higher than those investigated herein produced using the CC distribution while the values of ε_6 were lower. Mixture A had ε_6 lower than $50 \mu\text{m/m}$, whereas mixtures D and E ε_6 was about $60 \mu\text{m/m}$. Mixtures B and C reached ε_6 values similar to those obtained with mixtures produced using the distribution GG. The result indicates that the adoption of high strength cementitious binders, modified emulsion, and higher binder dosages did not penalise the fatigue resistance of CBE mixtures. In particular, when the continuous grading curve was used, the fatigue life of mixtures was enhanced.

Appendix G

Fatigue Behaviour of CBE Mixtures for Binder Courses Produced with High Strength Cements

Multiscale Approach for Characterising the Behaviour of Cold Bitumen Emulsion Materials

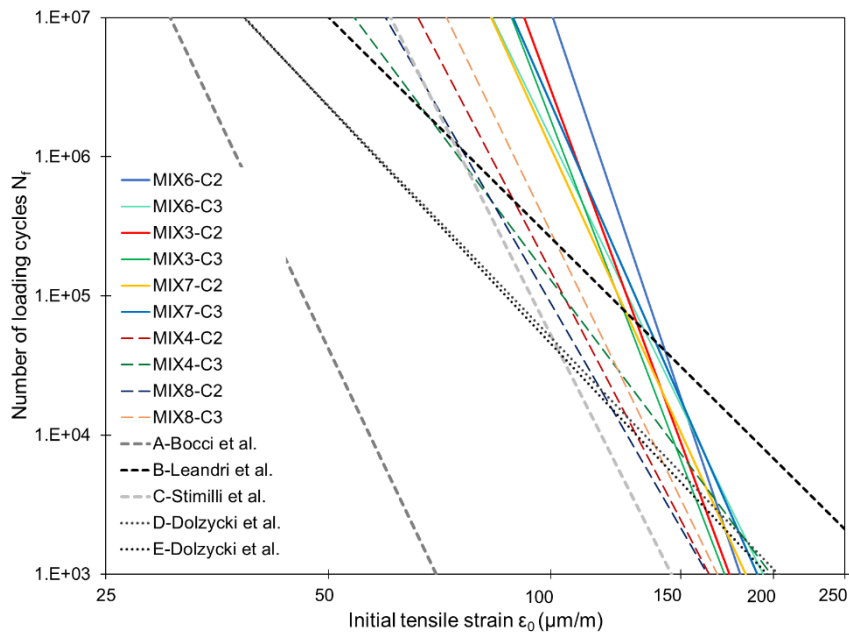


Figure G.4 Comparison between the fatigue law of the CBE mixtures investigated and mixtures from the literature.

Table G.2. Composition and testing methods of CBE mixtures found in literature

ID	Reference	Aggregate blend	Cement	Residual bitumen	Test
A	Bocci <i>et al.</i> (2011)	100% RA0/16	2,0% CEM II/B-LL, 32.5R	1,8% C60B10	ITFT, 20°C Stress control
B	Leandri <i>et al.</i> (2015))	100% RA0/16	2,0% Portland Cement, 32.5R	2,5%	ITFT, 20°C Stress control
C	Stimilli <i>et al.</i> (2013)	90% RA0/20	3.0% Portland Cement	2.4% C60BP7	ITFT, 20°C Stress control
D	Dolzycki <i>et al.</i> (2020)	70% RA 0/31.5	2.0% Portland cement CEM I 32.5R	2.4% C60B10	ITFT, 20°C Stress control
E	Dolzycki <i>et al.</i> (2020)	70% RA 0/31.5	2.0% Portland cement CEM I 32.5R	3.6% C60B10	ITFT, 20°C Stress control

G.4. Summary

The Appendix aimed at investigating the fatigue response in terms of ITFT of CBE mixtures suitable for binder courses. The influence of two types of high strength cement was evaluated as well as the effect of traditional and modified bitumen emulsion and the effect of two grading distribution.

The main findings are as follows:

- Cementitious binders C2 and C3 led to CBE mixtures having similar fatigue life;
- No significant differences in the fatigue response were observed due to the emulsion type. However, this could be due to different voids levels;
- The adoption of a gap graded distribution slightly reduced the fatigue life of CBE mixtures compared to a continuous distribution.

Appendix H

Cracking Resistance of CBE FAM mortars

H.1. Introduction

Cracking is one of the major distress of road pavements. This means that the structural performance of pavements is strictly related to the fracture behaviour of its constituent materials. Hence, the fracture resistance assessment is a fundamental aspect, especially for CBE mixtures that could be prone to cracking because of the presence of cement, aged bitumen and RA. This investigation focuses on the cracking resistance of CBE FAM mortars, which is related to the presence and relative effect of bituminous and cementitious bonds within the materials. The objective is to evaluate the influence of different cement types, B/C ratios and curing RH. The semi-circular bending (SCB) test was used to evaluate the cracking resistance of eight FAM mortar specimens whose composition was derived from eight mixtures composition (see Chapter 5 and Chapter 6).

H.2. Methodology

The CBE FAM mortars were composed of RA 0/2 aggregate, natural fine aggregate, limestone filler, bitumen emulsion, cement and additional water (Section 4.1). The bituminous binder was traditional bitumen emulsion (B), whereas, as co-binders, four different types of cement were adopted (C1, C2, C3 and C4). Details about the materials used are provided in Chapter 4.

Eight FAM mortars, derived from eight mixtures (Chapter 5) were considered (**Table 4.4**):

- FAM1a, FAM2a, produced with both C1 and C2;
- FAM1b, FAM2b, produced with both C3 and C4.

Appendix B details the FAM mortar mixing procedure, whereas the specimen compaction procedure is described in Section 4.2.2. Final specimens had a height of 50 mm and a diameter of 150 mm. The specimens mass was selected to get the target values of V_m (**Table 4.4**). After the compaction, specimens were cured for 28 days in a climatic chamber at $(25 \pm 2)^\circ\text{C}$ and $(70 \pm 5)\%$ RH. Both unsealed and sealed curing conditions were considered (Section 4.2.3). At the end of the curing, specimens were conditioned at 5°C for 12 hours. Afterwards, two half-cylindrical specimens were obtained by cutting. A notch with a width

Appendix H
Cracking Resistance of CBE FAM mortars

Multiscale Approach for Characterising the Behaviour of Cold Bitumen Emulsion Materials

of (0.35 ± 0.10) mm and a depth of (10.0 ± 1.0) mm was then cut in the middle of the base of each half-cylindrical specimen.

The SCB test (EN 12697-44) was carried out at 10°C , after 4 hours of temperature conditioning. The test requires applying of three-point bending load to a half-cylindrical specimen (**Figure H.1a**). In this test configuration, the middle base of the specimen is subjected to increasing tensile stress. As the test proceeds, the crack starts from the tip of the notch, where the concentration of the stress is highest, and then propagates vertically. The test was carried out at a constant vertical displacement rate of 5 mm/min. Four replicate specimens were tested for each mortar and curing condition.

The results were analysed in terms of fracture toughness K (EN 12697-44), fracture energy G_f (Li and Marasteanu 2010) and flexibility index FI (Ozer, Al-Qadi, Lambros, *et al.* 2016, Ozer, Al-Qadi, Singhvi, *et al.* 2016).

K describes the state of local stress around a crack and is defined as follows:

$$K = \sigma_{max} \cdot f\left(\frac{a}{A}\right) \quad (\text{H.1})$$

where σ_{max} is the maximum stress at failure and $f\left(\frac{a}{A}\right)$ is a geometric factor. K is an intrinsic property of the material that is commonly used to define its aptitude to resist cracking initiation (Saha and Biligiri 2016).

G_f describes the overall cracking potential of the mixture being a measurement of the work needed to increase the fractured surface until failure and is defined as follows:

$$G_f = \frac{W}{A_{lig}} \quad (\text{H.2})$$

where W is the work of fracture (area under the load-displacement curve until failure), and A_{lig} is the crack ligament area (Ozer, Al-Qadi, Singhvi, *et al.* 2016).

FI is related to the fracture energy and the slope of the post-peak load-displacement curve (crack propagation phase) according to the following equation:

$$FI = A \frac{G_f}{\text{abs}(m)} \quad (\text{H.3})$$

where G_f is the fracture energy, m is the slope of the post-peak curve at the inflexion point, and A is a unit conversion factor assumed equal to 0.01. FI was developed to discriminate the cracking resistance of different mixtures better, taking into account the crack propagation speed and fracture process zone. Indeed, it was observed that the post-peak segment of the load-deformation curve is susceptible to changes in the composition of the material (Ozer, Al-Qadi, Lambros, *et al.* 2016).

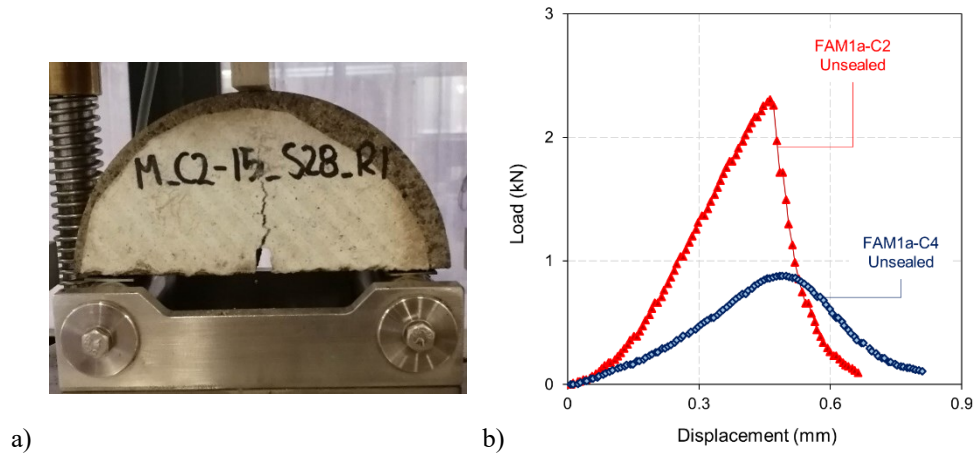


Figure H.1. SCB test a) configuration, b) typical load-displacement curves

H.3. Analysis of the Results

Figure H.1b shows two typical load-displacement curves obtained for the studied CBE FAM mortars. In particular, the curves of mortars with cements C2 and C4, with the B/C ratio of 1.3 and cured in unsealed condition, are depicted.

Figure H.2 shows the average values of K . As can be observed, the cement type influenced the K of the mortars. In particular, a hierarchy of the toughness can be highlighted: mortars produced with C2 always showed the highest K , followed by the mortars with C3 and C1. Mortars with C4 always showed the lowest K . Passing from FAM1 to FAM2, thus reducing the B/C ratio from 1.3 to 0.8, improved K of all the mortars investigated, regardless of cement type and curing condition. In particular, the average increase of K was about 40% for mortars with C1, C2 and C4, and it reached 80% for mortars with C3. As far as curing condition is concerned, generally, sealed condition of curing negatively influenced K of the mortars, especially for the lowest cement dosage. In particular, for mortars with B/C=1.3, K decreased by about 25% using C1, C2 and C3 and 39% when C4 was used.

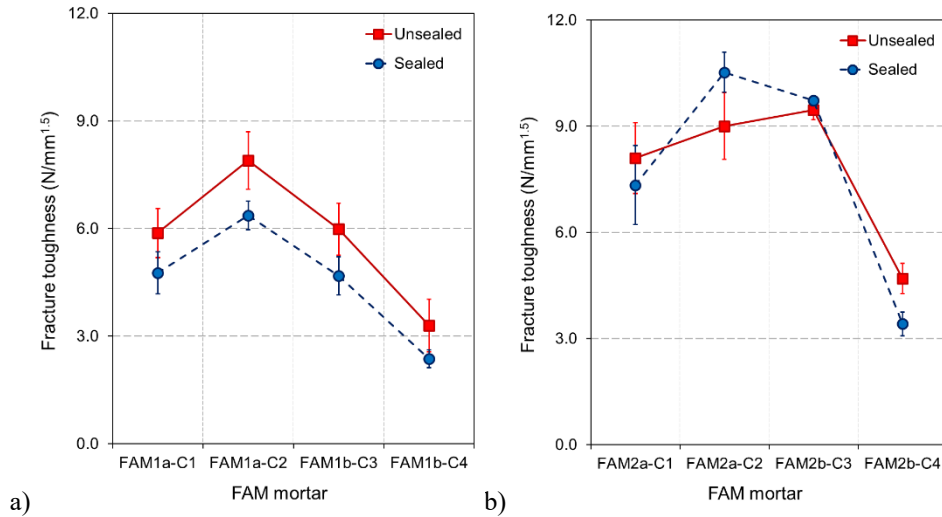


Figure H.2. K of the FAM mortars investigated a) $B/C=1.3$ (FAM1a and FAM1b), b) $B/C=0.8$ (FAM2a and FAM2b). Error bars represents the standard deviation

Figure H.3 shows the average values of G_f . The cement type influence on G_f was similar to those highlighted for K . Fracture energy was higher for mortars produced with C2 and C3 indeed. In contrast, lower values were achieved for the mortars with C4 regardless of curing conditions. Similar to the results obtained for K , the fracture energy increased with the increase in cement dosage (lower B/C ratio). The increase in G_f was particularly high for the mortars produced with C3 (more than doubled). Whereas the cement dosage had a lower influence on the mortars produced with C4 (average increase equal to 28%). Generally, the increase in cement dosage resulted in increased brittleness. However, the experimental results indicate that mortars maintained a good ability of deformation at failure due to the bituminous bonds. Allowing free water evaporation (unsealed conditions) resulted in increased G_f from 4% to 97% with respect to restricted evaporation (sealed conditions). The opposite effect was observed only for the mortar produced using FAM2a-C1.

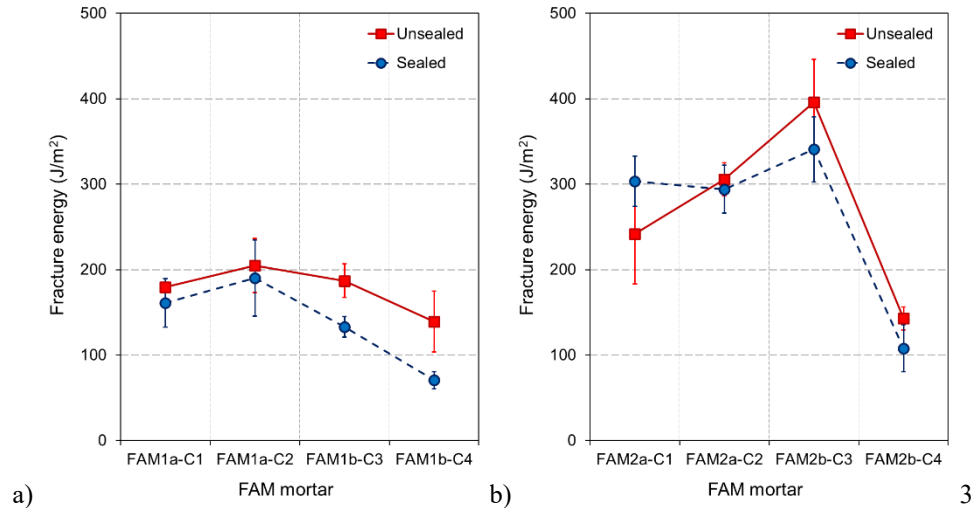


Figure H.3. G_f of the mortars investigated a) B/C=1.3, b) B/C=0.8. Error bars represents the standard deviation

Figure H.4 shows the average values of FI . Similar to the results obtained in terms of K and G_f , the influence of the dosage of cement (and consequently of the B/C ratio) was evident. In particular, the increase in cement dosage generally caused a decrease in FI , depending on the cement type and curing condition. FI allowed different post-peak behaviours due to the cement type to be distinguished more clearly. Generally, mortars produced using C2 and C3, which were characterised by higher K and G_f , showed lower FI values than mortars produced using C1 and C4. This behaviour can be explained considering the slope of the post-peak curve at the inflexion point. In fact, the values of the slope obtained testing the mortars produced with C2 and C3 was, in general, two or three times higher with respect to the slope of mortars with C1 and C4. In general, a lower slope of the post-peak peak segment is an index of a more ductile response to the crack propagation, whereas a higher slope is related to more brittle crack propagation. Thus, the lowest FI values clearly showed the increase of brittleness of the mortars produced with C2 and C3.

Figure H.5 shows the values of G_f and FI as a function of K . As can be observed, increasing the K value, G_f increased, whereas FI decreased. In general, brittle materials show high values of K associated with low values of G_f . FAM mortars did not follow this trend because high values of K were associated with high values of G_f . This may be an effect of the simultaneous presence of cementitious and bituminous bonds. The first ones contributed to high values of K , and the second led to high values of G_f . The FI values revealed that the positive effect of the bituminous bonds was limited to the crack initiation phase. In fact, high

Appendix H

Cracking Resistance of CBE FAM mortars

Multiscale Approach for Characterising the Behaviour of Cold Bitumen Emulsion Materials

values of K are associated with low values of FI , which indicated a brittle behaviour during crack propagation (post-peak phase).

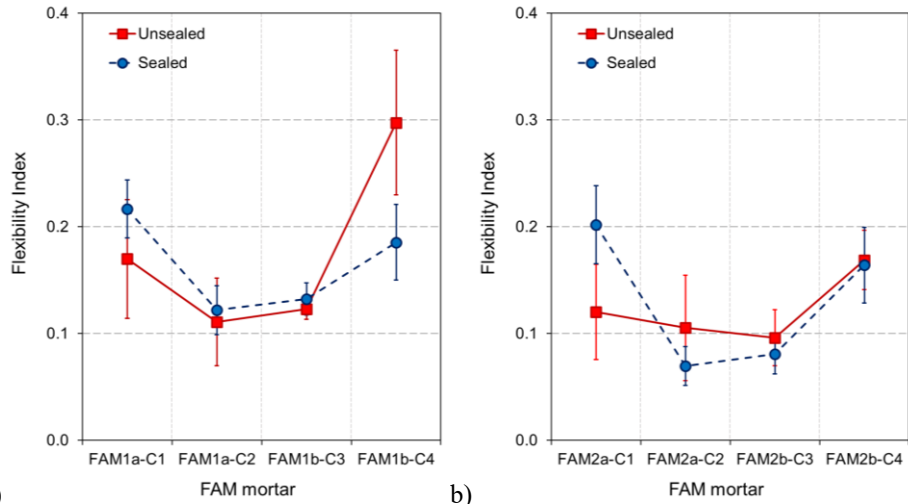


Figure H.4. FI of the mortars investigated a) B/C=1.3, b) B/C=0.8. Error bars represents the standard deviation

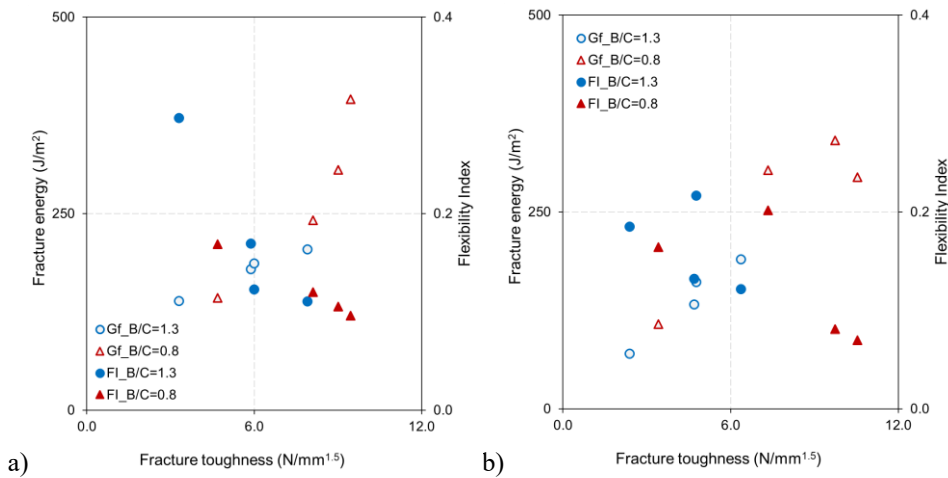


Figure H.5. G_f and FI as a function of K for mortars cured in a) unsealed conditions, b) sealed conditions

H.4. Summary

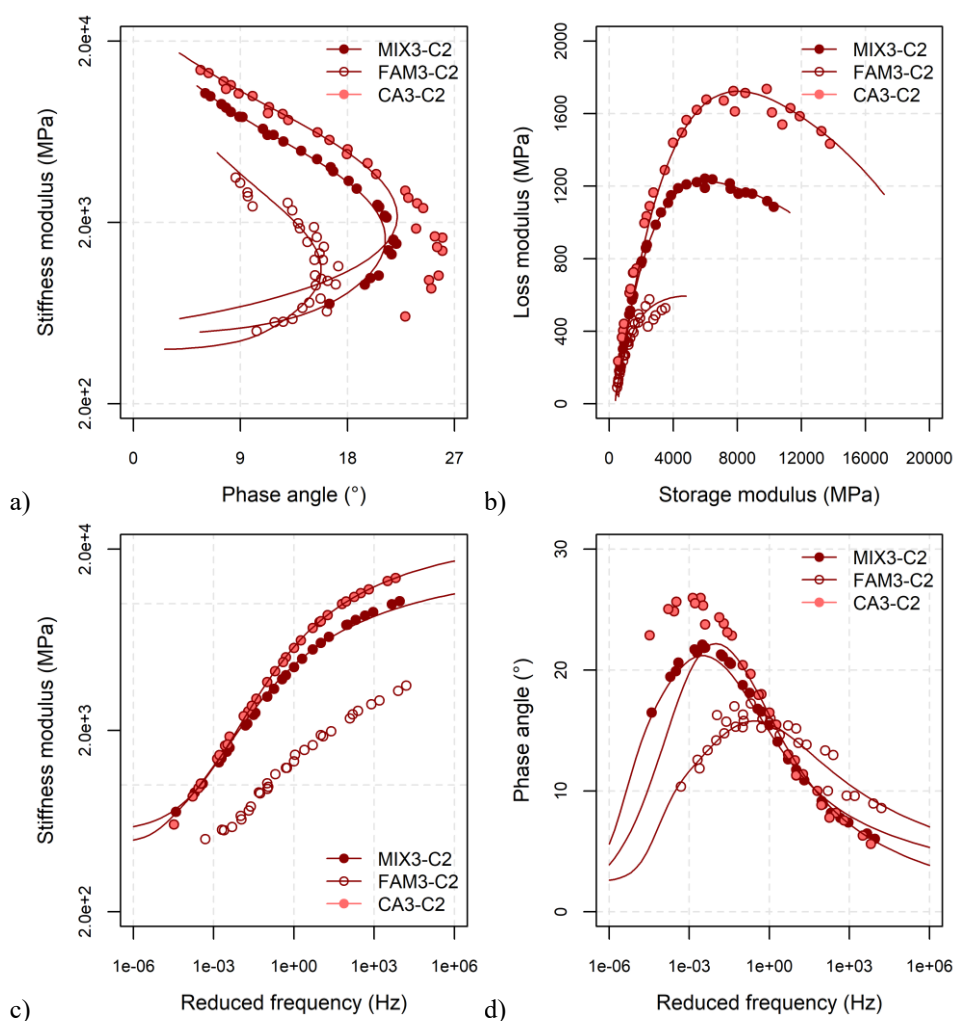
The present laboratory investigation evaluated the cracking resistance of FAM mortars. They were produced using four cement types, two cement dosages and one bitumen emulsion dosage. Tests were carried out after 28 days of curing in two RH conditions: unsealed and sealed.

The main findings are as follows:

- Fracture toughness K , fracture energy G_f and flexibility index FI allowed to discriminate among mortars produced with different types and dosages of cement;
- Mortars produced using cements C2 and C3 showed higher values of K and G_f , whereas the mortars produced using cements C1 and C4 showed higher values of FI ;
- In the crack initiation phase, the behaviour of mortars depended on the combined presence of cementitious and bituminous bonds. In the crack propagation phase, the effects of cement type and dosage prevailed and may have led to brittle behaviour.

Appendix I

Graphic Representation of the Results For Complex Modulus Test



Graphic Representation of the Results For Complex Modulus Test

Multiscale Approach for Characterising the Behaviour of Cold Bitumen Emulsion Materials

Figure I.1. Average complex modulus results and fitted 2S2P1D-HY obtained for CBE materials with grading CC and cement C2: a) Black diagram, b) Cole-Cole plan, c) stiffness modulus master curve, d) phase angle master curve

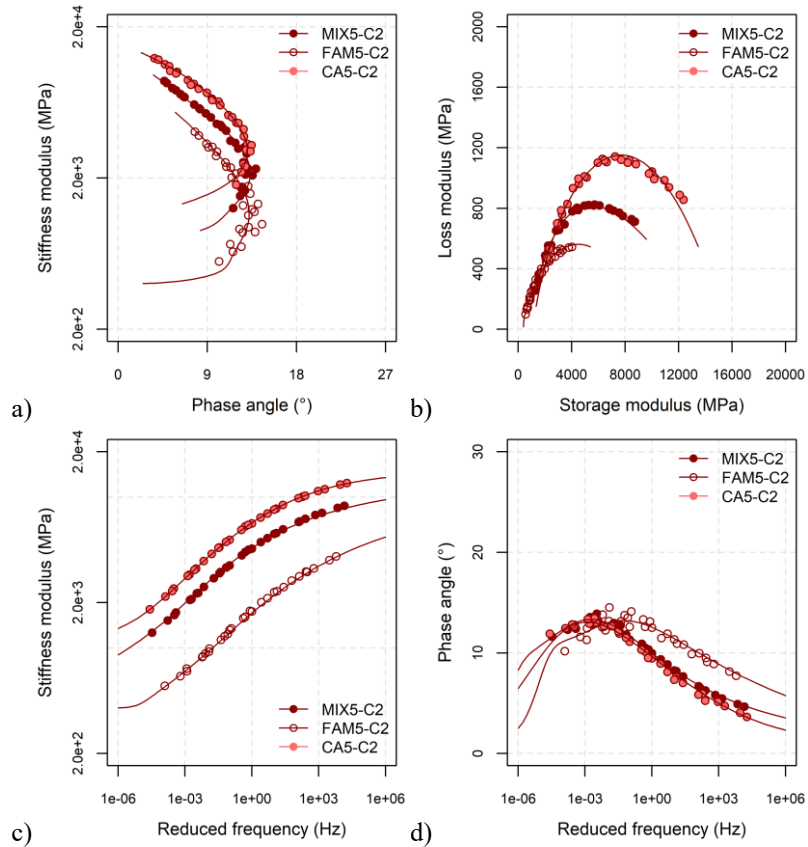


Figure I.2. Average complex modulus results and fitted 2S2P1D-HY obtained for CBE materials with grading GGallRA and cement C2: a) Black diagram, b) Cole-Cole plan, c) stiffness modulus master curve, d) phase angle master curve

Appendix I

Graphic Representation of the Results For Complex Modulus Test

Multiscale Approach for Characterising the Behaviour of Cold Bitumen Emulsion Materials

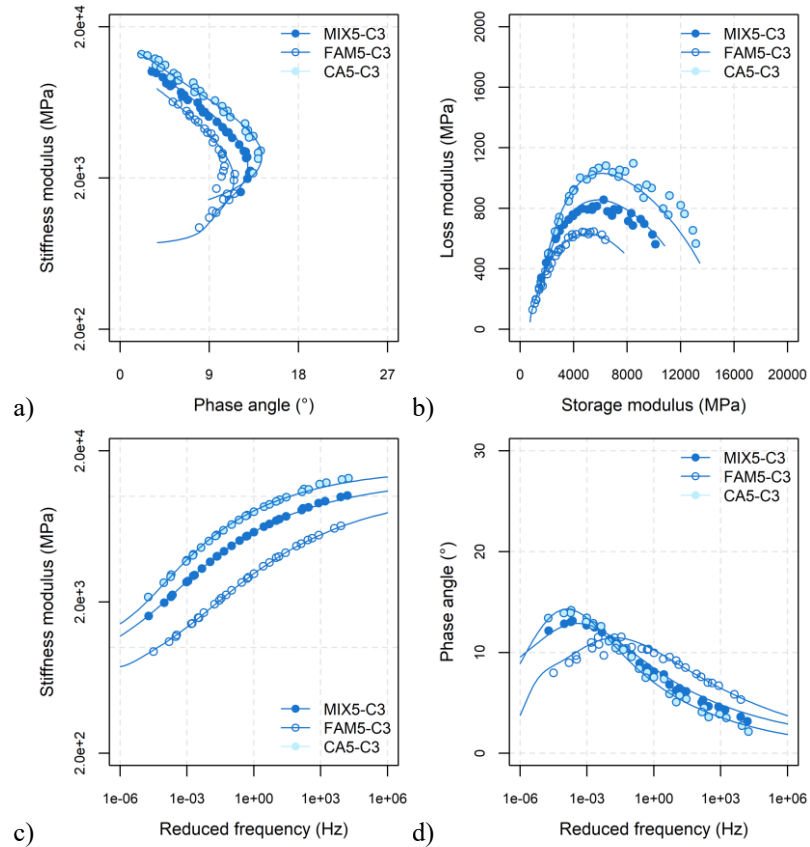


Figure I.3. Average complex modulus results and fitted 2S2P1D-HY obtained for CBE materials with grading GGallRA and cement C3: a) Black diagram, b) Cole-Cole plan, c) stiffness modulus master curve, d) phase angle master curve

Lists of 3-years PhD Publications

- Mignini, C., Cardone, F., & Graziani, A. (2018). Experimental study of bitumen emulsion–cement mortars: mechanical behaviour and relation to mixtures. *Materials and Structures*, 51(6), 149.
- Raschia, S., Mignini, C., Graziani, A., Carter, A., Perraton, D., & Vaillancourt, M. (2019). Effect of gradation on volumetric and mechanical properties of cold recycled mixtures (CRM). *Road Materials and Pavement Design*, 1-15.
- Graziani, A., Mignini, C., Bocci, E., & Bocci, M., (2019). Complex Modulus Testing and Rheological Modeling of Cold-Recycled Mixtures. *Journal of Testing and Evaluation*, 48(1).
- Ferrotti, G., Grilli, A., Mignini, C., & Graziani, A. (2020). Comparing the Field and Laboratory Curing Behaviour of Cold Recycled Asphalt Mixtures for Binder Courses. *Materials*, 13(21), 4697.
- Graziani, A., Raschia, S., Mignini, C., Carter, A., & Perraton, D. (2020). Use of fine aggregate matrix to analyze the rheological behavior of cold recycled materials. *Materials and Structures*, 53(4), 1-16.
- Mignini, C., Cardone, F., & Graziani, A. (2020). Using fine aggregate matrix mortars to predict the curing behaviour of cement bitumen treated materials produced with different cements. *Construction and Building Materials*, 121201.
- Mignini, C., Lo Presti, D., Airey, G., & Graziani, A. (2021). Rheological characterisation of cold bitumen emulsion slurries. *Road Materials and Pavement Design*, 1-19.
- Graziani, A., Mignini, C., Bocci, E., & Bocci, M. (2018, June). Complex modulus of cold recycled mixtures: measurement and modelling. In 13th ISAP conference on asphalt pavements. Fortaleza, Ceará, Brazil (pp. 19-21).
- Grilli, A., Mignini, C., & Graziani, A. (2019, March). Field behaviour of cold-recycled asphalt mixtures for binder courses. In Proceedings of the International Conference on Sustainable Materials, Systems and Structures (SMSS 2019), Rovinj, Croatia.
- Mignini, C., Cardone, F., Morbi A., Setti L. & Graziani, A., (2019, March). Evaluating the cracking resistance of cement-bitumen treated materials using the semi-circular bending test, In Proceedings of the International Conference on Sustainable Materials, Systems and Structures (SMSS 2019), Rovinj, Croatia.

List of 3-years PhD Publications

Multiscale Approach for Characterising the Behaviour of Cold Bitumen Emulsion Materials

- Mignini C., Cardone F., Graziani A., Morbi A., & Setti L. (2019) Effect of curing on the indirect tensile failure energy of cement-bitumen treated materials, Bituminous Mixtures and Pavements VII: Proceedings of the 7th International Conference Bituminous Mixtures and Pavement, June 12-14, Thessaloniki, Greece.
- Graziani, A., Raschia, S., Mignini, C., Carter, A., & Perraton, D. (2020, January). Use of Fine Aggregate Matrix to Analyze the Rheological Behavior of Cold Recycled Materials, 99th Annual Meeting Transportation Research Board, Washington (POSTER).
- Winter, M., Mollenhauer, K., Graziani, A., Mignini C., Giancontieri, G., Lo Presti, D., Bjurström, H. & Kalman, B. Design of flexible pavements with cold recycled asphalt bases: Comparison of four national approaches, Proceedings of 8th Transport Research Arena TRA 2020, April 27-30, 2020, Helsinki, Finland.
- Bjurström, H., Kalman, B., Mollenhauer, K., Winter, M., Graziani, A., Mignini, C., Lo Presti, D., Giancontieri, G., Gaudefroy, V. Experiences from cold recycled materials used in asphalt bases: a comparison between five European countries, accepted to 7th Euroasphalt and Eurobitume Congress, June 16-18, 2021, Madrid.
- Mignini, C., Cardone, F., & Graziani, A. (2020). Mechanical Behaviour of Cold Recycled Asphalt Mixtures for Binder Courses Produced with Bitumen Emulsion and High Strength Cement. In Proceedings of the 9th International Conference on Maintenance and Rehabilitation of Pavements—Mairepav9 (pp. 365-374). Springer, Cham.
- Mignini, C., Cardone, F. & Graziani, A., Experimental study on the grading distribution of cold recycled asphalt mixtures produced with bitumen emulsion and high strength cement, RILEM International Symposium on Bituminous Materials, December 14-16, 2020, Lyon.
- Miljković M., Graziani, A. & Mignini, C. Interphase relations in the characterisation of bitumen emulsion-cement composites, RILEM International Symposium on Bituminous Materials, December 14-16, Lyon.
- Winter, M., Mollenhauer, K., Graziani, A., Mignini, C., Bjurström, H., Kalman, B., Hornych, P., Gaudefroy, V. Lo Presti, D., Giancontieri, G. Validation of national empirical pavement design approaches for cold recycled asphalt bases, submitted to 11th International Conference on the Bearing Capacity of Roads, Railways and Airfields. 28 -30 June 2022 in Trondheim, Norway.

Lists of 3-years PhD Awards

Outstanding Paper published in 2018 by the Board of Editors of Materials and Structures to Mignini, C., Cardone, F., & Graziani, A. (2018). Experimental study of bitumen emulsion–cement mortars: mechanical behaviour and relation to mixtures. *Materials and Structures*, 51(6), 149

SIIV Arena Best Presentation award, 2nd SIIV International Winter School, December 15-18, 2019, Moena Italy

Outstanding Paper published in 2020 by the Board of Editors of Materials and Structures to Graziani, A., Raschia, S., Mignini, C., Carter, A., & Perraton, D. (2020). Use of fine aggregate matrix to analyze the rheological behavior of cold recycled materials. *Materials and Structures*, 53(4), 1-16.